AEDC-TR-73-47

cy 2

AUG 1 1973
AUG 17 1973

MAY 29 1990

WIND TUNNEL MODEL PARAMETRIC STUDY FOR USE IN THE PROPOSED 8 FT × 10 FT HIGH REYNOLDS NUMBER TRANSONIC WIND TUNNEL (HIRT) AT ARNOLD ENGINEERING DEVELOPMENT CENTER

W. K. Alexander, S. A. Griffin, R. L. Holt, et al.

General Dynamics Corporation

Convair Aerospace Division

March 1973

Approved for public release; distribution unlimited.

ARNOLD ENGINEERING DEVELOPMENT CENTER

AIR FORCE SYSTEMS COMMAND

ARNOLD AIR FORCE STATION, TENNESSEE

Property of U. S. Air Force
AEDC LIBRARY
F40600-74-C-0001

NOTICES

When U. S. Government drawings specifications, or other data are used for any purpose other than a definitely related Government procurement operation, the Government thereby incurs no responsibility nor any obligation whatsoever, and the fact that the Government may have formulated, furnished, or in any way supplied the said drawings, specifications, or other data, is not to be regarded by implication or otherwise, or in any manner licensing the holder or any other person or corporation, or conveying any rights or permission to manufacture, use, or sell any patented invention that may in any way be related thereto.

Qualified users may obtain copies of this report from the Defense Documentation Center.

References to named commercial products in this report are not to be considered in any sense as an endorsement of the product by the United States Air Force or the Government.

WIND TUNNEL MODEL PARAMETRIC STUDY FOR USE IN THE PROPOSED 8 FT X 10 FT HIGH REYNOLDS NUMBER TRANSONIC WIND TUNNEL (HIRT) AT ARNOLD ENGINEERING DEVELOPMENT CENTER

W. K. Alexander, S. A. Griffin, R. L. Holt, et al.
General Dynamics Corporation
Convair Aerospace Division

Approved for public release; distribution unlimited.

FOREWORD

This report describes the work performed on Air Force contract F-40600-72-C-0015 by the Convair Aerospace Division of General Dynamics Corporation, San Diego operation, San Diego, California. The report is identified by contractor's number GDCA-DHJ72-001.

The work was administered by the Department of the Air Force, Headquarters, Arnold Engineering Development Center (TMP), Arnold Air Force Station, Tennessee. Mr. Ross G. Roepke, AEDC (DYX), is the Air Force technical representative.

This program was conducted in the research and engineering department of Convair and was managed by S. A. Griffin with W. K. Alexander as coordinating engineer. The work was accomplished between June and December 1972.

Principal contributors to the study include:

Wind Tunnel Design	W. K. Alexander, S. B. Harkey
Dynamics	R. L. Holt
Materials Evaluation	R. T. Torgerson, R. W. Tryon
Aerodynamics	T. J. Fleck, G. J. Fatta
Structural Analysis	W. W. Johnstone, C. E. Edenfield
Test Operations	W. H. Lowe
Aerodynamic Consultant	H. Yoshihara

The reproducibles used in the reproduction of this report were supplied by the author.

This technical report has been reviewed and is approved.

ROSS G. ROEPKE
Requirements Planning Division
Directorate of Technology

ROBERT O. DIETZ
Director of Technology

Col. Roland R.

Marshall K. Kingery
Facilities Div. Div
Deputy

ABSTRACT

The need for a High Reynolds Number Transonic Wind Tunnel (HIRT) has been recognized throughout the industry for some years. The proposed HIRT facility at Arnold Engineering Development Center will provide a much needed tool for the study of phenomena sensitive to Reynolds number. The usefulness of the HIRT facility will be largely influenced by the ability of industry to design and build wind-tunnel models for an acceptable cost capable of operating within the severe environment of the tunnel. The object of this study is to determine the feasibility of designing and building models capable of withstanding the loads and environmental conditions of the facility. The aircraft configurations chosen for study cover a wide spectrum of flight conditions. A test plan is developed for each configuration which encompasses its complete flight envelope. Model loads and distortions are computed and presented to illustrate their magnitude under HIRT test conditions. Stress analyses of each aircraft configuration are presented for three different types of model. A summary of materials suitable for use in the HIRT facility is presented, and specific recommendations are made for model materials. Cost comparisons are made between models for testing in HIRT and similar models for testing in existing transonic wind tunnels. The study concludes that models capable of running in the HIRT facility can be built at a reasonable cost with present-day techniques and materials.

TABLE OF CONTENTS

Section		Page
I	INTRODUCTION	1
II	PROGRAM ORGANIZATION	4
III	MODEL CONFIGURATION SELECTION	5
IV	MODEL SIZING	6
V	DESIGN PARAMETERS	11
	5.1 MODEL TYPES	11
	5.2 MATERIALS	11
	5.3 LOADS	11
	5.4 SURFACE FINISHES	11
	5.5 SCALE EFFECTS	12
VI	BASIC DESIGN PHILOSOPHY	13
	6.1 BALANCE AND SUPPORT SYSTEMS	13
	6.2 BASIC FORCE MODELS	14
	6.3 PRESSURE MODELS	19
	6.4 BASELINE MATERIAL SELECTION	27
	6.5 SURFACE FINISH	27
	6.6 MISCELLANEOUS OBSERVATIONS	27
VII	TEST PLAN	29
	7.1 TUNNEL USE	29
	7.2 OPERATING ENVELOPES	29
	7.3 TEST PLAN DEVELOPMENT	36
	7.4 DATA STORAGE	36
VIII	AEROELASTIC ANALYSIS	38
	8.1 METHODS	38
	8.2 TUNNEL OPERATING CONDITIONS INFLUENCE ON MODEL LOADS	39
	8.3 MODEL LOADS	46
	8.4 MODEL WING DEFORMATION	63
	8.5 MODEL SCALE EFFECTS ON WING DEFORMATION	70
	8.6 REYNOLDS NUMBER EFFECT ON WING DEFORMATION	71

TABLE OF CONTENTS, Contd

Section		Page
IX	STRUCTURAL ANALYSIS	72
	9.1 ATT MODEL	72
	9.2 F-111 AIRCRAFT	96
	9.3 DELTA CANARD FIGHTER	108
	9.4 SPACE SHUTTLE BOOSTER	116
X	MATERIALS ANALYSIS	120
	10.1 CURRENT MODEL MATERIALS	120
	10.2 HIRT MODEL REQUIREMENTS	120
	10.3 MATERIALS SEARCH	121
	10.4 GENERAL DISCUSSION OF MATERIAL CLASSES	121
	10.5 PROMISING MATERIAL CANDIDATES	123
	10.6 ALLOY SELECTION	125
	10.7 PROCUREMENT SPECIFICATIONS	127
	10.8 DESIGN ALLOWABLES	127
	10.9 SURFACE FINISH	129
	10.10 PROTECTIVE COATINGS	130
XI	MODEL COSTS	131
XII	CONCLUSIONS	133
XIII	RECOMMENDATIONS	135
	13.1 RECOMMENDATIONS FOR FURTHER ANALYSES	135
	13.2 ADDITIONAL STUDY AREAS	135
XIV	REFERENCES	137
Appendix		
I	TYPICAL COMPUTER RUN PROGRAM 4278	139
II	SAFETY FACTOR BASED ON FRACTURE MECHANICS	159

LIST OF FIGURES

Figure		Page
1	Program Operations Chart	4
2	Basic Geometry — ATT	7
3	Basic Geometry — F-111	8
4	Basic Geometry — Space Shuttle Booster	9
5	Basic Geometry — Delta Canard	10
6	Balance Diameter vs Normal Force Capability	13
7	ATT Basic Force Model	15
8	F-111 Basic Force Model	16
9	Delta Canard Fighter Basic Force Model	17
10	Space Shuttle Booster Basic Force Model	18
11	ATT Pressure Wing, Method I	21
12	ATT Pressure Wing, Method II	22
13	F-111 Pressure-Instrumented Wing	23
14	Delta Canard Fighter Pressure Wing	24
15	Space Shuttle Booster Pressure Wing	25
16	Reynolds Number Ranges of Aircraft Chosen for Study	29
17	ATT Operating Envelope	30
18	Delta Canard Operating Envelope	31
19	Space Shuttle Booster Operating Envelope	32
20	F-111 (50 deg) Operating Envelope	33
21	F-111 (26 deg) Operating Envelope	34
22	F-111 (72-1/2 deg) Operating Envelope	35
23	Aeroelastic Program Geometry	41
24	Reynolds Number vs Dynamic Pressure at 300°K	43
25	Reynolds Number vs Dynamic Pressure at 240°K	44
26	ATT – Effects of 300°K vs 240°K Tunnel Operation	45
27	ATT — Model Loads — Condition 5	47
28	ATT — Model Loads — Condition 6	48
29	ATT — Model Loads — Condition 7	49
30	ATT — Model Loads — Condition 1	50
31	ATT — Model Loads — Condition 3	51
32	ATT — Model Loads, 1/16 Scale — Conditions 37 and 41	52
33	ATT — Model Loads, 1/16 Scale — Conditions 38 and 42	53
34	ATT — Model Loads, 1/12 Scale — Conditions 39 and 43	54
35	ATT — Model Loads, 1/12 Scale — Conditions 40 and 44	55
36	F-111 (50 Deg) — Model Loads — Condition 14	56
37	F-111 (50 Deg) — Model Loads — Condition 17	57
38	F-111 (26 Deg) — Model Loads — Condition 20	58
39	F-111 (72-1/2 Deg) — Model Loads — Condition 22	59

LIST OF FIGURES, Contd

Figure		Page
40	Delta Canard — Model Loads — Condition 24	60
41	Delta Canard — Model Loads — Condition 27	61
42	Space Shuttle Booster — Model Loads — Condition 29 (T = 300°K)	62
43	ATT — Elastic Wing Twists	64
44	ATT — Model Wing and Airplane Wing Twist Due to Matching Operating Envelope	65
45	ATT — Wing Deflections — 1/24 Scale Model and Full-Scale Airplane	66
46	ATT — Effect on Deflection Due to Removing Aft 35% Chord	66
47	F-111 (50 Deg) — Elastic Wing Twist	67
48	F-111 (50 Deg) — Wing Deflections	67
49	F-111 — Elastic Wing Twist vs Wing Sweep	68
50	F-111 — Wing Deflections vs Wing Sweep	68
51	Delta Canard — Elastic Wing Twist	69
52	Delta Canard — Wing Deflection	69
53	Space Shuttle Booster — Elastic Wing Twist	70
54	Space Shuttle Booster — Wing Deflection	70
55	ATT — Elastic Wing Twist vs Tunnel Temperature and Model Scale	71
56	ATT — Effect of Reynolds Number on Wing Twist	71
57	ATT Wing — Location of Sections Used For Structural Analysis	74
58	ATT — Comparison of Wing Types vs Stress (Condition 7)	75
59	ATT — Wing Stress at Wing Section 4 Resulting from Matching Flight Conditions for M=1.0 at 30,000 ft from 1.0 g to 2.5 g's	76
60	ATT — Comparison of Wing Stresses vs Tunnel Temperature and Model Scale	78
61	ATT Wing — Minimum Inertias	79
62	F-111 — Wing Stresses vs Wing Sweeps (Solid Wing)	97
63	F-111 — Wing Types vs Stress at 50-Degree Sweep	97
64	F-111 — Horizontal Tail Bracket Stress vs Incidence	97
65	Delta Canard — Wing Section Properties	110
66	Strength and Room Temperature Fracture Toughness Relationships	126
67	Strength and Low Temperature Fracture Toughness Relationships	126

LIST OF TABLES

Table		Page
1	Admissible Roughness Estimates (Surface Finish)	28
2	Test Plan	37
3	Model Loads, Empennage, and Total Lift	63
4	Model Loads Directory	64
5	Stress Analysis — Minimum Safety Factor Summary	73
6	ATT Wing Section Properties and Bending Analysis — 100% Chord Solid Wing	80
7	ATT Wing Section Properties and Bending Analysis — 65% Chord Solid Wing	81
8	ATT Wing Section Properties and Bending Analysis — 100% Chord Pressure Model (Method I)	82
9	ATT Wing Section Properties and Bending Analysis — 65% Chord Pressure Model (Method II)	83
10	Comparative Properties of General Classes of Materials (Ambient Temperature)	122
11	Material Specification for Recommended Alloys	127
12	Design Mechanical and Physical Properties of Materials Recommended for HIRT Test Models	128
13	Model Fabrication Cost Comparisons	131

ABBREVIATIONS AND SYMBOLS

Symbol	Nomenclature	Units
A	Area	$in.^2$
B.L.	Buttock line station	in.
C	Chord or dimension	in.
C	Specific heat	BTU/lb F
C_L	Coefficient of lift	in.
C.P.	Center of pressure	
c_L	Distance to lower fibers	in.
c_U	Distance to upper fibers	in.
D	Diameter	in.
E	Modulus of elasticity	$lb/in.^2$
E.A.	Elastic axis	
E_c	Modulus of elasticity in compression	$lb/in.^2$
e/D	Edge distance/diameter	
e	Elongation	%
F	Fahrenheit	degrees
F_A	Axial force	lb
F_b	Allowable bending stress	$lb/in.^2$
F_{bru}	Ultimate bearing stress	$lb/in.^2$
F_{bry}	Bearing yield stress	$lb/in.^2$
F_{cy}	Compressive yield stress	$lb/in.^2$
F_n	Ultimate tension allowable	$lb/in.^2$
F_{su}	Ultimate shear allowable	$lb/in.^2$
F_{tu}	Ultimate tension allowable	$lb/in.^2$
F_{ty}	Tensile yield stress	$lb/in.^2$
F.S.	Fuselage station	in.
f_b	Calculated bending	$lb/in.^2$
f_{br}	Calculated bearing stress	$lb/in.^2$

Symbol	Nomenclature	Units
f_c	Calculated compressive stress	lb/in.^{2}
f_n	Calculated principal stress	lb/in.^{2}
f_s	Calculated shear stress	lb/in.^{2}
f_{st}	Calculated shear stress (torsion)	lb/in.^{2}
f_t	Calculated tension stress	lb/in.^{2}
G	Modulus of rigidity	lb/in.^{2}
I	Moment of inertia	in.^{4}
J	Polar moment of inertia	in.^{4}
K	Thermal conductivity	BTU/hr ft^2°F
K_{1c}	Plane strain fracture toughness	ksi in.
L	Load	lb
l	Length	in.
M	Moment	in-lb
MAC	Mean aerodynamic chord	ft
Method I	ATT Model gun-drilled pressure wing (Figure 11)	
Method II	ATT Model removeable T.E. pressure wing (Figure 12)	
n	Designates a number	
P	Load	lb
P_S	Shear load	lb
P_{SA}	Allowable shear load	lb
P_T	Tensile load	lb
P_{TA}	Allowable tensile load	lb
Q	Static moment of a cross-section	in-lb
q_∞	Freestream dynamic pressure	lb/ft^2
R_e	Reynolds number	
S	Translational deflection	in.
S.F.	Safety factor	

Symbol	Nomenclature	Units
S.S.	Span station	in.
T	Torsion	in.-lb
T.E.	Trailing edge	
T.S.	Tail panel station	in.
t	Thickness	in.
u	Median length	in.
V	Shear load	lb
W.S.	Wing station	in.
x_{cp}	Axial center of pressure location	in.
y_L	Distance to lower fibers	in.
y_T	Distance to upper fibers	in.
z_{cp}	Polar section modulus	$in.^3$
α	Coefficient of thermal expansion	
Δ	Incremental or differential	
Λ L.E.	Leading edge sweep angle	deg.
μ-in.	Microinch	$in. \times 10^{-6}$
χ	Rotational deflection	deg.
ω	Density	$lb/in.^3$
°K	Degrees Kelvin	deg.
$\parallel$	Parallel	
$\perp$	Perpendicular	
$+$	Vectorial addition symbol	

SECTION I

INTRODUCTION

The international concern over the inability of existing wind-tunnel facilities to approach or match full-scale Reynolds numbers has led to the development of a variety of plans to construct high Reynolds number transonic wind tunnels. One proposed facility is HIRT, a large Ludwieg tube tunnel (8 ft × 10 ft test section), to be located at Arnold Engineering Development Center, Arnold Air Force Station, Tennessee (References 1 and 2). HIRT will operate over a range of Reynolds numbers from those available in present-day wind tunnels up to full-scale values for future flight vehicles.

Reynolds number performance in a wind tunnel is achieved through a balance of tunnel size, dynamic pressure, and temperature. Tunnel size is the prime parameter when relating to facility cost. The financial gains resulting in tunnel size reduction must be weighed against the restraints on testing capability due to model limitations. As the test section size is reduced (with a corresponding reduction in allowable model scale), the dynamic pressure must increase to maintain the desired Reynolds number performance. Model, balance, and support system stresses and deflections increase, while allowable surface finishes and model tolerances decrease. Model design, fabrication techniques, materials selection, balance system requirements, and, of course, model costs must be considered along with tunnel fabrication and operating costs when selecting an optimum tunnel size.

The objective of this study is to identify and analyze various problem areas associated with the design and fabrication of four configurations of wind tunnel models for use in the HIRT facility. The variety of aircraft studied included:

a. A variable wing sweep supersonic airplane (F-111).

b. A high-performance delta-wing fighter (Delta Canard).

c. An advanced technology transport (ATT).

d. A space shuttle booster.

Section III and Section IV respectively cover the selection of the specific aircraft to be studied and the sizing of models for use in the 8 ft × 10 ft HIRT test section. Basic model geometry drawings are presented.

The design parameters are discussed in Section V:

a. Types of models.

b. Model materials.

c. Model loads.

d. Surface finishes.

e. Model scale effects.

The basic design philosophy applied to this study is discussed in Section VI. Model conceptual drawings for each of the four model configurations are presented. Balance requirements and various support system stings are shown. Pressure-instrumented wings with approximately 400 pressure orifices are shown for each configuration. The ATT model is used to present two pressure wing design concepts. Baseline material selections were made for the basic model construction and model support system. Model surface finish requirements due to aerodynamics are discussed and admissible roughness computed for each of the models.

It is anticipated that the proposed HIRT facility will be heavily used and, unlike present-day transonic tunnels, that test plans will be very sensitive to the high Reynolds number capability. The high demand for occupancy will require a more limited test plan, with emphasis placed on testing critical areas of the operating envelope to confirm configuration performance.

A computer program was developed to compute design loads for each model and the corresponding deformations due to twisting and bending. In Section VIII each design point in the test plan was analyzed, and data were plotted to show wing loadings and deformations including:

a. Shear load.

b. Bending moment and pitching torque.

c. Wing loading.

d. Vertical deflection.

e. Elastic wing twist.

Basic structural analyses are performed on each of the models presented. Basic wing stresses, wing-to-fuselage attachments, empennage stresses, and the degradation of allowable loading due to the installation of pressure instrumentation in the model wings are analyzed and presented in Section IX.

The ATT model is used to analyze the effects on model stresses and model deformation resulting from increasing the model scale. The HIRT scale (1/24) was increased by factors of 1.5 (1/16 scale) and 2.0 (1/12 scale). Scale effects are covered in Sections VIII and IX.

Materials suitable for use in the fabrication of wind-tunnel models for the HIRT facility are presented in Section X. Alloy selections, procurement specifications, design

allowables, surface-finish procedures, and protective coatings for models are also presented.

In Section XI, model cost estimates are given, and comparisons are made between HIRT model costs and model costs for existing wind tunnels. Cost increments are given for various model surface finishes and model scales.

Due to the large scope of the subject of the design of wind-tunnel models for the HIRT tunnel, this study had to be very selective in the choice of subjects to be explored. Several interesting problem areas were recognized but were not analyzed in detail in this report. Section XIII contains recommendations for subjects for future detailed analyses.

SECTION II

PROGRAM ORGANIZATION

Convair Aerospace Division established a program team within its research and engineering department to conduct the parametric study of high Reynolds number wind-tunnel models. The team organized to conduct this study was led by Mr. S. A. Griffin, who reports to Mr. W. T. MacCarthy, manager of wind tunnels. The entire organization is under the senior management of the division vice president of research and engineering, Mr. R. H. Widmer.

The program operations chart, Figure 1, illustrates the flow of information from the various technical groups, through design, to the final report.

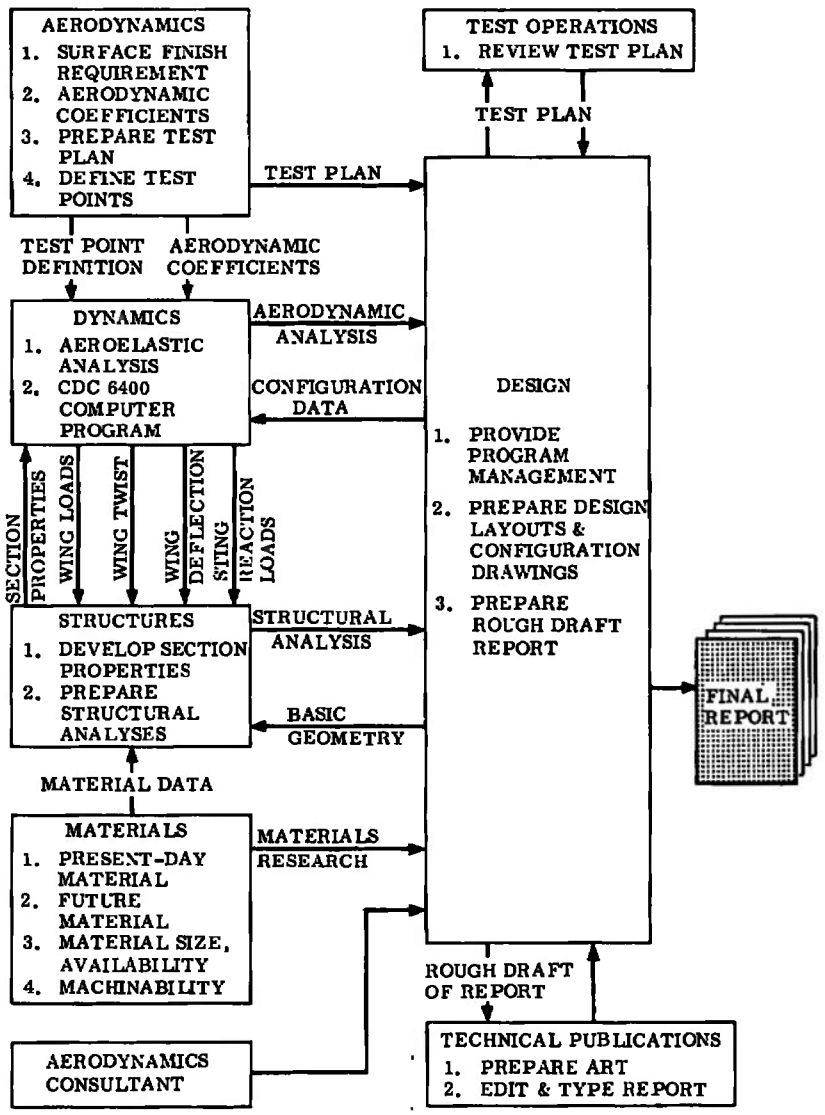

Figure 1. Program Operations Chart

SECTION III

MODEL CONFIGURATION SELECTION

Four types of aircraft have been selected to be analyzed during this study. These models are typical of the type of aircraft that would be likely candidates for testing in the HIRT facility. The wind tunnel model configurations selected are:

a. Advanced Technology Transport (ATT) – a highly loaded, large, swept-wing transport aircraft.

b. Convair Aérospace F-111 – a swing-wing supersonic aircraft.

c. Convair Aerospace space shuttle booster – a large delta-wing space vehicle capable of launching an orbiter space vehicle and returning to earth for a landing.

d. Convair Aerospace delta canard fighter (delta canard) – a highly maneuverable fighter aircraft consisting of delta planform wings and canards.

SECTION IV

MODEL SIZING

Model sizing was accomplished using criteria based on model size requirements recommended by the General Dynamics high speed wind tunnel and AGARD data (Reference 3). Sizing criteria:

a. Wing span ≤60% of the tunnel width.

b. Frontal area of the model at zero angle of attack ≤ 1% of the test section cross sectional area.

c. Wing area ≤ 5% of the test section cross sectional area.

d. Model length ≤ test section height.

HIRT test section dimensions:

a. Height = 8 feet

b. Width = 10 feet

c. Cross sectional area = 80 feet^2

Resulting model scales, wing spans, and body lengths:

Model	Scale	Wing span (in.)	Fuselage length (in.)
ATT	1/24	67.55	91.67
F-111 (26 deg sweep)	1/12	60.0	71.20
(50 deg sweep)	1/12	48.22	71.20
(72 1/2 deg sweep)	1/12	32.0	71.20
Delta Canard	1/9.6	35.61	56.00
Space Shuttle Booster	1/46.5	37.40	59.80

Basic model geometries are shown in Figures 2 through 5.

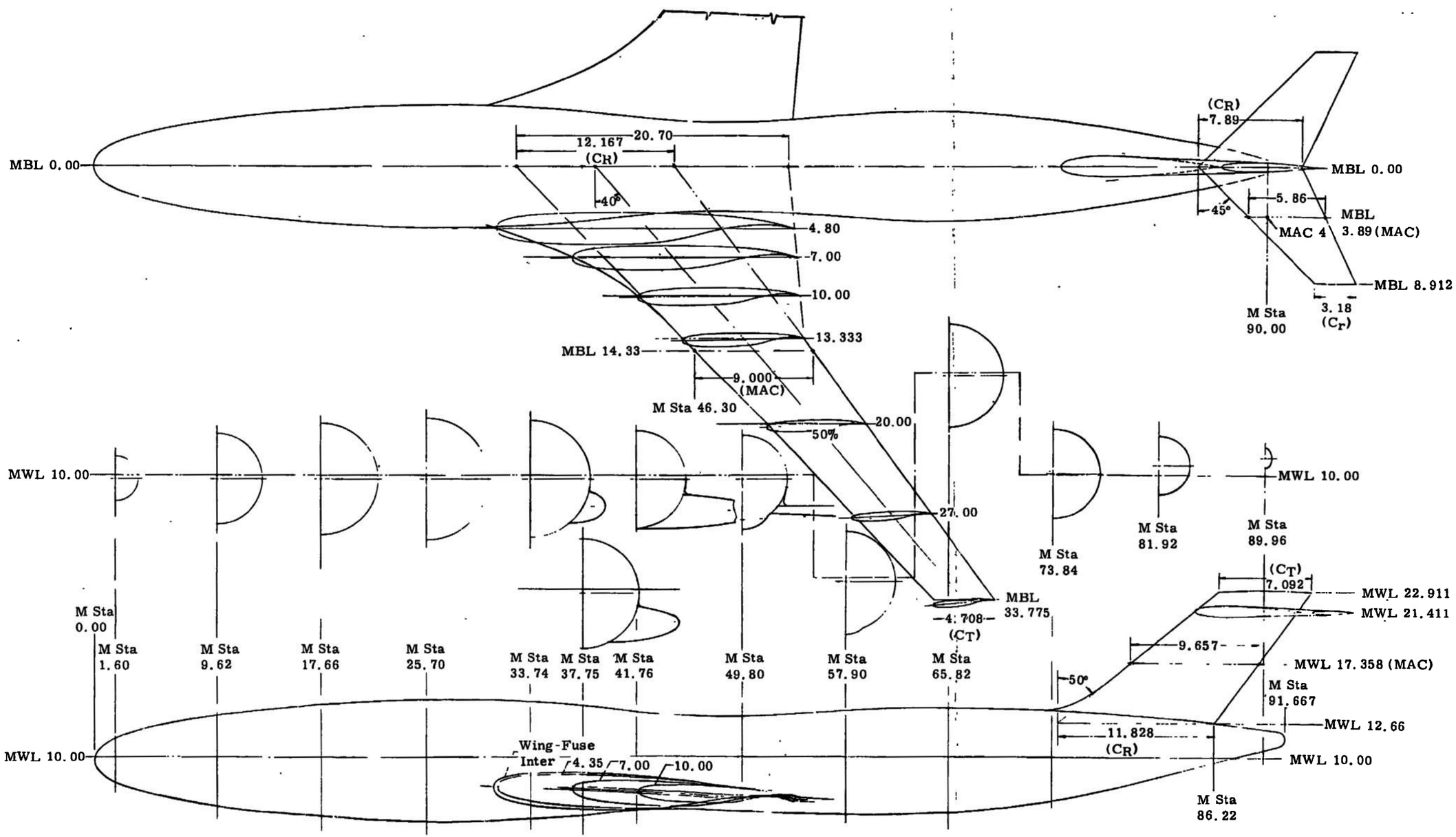

1/2 MODEL SCALE
Ref. FN 7197120

Figure 2. Basic Geometry – ATT

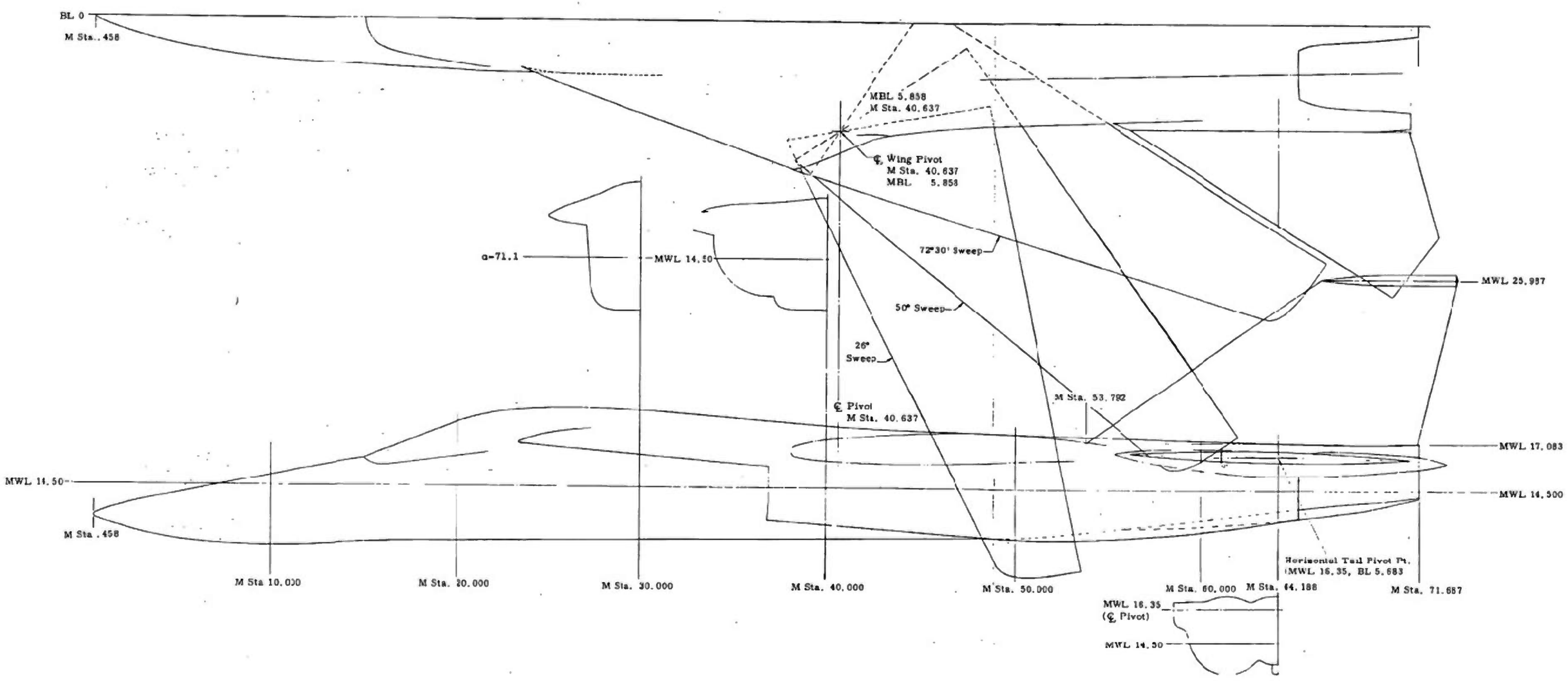

Figure 3. Basic Geometry – F-111

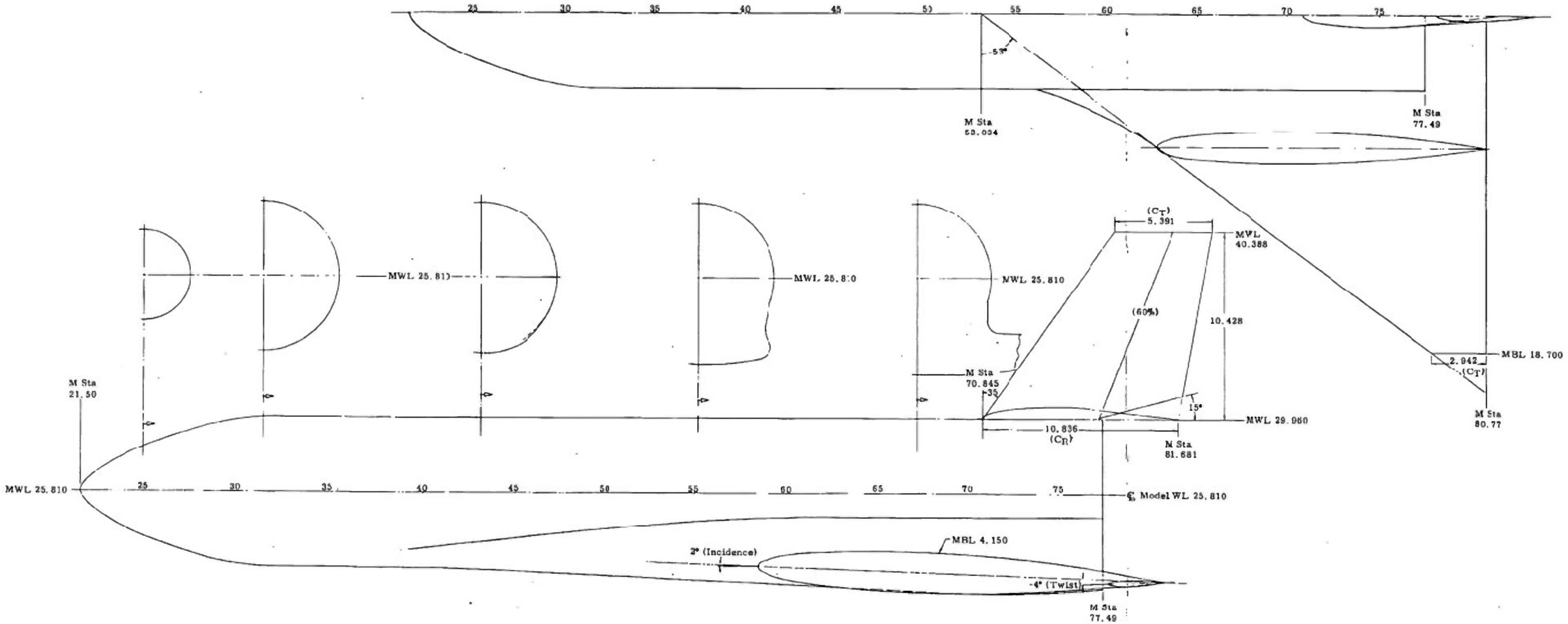

Figure 4. Basic Geometry – Space Shuttle Booster

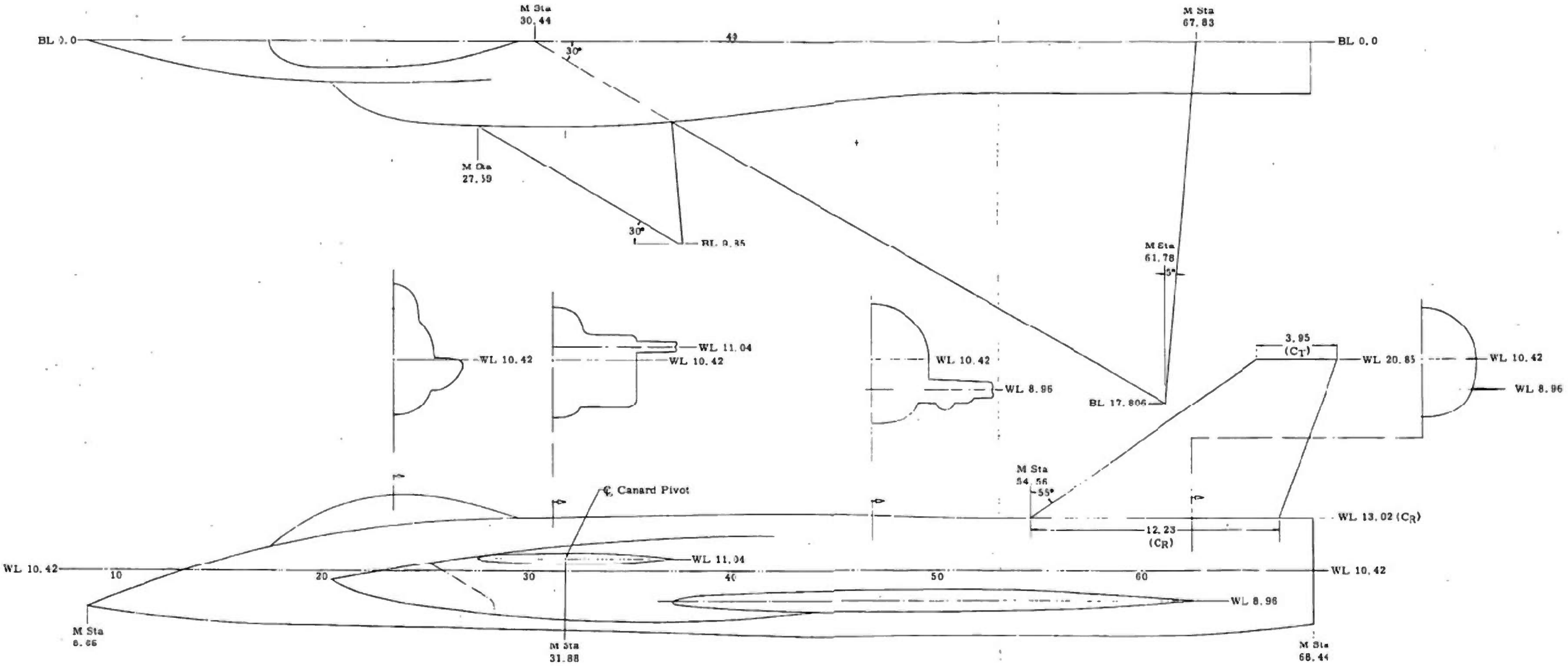

Figure 5. Basic Geometry – Delta Canard

SECTION V

DESIGN PARAMETERS

The study of the design and fabrication of wind tunnel models for use in the HIRT facility is multi-faceted with an infinite number of challenging problems. This report limits the areas of study to a number of parameters considered basic to the argument as to the usability of HIRT due to model/tunnel operating limitations.

5.1 MODEL TYPES

Each aircraft configuration is analyzed by considering at least three basic types of models per configuration:

a. Basic force model with a solid (no variable geometry capability) wing.

b. Solid wing model with provisions to vary flap or control surfaces.

c. Instrumented model with 100 to 400 pressure orifices in the wings.

5.2 MATERIALS

The same state-of-the-art material is used as a baseline material for the structural, aeroelastic, and cost analysis of each model type.

5.3 LOADS

All model loads are computed based on the actual or predicted aircraft operating envelopes for each configuration (Reference Figures 17 through 22). The points selected for analyses are discussed in the test plan (Section VII).

5.4 SURFACE FINISHES

Model surface finishes are analyzed with regard to the impact of special finishes on model costs. Three conditions were considered:

a. Complete model finished to a surface finish of 32 to 16 microinches.

b. First 30% of the airfoil and fuselage finished to 8 microinches with the remainder of the model finished to 16 microinches.

c. A 4 microinch finish for the first 30% of the airfoil and fuselage with the remainder of the model finished to 16 microinches.

The impact of model surface finishes on model cost is shown in Section XI, Table 13.

5.5 SCALE EFFECTS

The ATT model configuration was checked to determine the structural and aeroelastic effects of two larger model scales on the solid-wing model. Alternate model scales are:

a. 1.5 basic model size (1/16 scale).

b. 2.0 basic model size (1/12 scale).

The impact of model scale on model cost is shown in Section XI, Table 13.

SECTION VI

BASIC DESIGN PHILOSOPHY

Since detail design of any model for the HIRT facility will most certainly be greatly influenced by aircraft geometry and/or testing mission, this study does not dwell on some of the details that are most influenced by geometry. No attempt is made to perform detailed designs of these models. Model geometry drawings (Figures 2 through 5), basic force model assembly drawings (Figures 7 through 10), and typical pressure wing drawings (Figures 11 through 15) for each configuration illustrate possible model details and assemblies.

6.1 BALANCE AND SUPPORT SYSTEMS

The effects of the interference of the model support system on the flow over the model wing and fuselage are very real and difficult to analyze. Various techniques have been developed to account for these effects. Acceptable techniques depend on company and/or facility preferences or policies. No attempt has been made to explore this problem.

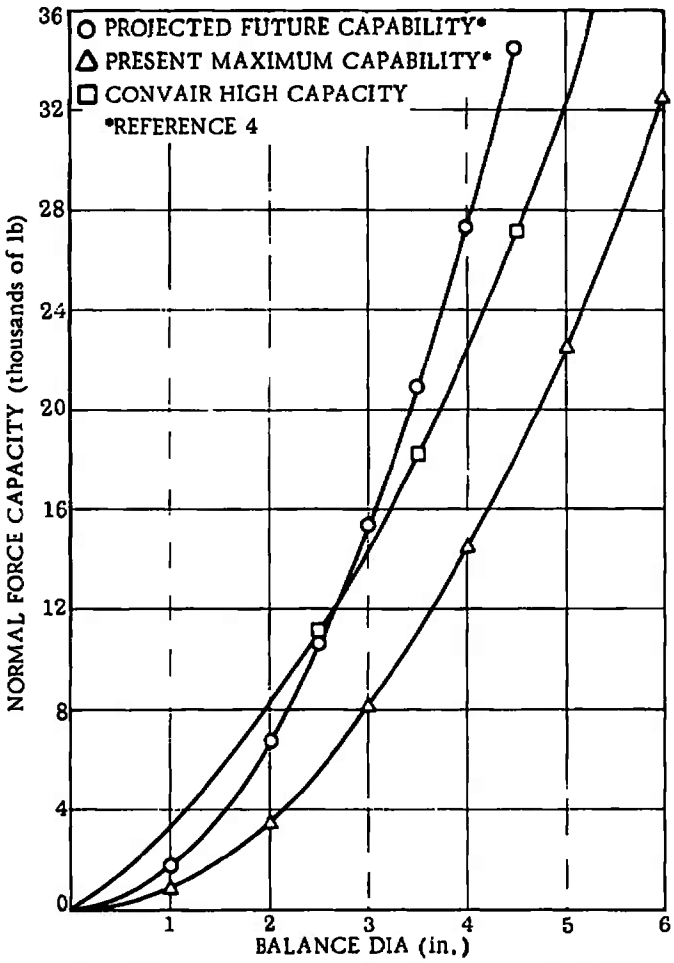

Figure 6. Balance Diameter vs Normal Force Capability

All models are supported by a sting/balance arrangement. Balances are sized to be consistent with the anticipated high capacity balances, with a balance load carrying capability (NF/diameter^2) of 1,700 psi. This load range appears to be consistent with current General Dynamics Convair Aerospace work and other studies (see Figure 6). No consideration is given to the problems of sting-to-balance attachment (it is recognized that a one-piece sting/balance combination might be required in some cases). It has been assumed that a conventional balance-to-model attachment (i.e., pins, etc.) will be required. Sting sizes are based on high-strength, maraging type steels. No attempt has been made to optimize sting shapes. All stings are assumed to have a circular cross section.

The aft portions of the fuselages on the F-111, ATT, and delta canard models have been revised to accept the model sting. The resulting shapes are noted in Figures 7, 8 and 9.

6.2 BASIC FORCE MODELS

6.2.1 Advanced Transonic Transport Model

Figure 7 presents a basic force model design for the ATT. A solid steel wing, split at the fuselage ℄ is used. Based on a maximum model load of 24,000 lb (Table 3), a 3.7-inch-diameter balance (Figure 6) is shown. Two sting sizes are shown to illustrate the relative size of stings required for a cruise versus a maximum maneuver loading condition. The horizontal tail is shown as a one-piece design mounted on a conventional vertical tail arrangement. Flow-through nacelles are mounted to the aft fuselage.

6.2.2 F-111 Aircraft

Figure 8 presents a basic force model design for the F-111. Individual wings are shown for each of the three wing sweeps considered, (26, 50, and 72-1/2 degrees). A maximum model load of 30,370 lb (Table 3) requires a 4.125-inch-diameter balance (Figure 6) for this configuration. A 65% chord alternate wing construction method is shown. This wing was analyzed to simulate a wing that was modified to allow flaps, ailerons, etc., to be carried by a portion of the total airfoil. Horizontal tails are attached with brackets to accommodate changes in tail incidence.

6.2.3 Delta Canard Fighter

Figure 9 is a basic force model of the delta canard fighter. A solid steel wing and an alternate wing with elevons are shown. The total model load, 22,000 lb at ambient tunnel conditions and 14,700 lb at 240°K (Table 3), are noted by the presentation of two balance and sting diameters. This design features a movable canard through the use of incidence blocks and cover plate fairings.

6.2.4 Space Shuttle Booster

Figure 10 is a basic force model of the space shuttle booster. The wing is shown as a one-piece wing using a keyway or tongue-and-groove attachment to the fuselage. A total model load, at ambient tunnel conditions, of 34,950 lb (Table 3) indicates that a 4.5-inch-diameter balance (Figure 6) is required. This model is the most straightforward design of all the configurations chosen.

ALTERNATE WING CONSTRUCTION
Typical Section for Wing with Removable Section for Control Surface Deflections

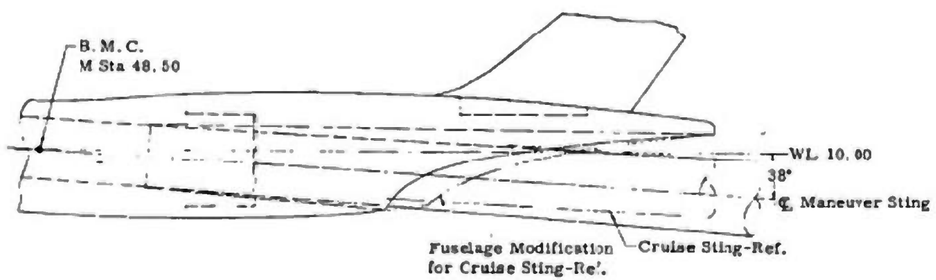

ALTERNATE FUSELAGE CONFIGURATION FOR MANEUVER STING

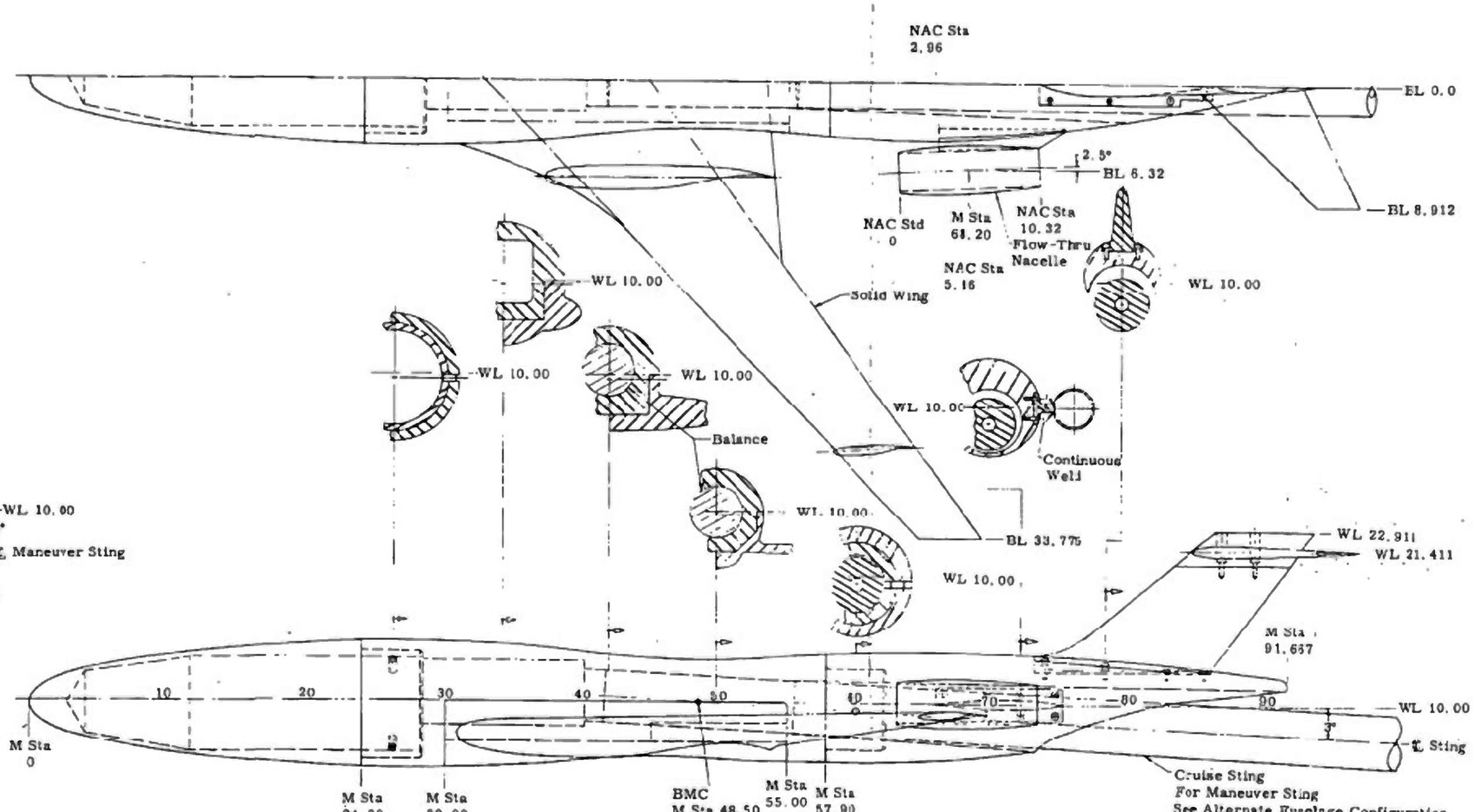

1/2 MODEL SCALE

Figure 7. ATT Basic Force Model

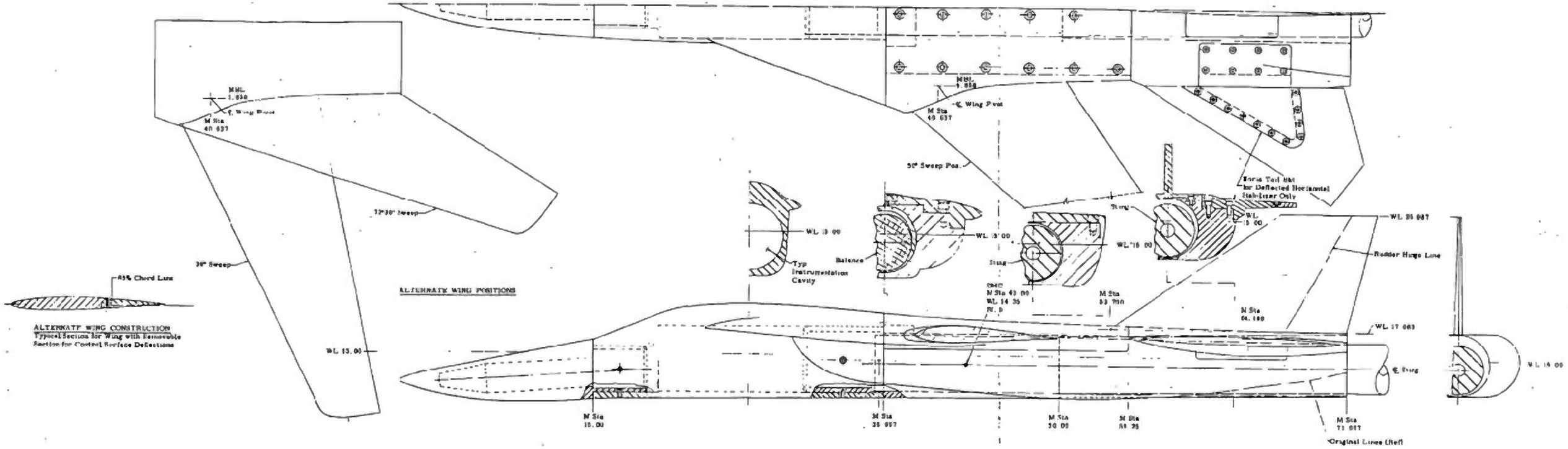

Figure 8. F-111 Basic Force Model

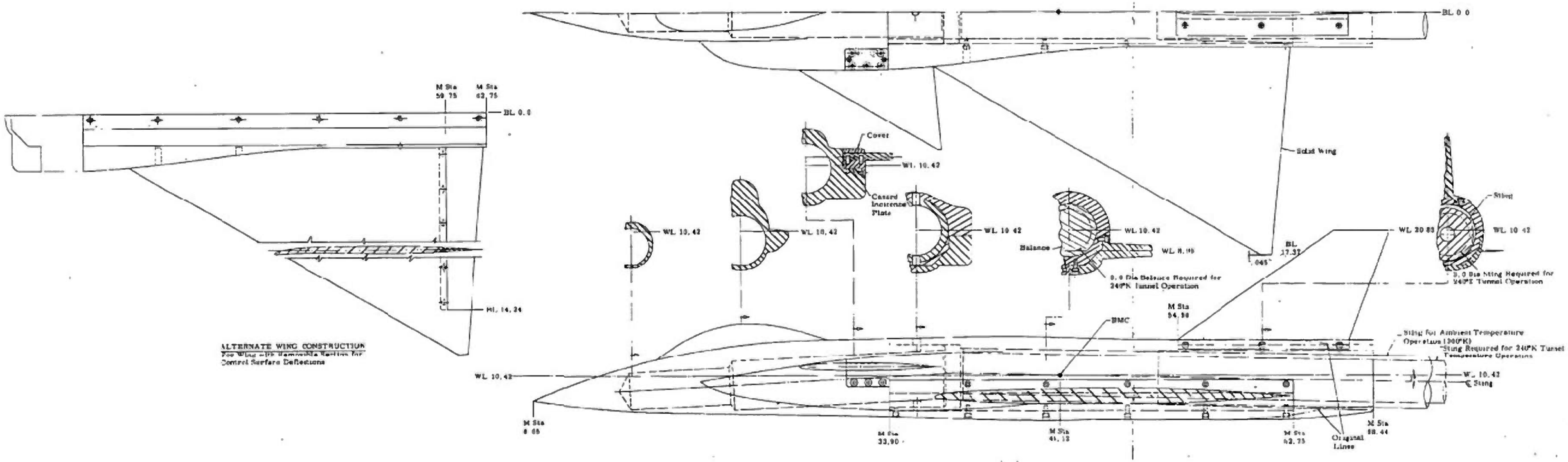

Figure 9. Delta Canard Fighter Basic Force Model

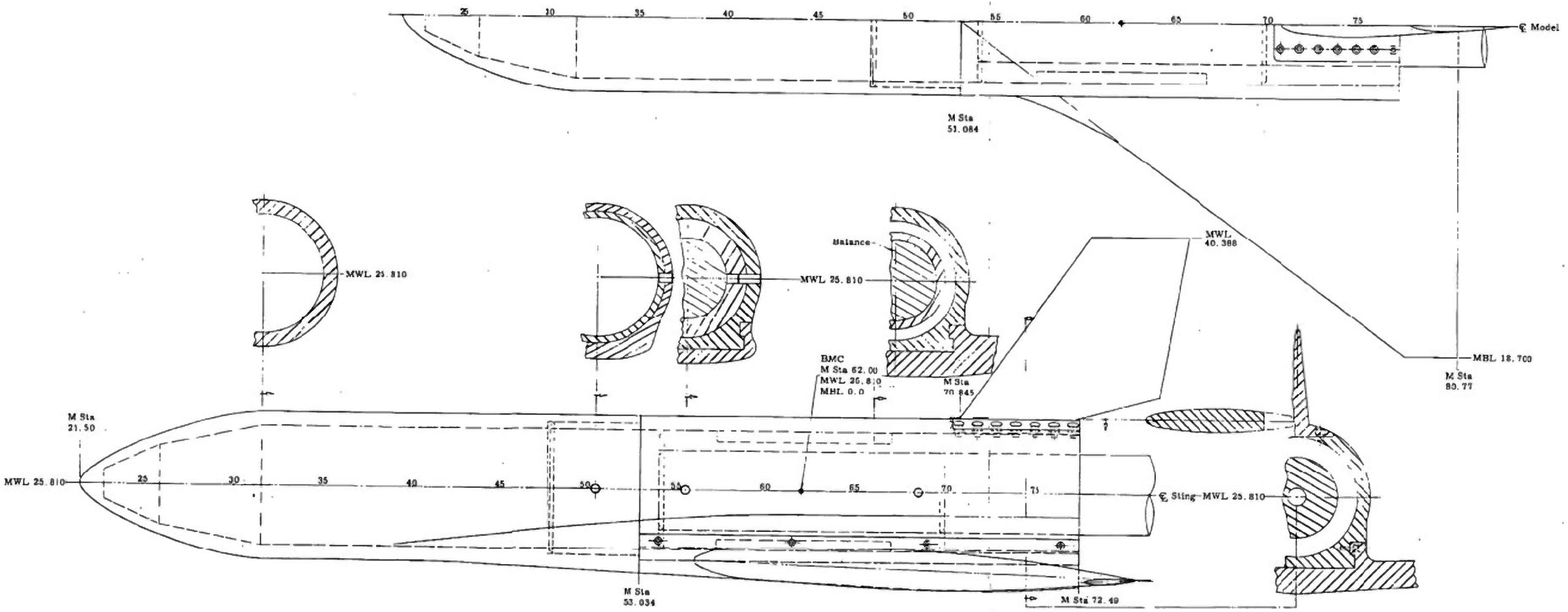

Figure 10. Space Shuttle Booster Basic Force Model

6.3 PRESSURE MODELS

Pressure models for use in the HIRT facility do not present any unique design problems. Conventional state-of-the-art methods of designing and fabricating pressure models are adequate. A requirement for superfine surface finishes appears to be a moot point when compared to the effect of several rows of pressure orifices.

The size of models used in the HIRT facility should provide adequate room for storage of transducer packages in nose/fuselage cavities. Errors in pressure measurements due to the tubing and transducer volume lag can be made small (0.5 percent) by selecting proper tube length-to-diameter ratio (Ref. 5). Pressure tubing with 0.049-inch outside diameter (0.025 I.D.) was selected for this study. Larger tubing is not compatible with HIRT scale-model airfoil sections.

Two methods of designing pressure wings for the ATT model are shown in Figures 11 and 12.

a. Method I, Figure 11, features gun-drilled spanwise tube routing holes with locally machined tube routing slots on the outside surface for each pressure orifice. The tube routing slots are filled with a material such as soft solder and finished to wing contour.

b. Method II, Figure 12, features a removable trailing-edge portion, which facilitates pressure-tube routing. Slots (located near the neutral axis) are eloxed at each row of pressure orifices to allow room for pressure tube installation and routing.

Method II is preferred from both a structural and a manufacturing standpoint. Pressure-tube installation and routing are easier to accomplish, and this method is not nearly as configuration-limited as the gun-drilled hole method. Method II was used for the design of pressure-instrumented wings for the F-111, delta canard, and space shuttle booster. Figure 13 is a pressure installation on the 50-deg sweep F-111 wing. Figures 14 and 15 show the pressure-tube installation for the two delta-wing models (delta canard fighter and space shuttle booster).

Results of the structural analysis of each method are presented in Section IX. It should be noted that all upper surface pressure orifices have been located on the left-hand wing panel and all lower surface pressure orifices on the right-hand panel. This procedure was followed to minimize the decline in allowable wing loading due to the installation of pressure tubes. The small size of wing airfoil sections for HIRT scale models is not compatible with the removal of material from the upper and lower surfaces at the same span station: approximately four hundred orifices (two hundred per side) are considered in this study.

Installation of fuselage orifices is basically straightforward.

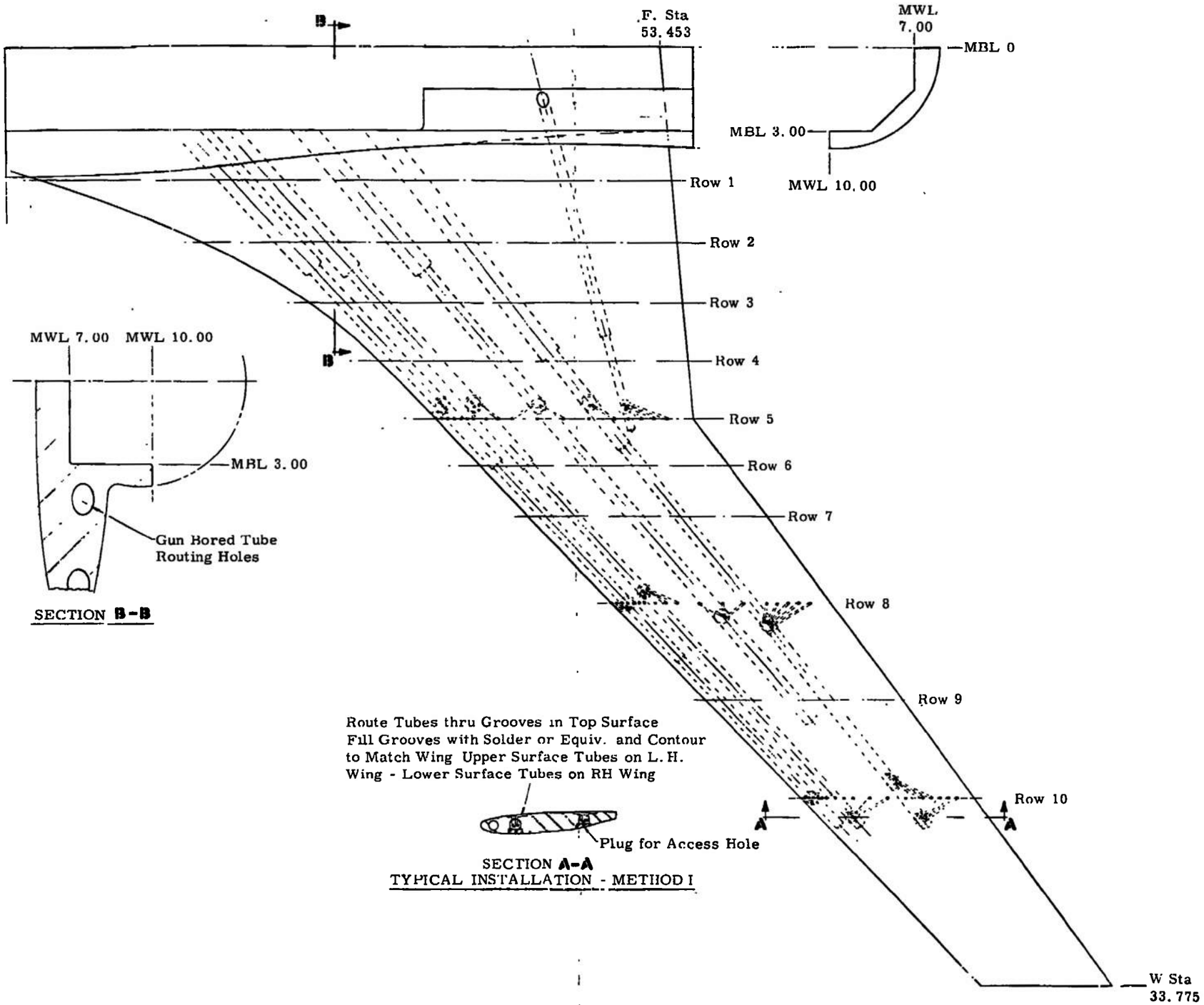

Figure 11. ATT Pressure Wing, Method I

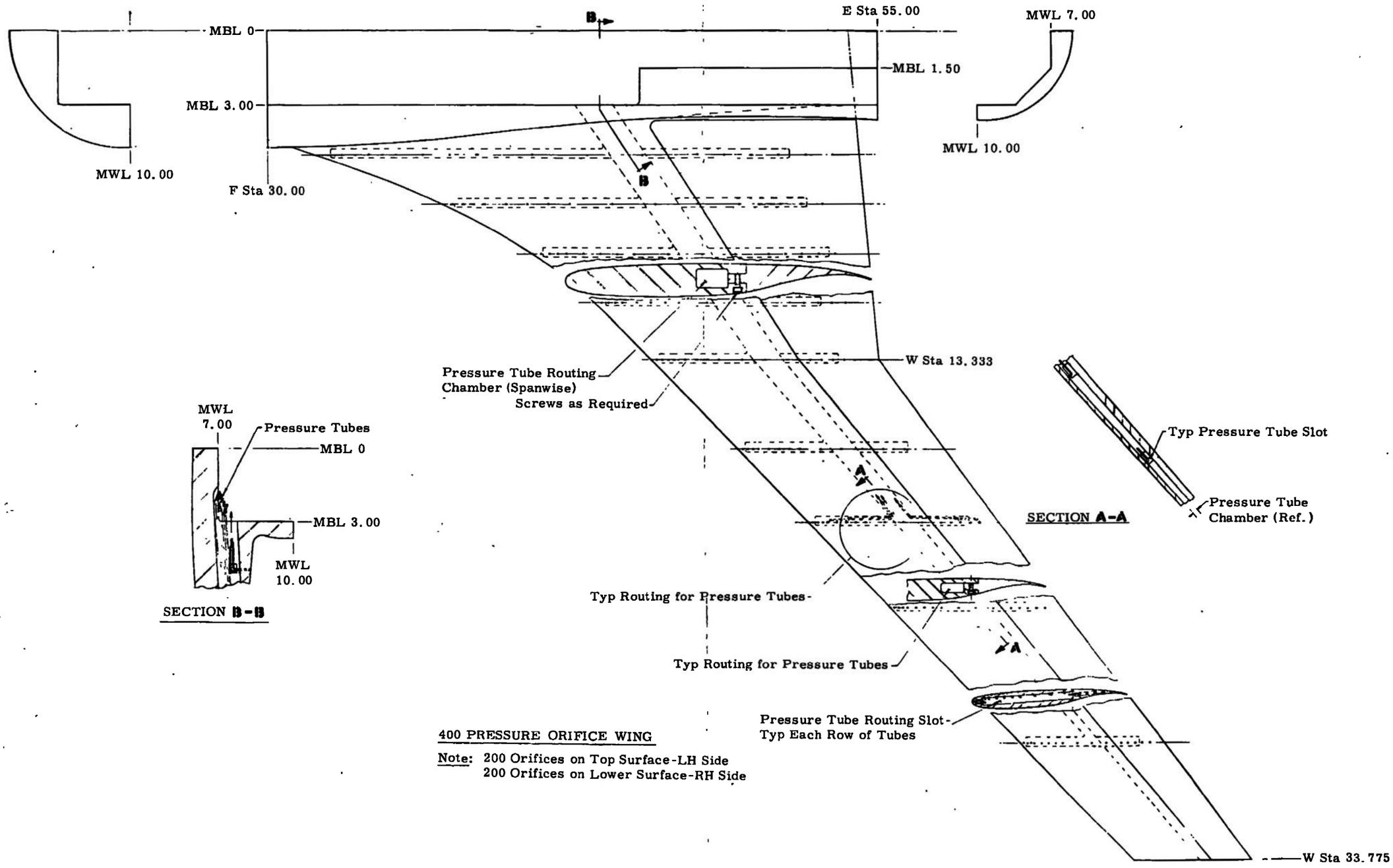

400 PRESSURE ORIFICE WING

Note: 200 Orifices on Top Surface-LH Side
200 Orifices on Lower Surface-RH Side

Figure 12. ATT Pressure Wing, Method II

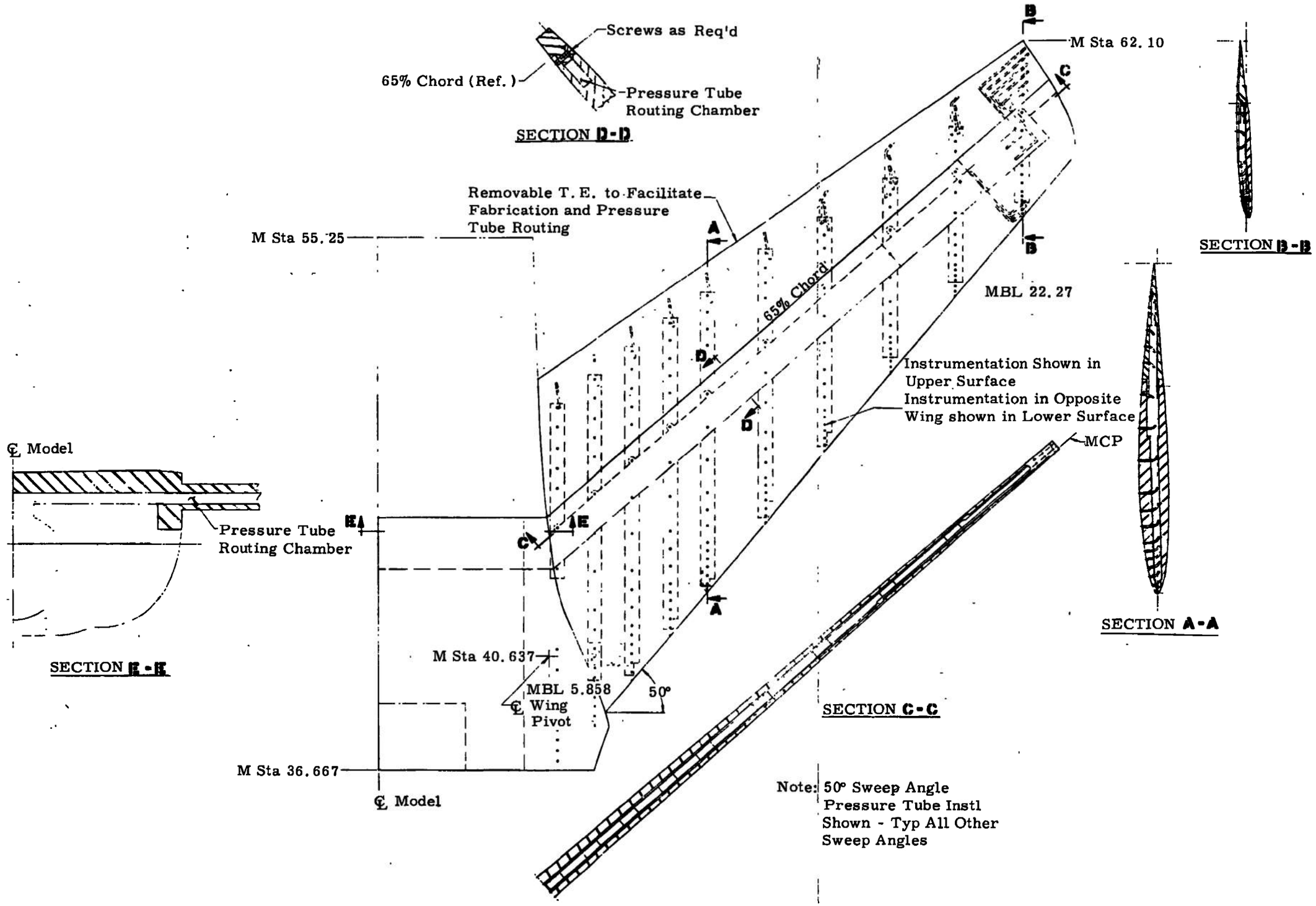

Figure 13. F-111 Pressure-Instrumented Wing

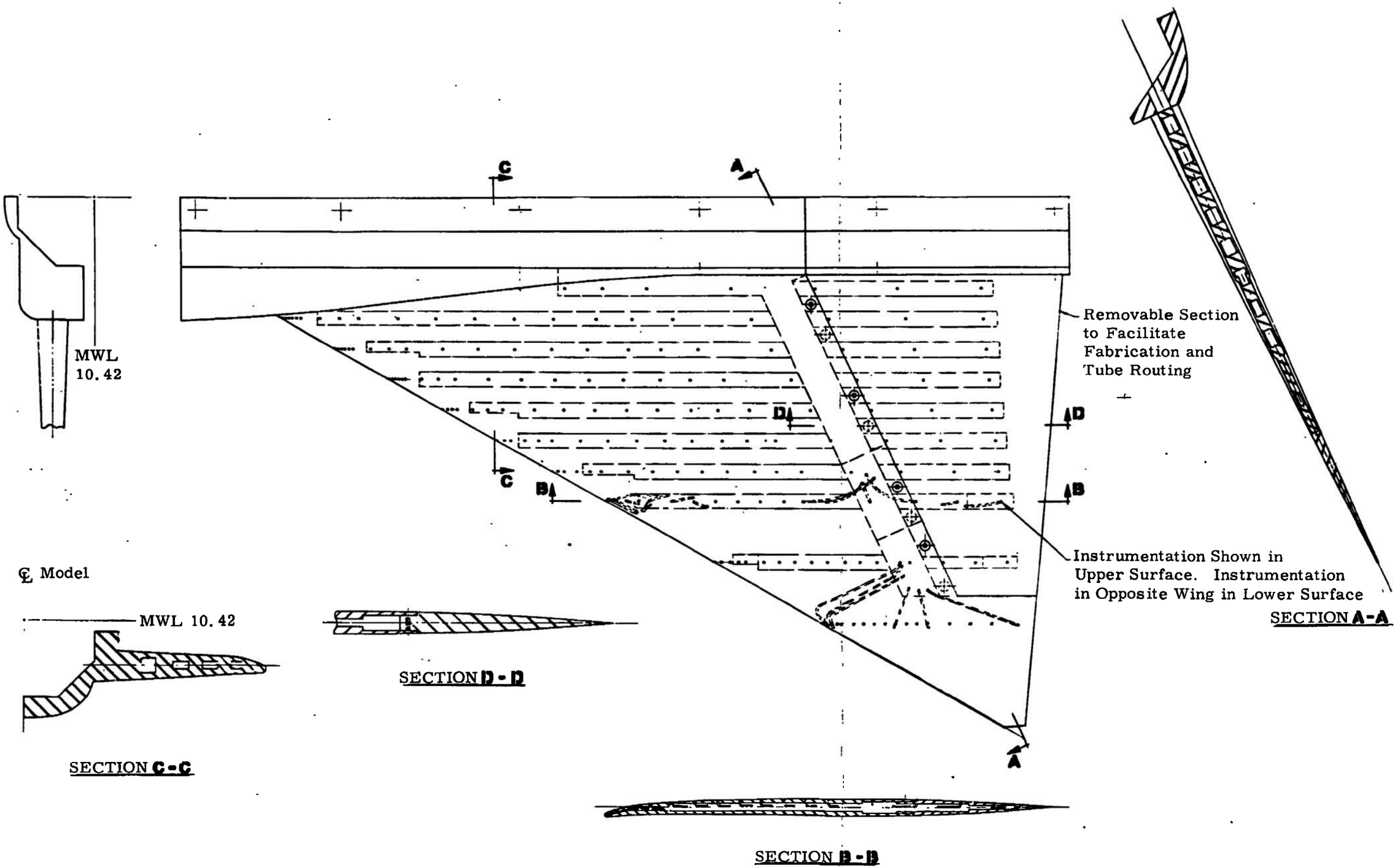

Figure 14. Delta Canard Fighter Pressure Wing

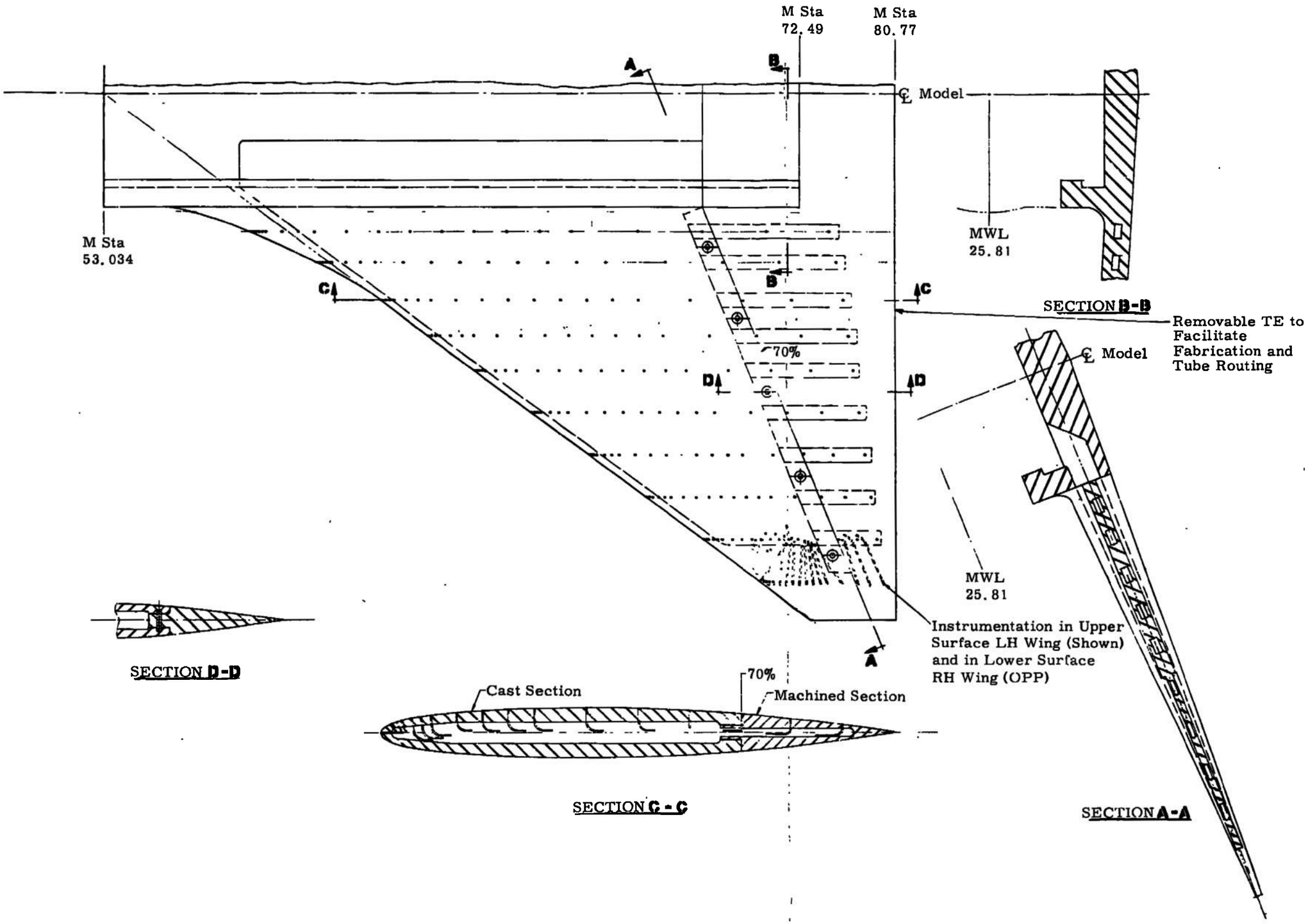

Figure 15. Space Shuttle Booster Pressure Wing

6.4 BASELINE MATERIAL SELECTION

Model cost and structural analyses were performed using one basic material for all model fabrication and another basic material for the stings. The present state-of-the-art materials selected for each task are:

a. Model details – PH 13-8 Mo steel; HT – H1000.

b. Stings – PH 13-8 Mo steel or 18Ni-300 grade (or -350 grade) maraging steel.

An analysis of candidate materials for use in the HIRT facility is presented in Section X.

6.5 SURFACE FINISH

The HIRT facility will produce very thin model boundary layers. As a consequence, surface roughness should be scaled down accordingly so that it does not contribute appreciably to drag or the momentum thickness of the boundary layer. The latter would influence the configuration characteristics associated with the shock boundary layer interaction.

For study purposes, Schlichting's admissible roughness criterion was used (Reference 6). Table 1 shows the admissible wing roughness for the study configurations. These values of roughness would pertain to a flat plate at zero incidence and should be a reasonable indication of leading edge requirements. Since the laminar sublayer will become larger with increasing distance from the leading edge, the admissible roughness will be increased.

The impact of the required surface finish qualities on the models is shown in Section XI, Table 9.

6.6 MISCELLANEOUS OBSERVATIONS

Special emphasis should be placed on some basic design rules when designing a model for a high Reynolds number test.

a. Careful attention should be given to the design of wing/fuselage attachment joints. Streamwise parting lines (located in the least critical flow area possible) should be used. It should be noted that the deflection between two parts in a joint under load is much more critical due to the added emphasis on surface finishes.

b. Basic split lines and attachments will greatly influence the ultimate surface finish achieved on the model. Tradeoff studies will be needed to obtain the maximum versatility/structural integrity/surface finish required for each test situation.

c. Each model must be analyzed to determine whether it is best to seal the internal model cavities or to provide passages for venting air from within the model to the tunnel during the start of a run. For example, calculations based on test condition 8, Table 2, (ATT model at M = 0.5, sea level, T = 300°K, storage pressure = 500 psia, Re/ft = 85.33 × 10^6) indicate that approximately 0.06 second would be required to equalize the pressure of the volume of air (approximately 1,100 in.^{3}) of the nose cavity forward of the model balance through a 1.0-in.^{2} venting duct.

Table 1. Admissible Roughness Estimates (Surface Finish)

Condition	Advanced transonic transport			F-111	Delta Canard	Space shuttle Booster
	Basic model 1/24 scale	1.5 × size 1/16 scale	2.0 × size 1/12 scale	1/12 scale	1/9.6 scale	1/46.5 scale
MAC (ft)	0.750	1.125	1.500	0.753	1.800	1.558
$R_{e_{MAC}} \times 10^6$						
Cruise	57.33	38.30	28.75	60.45	16.50	107.23
Maneuver	85.33	41.75	31.35	59.30	35.44	89.04
Maneuver	62.72			45.05	28.90	43.44
$K_{admissible}$ (in.)						
Cruise	0.000020	0.000031	0.000042	0.000019	0.000072	0.000011
Maneuver	0.000014	0.000023	0.000038	0.000020	0.000034	0.000013
Maneuver	0.000019			0.000026	0.000042	0.000028

$$K_{ADM} = MAC \frac{100}{R_{e_{MAC}}} \text{ (Reference 6)}$$

$$\left.\begin{array}{l} 16\sqrt{} = 16 \text{ microinches } (0.000016) \\ 8\sqrt{} = 8 \text{ microinches } (0.000008) \\ 4\sqrt{} = 4 \text{ microinches } (0.000004) \end{array}\right\} \text{ (Reference 24)}$$

SECTION VII

TEST PLAN

7.1 TUNNEL USE

It is anticipated that a great demand for test time in the HIRT facility will result in a situation where testing will necessarily be restricted to tests that are very Reynolds-number dependent (as is the case with the Canadian N. A. E. high Reynolds number 15 in. x 60 in. two-dimensional facility). Hence, use of the HIRT facility will be somewhat unlike that of current transonic wind tunnels in that test plans will probably be much more operating envelope oriented or will concentrate on one particular test problem. It is current practice to test a configuration without particular regard to its flight envelope so that data is obtained beyond the limits that the flight article can achieve. Such practice cannot be justified for HIRT testing because of the impact of high model loads and model deformation. HIRT testing will best be carried out by testing in critical areas of the operation envelope to obtain the configuration performance (typically design point cruise and maneuvering parameters.)

7.2 OPERATING ENVELOPES

For the purpose of this study, the points of interest in an operation envelope are the maximum loading conditions, for if the model can be designed to take the full-scale R_e at these conditions, it is feasible to test at full-scale R_e throughout the envelope. Reynolds number ranges for the aircraft covered in this test plan are illustrated in Figure 16.

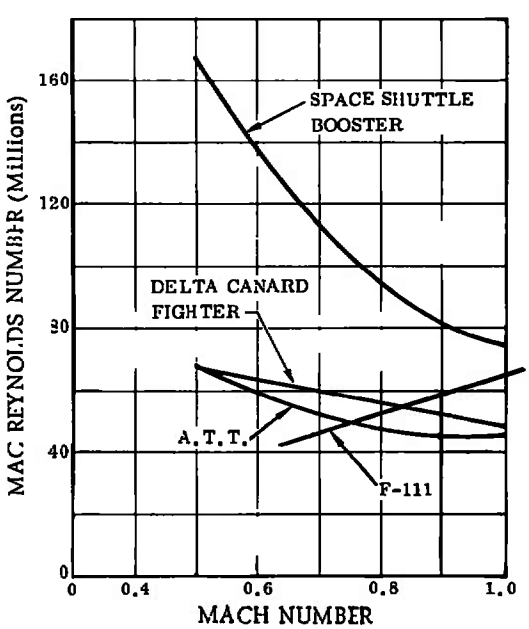

Figure 16. Reynolds Number Ranges of Aircraft Chosen for Study

Flight article operational envelopes for the four study configurations are shown in Figures 17 through 22. Two plots are presented for each configuration. The (a) plot shows $Re_{MAC}\ C_L$ as a function of Mach number and altitude up to the structural limit load factor. The critical high loading corners are readily apparent. The (b) plots show the HIRT tunnel dynamic pressures for the equivalent envelope.

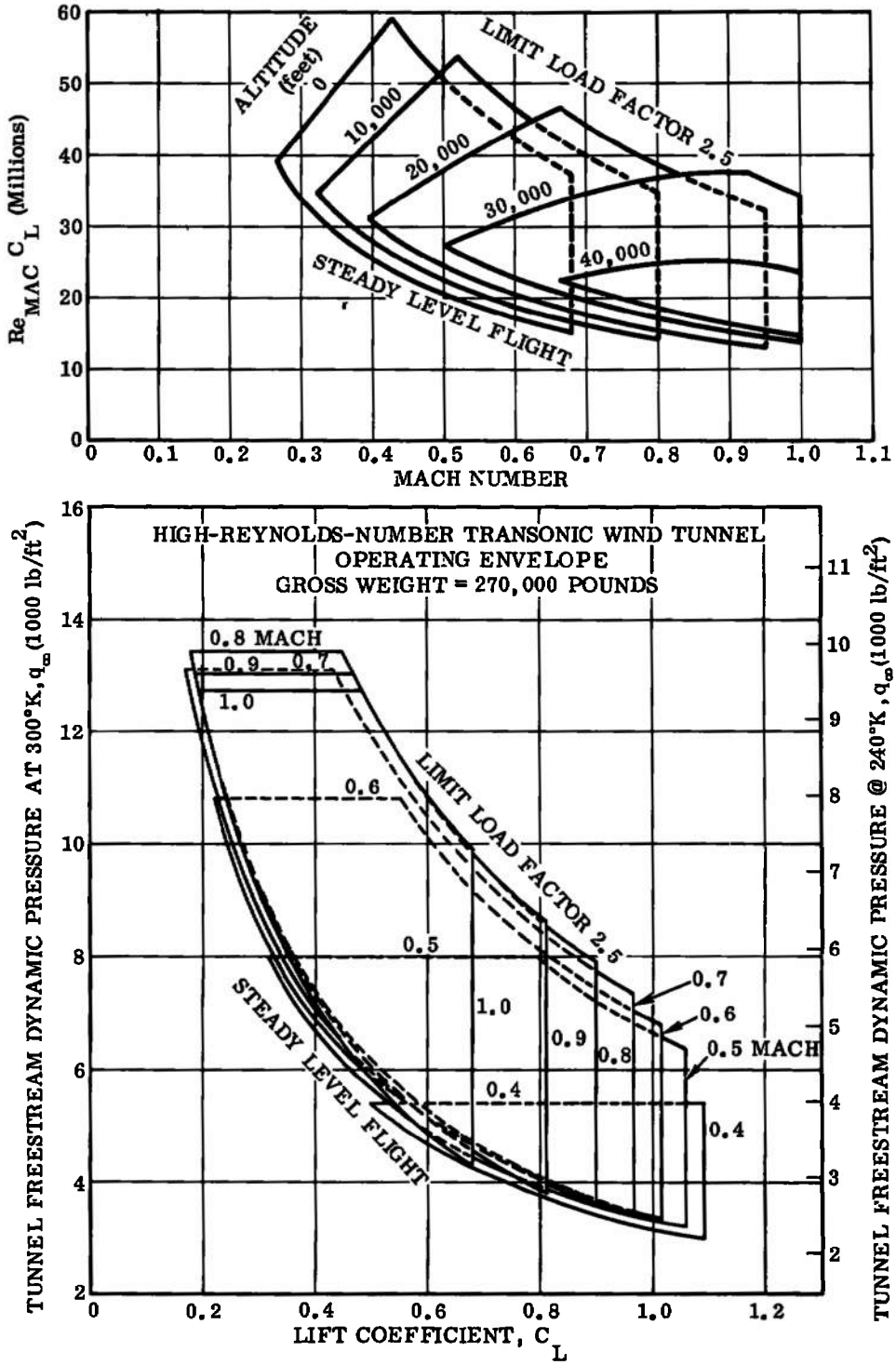

Figure 17. ATT Operating Envelope

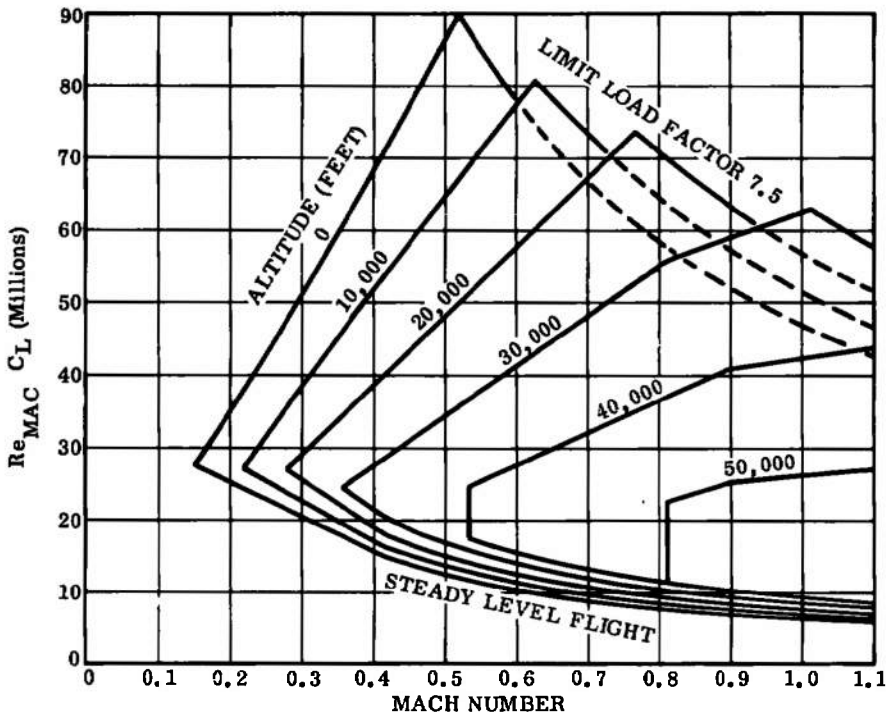

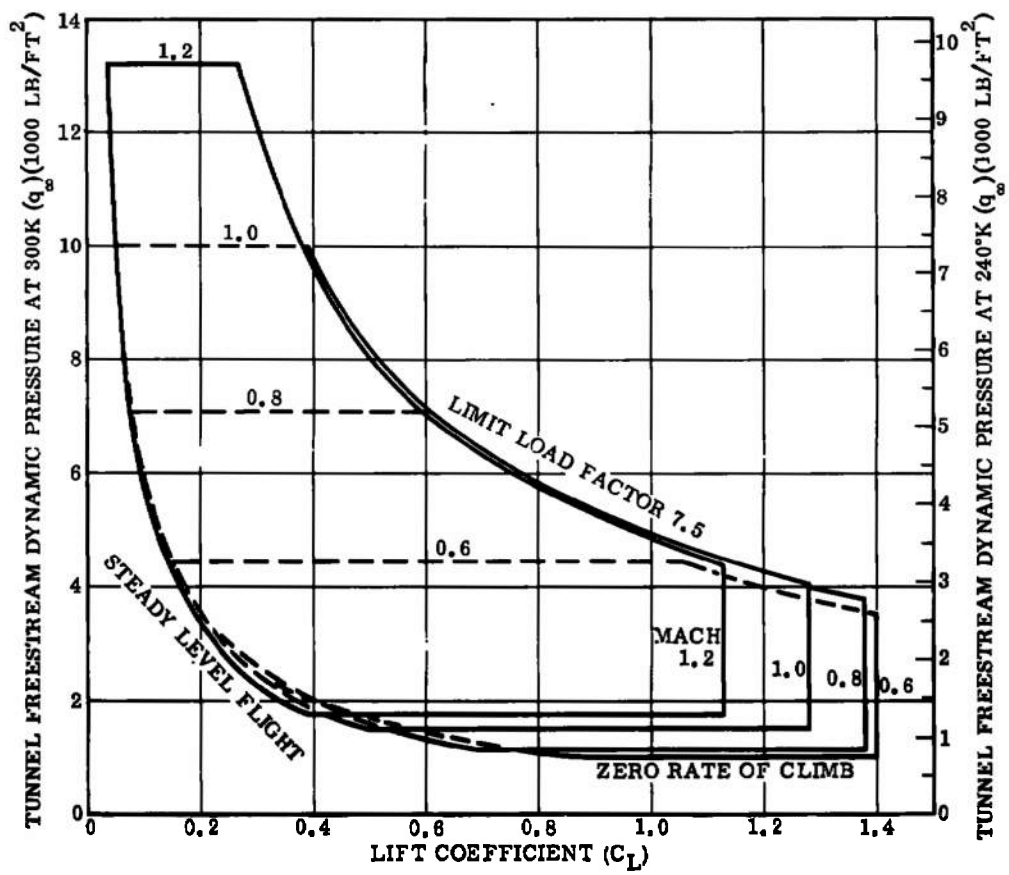

Figure 18. Delta Canard Operating Envelope

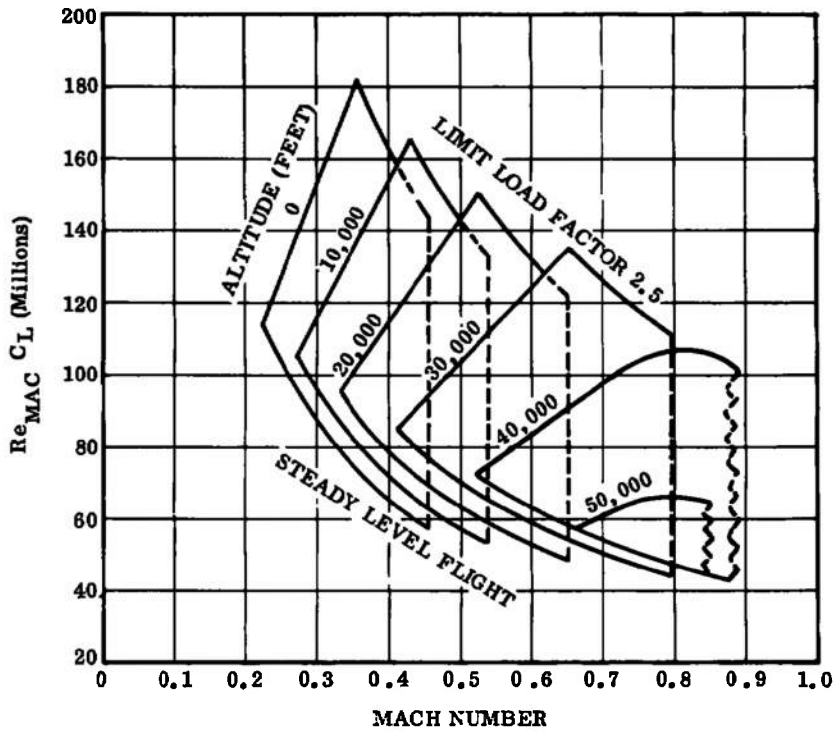

HIGH REYNOLDS NUMBER TRANSONIC WIND TUNNEL OPERATING ENVELOPE

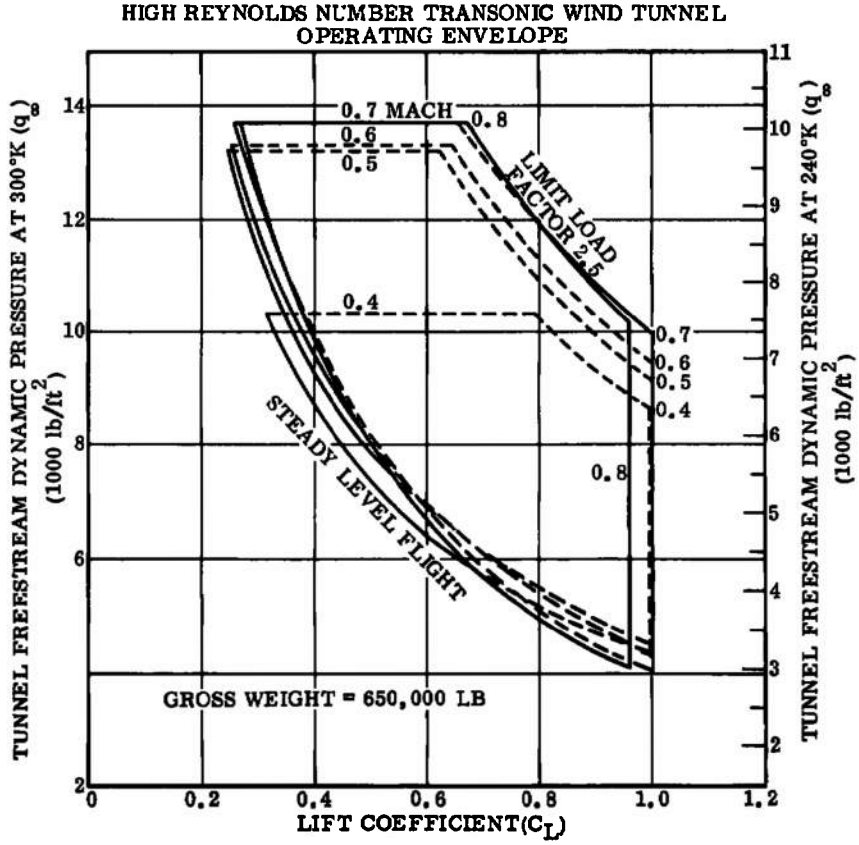

Figure 19. Space Shuttle Booster Operating Envelope

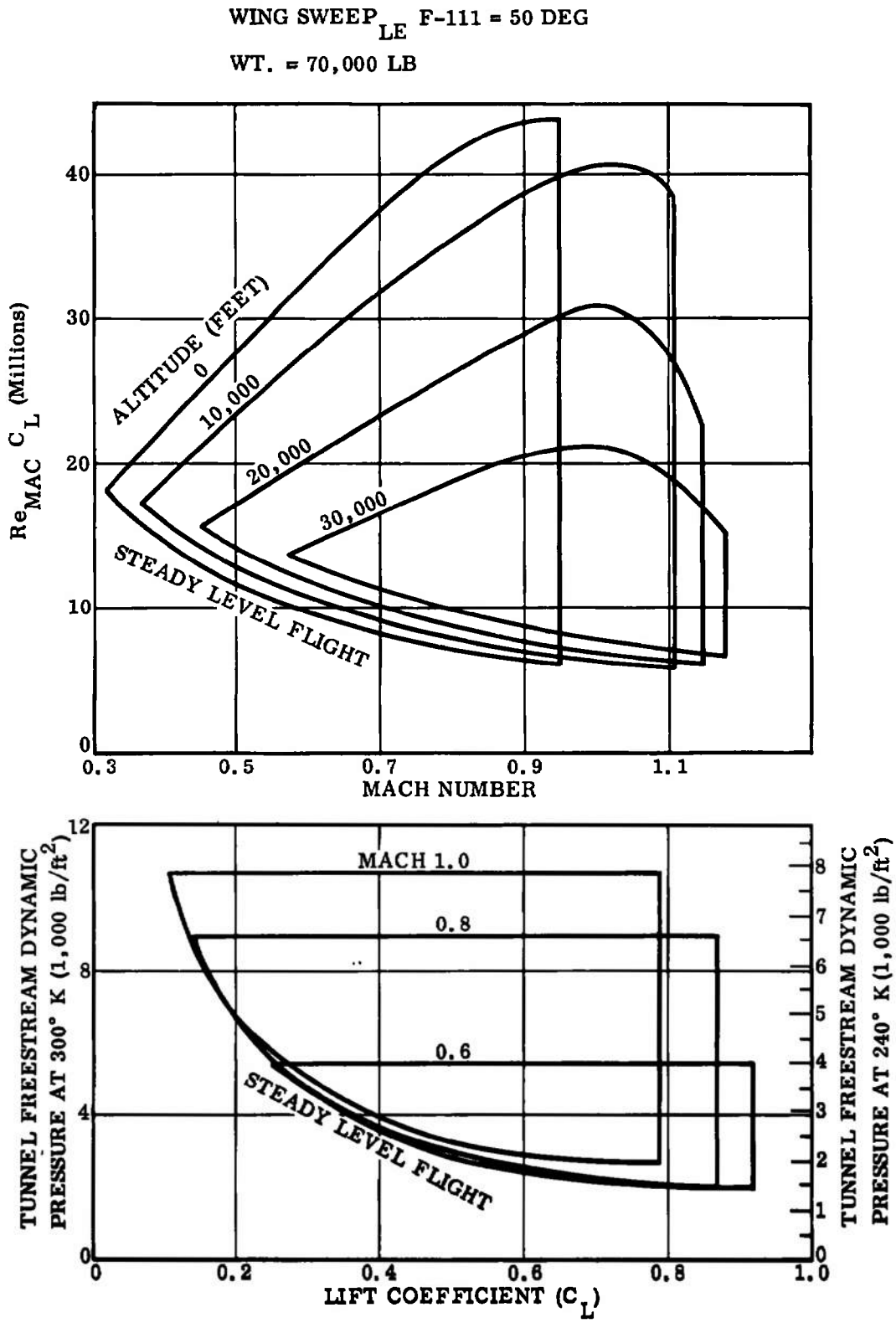

Figure 20. F-111 (50 deg) Operating Envelope

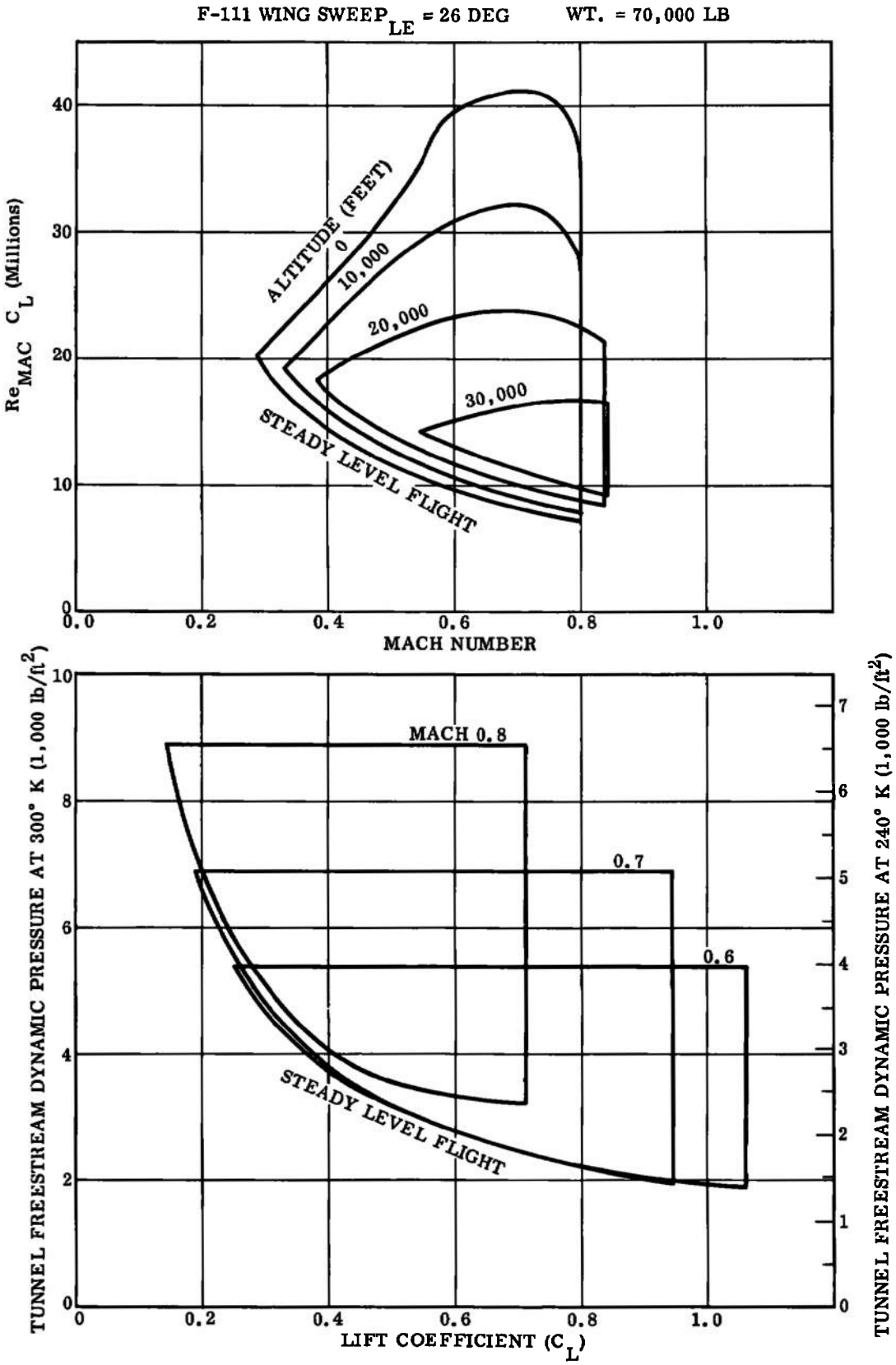

Figure 21. F-111 (26 deg) Operating Envelope

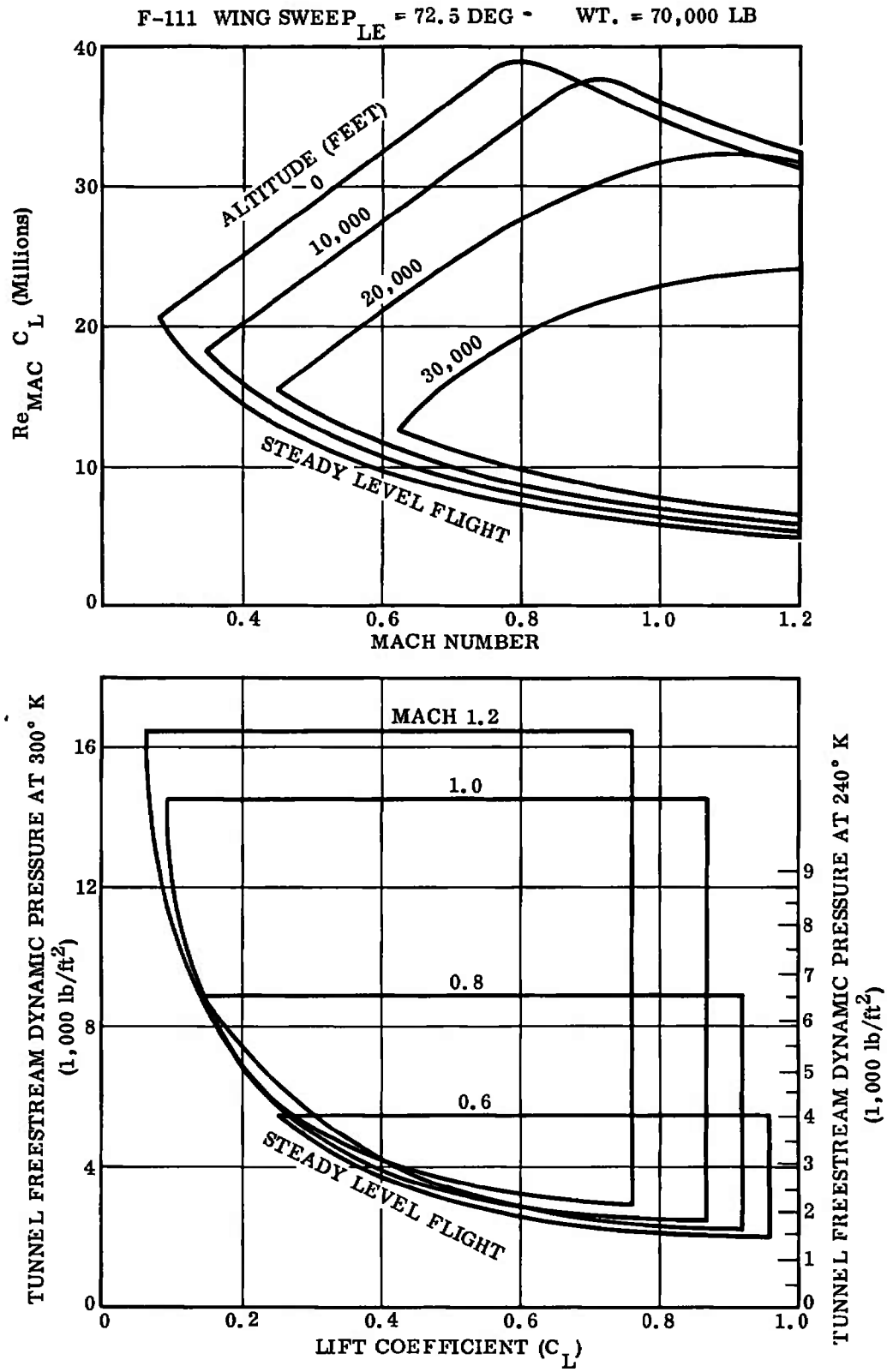

Figure 22. F-111 (72-1/2 deg) Operating Envelope

The conditions selected for detailed study are:

a. The maximum loaded condition the airplane could experience within its operating envelope.

b. A typical cruise condition.

c. Item a. (maximum loaded condition) with a reduced angle of attack or Reynolds number.

Note that Item c. is used if required for an acceptable stress level for a given model.

7.3 TEST PLAN DEVELOPMENT

Table 2, Test Plan, presents a summary of all the model test conditions selected for analysis in this study. Each of the test conditions was analyzed to determine:

a. Wing shear loads.

b. Wing pitching torques.

c. Wing bending moments.

d. Wing loading.

e. Wing distortions (vertical deflection and wing twist).

f. Wing section properties (EI, GJ).

g. Total model vertical force.

h. Model angle of attack.

i. Horizontal tail loads.

The results of each test condition were analyzed and the most pertinent information used to compute model stresses and distortions as presented in Sections VIII and IX.

7.4 DATA STORAGE

Complete computer printouts from program P4278 for each of the test conditions are on file at General Dynamics Convair Aerospace. A typical computer run (test condition 7 – 1/24 scale ATT at Mach 1.0, 2.5g maneuver, 30,000 feet, R_e/ft = 69.5×10^6, tunnel temperature = 240°K) is presented in Appendix I of this report.

Table 2. Test Plan

Model	Condition no.	Load factor (g)	Mach no.	Altitude (10^3 ft)	Tunnel temperature (degrees Kelvin)	Tunnel dynamic pressure (psi)	Tunnel storage pressure (psi)	Tunnel Model Re/ft (millions)	Model angle of attack (degrees)	Wing structural cross section (%)	Computer code	Run description
ATT (1/24 scale)	1	2.5	0.5	S. L.	240	40.84	360	85.33	9.79	100	A24-9	Maneuver
	2	2.5	0.5	S. L.	240	40.84	380	85.33	9.79	65	A24-13	Maneuver
	3	1.0	1.0	35	240	43.75	190	57.53	3.55	100	A24-1	Cruise
	4	1.0	1.0	35	240	43.75	190	57.63	3.55	65	A24-11	Cruise
	5	1.0	1.0	30	240	52.76	225	69.5	3.23	100	A24-3	Cruise
	6	1.75	1.0	30	240	52.76	225	69.5	5.59	100	A24-5	Intermediate
	7	2.5	1.0	30	240	52.78	225	69.5	7.95	100	A24-7	Maneuver
	8	2.5	0.5	S. L.	300	55.55	500	85.33	9.79	100	A23-5	Maneuver
	9	1.0	1.0	35	300	57.64	250	57.53	3.55	100	A23-1	Cruise
	10	1.0	1.0	30	300	69.60	300	69.5	3.23	100	A23-2	Cruise
	11	1.75	1.0	30	300	69.60	300	69.5	5.59	100	A23-3	Intermediate
	12	2.5	1.0	30	300	69.60	300	69.5	7.95	100	A23-4	Maneuver
F-111 (1/12 scale)												
50°	13	6.0	0.9	S. L.	300	73.60	340	76.56	22.47	100	F11-3	Maneuver
50°	14	6.0	0.9	S. L.	240	54.12	255	76.55	22.47	100	F13-4A	Maneuver
50°	15	6.0	0.9	S. L.	240	54.12	255	76.55	22.47	65	F13-5A	Maneuver
50°	16	1.0	1.0	40	300	23.26	100	22.96	12.64	100	F11-9	Cruise
50°	17	1.0	1.0	40	240	17.10	60	22.96	12.64	100	F13-10A	Cruise
50°	18	1.0	1.0	40	240	17.10	60	22.98	12.64	65	F13-11A	Cruise
26°	19	5.2	0.75	S. L.	300	54.17	310	63.90	13.13	100	F11-1	Maneuver
26°	20	5.2	0.75	S. L.	240	39.83	235	63.90	13.13	100	F13-2A	Maneuver
72 1/2°	21	6.0	1.0	S. L.	300	64.72	370	85.1	25.16	100	F11-7	Maneuver
72 1/2°	22	6.0	1.0	S. L.	240	62.29	270	85.1	25.16	100	F13-8A	Maneuver
Delta canard fighter (1/9.6 scale)	23	7.5	0.52	S. L.	300	22.92	240	35.44	31.03	100	C01-1	Maneuver
	24	7.5	0.52	S. L.	240	16.85	210	35.44	31.03	100	C02-2A	Maneuver
	25	7.5	0.52	S. L.	240	16.65	210	35.44	31.03	65	C02-3A	Maneuver
	26	1.0	0.90	40	300	15.97	65	16.52	6.62	100	C01-5	Cruise
	27	1.0	0.90	40	240	11.74	30	16.52	6.62	100	C02-6A	Cruise
	28	1.0	0.90	40	240	11.74	30	16.52	6.62	65	C02-7A	Cruise
Space shuttle booster (1/46.5 scale)	29	2.5	0.6	30	300	95.14	490	106.097	16.74	100	S08-12	Maneuver
	30	2.5	0.6	30	240	70.83	360	106.097	16.74	100	S09-14	Maneuver
	31	2.5	0.8	30	240	70.83	360	106.097	16.74	70	S09-16	Maneuver
	32	2.5	0.3	S. L.	300	46.61	—	99.04	38.21	100	S07-10A	Landing
	33	2.5	0.3	S. L.	240	35.74	—	99.04	36.21	100	S07-5A	Landing
	34	2.5	0.3	S. L.	240	35.74	—	99.04	36.21	70	S07-6A	Landing
	36	2.5	0.3	S. L.	300	46.61	—	99.04	38.21	70	S07-11A	Landing
	36	2.5	0.6	30	300	95.14	490	106.097	16.74	70	S09-15	Maneuver
ATT 1/16 scale	37	1.0	1.0	30	240	35.4	225	69.5	3.23	100	A27-21	Cruise
1/16 scale	38	2.5	1.0	30	240	35.4	225	69.5	7.95	100	A27-22	Maneuver
1/12 scale	39	1.0	1.0	30	240	26.5	225	69.5	3.23	100	A27-25	Cruise
1/12 scale	40	2.5	1.0	30	240	26.5	225	69.5	7.95	100	A27-26	Maneuver
1/16 scale	41	1.0	1.0	30	300	47.2	300	69.5	3.23	100	A27-19	Cruise
1/16 scale	42	2.5	1.0	30	300	47.2	300	69.5	7.95	100	A26-20	Maneuver
1/12 scale	43	1.0	1.0	30	300	35.4	300	69.5	3.23	100	A27-23	Cruise
1/12 scale	44	2.5	1.0	30	300	35.4	300	69.5	7.95	100	A27-24	Maneuver
1/24 scale	7a	2.5	1.0	30	240	22.7	225	69.5	7.95	100	A29-7a	Maneuver
1/24 scale	7b	2.5	1.0	30	240	30.3	225	69.5	7.95	100	A29-7b	Maneuver
1/24 scale	7c	2.5	1.0	30	240	37.9	225	69.5	7.95	100	A29-7c	Maneuver
Full scale	5x	1.0	1.0	30	—	—	—	—	3.23	—	3 ATT	Cruise
Full scale	6x	1.75	1.0	30	—	—	—	—	5.59	—	5 ATT	Intermediate
Full scale	7x	2.5	1.0	30	—	—	—	—	7.95	—	7 ATT	Maneuver

SECTION VIII

AEROELASTIC ANALYSIS

8.1 METHODS

Considerable aeroelastic deformation of models in the HIRT facility are a certainty. A means of accounting for the model elasticity is necessary before the test data can be rationally applied to the full-scale design problem. Simultaneous solution of equations that contain both the aerodynamic influence function and the structural influence function are necessary for this task. A method and digital program, P4278, (Reference 7) in FORTRAN IV language for computing steady-state spanwise load distribution on an elastic airplane wing for specified airplane weights and load factors was used to accomplish this analysis. The method is based on a modification of the Weissinger L-Method, from theory originally developed for subsonic flow. It is valid for supersonic flight, providing that the flow over the wing is subsonic (this is a possible case for swept wings that operate in the low supersonic Mach number range in which the shock cone lines are ahead of the leading edge and no other shocks are generated on the wing.) Program 4278 capabilities include the effects of external stores, fuselage, and tail boom on spanwise loading.

The Weissinger L-Method of digital program 4278 is an outgrowth of NACA TN 3030 (Reference 8). Surveys and texts on the methods of calculating aerodynamic loads on aircraft structures invariably reference TN 3030. TN 3030 was used in the design of the CV880 and CV990 jet transports, and more recently Boeing employed this method in the design analysis of the 747 transport. Approximately one-half of the technical papers being written today on the subject of interaction between fuselage and wing make use of the principle of image vortices as described by Gray, Schenk, and Lennertz. The Air Force Flight Dynamics Laboratory has revived interest in this method (References 9 and 10). More recently Blackwell at NASA Langley extended the method to include sidewash and backwash (Reference 11) in addition to the usual downwash.

Convair Aerospace continues to use the Weissinger L-Method in proposal work for subsonic aircraft and transonic wings that have enough leading edge sweep so that the Mach cone lies ahead of the wing.

The digital program performs symmetric and asymmetric balances and then distributes the shears, moments, and torques over the vehicle for each condition. Angles of attack along the wing span are calculated for checking stall characteristics and for recommendation of the wing twist to counter this problem.

Program 4278 was used to provide design loads for each model and the corresponding deformations due to twisting and bending. Program 4278 is a strip theory program and solves the aeroelastic distribution of a load in a single run on the digital computer.

Model geometries used for the aeroelastic analyses are presented in computer format in Figure 23.

In order to determine the distributed loads and aeroelastic deflections, the rigid aerodynamic characteristics of the study configurations were determined. This was accomplished by using wind-tunnel data, when it was available, and DATCOM (Reference 12).

Each design test point as shown in Table 2 was analyzed and the following data were plotted using the conventional SC4020 plotting output:

a. Shear load (air + inertia).

* b. Bending moment and pitching torque (air + inertia)

c. Wing loading ($C_L cq$) (air only)

d. Wing vertical deflection (y)

e. Elastic wing twist (θ)

Note that all plots are presented versus wing semispan.

A typical computer printout is included in the appendix of this report.

8.2 TUNNEL OPERATING CONDITIONS INFLUENCE ON MODEL LOADS

8.2.1 Cooled Storage Air

Tunnel operating conditions were obtained from a set of estimated flow property curves for the proposed HIRT facility (Reference 13). These curves were supplied by the government for use in this study. Dynamic pressure (q_∞) versus Reynolds number per foot (R_e/ft) for two storage temperatures, ambient (300°K) and cooled (-30°F, 240°K) are presented in Figures 24 and 25. Since Reynolds number is very sensitive to free-stream temperature, a significant lowering of dynamic pressure can be obtained by using cooled storage air. Figure 26 illustrates the effects of cooled air versus ambient air on the elastic twist, deflection of the wing, maximum wing stress, and the maximum lift force on the ATT model.

Note that model loads are based on using 240°K storage air unless noted otherwise.

8.2.2 Model Problems Due to Temperature

Running models in a 240°K (-30°F) environment does not present any large physical problems. Model material selection must be accomplished with the temperature in mind. The material selected for use as a baseline material for this study (PH 13-8 Mo steel) has few restrictions at these temperatures (Reference Section X).

* Bending moments & torque taken about wing elastic axis (see Figure 23 for E.A. location).

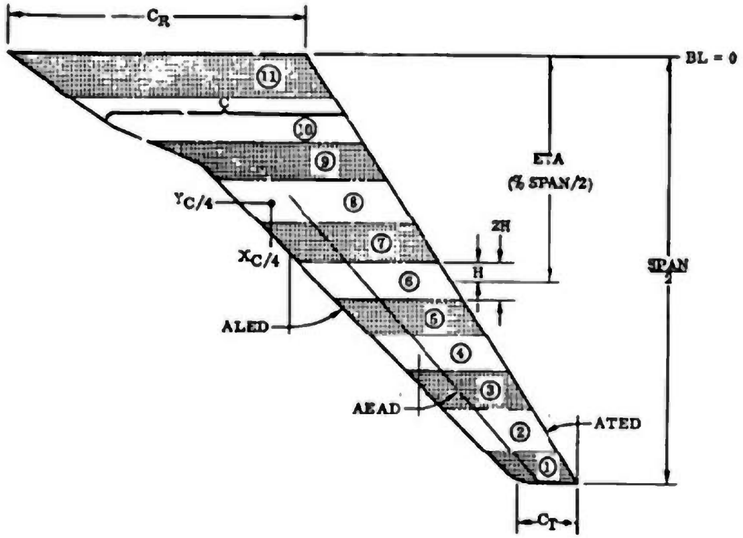

LEGEND

ETA = DISTANCE FROM BL = 0 TO CENTER OF STRIP (% SEMISPAN)
C = CHORD LENGTH AT A GIVEN ETA
2H = WIDTH OF STRIP
$X_{C/4}$ = FUSELAGE STATION LOCATION OF QUARTER CHORD OF AIRFOIL AT ETA
$Y_{C/4}$ = BUTTOCK LINE LOCATION OF QUARTER CHORD OF AIRFOIL AT ETA
$Z_{C/4}$ = WATER LINE LOCATION OF QUARTER CHORD OF AIRFOIL AT ETA
EA = ELASTIC AXIS (% CHORD)
ALED = SLOPE OF WING LEADING EDGE (deg)
AEAD = SLOPE OF ELASTIC AXIS (deg)
ATED = SLOPE OF WING TRAILING EDGE (deg)

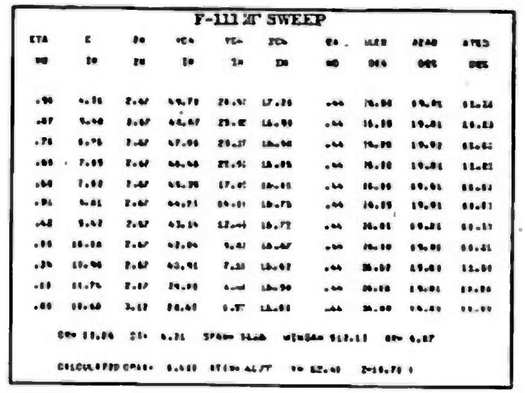

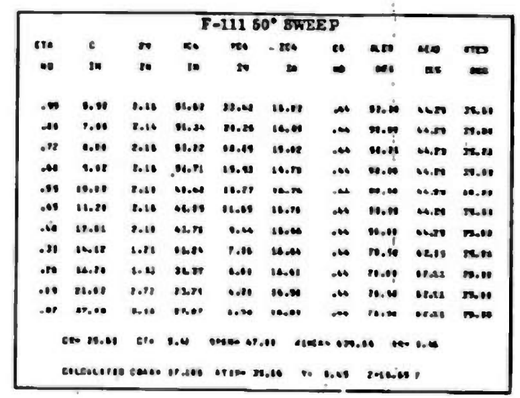

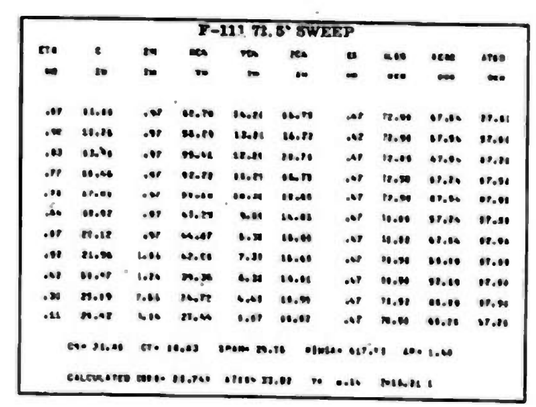

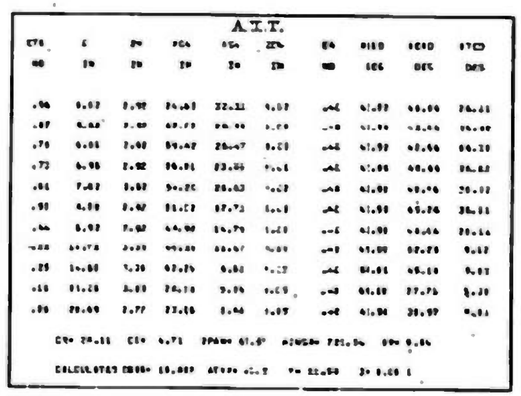

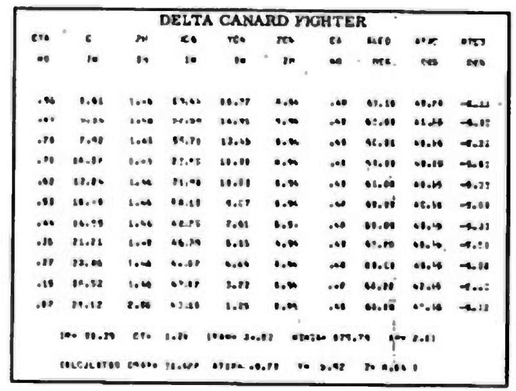

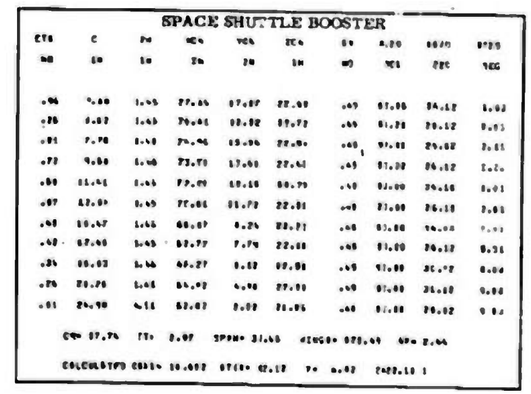

Figure 23. Aeroelastic Program Geometry

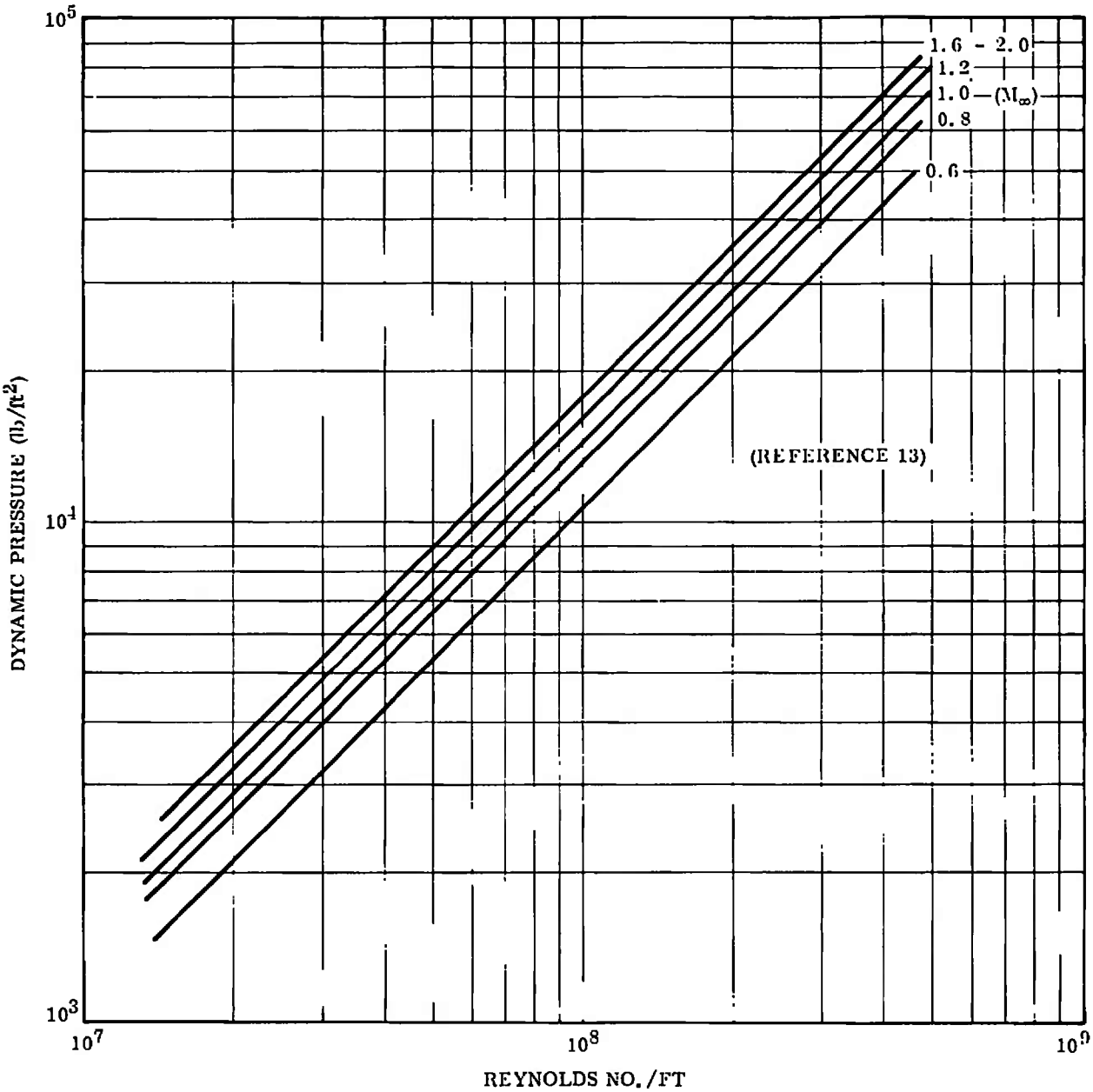

Figure 24. Reynolds Number vs Dynamic Pressure at 300°K

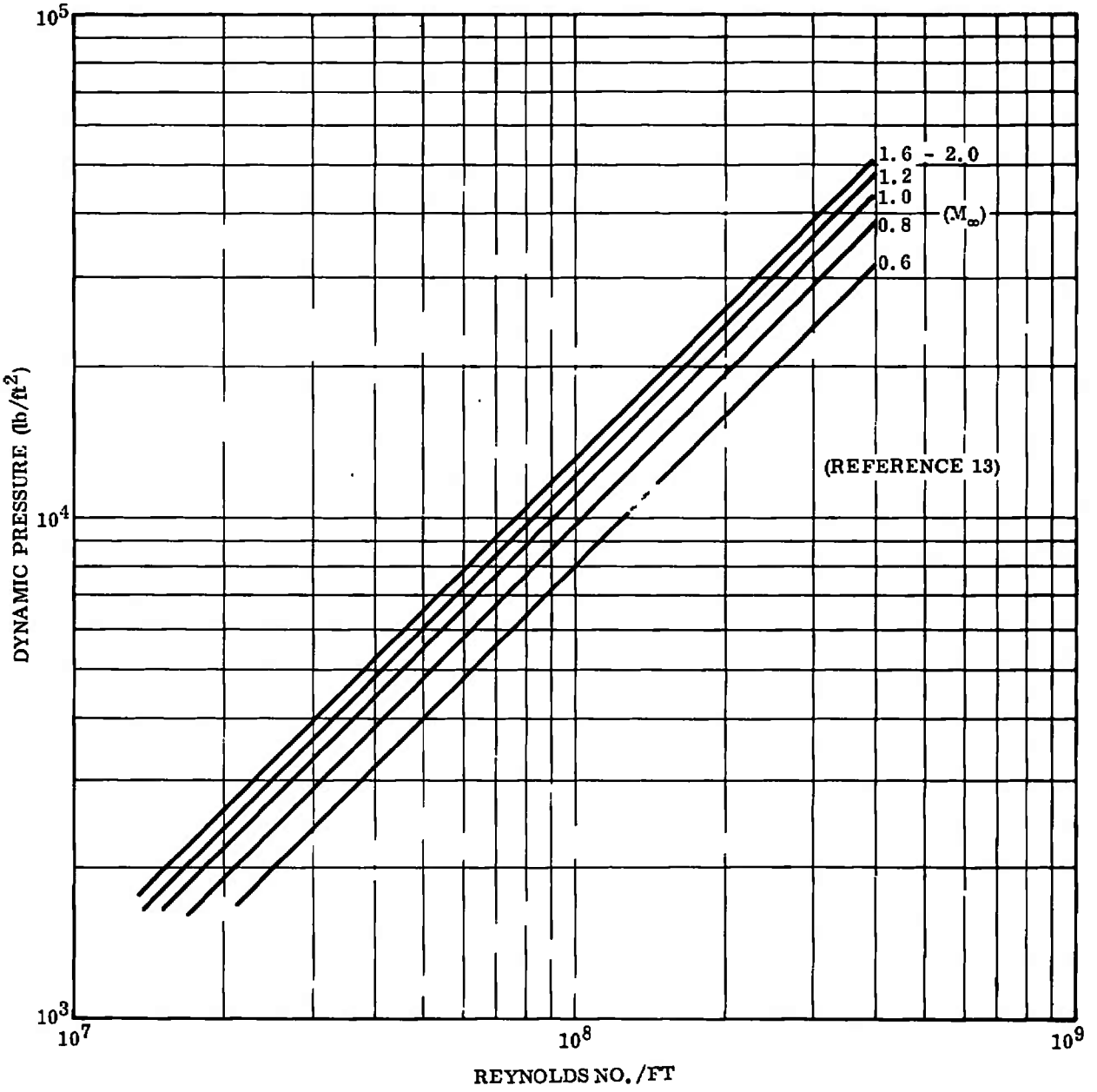

Figure 25. Reynolds Number vs Dynamic Pressure at 240°K

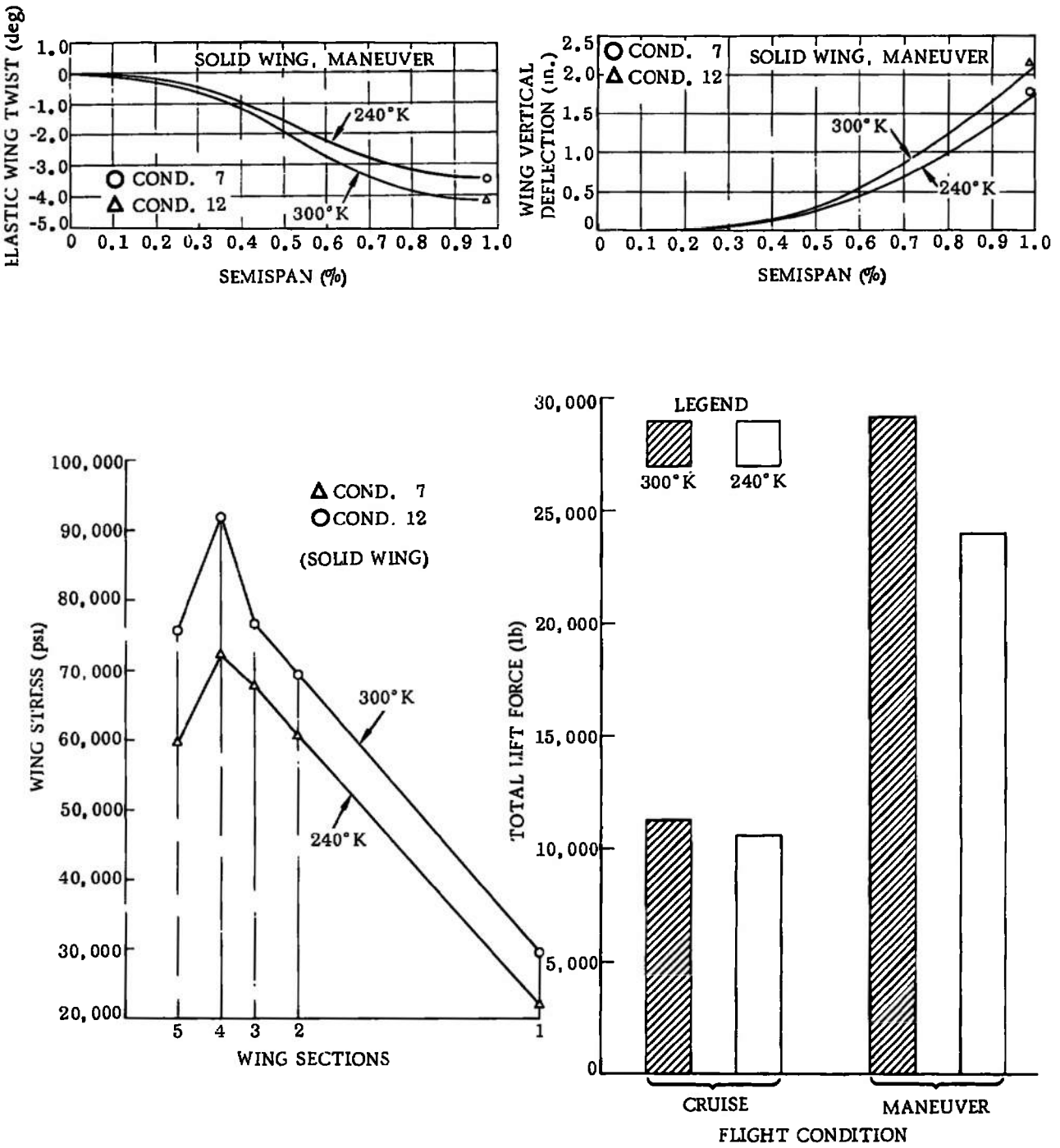

Figure 26. ATT — Effects of 300°K vs 240°K Tunnel Operation

Model balances and onboard instrumentation, such as pressure transducers, will have to be temperature compensated and/or thermally protected to minimize temperature effects.

Model change procedures must be developed to handle -30°F models.

8.3 MODEL LOADS

Model loads were computed using Program 4278 supplemented by hand calculations as required. Loads are based on actual or estimated operating envelopes for each of the aircraft configurations. These operating envelopes were presented in Figures 17 through 22. Wing shear, bending moment, pitching torque, and $C_L cq$ (wing loading) were computed for each model configuration and condition shown in the test plan (Table 2). These data were used for all structural analysis work.

All model loads are based on steady-state conditions only.

8.3.1 ATT Model – Wing Loads

Loads for the Advanced Technology Transport configuration were computed for several test points. Low-speed, low-altitude maneuvering; high-speed, high-altitude maneuvering, and various high speed cruise conditions. Test plan (Table 2) conditions 5, 6 and 7, (Figures 27 through 29) were selected as most representative of cruise, mid-maneuver (1.75g) and maximum maneuver (2.5g) conditions. Loads for conditions 1 and 3 are presented in Figures 30 and 31.

The ATT configuration was selected to explore the results of increasing the model scale by 150% and 200%. The loads resulting from these model scales are shown in Figures 32 through 35.

8.3.2 F-111 Model – Wing Loads

The 50-degree wing sweep version of the F-111 is the highest loaded configuration. Loads for a 40,000-foot cruise and a sea-level, 6-g maneuver condition are shown in Figures 36 and 37. Maximum maneuvering loads for the 26-degree sweep and 72-1/2-degree sweep configurations are presented in Figures 38 and 39.

8.3.3 Delta Canard Fighter – Wing Loads

The loads for this delta-wing fighter are shown in Figures 40 and 41. A 40,000-foot cruise condition and a sea-level, 7.5-g maneuvering condition are represented.

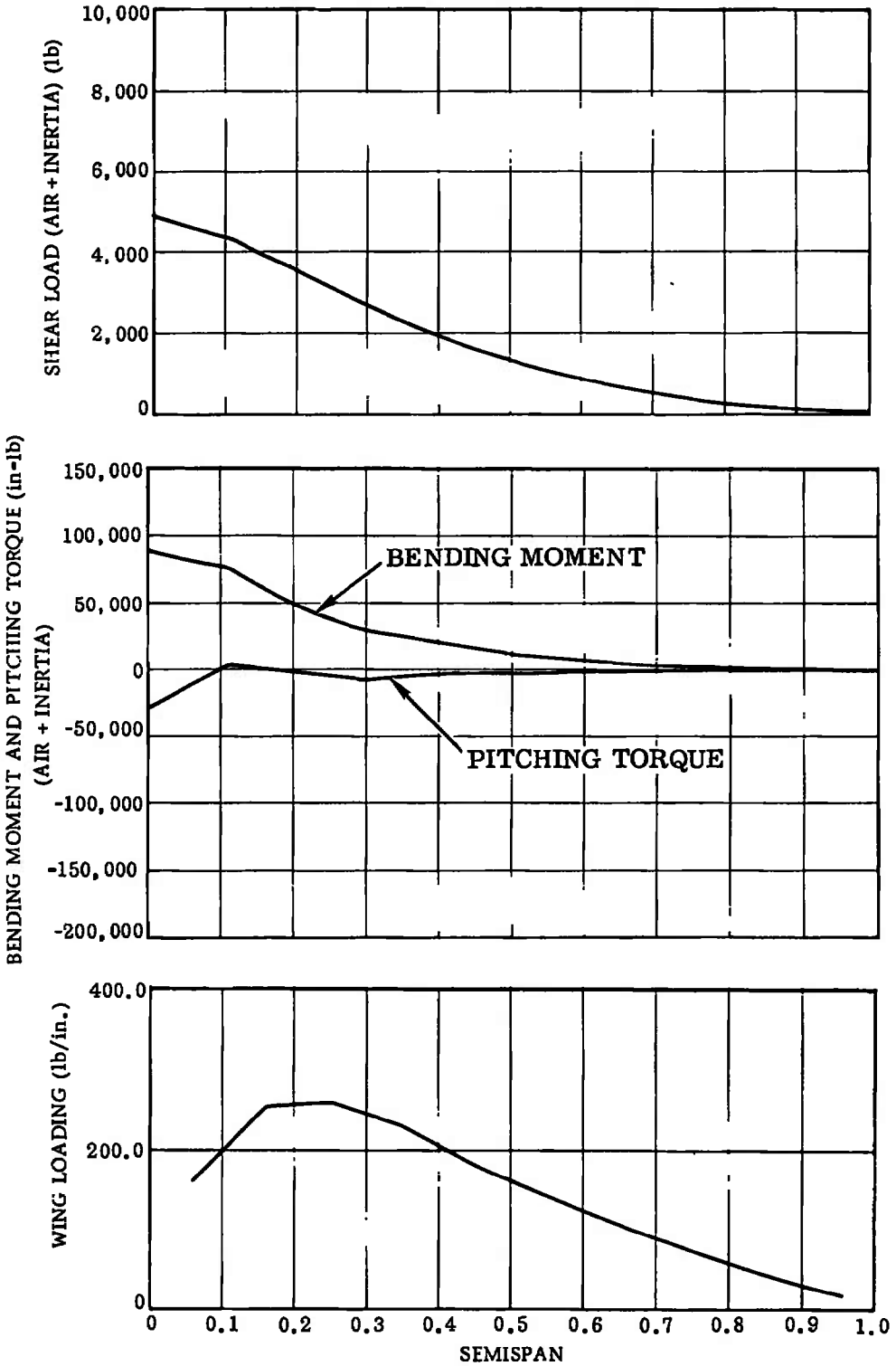

Figure 27. ATT — Model Loads – Condition 5

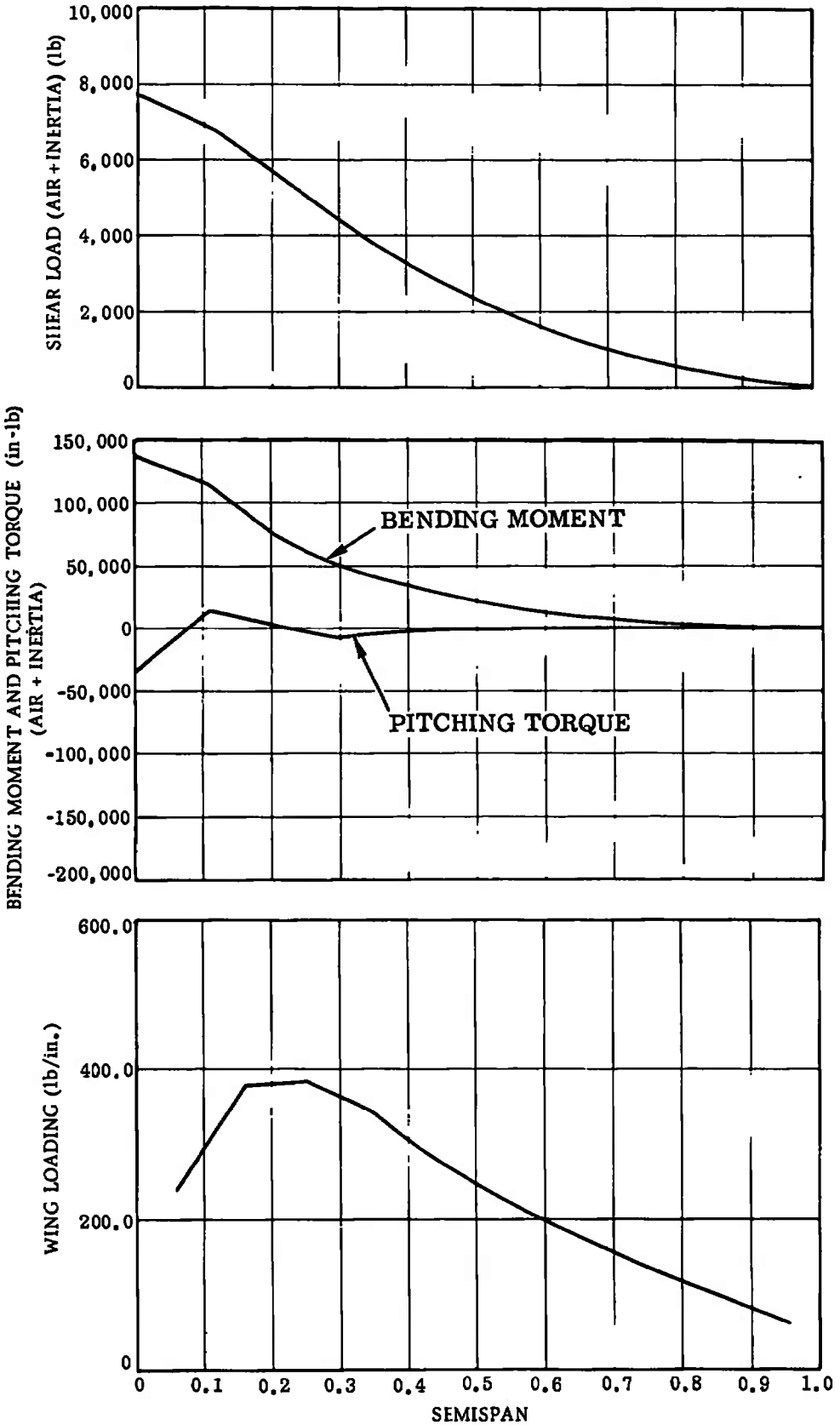

Figure 28. ATT – Model Loads – Condition 6

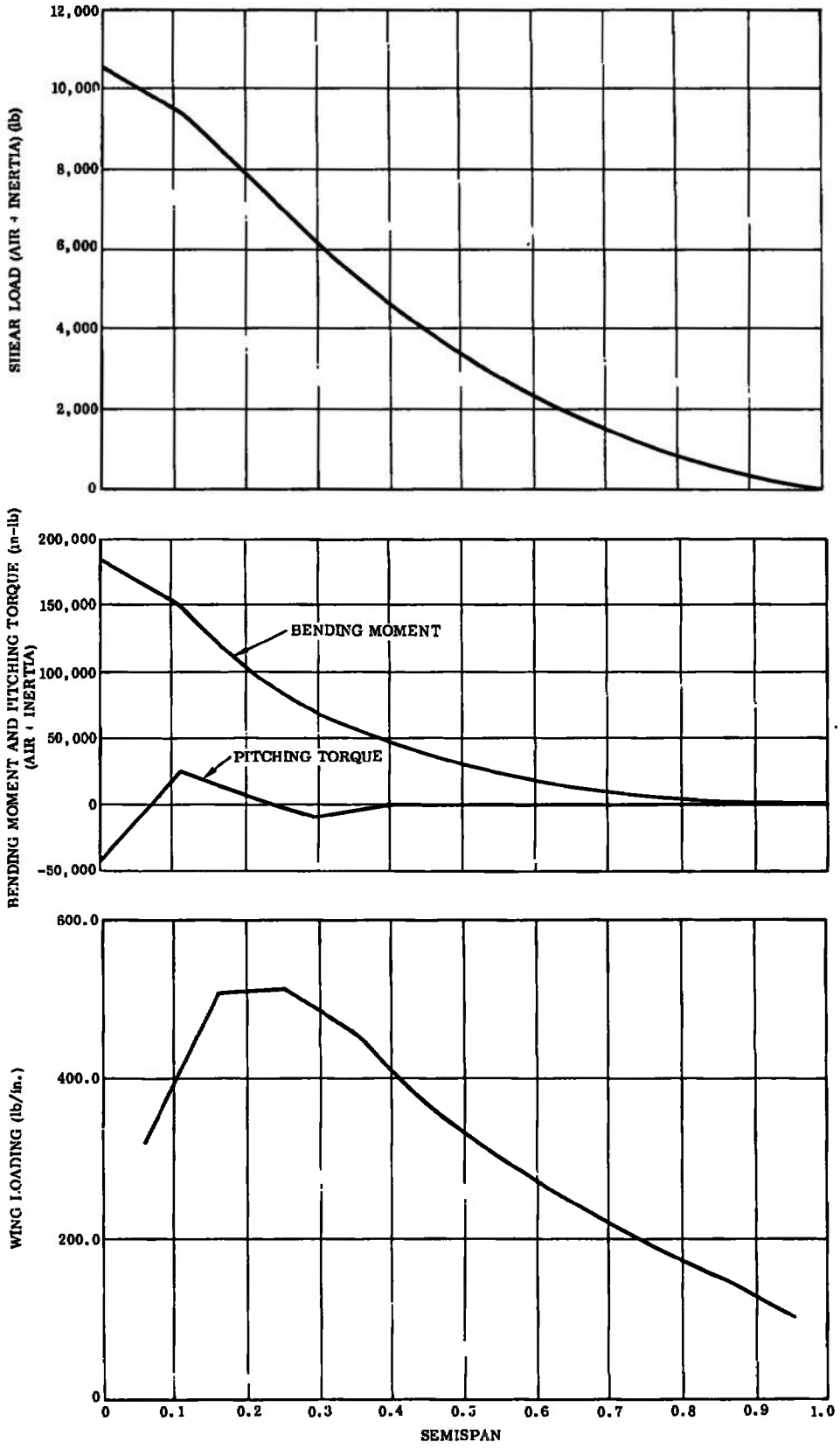

Figure 29. ATT — Model Loads — Condition 7

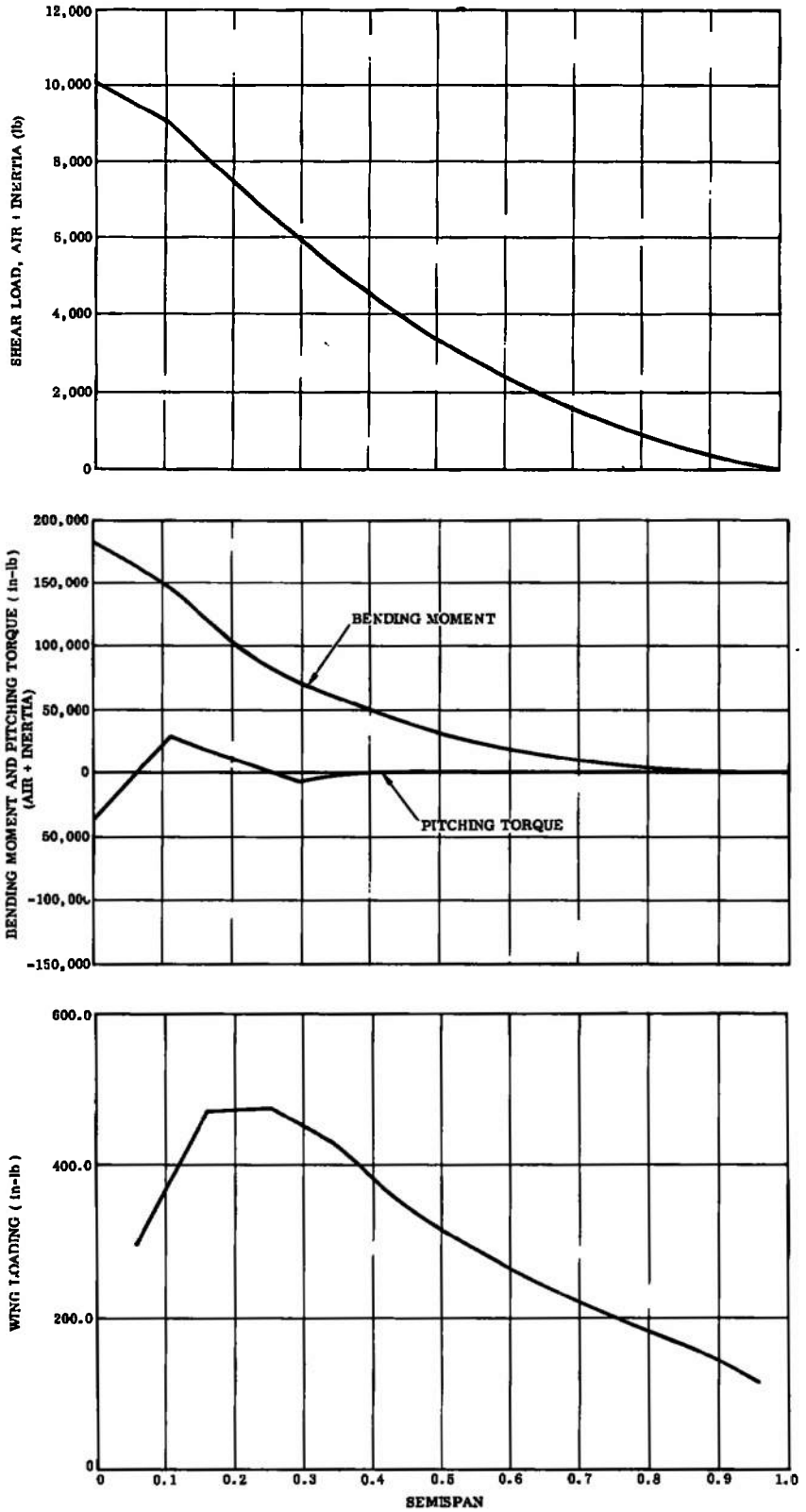

Figure 30. ATT — Model Loads — Condition 1

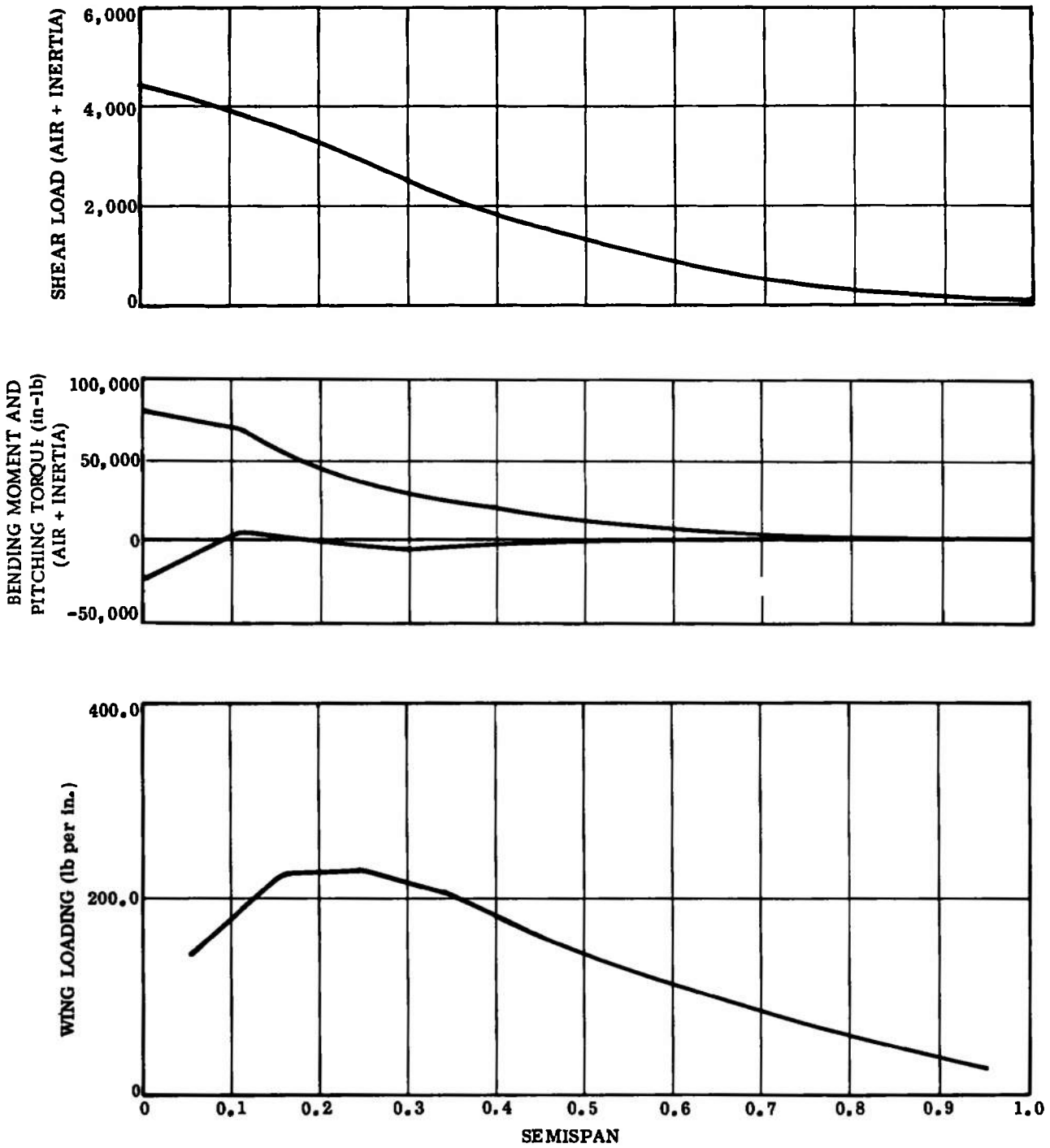

Figure 31. ATT – Model Loads – Condition 3

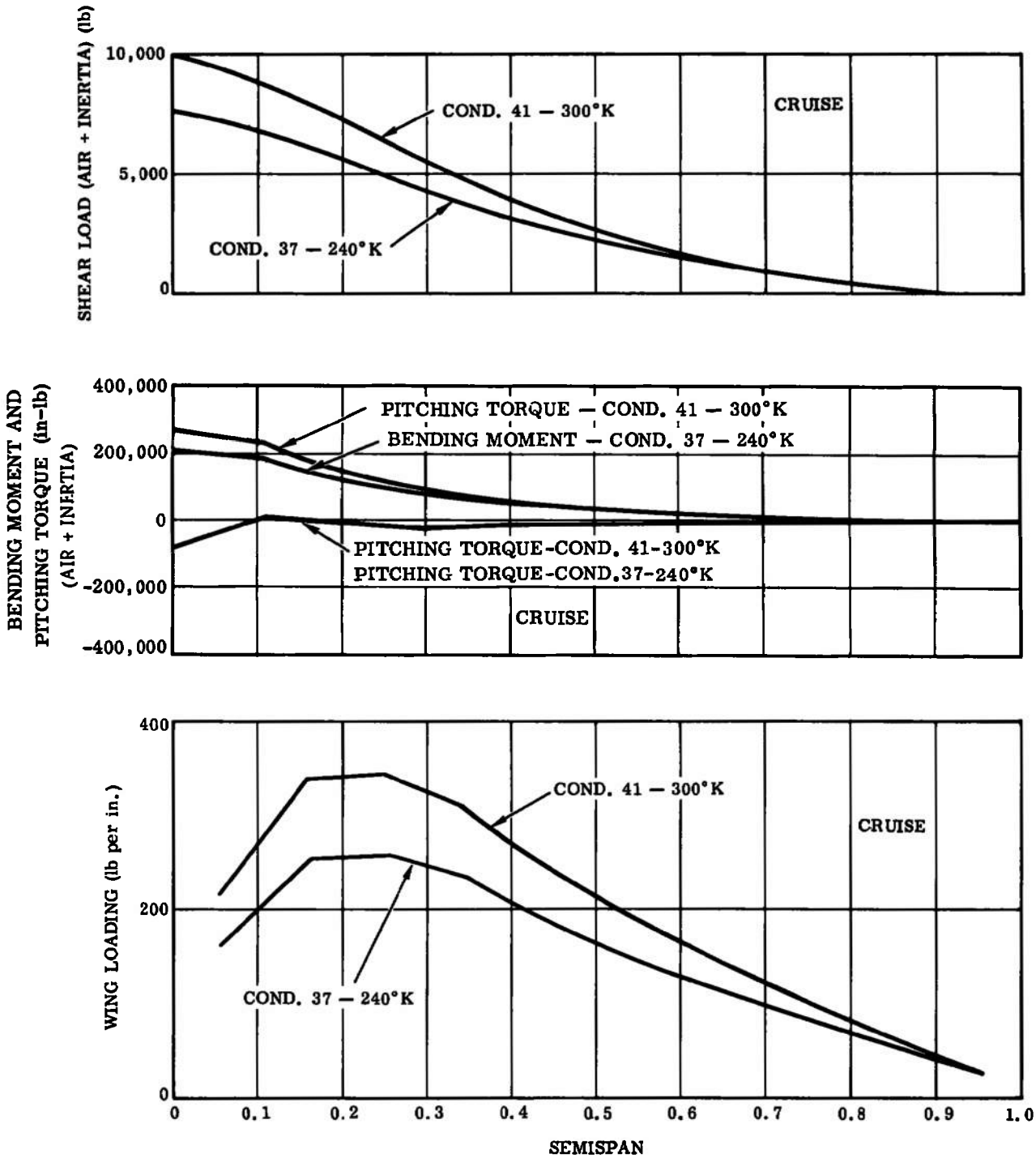

Figure 32. ATT — Model Loads, 1/16 Scale — Conditions 37 and 41

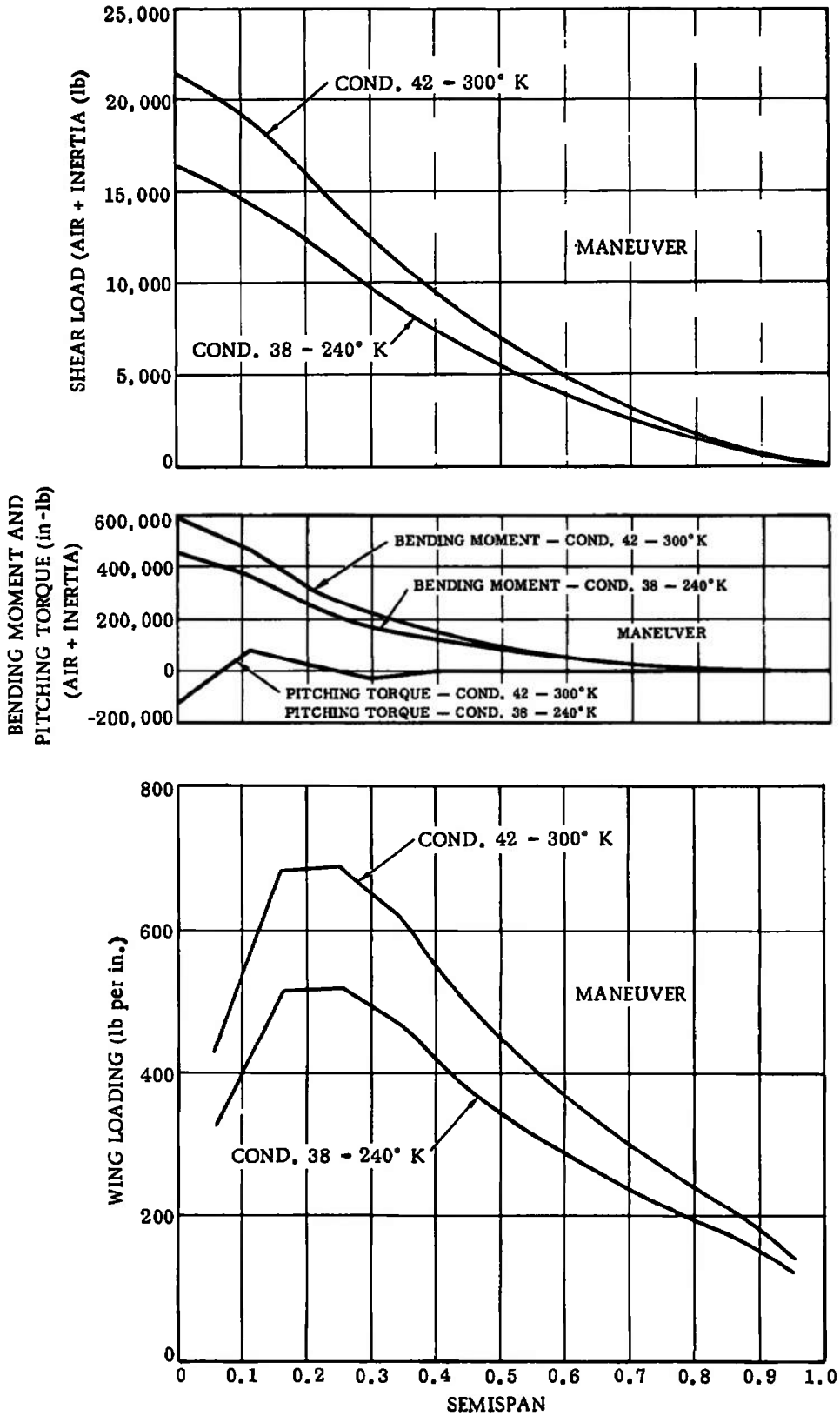

Figure 33. ATT – Model Loads, 1/16 Scale – Conditions 38 and 42

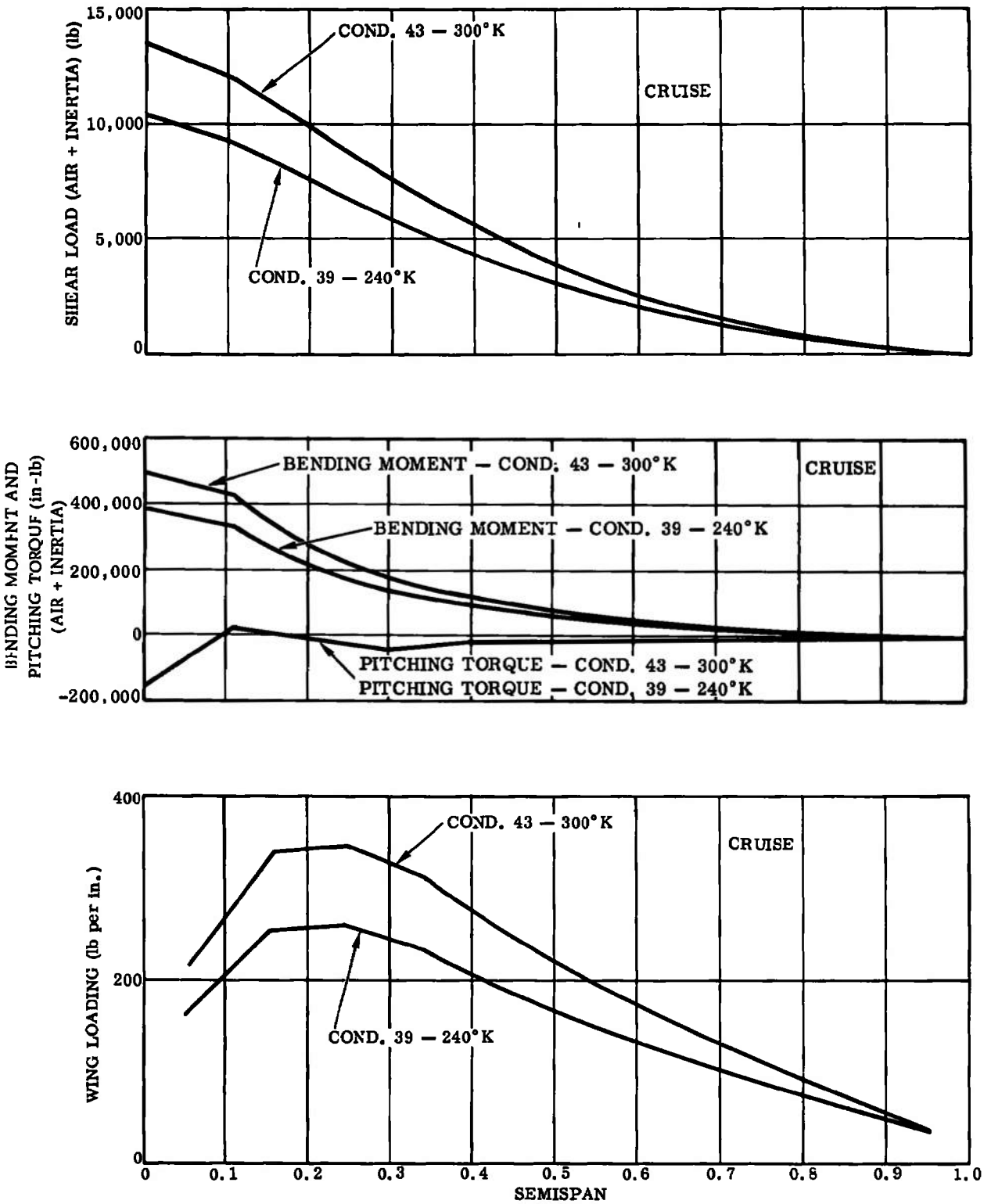

Figure 34. ATT – Model Loads, 1/12 Scale — Conditions 39 and 43

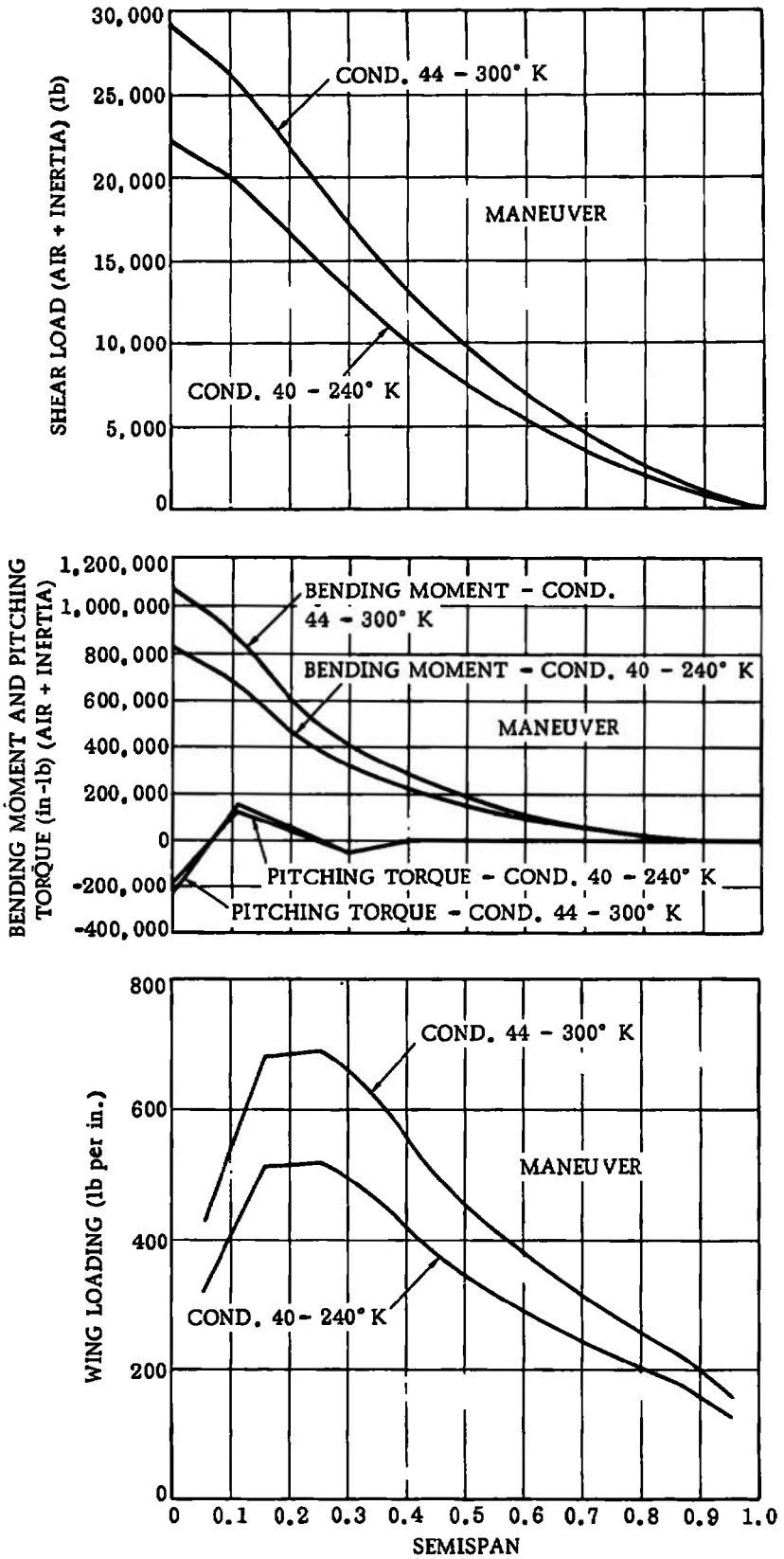

Figure 35. ATT – Model Loads, 1/12 Scale – Conditions 40 and 44

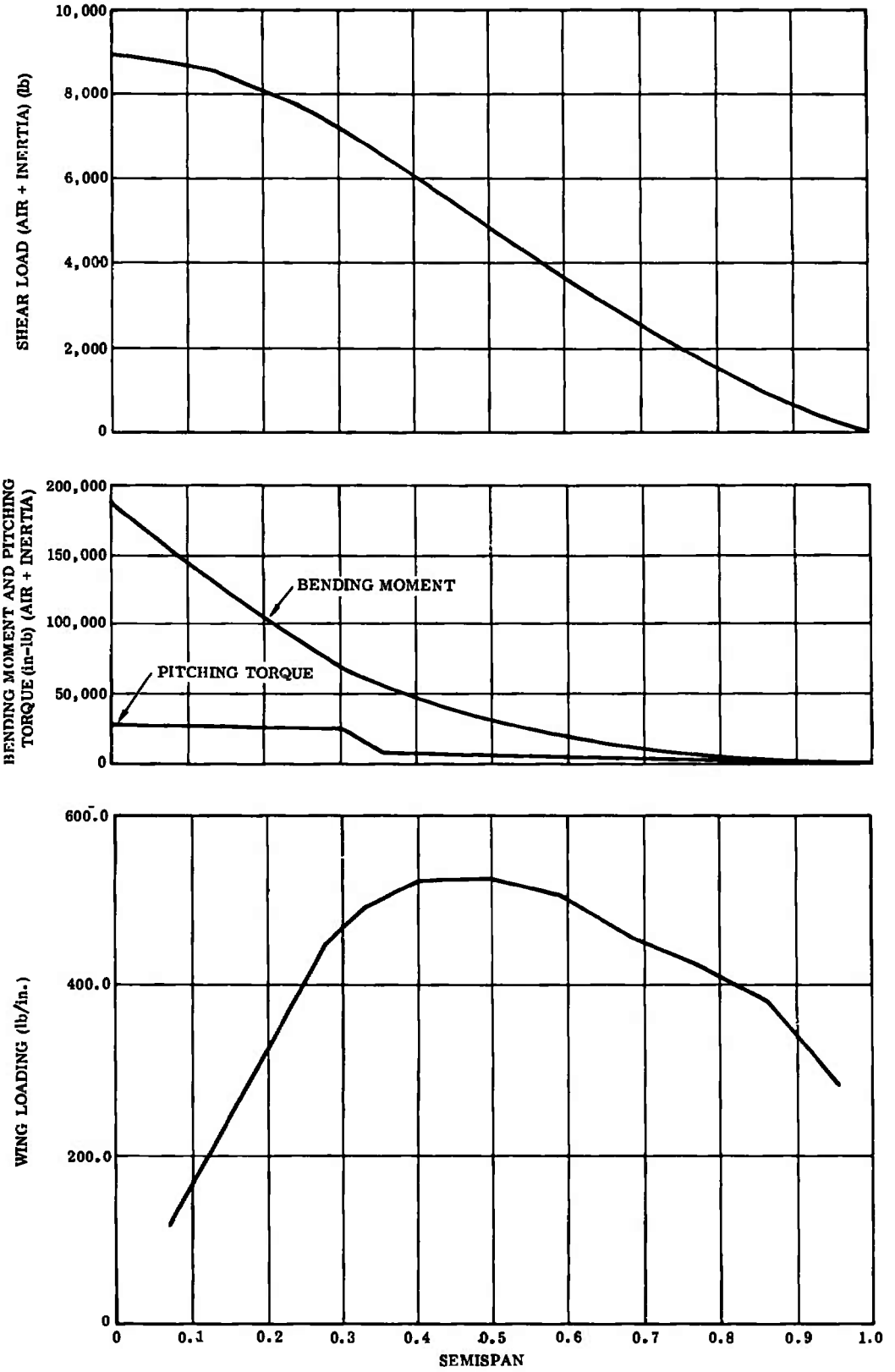

Figure 36. F-111 (50 Deg) – Model Loads – Condition 14

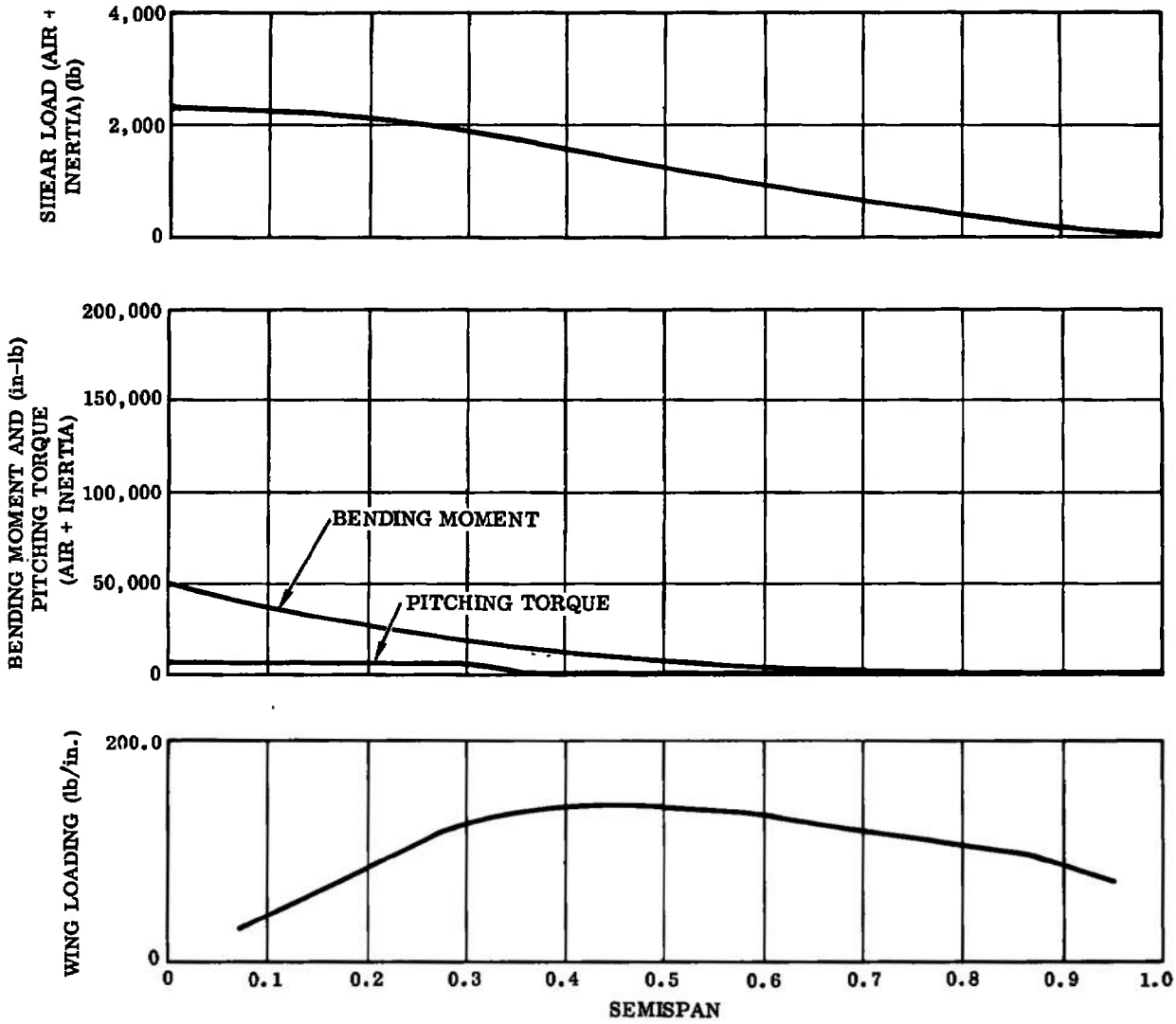

Figure 37. F-111 (50 Deg) – Model Loads – Condition 17

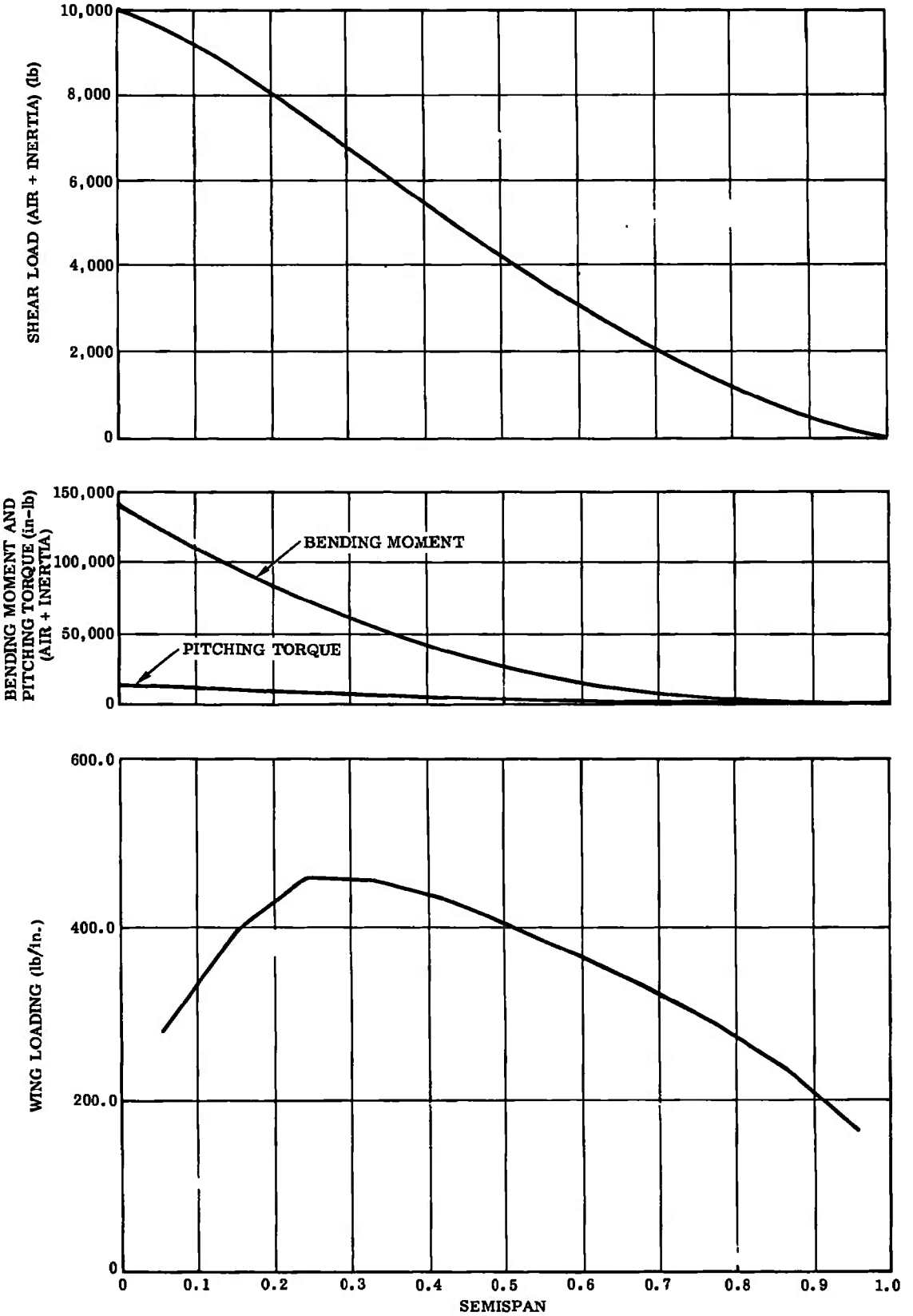

Figure 38. F-111 (26 Deg) – Model Loads – Condition 20

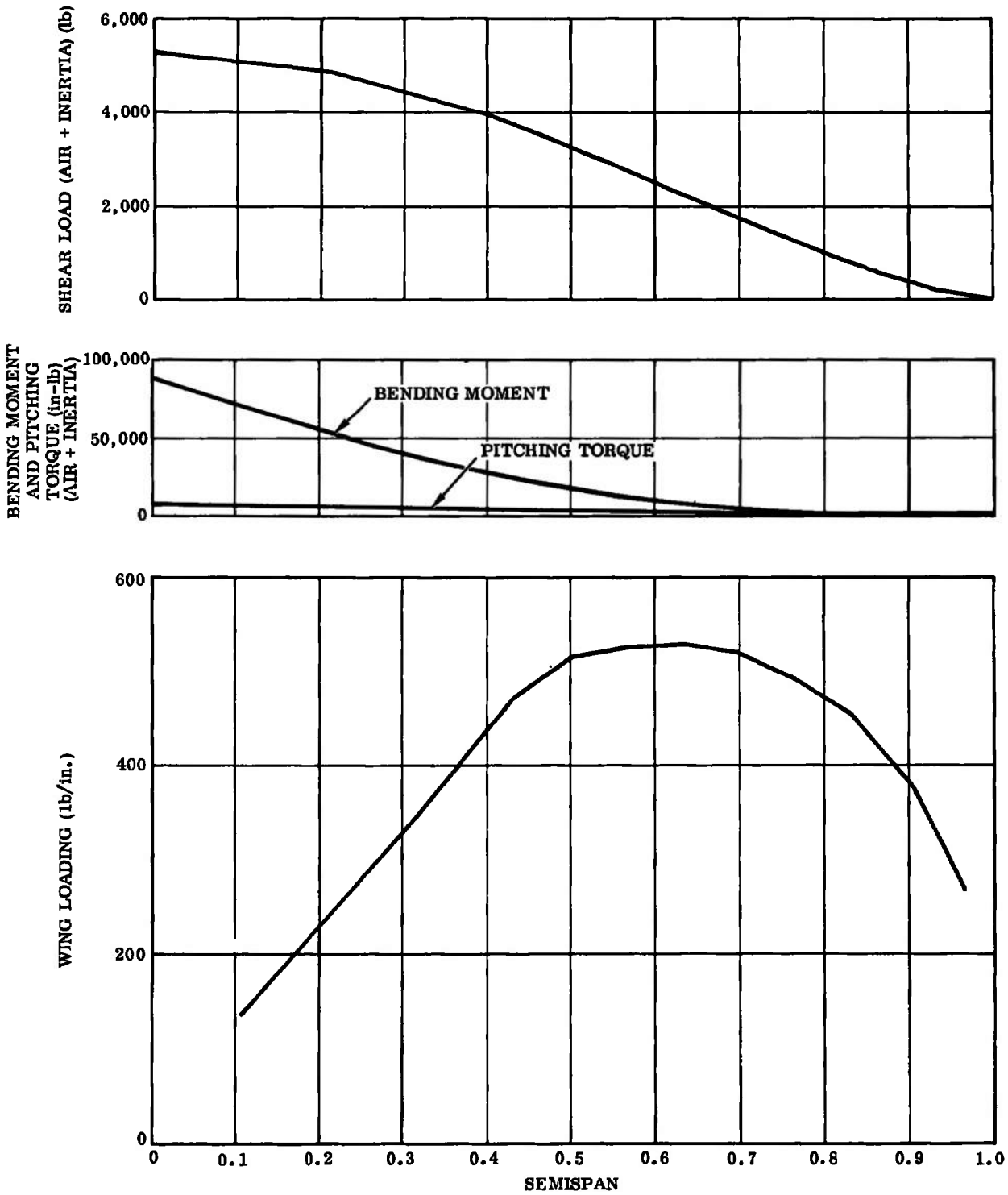

Figure 39. F-111 (72-1/2 Deg) – Model Loads – Condition 22

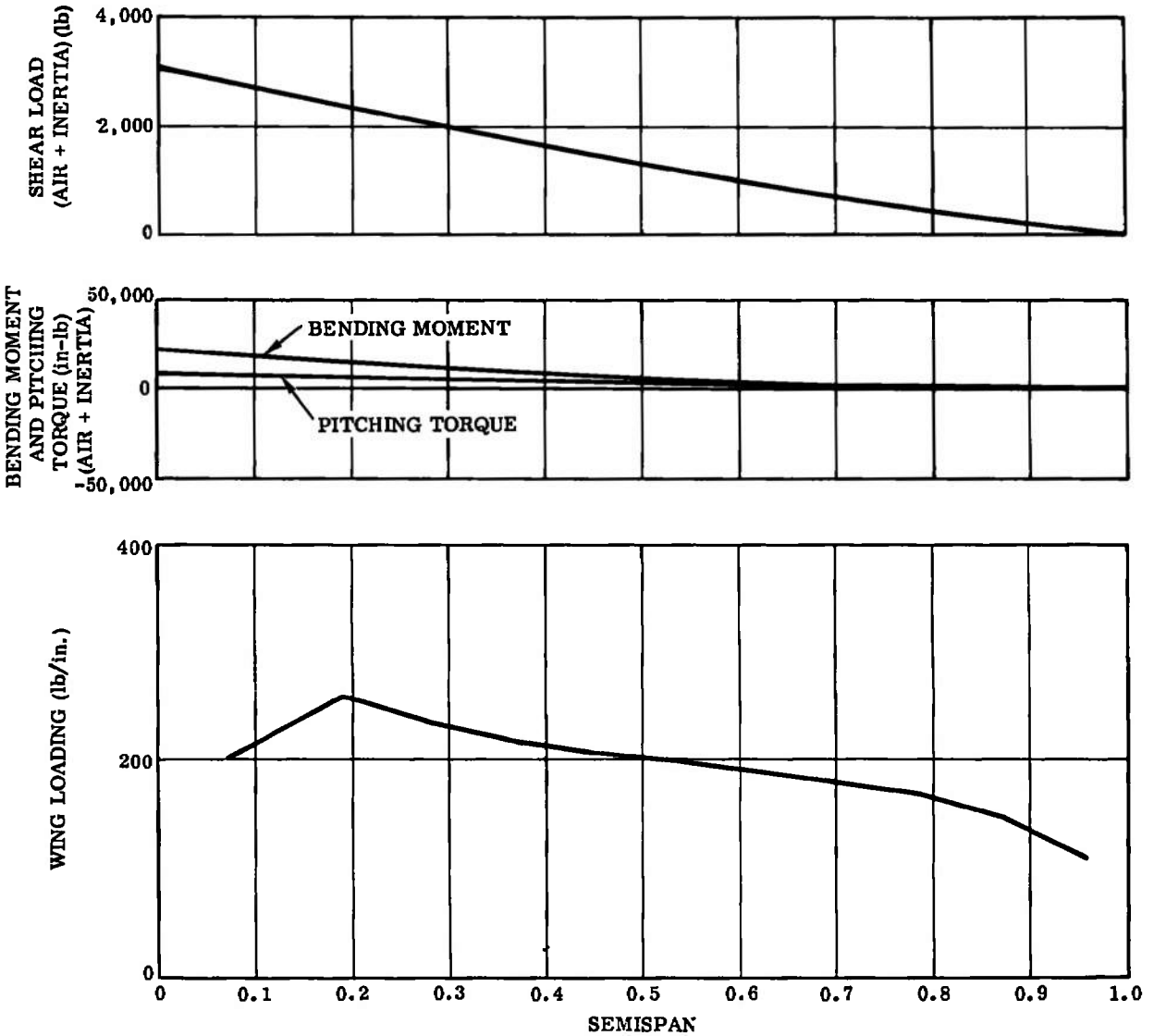

Figure 40. Delta Canard – Model Loads – Condition 24

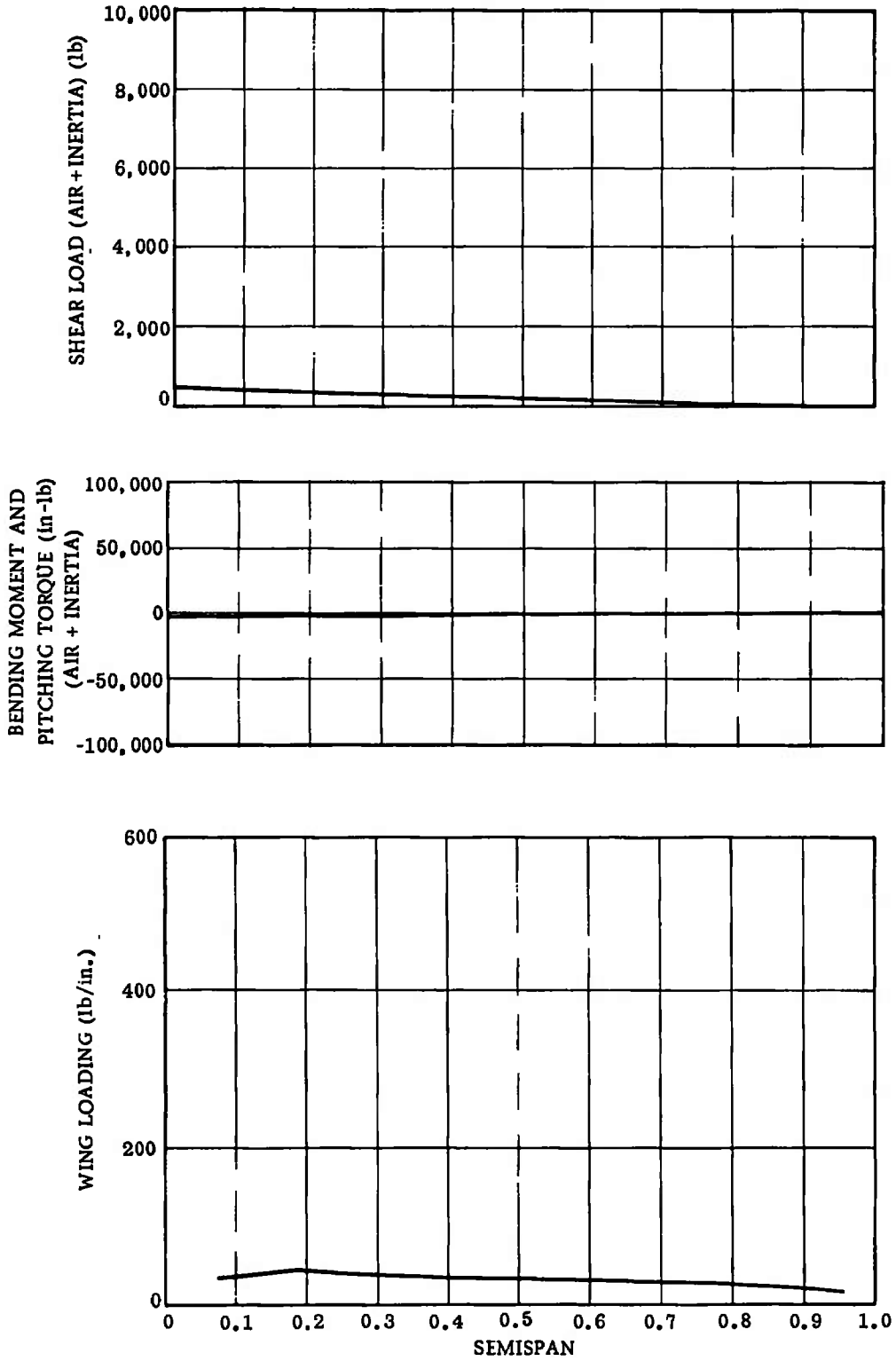

Figure 41. Delta Canard – Model Loads – Condition 27

8.3.4 Space Shuttle Booster – Wing Loads

The space shuttle booster model loads are representative of a 2.5-g, 30,000-foot maneuver condition. These loads are presented in Figure 42.

Note that these loads are for ambient tunnel temperature operation (300°K).

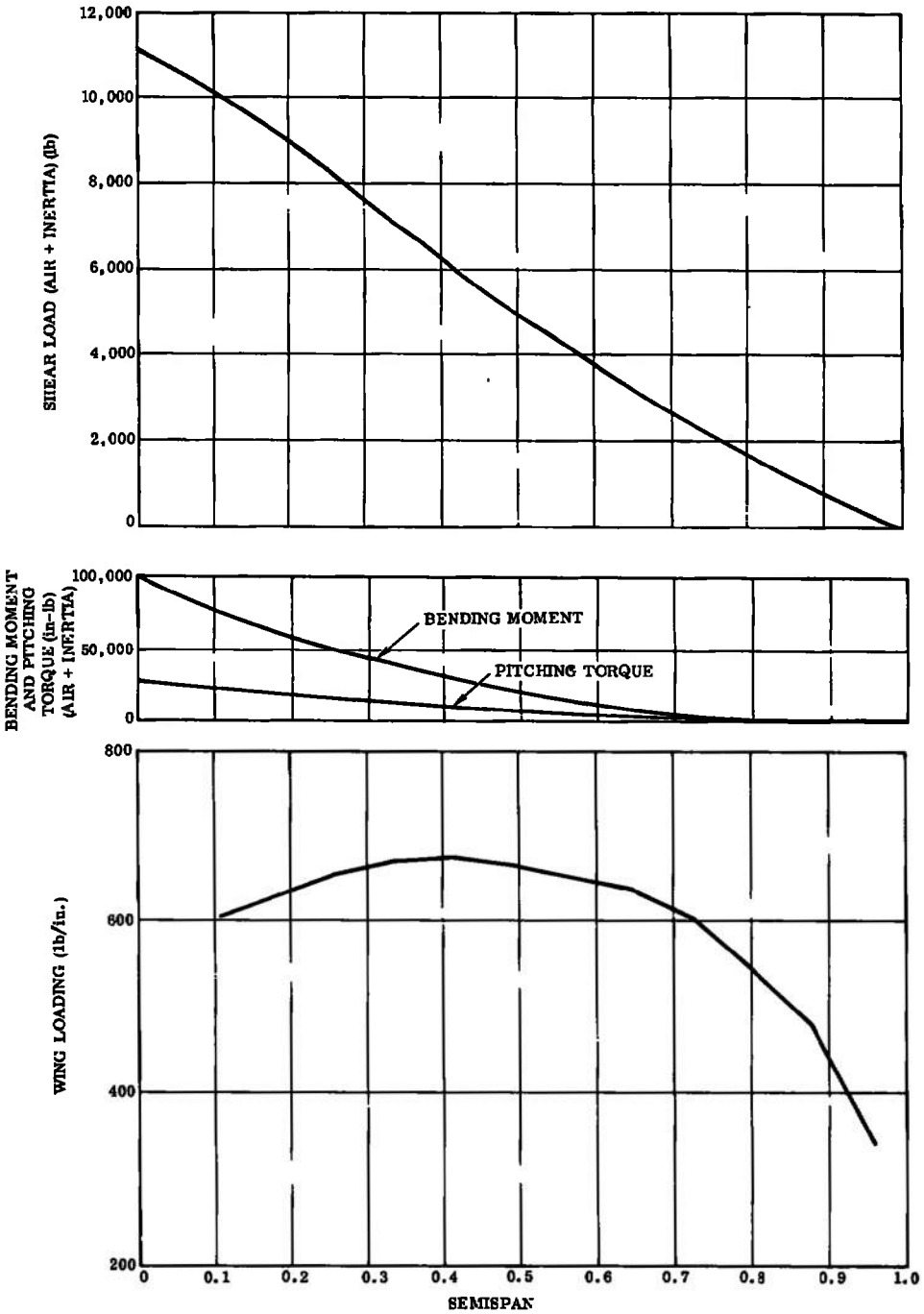

Figure 42. Space Shuttle Booster — Model Loads — Condition 29 (T = 300°K)

8.3.5 Empennage and Balance Loads

The total vertical force acting on each of the models was computed using Program 4278. The maximum vertical force value for each of the model configurations was used as a representative load for balance cavity and sting sizing. Balance and stings are shown only to represent feasibility.

Vertical tail and horizontal loads were computed by hand and represent general values for each configuration.

Empennage and total vertical force values for each of the models are shown in Table 3.

Table 3. Model Loads, Empennage, and Total Lift

Configuration	Vertical tail load (lb)	Horizontal tail (per side) (lb)	Temperature (°K)	Maximum total lift (balance load) and location (lb)
ATT	3,070	950	240	24,100 at F. STA. 44.790
F-111	2,500	4,500	240	30,370 at F. STA. 43.105
Delta canard	2,450	---	300	22,000 at F. STA. 46.136
	1,800		240	14,700
Space shuttle booster	8,320	---	300	34,950 at F. STA. 66.820
	6,200		240	30,761
ATT (1.5 size)	---	1,435	240	37,370
	---	1,910	300	48,900
ATT (2.0 size)	---	1,910	240	50,473
	---	2,550	300	66,400

8.3.6 Model Loads Directory

Table 4 may be used as an index to the location of the various model loads.

8.4 MODEL WING DEFORMATION

8.4.1 1/24 Scale ATT Model

Some representative aeroelastic wing twists for the ATT model wing are shown in Figure 43. Aeroelastic twists are shown for a 100% chord solid steel wing and for a solid steel wing with the aft 35% chord removed to illustrate the effect of simulating deflected surfaces, etc. Solid steel wings (100% chord) twist from a maximum of 1.5 degrees at a Mach 1.0 cruise, 30,000 feet, to a maximum of 3.4 degrees at a 2.5 g

Table 4. Model Loads Directory

Configuration	Test condition no. (see Table 2)	Figure no. Bending moment Pitching torque Shear Wing loading	Table no. Vertical tail Horizontal tail Total lift
ATT	1	30	3
	3	31	
	5	27	
	6	28	
	7	29	
F-111			
50 deg	14	36	
50 deg	17	37	
26 deg	20	38	
72-1/2 deg	22	39	
Delta canard fighter	24	40	
	27	41	
Space shuttle booster	29	42	
ATT			
1.5 size	37 & 41	32	
	38 & 42	33	
2.0 size	39 & 43	34	
	40 & 44	35	3

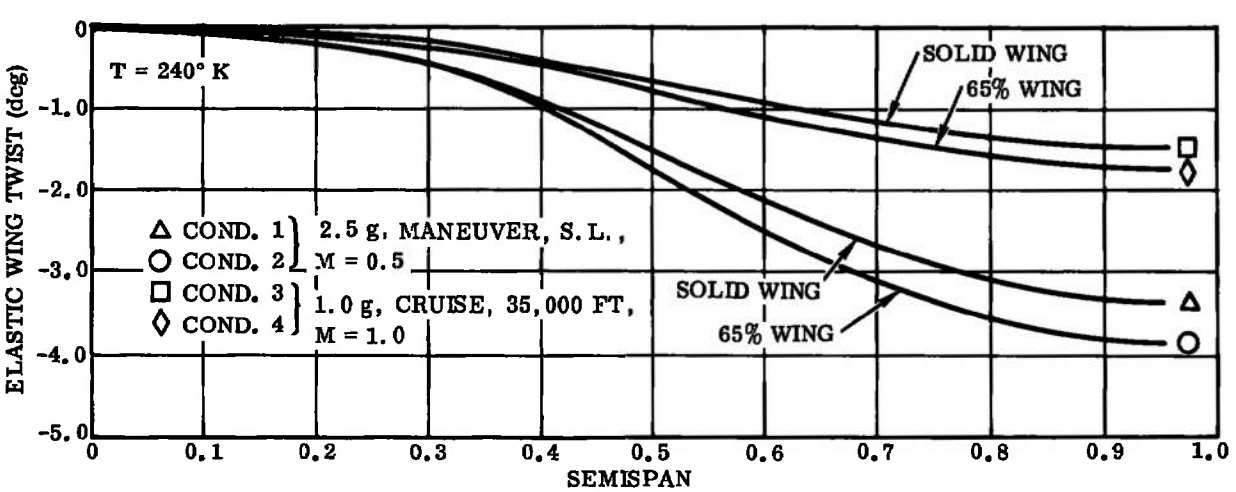

Figure 43. ATT – Elastic Wing Twists

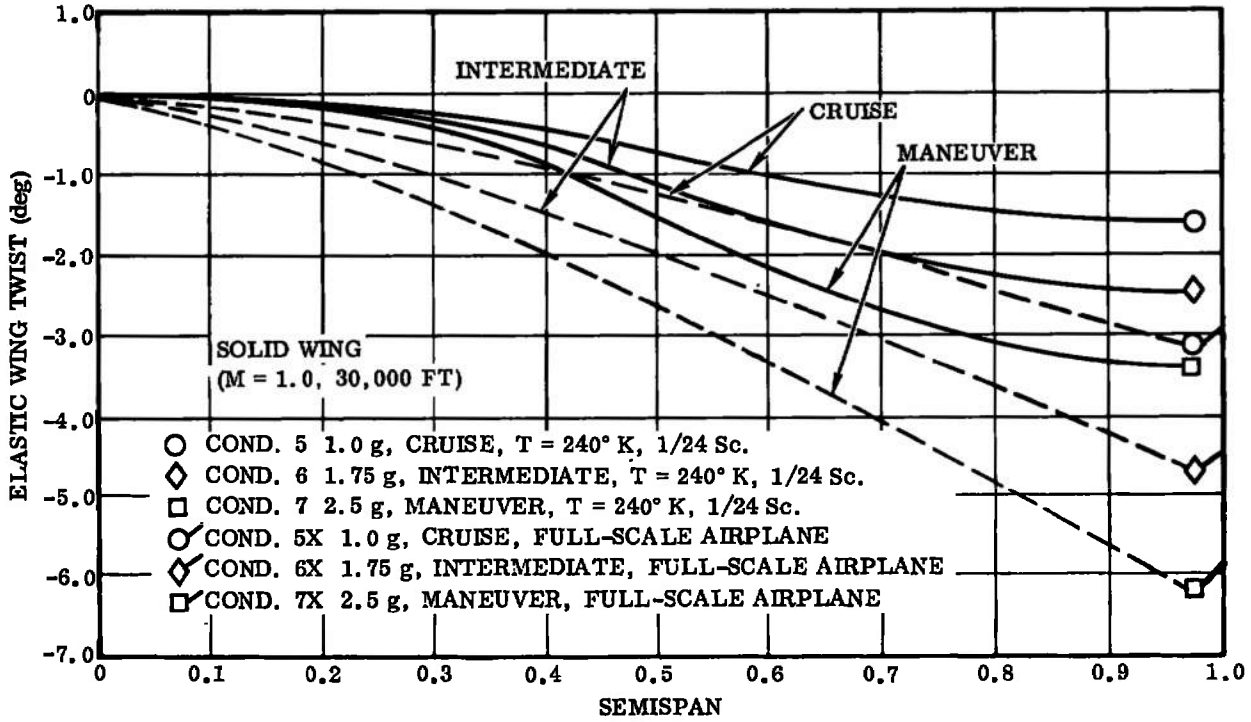

Figure 44. ATT – Model Wing and Airplane Wing Twist Due to Matching Operating Envelope

maneuver at 30,000 feet (reference Figure 44). Figure 44 is a plot of the change in elastic twist of a solid wing model due to varying the angle of attack to match the airplane operating envelope for Mach 1.0, 30,000 feet - cruise (α = 3.23 degrees), intermediate (α = 5.59 degrees), and 2.5 g maneuver (α = 7.95 degrees) conditions.

Wing deflections vary from 0.7 to 1.75 inches for solid wings and from 0.75 to 2.0 inches for 65% chord wings (cruise to 2.5 g maneuver conditions). The wing deflections for the solid-wing model are shown in Figure 45. The effect of removing the aft 35% of the wing is illustrated in Figure 46.

8.4.2 Full-Scale ATT Airplane

The predicted aeroelastic twist and deflection for the full-scale ATT airplane are included in Figures 44 and 45. The aeroelastic solutions for the airplane are based on representative airplane structure for this type of wing. The twist for the airplane is -6.2 degrees at a 2.5 g maneuver and -3.1 degrees at a 1 g cruise condition (compared to -3.4 degrees and -1.5 degrees for a solid-wing model). The airplane wing vertical deflection varies from 103.6 inches (4.3 inches at 1/24 scale) to 42.2 inches (1.8 inches at 1/24 scale) compared to 1.75 inches and 0.7 inch for a solid-wing model.

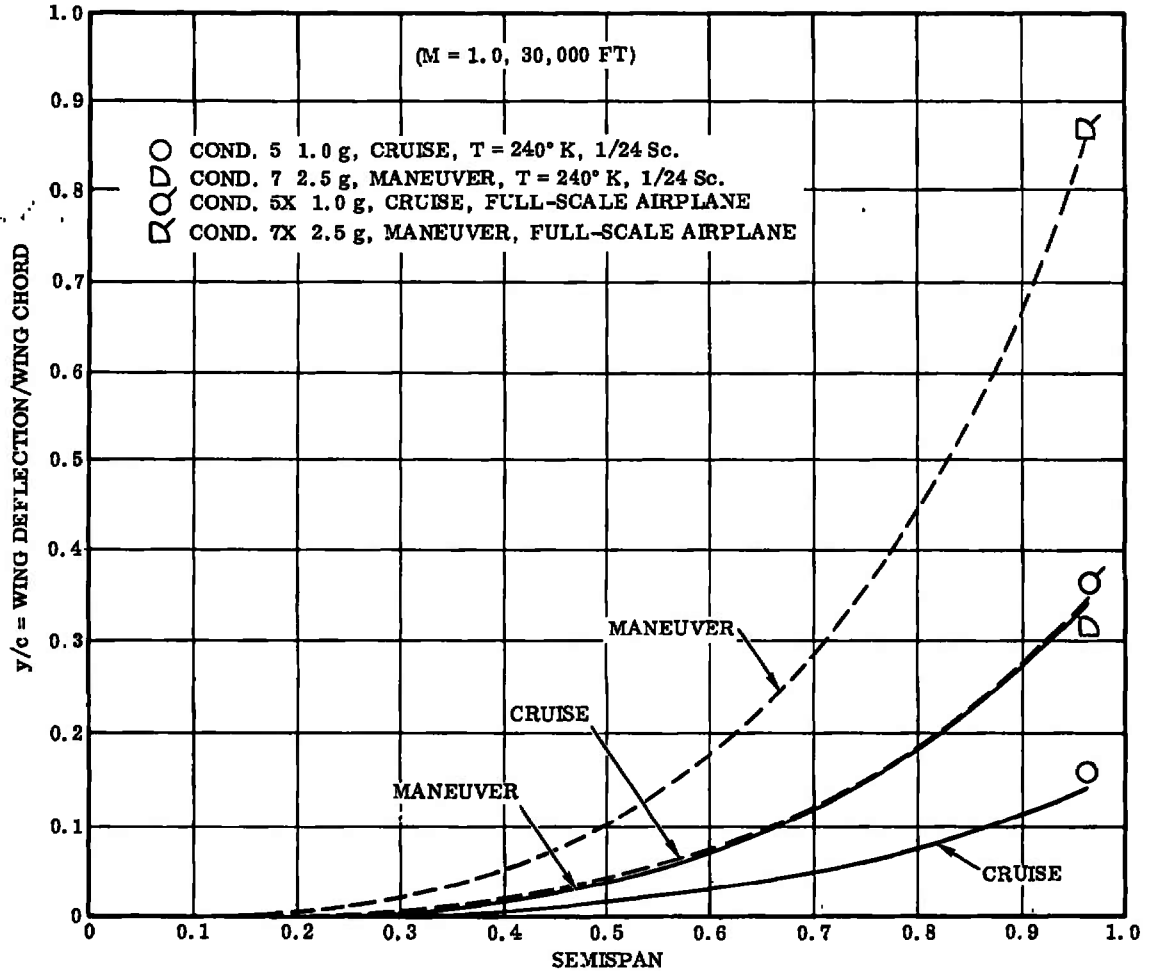

Figure 45. ATT – Wing Deflections – 1/24 Scale Model and Full-Scale Airplane

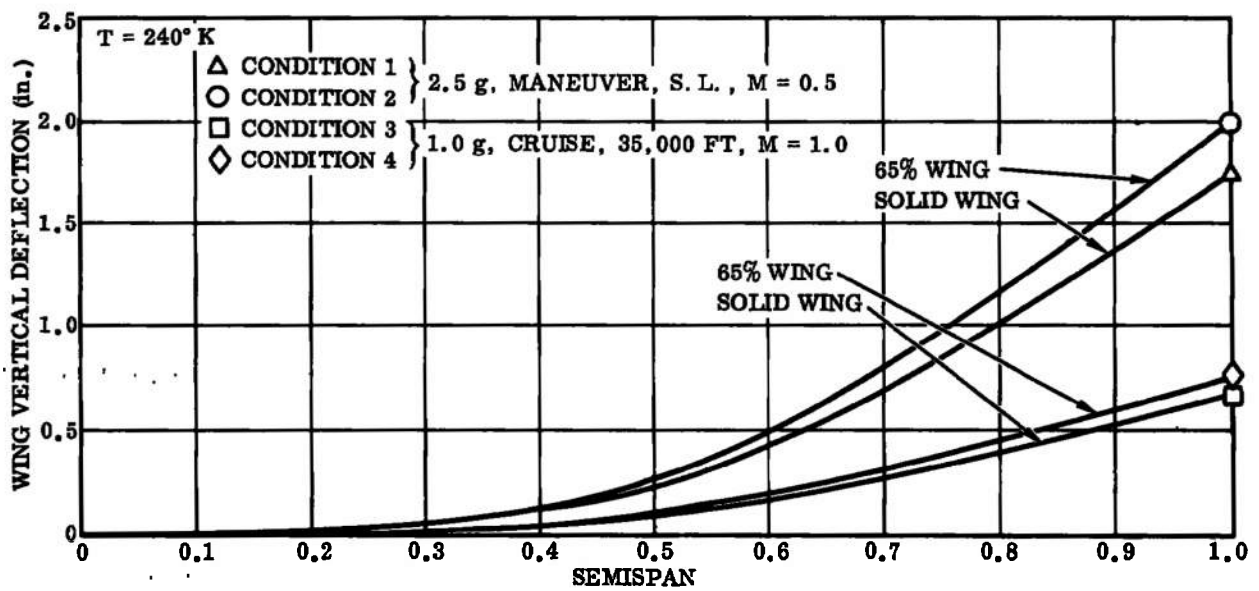

Figure 46. ATT — Effect on Deflection Due to Removing Aft 35% Chord

8.4.3 1/12 Scale F-111 Model

The 50-degree sweep version of the F-111 is the highest loaded configuration. The aeroelastic wing twists for the 50-degree wing sweep version of the F-111 model are presented in Figure 47. Maximum wing twists vary from -1.29 degrees (solid) and -1.4 degrees (65% C) at cruise to -4.83 degrees (solid) and -5.42 degrees (65% C) at 6.0 g maneuver.

Maximum wing deflections vary from 0.42 inch to 2.37 inches. The wing deflections for the F-111 configurations are shown in Figure 48.

The effects of wing sweep and airplane envelope restrictions on the F-111 solid-wing elastic twists and deflections are illustrated in Figures 49 and 50.

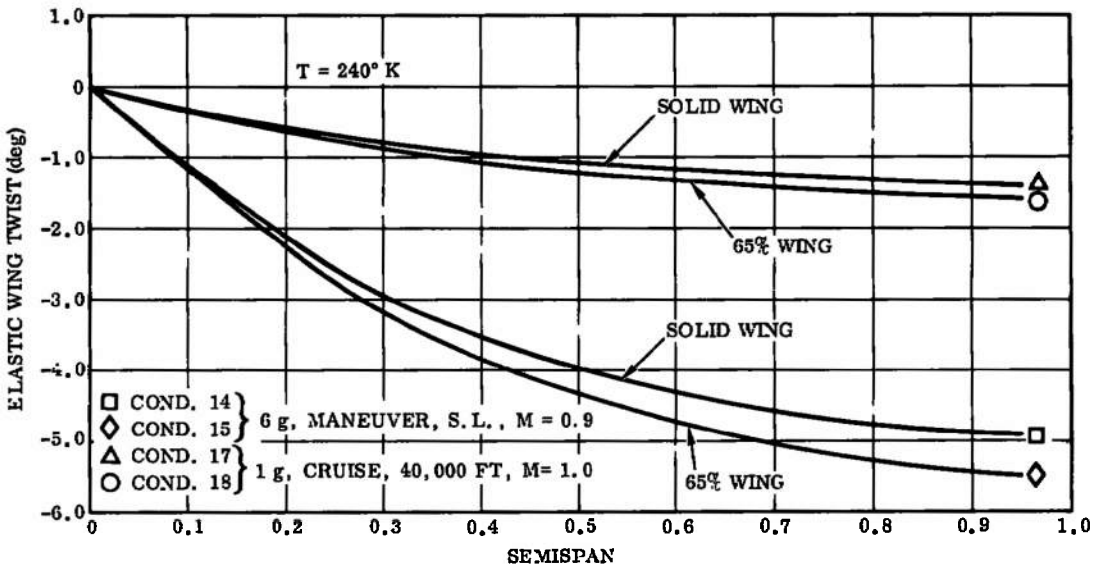

Figure 47. F-111 (50 Deg) – Elastic Wing Twist

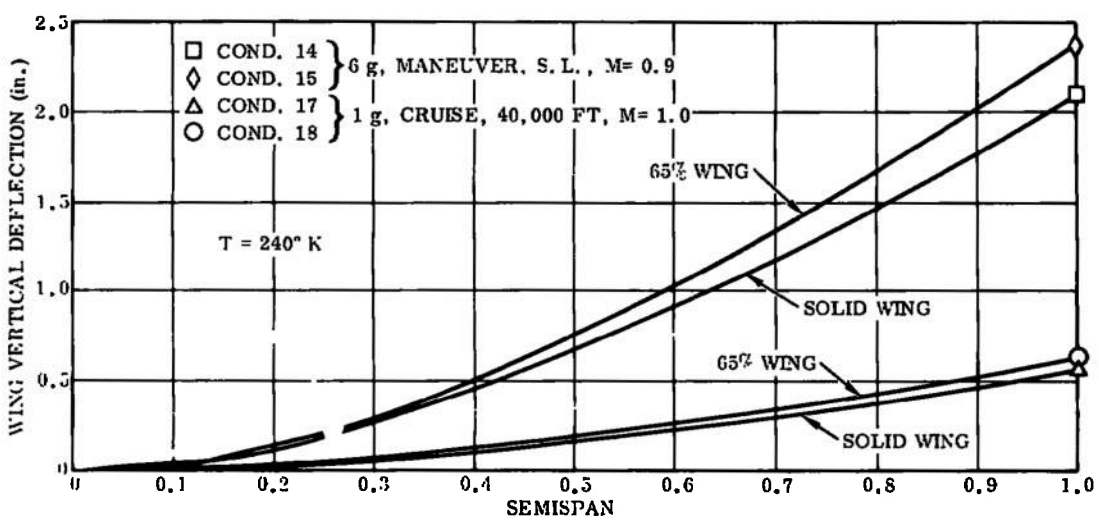

Figure 48. F-111 (50 Deg) – Wing Deflections

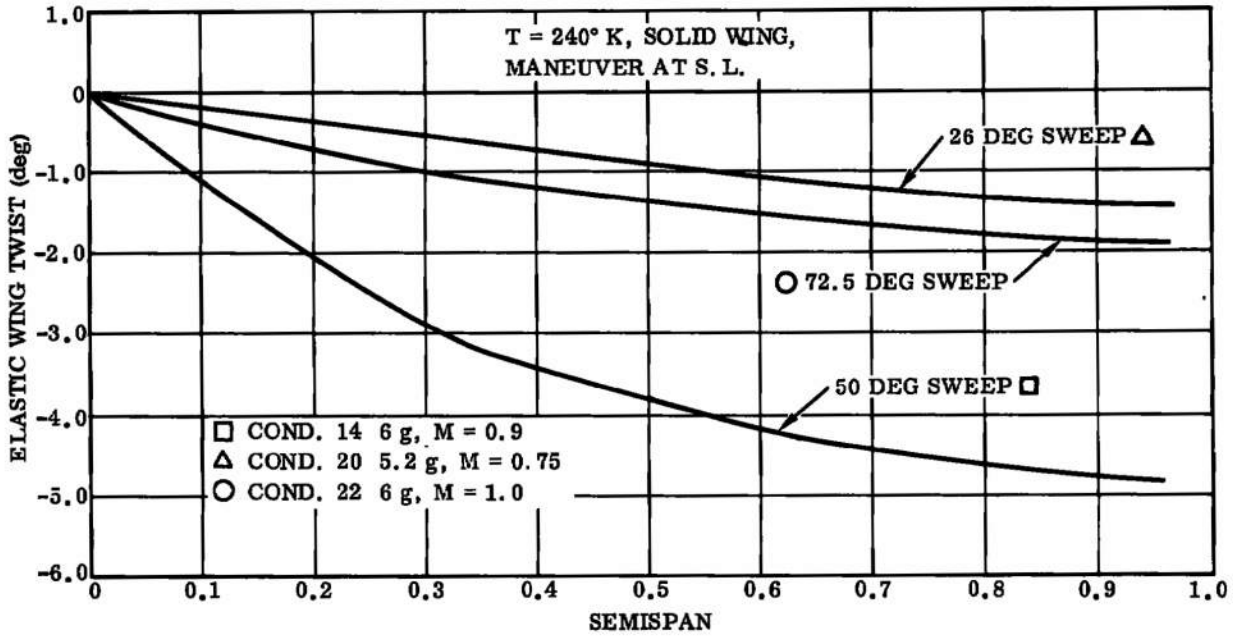

Figure 49. F-111 - Elastic Wing Twist vs Wing Sweep

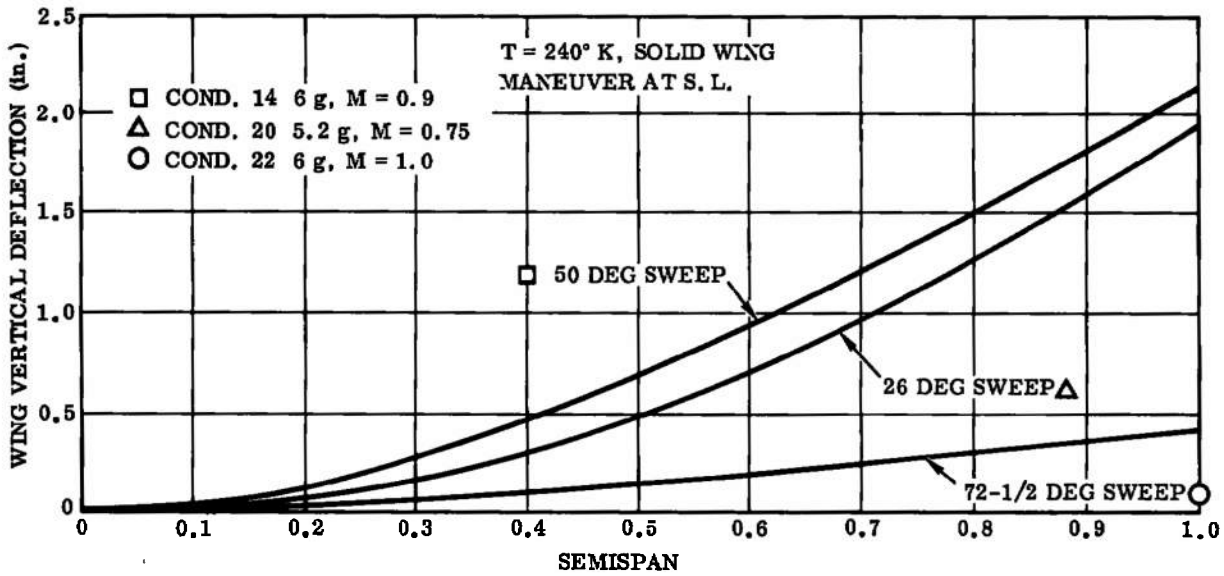

Figure 50. F-111 – Wing Deflections vs Wing Sweep

8.4.4 Delta Canard Fighter

The maximum aeroelastic twists on the delta canard fighter model solid wing vary from 0.4 degree at cruise to 1.73 degrees in a 7.5 g maneuver at 240°K tunnel conditions and up to 2.35 degrees for an ambient temperature condition. Removal of the aft 35% of the wing structure for control surfaces, etc., results in a twist of 4.92 degrees at 240°K. (Note: excessive wing twist outboard of 0.65 semispan due to removing a constant percent chord from a delta wing. In practice, this would be avoided.) Wing-tip deflections vary from zero to 0.4 inch for solid wings and zero to 0.7 inch for the 70% version. Model wing twists and deflections for the delta canard are shown in Figures 51 and 52.

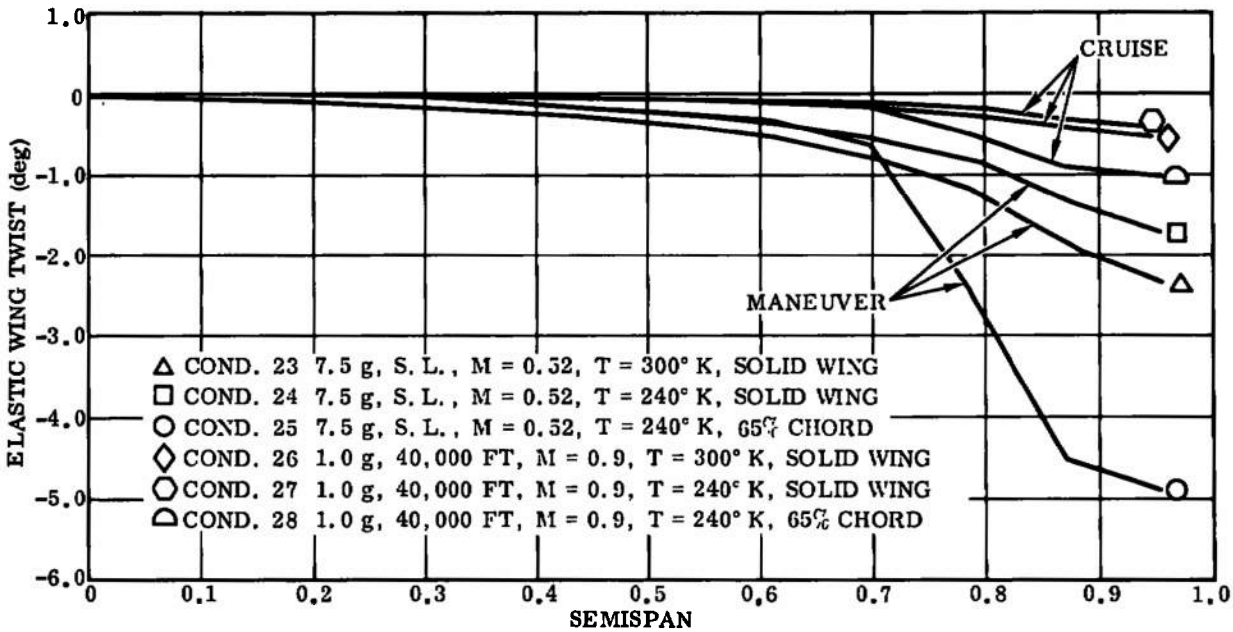

Figure 51. Delta Canard — Elastic Wing Twist

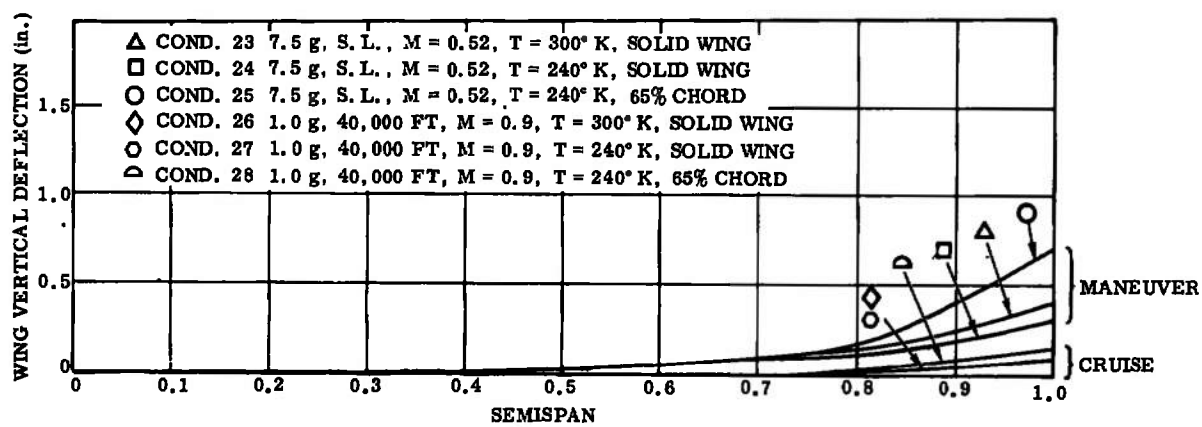

Figure 52. Delta Canard — Wing Deflection

8.4.5 Space Shuttle Booster

The space shuttle booster wing has a relatively low wing loading when compared to high aspect ratio vehicles. The deformation of this wing under the maximum loading conditions at 300°K results in only 0.25 degree twist and 0.8 inch deflection at the wing tip. Model wing twist is illustrated in Figure 53 and model wing deflection in Figure 54.

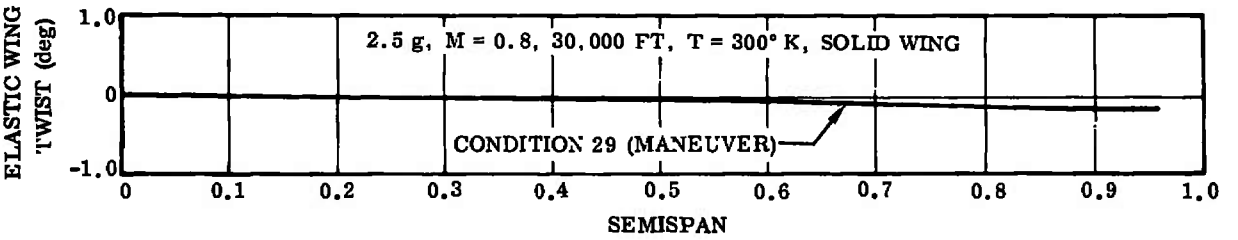

Figure 53. Space Shuttle Booster – Elastic Wing Twist

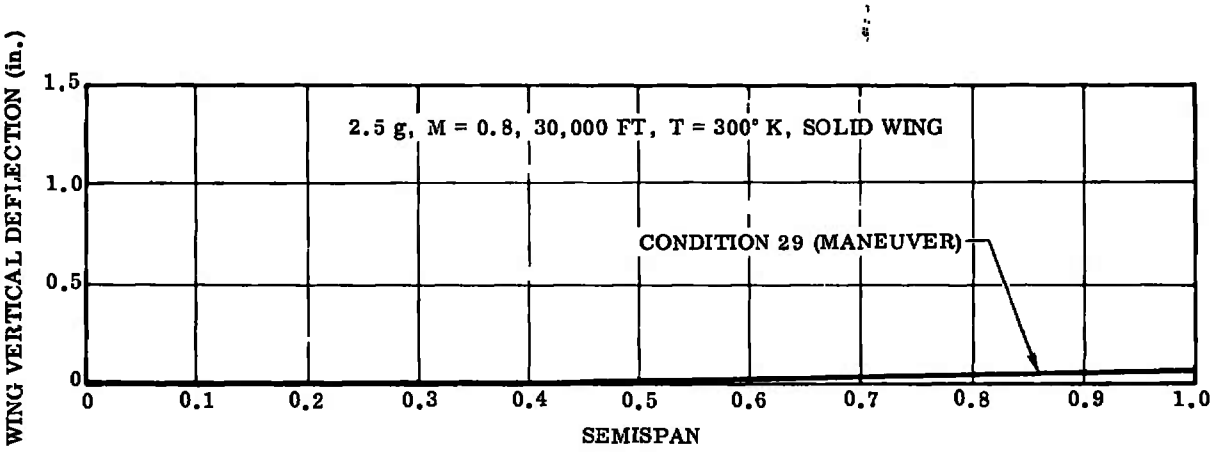

Figure 54. Space Shuttle Booster – Wing Deflection

8.5 MODEL SCALE EFFECTS ON WING DEFORMATION

The ATT model was selected to illustrate the effects on various model parameters due to a change in model scale of 1.5 and 2.0. Model test conditions 37 through 44 (Table 2), were computed for this study. Conditions 37, 38 and 39, 40 are equivalent to conditions 5 and 7. Conditions 41, 42 and 43, 44 are equivalent to conditions 10 and 12. Tunnel operating pressure and temperature were varied to provide the same $R_{e_{MAC}}$ for each of the three model sizes.

The effects of scale and temperature on wing twist are illustrated in Figure 55. The maximum wing twist at ambient temperature (300°K) and basic model scale (1/24) at the 2.5-g maneuvering condition is 4.1 degrees. The twist is reduced from 4.1 degrees to 3.1 degrees and to 2.5 degrees by changing the model scale from 1/24 to 1/16 and to 1/12. Note that the 4.1-degree twist can be reduced to 3.25 degrees by operating the tunnel at -30° F (240°K).

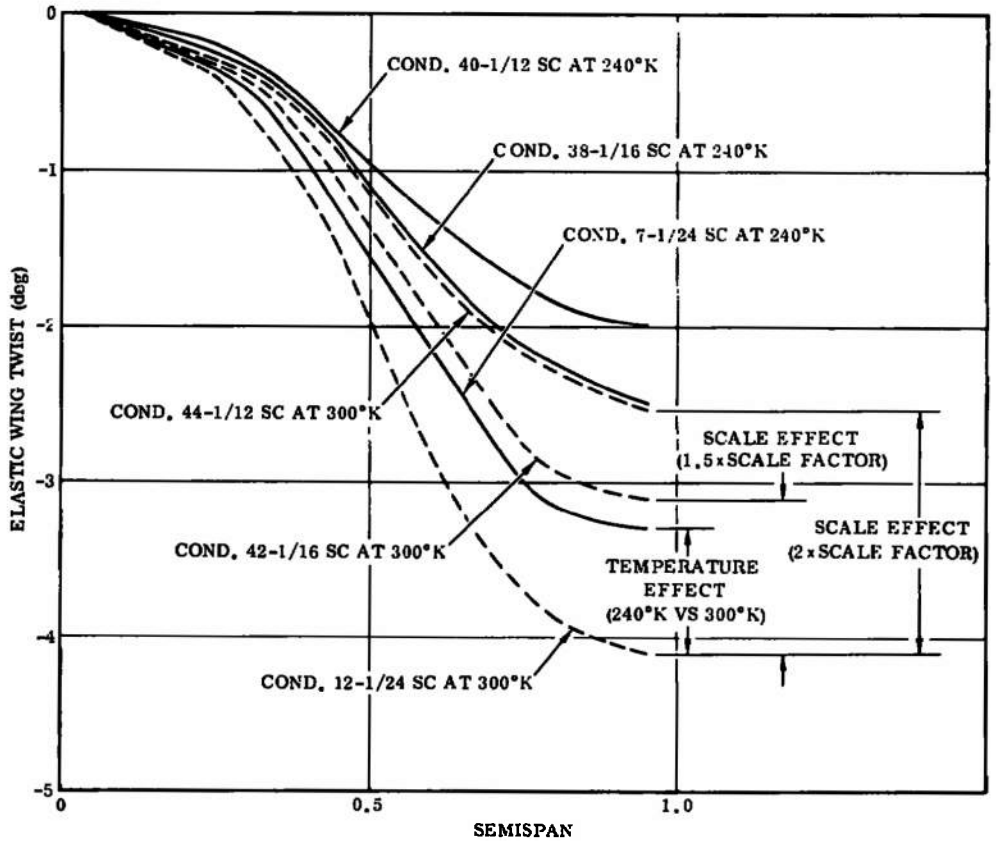

Figure 55. ATT – Elastic Wing Twist vs Tunnel Temperature and Model Scale

8.6 REYNOLDS NUMBER EFFECT ON WING DEFORMATION

The effect on wing twist due to running at a reduced Reynolds number (i.e., dynamic pressure) is shown in Figure 56. Test conditions 7a, 7b, and 7c (Table 2) are the same as condition 7 except that they represent a variety of Reynolds numbers, all of which are less than full scale. The maximum wing twist for the 1/24-scale ATT model at -30°F (240°K) tunnel operating temperature is -3.4 degrees at $R_e/ft = 70 \times 10^6$ (a model $R_{e_{MAC}}$ equivalent to the full-scale airplane $R_{e_{MAC}}$). Wing twist is reduced to 2.6 degrees, 2.1 degrees, and 1.8 degrees by reducing the Reynolds numbers to 49.5×10^6, 39.5×10^6, and 29.5×10^6 respectively. Note that decreasing the Reynolds number by 50% reduces the wing twist to the same value as computed for the 1/12 scale model (Figure 55).

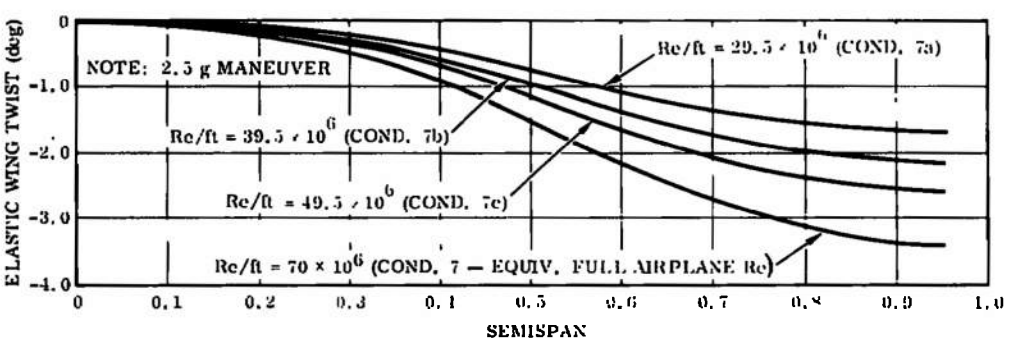

Figure 56. ATT — Effect of Reynolds Number on Wing Twist

SECTION IX

STRUCTURAL ANALYSIS

The basic structural analyses performed on each of the model configurations are:

a. Basic wing stresses.

b. Wing/fuselage attachment.

c. Empennage stresses.

d. Empennage attachment.

e. The degradation of maximum allowable loading due to:

   1. Incorporation of pressure orifices in the wing.

   2. Removal of an aft portion of the wing to allow for control-surface attachments.

f. Model sting stress and deflection. Note: since no balance stiffness data is available, an estimated angle of rotation was used for sting/balance deflection analysis.

Each model is analyzed to determine working stress levels. PH13-8 Mo steel, heat treated to an H1000 condition, is used as a baseline material for each configuration. (The mechanical properties of 13-8 PH steel are found in Table 12.)

Structural analyses are based on 240°K operation unless noted otherwise. Table 5 presents a summary of model achieved safety factor.

9.1 ATT MODEL

The critical section for the ATT model wing is located at the intersection of wing station 14.87 and the elastic axis and is labeled Section 4. (Figure 57.) The maximum wing bending stress varies from 72,200 psi for a solid wing to 94,000 psi for the pressure wing configuration. Stresses for the various wing configurations at the maximum maneuver test condition (Condition 7) are shown in Figure 58.

The change in stress level of the critical wing section (Section 4) due to varying the model angle of attack and $Re\,C_L$ to match the aircraft operating envelope is illustrated in Figure 59. The values of $Re\,C_L$ (13.73, 24.07 and 34.40 millions) represent 1.0 g, 1.75 g, and 2.5 g conditions at M = 1.0, 30,000 feet (conditions 5, 6 and 7 in Table 2).

A wing-to-fuselage attachment analysis shows that there are no particular problems in that area.

Table 5. Stress Analysis – Minimum Safety Factor Summary

Model	Location	Mode	S. F.
Delta-Canard 1/9.6 scale			
Screws, wing to fuselage	Juncture, wing to fuselage	Shear	2.26
Screws, tail to fuselage	Juncture, tail to fuselage	Tension	2.12
Tail	Base section	Bending	2.32
Screws, canard to fuselage	Juncture, canard to fuselage	Tension	3.61
Sting support	Station 68.44	Bending	2.88
F-111 – 1/12 scale			
Solid wing	Section A (ref. page 114)	Bending + torsion	2.86
65% solid wing	Section A (ref. page 114)	Bending + torsion	2.48
100% pressure wing	Section A (ref. page 114)	Bending + torsion	2.11
65% pressure wing	Section A (ref. page 114)	Bending + torsion	1.92
Horizontal tail	Section AA (10 deg incidence)	Bending + torsion	1.29
Sting (constant dia)	Station 71.667	Bending	2.43
Sting (tapered)	Station 71.667	Bending	2.43
Space Shuttle			
Solid wing	B. L. 4.15	Bending + torsion	32.27
Pressure wing	B. L. 4.15	Bending + torsion	25.16
Tail	Base section	Bending + torsion	5.63
Screws, tail to fuselage	Juncture, tail to fuselage	Tension	3.91
Sting support	Station 77.49	Bending	4.94
ATT 1/24 scale			
Solid wing	Station 14.87	Bending	2.78
65% solid wing	Station 14.87	Bending	2.61
100% pressure wing	Station 14.87	Bending	2.14
65% pressure wing	Station 14.87	Bending	2.69
Screws, T.E. joint	Station 13.33	Shear	1.93
Dowels, wing-fuselage	Juncture, wing to fuselage	Shear	2.15
Screws, horizontal tail	Horizontal to vertical tail	Tension	2.80
Screws, vertical tail	Vertical tail to fuselage	Tension	3.12
Maneuver sting	Station 91.667	Bending	3.81
Cruise sting	Station 91.667	Bending	3.26
ATT 1/16 scale			
Solid wing	Station 22.305	Bending	2.91
ATT 1/12 scale			
Solid wing	Station 29.74	Bending	3.63

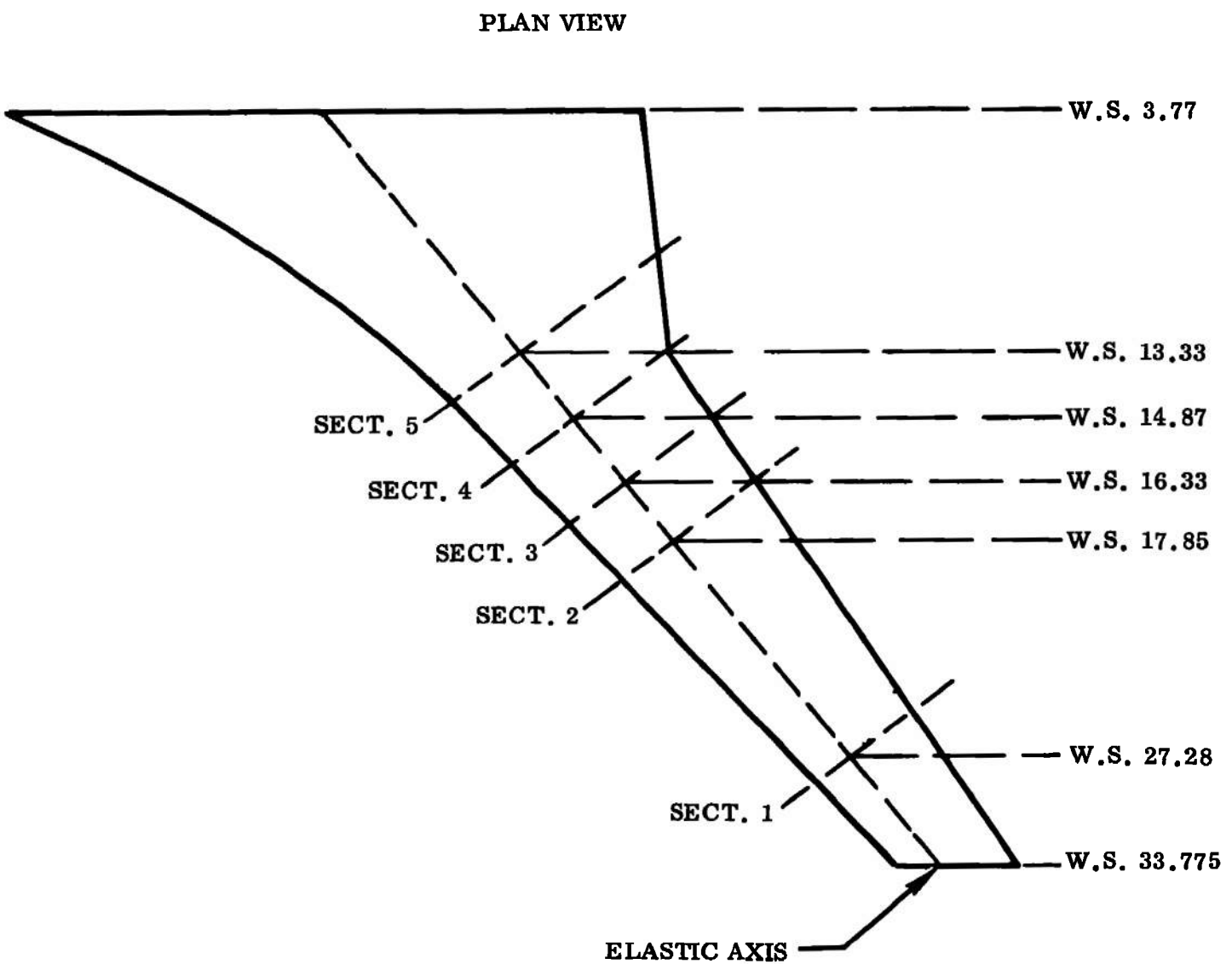

Figure 57. ATT Wing — Location of Sections Used For Structural Analysis

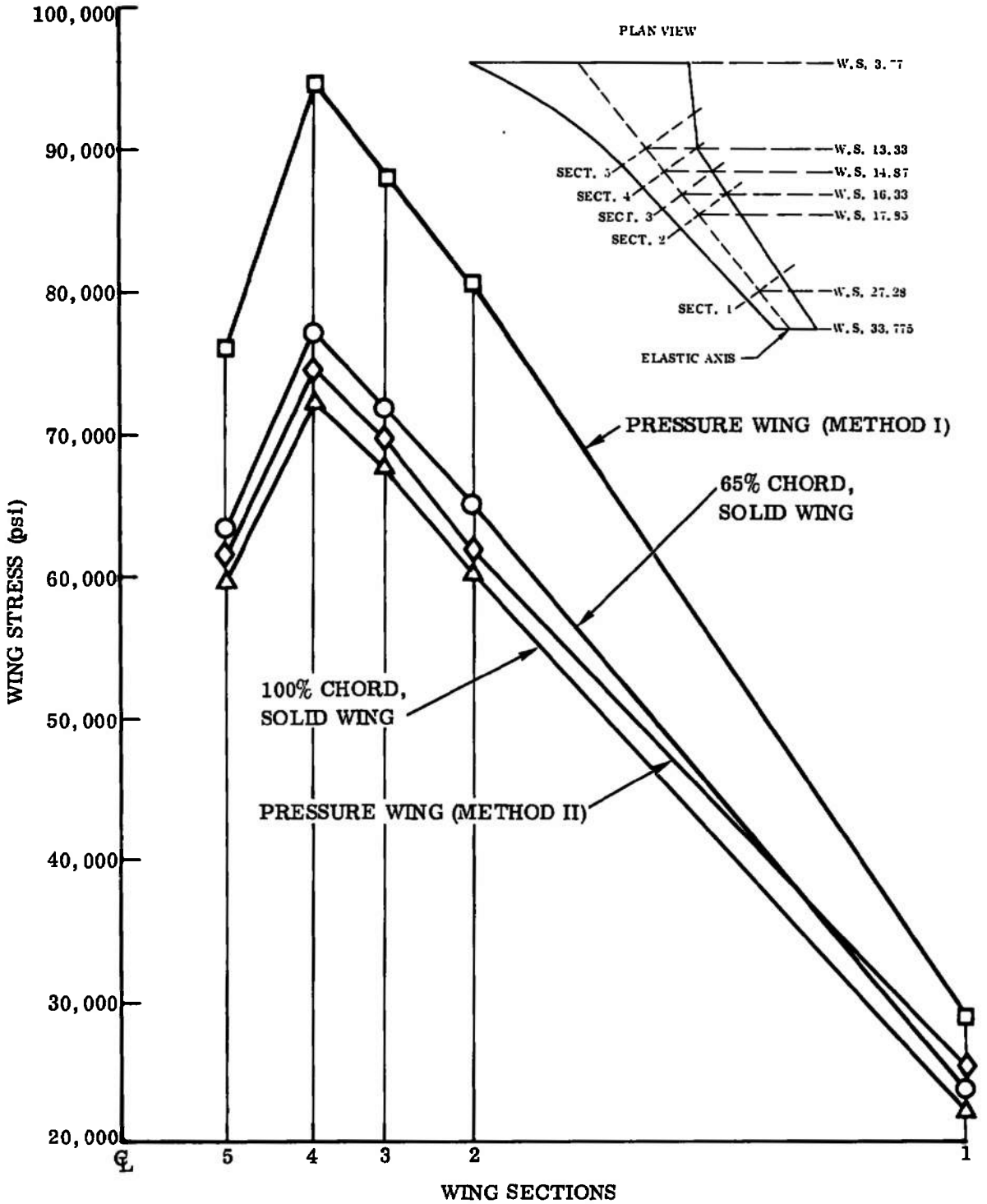

Figure 58. ATT – Comparison of Wing Types vs Stress (Condition 7)

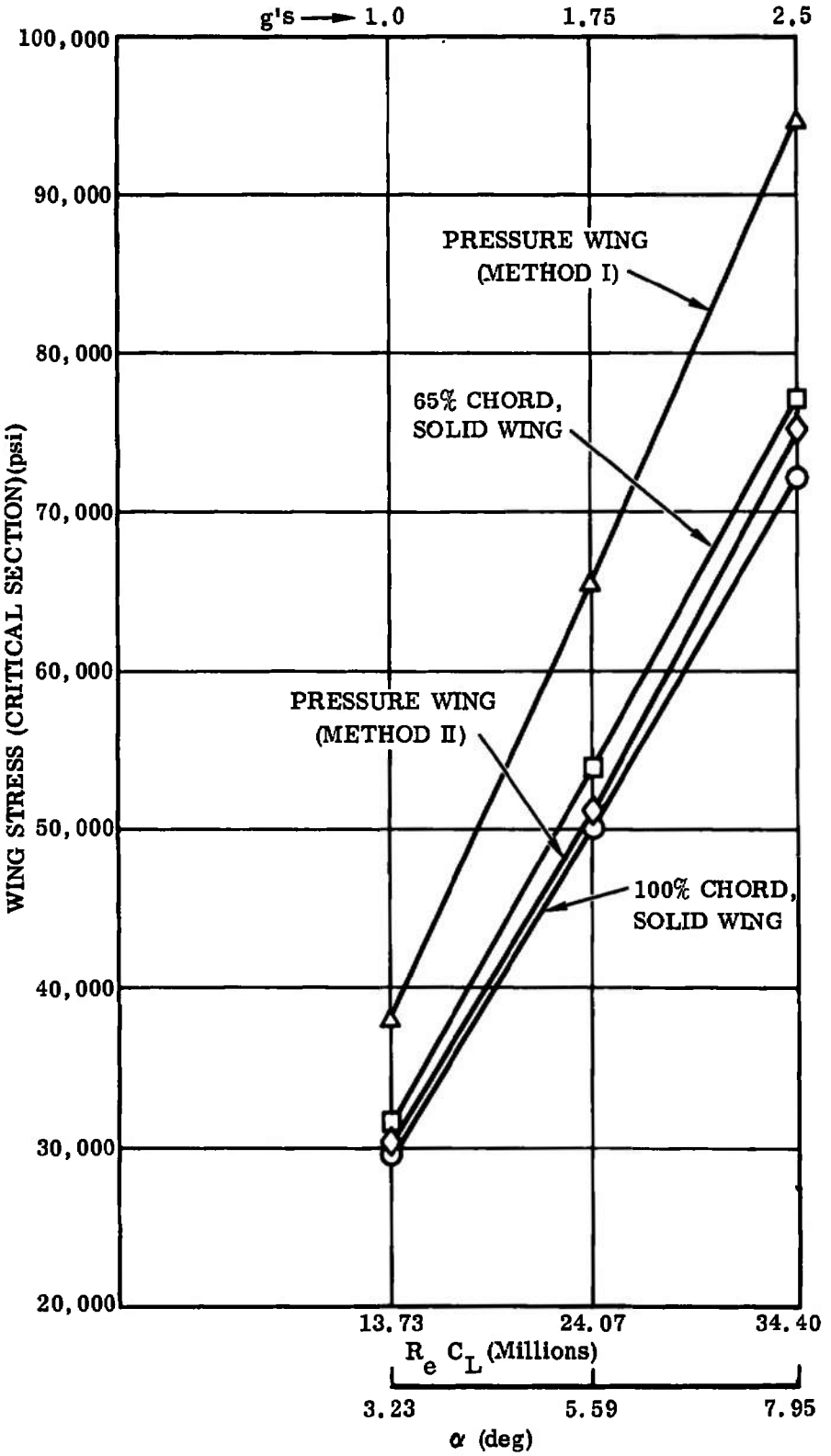

Figure 59. ATT — Wing Stress at Wing Section 4 Resulting from Matching Flight Conditions for M = 1.0 at 30,000 ft from 1.0 g to 2.5 g's.

Horizontal tail stresses are small if the horizontal tail is fabricated in one piece. The vertical tail stresses are also quite standard.

The attachment of fuselage-mounted, flow-through type engine nacelles is no structural problem. Engine simulators should not be too difficult to install physically but may be very difficult or even impossible to operate in the high dynamic pressure environments of the HIRT tunnel.

A representative sting and balance combination indicates that combinations of sting diameter and model cavities can be found to handle the model loads.

9.1.1 ATT Model Scale Effects on Stress

The basic ATT configuration is 1/24 scale. When model loads were revised to simulate the same test conditions ($R_{e_{MAC}}$ of the model equal to $R_{e_{MAC}}$ of the airplane) for 1/16 scale and 1/12 scale models, the stress levels were reduced. Maximum wing stress for a solid-wing configuration decreased from 72,200 psi for 1/24 scale to 69,000 psi for 1/16 scale and 55,295 psi for 1/12 scale. Figure 60 illustrates the effects of model scale and tunnel operating temperature on the ATT model wing stresses.

9.1.2 Detailed Stress Analysis — 1/24 - Scale Model

The analysis is performed on four different ATT wing configurations:

a. 100% chord solid wing.

b. 65% chord solid wing.

c. 100% chord pressure wing (Method I).

d. 65% chord pressure wing (Method II).

Bending stresses have been calculated for three conditions: Conditions 5, 6, and 7 (reference Table 2). (The resulting range of stresses experienced are plotted versus Reynolds numbers in Figure 59.)

The following analyses use section properties contained in Figure 61.

Solid Wing Configuration (Reference Figure 7)

The wing is machined from PH 13-8 Mo stainless steel and heat treated to condition H1000. Wing Sections 1 through 5 (Figure 57) are used for each of the wing analyses. Section properties and the results of the 100% chord solid wing analysis are presented in Table 6.

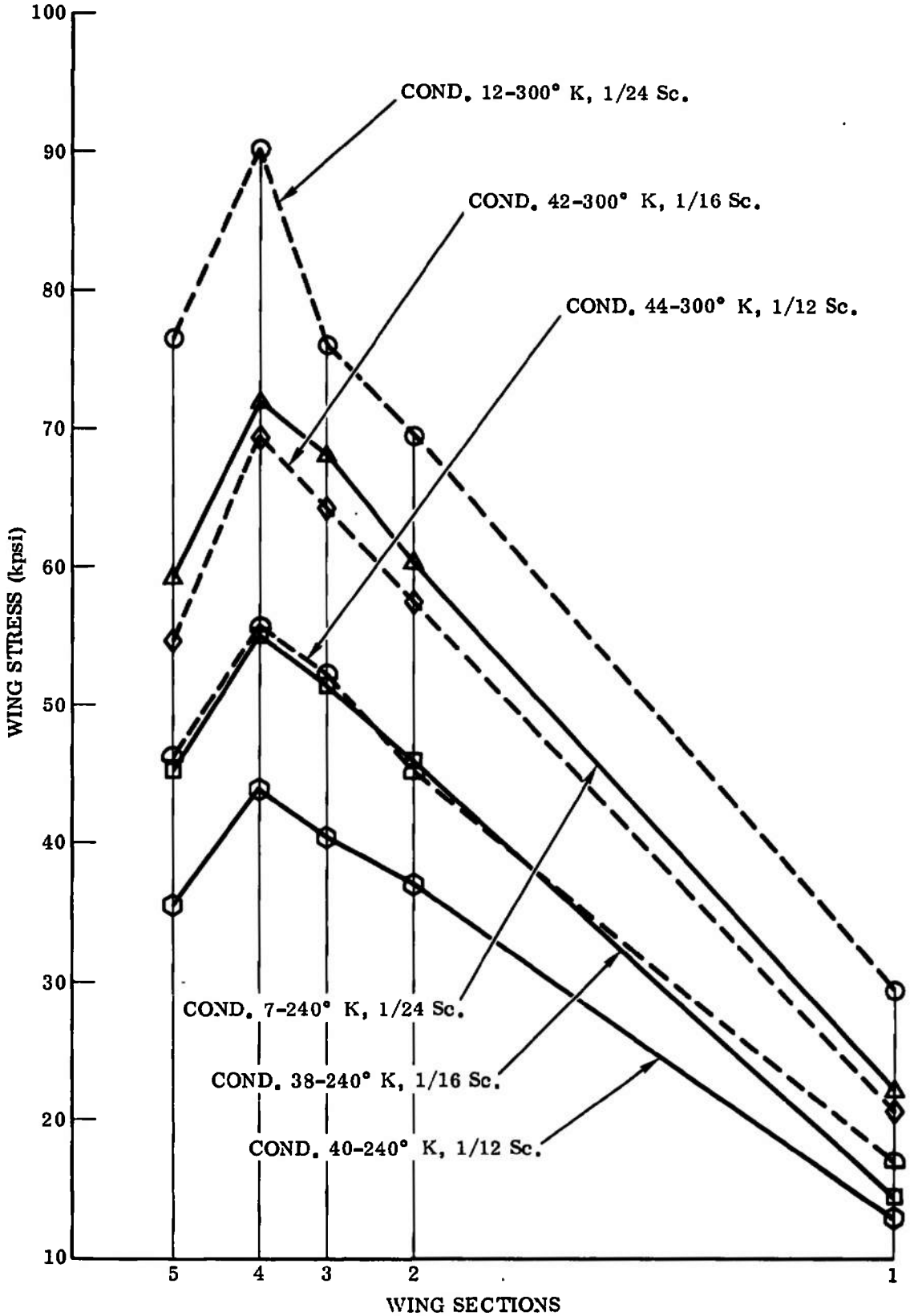

Figure 60. ATT – Comparison of Wing Stresses vs Tunnel Temperature and Model Scale

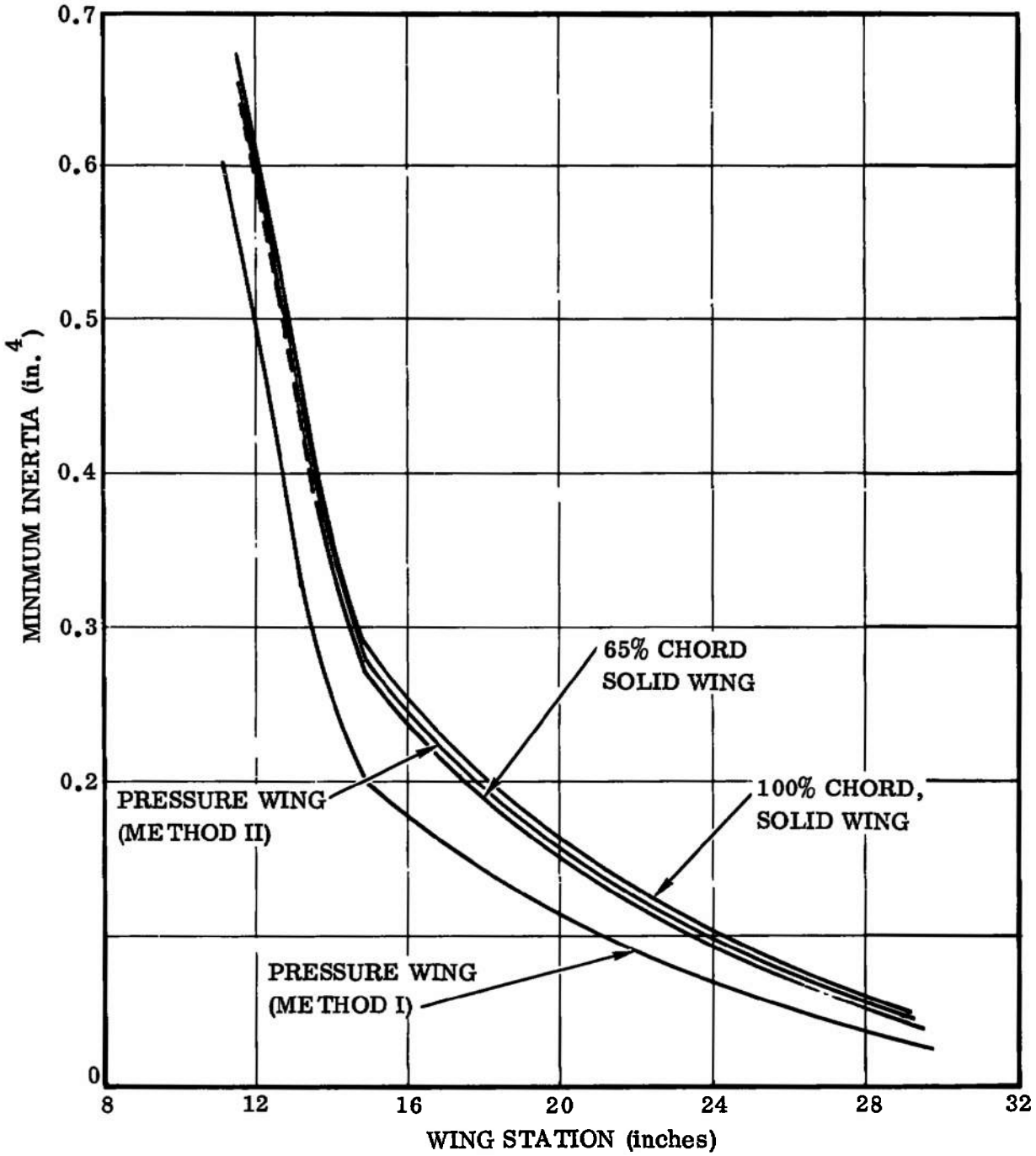

Figure 61. ATT Wing — Minimum Inertias

Table 6. ATT Wing Section Properties and Bending Analysis — 100% Chord Solid Wing

TYPICAL CROSS SECTION

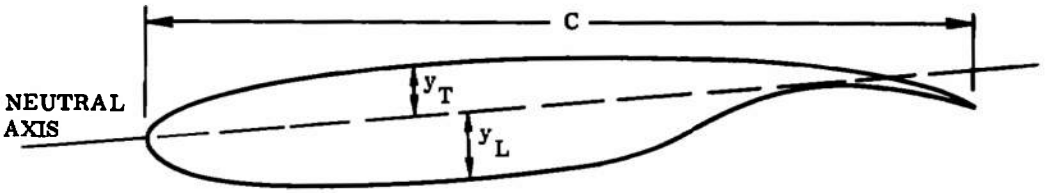

SECTION PROPERTIES

Section (Ref. Fig. 57)	Wing station (in.)	C (in.)	y_T (in.)	y_L (in.)	I_{min} (in.^{4})
1	27.28	4.78	0.32	0.37	0.0637
2	17.85	6.42	0.44	0.48	0.2074
3	16.33	6.69	0.46	0.50	0.2446
4	14.87	8.20	0.48	0.52	0.2880
5	13.33	9.78	0.51	0.55	0.4470

BENDING ANALYSIS (240°K)

Condition	Section	Wing station (in.)	$M_{E.A.}$ (in-lb)	f_b (psi)	F_b (psi)	S. F.
5	1	27.28	2,310	13,418	201,000	14.98
	2	17.85	10,000	23,144	201,000	8.68
	3	16.33	13,100	26,778	201,000	7.51
	4	14.87	16,200	29,250	201,000	6.87
	5	13.33	20,000	24,608	201,000	8.17
6	1	27.28	3,080	17,890	201,000	11.24
	2	17.85	18,500	42,816	201,000	4.69
	3	16.33	21,600	44,154	201,000	4.55
	4	14.87	27,700	50,014	201,000	4.02
	5	13.33	34,600	42,573	201,000	4.72
7	1	27.28	3,850	22,362	201,000	8.99
	2	17.85	26,200	60,636	201,000	3.31
	3	16.33	33,100	67,661	201,000	2.97
	4	14.87	40,000	72,222	201,000	2.78
	5	13.33	48,300	59,429	201,000	3.38
			300°K			
12	1	27.28	5,000	29,000	201,000	6.94
	2	17.85	30,000	69,400	201,000	2.90
	3	16.33	38,000	76,500	201,000	2.63
	4	14.87	50,000	90,200	201,000	2.23
	5	13.33	62,000	76,300	201,000	2.64

65% Chord Solid Wing (Ref. Figure 7)

The aft 35% of the wing is removable. The material for both portions is PH 13-8 Mo H1000 stainless steel. The bending sections considered have the same locations as the solid wing sections. Section properties and the results of the bending analysis of the 65% chord solid wing configuration are presented in Table 7.

Table 7. ATT Wing Section Properties and Bending Analysis — 65% Chord Solid Wing

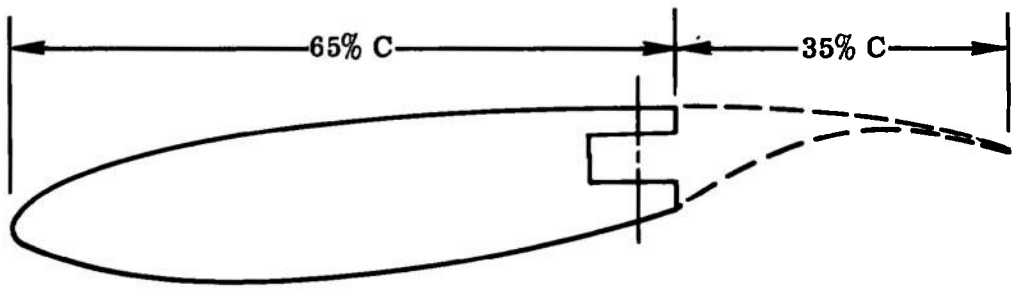

SECTION PROPERTIES (T.E. CONSIDERED INEFFECTIVE)

Section (Ref. Fig. 57)	Wing station (in.)	C (in.)	y_T (in.)	y_L (in.)	I_{min} (in.^{4})
1	27.28	4.78	0.32	0.37	0.0599
2	17.85	6.42	0.45	0.47	0.1893
3	16.33	6.69	0.46	0.50	0.2294
4	14.87	8.20	0.48	0.52	0.2698
5	13.33	9.78	0.51	0.55	0.4183

PRIMARY BENDING ANALYSIS (240°K)

Condition	Section	Wing station (in.)	$M_{E.A.}$ (in-lb)	f_b (psi)	F_b (psi)	S. F.
5	1	27.28	2,310	14,269	201,000	13.74
	2	17.85	10,000	24,828	201,000	8.10
	3	16.33	13,100	28,553	201,000	7.04
	4	14.87	16,200	31,223	201,000	6.44
	5	13.33	20,000	26,297	201,000	7.64
6	1	27.28	3,080	19,025	201,000	10.57
	2	17.85	18,500	45,932	201,000	4.38
	3	16.33	21,600	47,079	201,000	4.27
	4	14.87	27,700	53,388	201,000	3.76
	5	13.33	34,600	45,498	201,000	4.42
7	1	27.28	3,850	23,781	201,000	8.45
	2	17.85	26,200	65,051	201,000	3.09
	3	16.33	33,100	72,145	201,000	2.79
	4	14.87	40,000	77,094	201,000	2.61
	5	13.33	48,300	63,507	201,000	3.19

100% Chord Pressure Model (Method I) (Ref. Figure 11)

The wing is machined from PH 13-8 Mo H1000 stainless steel. The bending sections under consideration have the same locations as those used for the other ATT wing configurations. The results of the stress analysis and the section properties for the Method I pressure model are presented in Table 8.

Table 8. ATT Wing Section Properties and Bending Analysis — 100% Chord Pressure Model (Method I)

EFFECTIVE CROSS SECTION AT PRESSURE PICKUP LOCATION

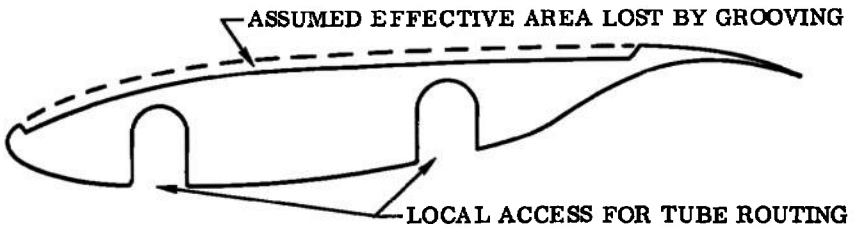

SECTION PROPERTIES

Section (Ref. Fig. 57)	Wing station (in.)	C (in.)	y_T (in.)	y_L (in.)	I_{min} (in.^{4})
1	27.28	4.78	0.29	0.33	0.0441
2	17.85	6.42	0.40	0.44	0.143
3	16.33	6.69	0.42	0.45	0.169
4	14.87	8.20	0.43	0.47	0.200
5	13.33	9.78	0.46	0.49	0.310

BENDING ANALYSIS (240°K)

Condition	Section	Wing station (in.)	$M_{E.A.}$ (in-lb)	f_b (psi)	F_b (psi)	S. F.
5	1	27.28	2,310	17,286	201,000	11.63
	2	17.85	10,000	30,769	201,000	6.53
	3	16.33	13,100	34,881	201,000	5.76
	4	14.87	16,200	38,070	201,000	5.28
	5	13.33	20,000	31,613	201,000	6.36
6	1	27.28	3,080	23,048	201,000	8.72
	2	17.85	18,500	56,923	201,000	3.53
	3	16.33	21,600	57,515	201,000	3.49
	4	14.87	27,700	65,095	201,000	3.09
	5	13.33	34,600	54,690	201,000	3.68
7	1	27.28	3,850	28,810	201,000	6.98
	2	17.85	26,200	80,615	201,000	2.49
	3	16.33	33,100	88,136	201,000	2.28
	4	14.87	40,000	94,000	201,000	2.14
	5	13.33	48,300	76,345	201,000	2.63

65% Chord Pressure Model (Method II) (Ref. Figure 12)

The aft 35% of the wing is removable. The material for both portions is PH 13-8 Mo H1000 stainless steel. The bending sections under consideration have the same locations as those used for the solid wing sections. The stress analysis and section properties for this configuration are presented in Table 9.

Table 9. ATT Wing Section Properties and Bending Analysis — 65% Chord Pressure Model (Method II)

TYPICAL CROSS SECTION

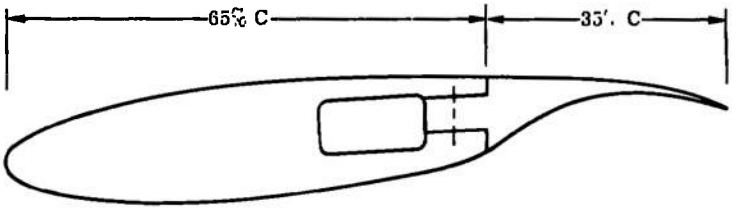

SECTION PROPERTIES (T.E. CONSIDERED EFFECTIVE)

Section (Ref. Fig. 57)	Wing section (in.)	C (in.)	y_T (in.)	y_L (in.)	I_{min} (in.^{4})
1	27.28	4.78	0.32	0.37	0.0563
2	17.85	6.42	0.45	0.47	0.2000
3	16.33	6.69	0.46	0.50	0.2371
4	14.87	8.20	0.48	0.52	0.2780
5	13.33	9.78	0.51	0.55	0.4350

BENDING ANALYSIS (240°K)

Condition	Section	Wing station (in.)	$M_{E.A.}$ (in-lb)	f_{bmax} (psi)	F_b (psi)	S. F.
5	1	27.28	2,310	15,181	201,000	13.24
	2	17.85	10,000	23,500	201,000	8.55
	3	16.33	13,100	27,625	201,000	7.28
	4	14.87	16,200	30,302	201,000	6.63
	5	13.33	20,000	25,287	201,000	7.95
6	1	27.28	3,080	20,242	201,000	9.93
	2	17.85	18,500	43,475	201,000	4.62
	3	16.33	21,600	45,550	201,000	4.41
	4	14.87	27,700	51,813	201,000	3.93
	5	13.33	34,600	43,747	201,000	4.59
7	1	27.28	3,850	25,302	201,000	7.94
	2	17.85	26,200	61,570	201,000	3.26
	3	16.33	33,100	69,802	201,000	2.88
	4	14.87	40,000	74,820	201,000	2.69
	5	13.33	48,300	61,069	201,000	3.29

Trapezoidal Distribution for C.P. at 40.5%

From the torsional load plots, Figure 29, the c.p. coincides with the E.A. at 40.5% C.

For Section 3,

		% of Section Stiffness
$I_{42\%}$	= 0.159 in.^{4}	67
$I_{48.5\%}$	= 0.181 in.^{4}	76
$I_{65\%}$	= 0.221 in.^{4}	93
$I_{100\%}$	= 0.237 in.^{4}	100

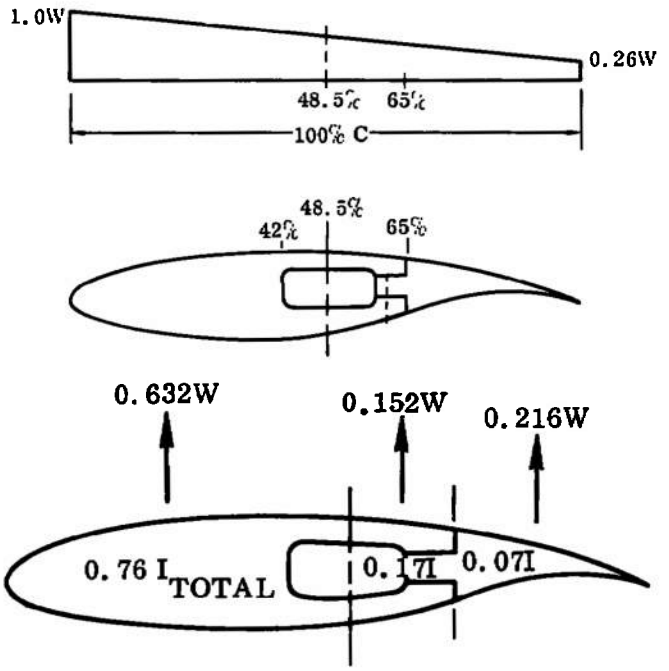

For the preceding chordwise distribution (running chordwise load, W) the distribution over three segments is shown at right.

From shear plot, Figure 29, W = 300 lb/in. at Section 3.

Since the 35% trailing edge portion of the wing deflects in unison with the 65% portion, it tends to carry loads in direct proportion between its stiffness and the stiffness offered by the 65% portion. Therefore loads in excess of this amount must be transferred to the forward section.

Using this approach, the following analysis of the trailing edge attachments and relieved out area is made:

Amount of load carried by T. E. (aft 35% chord) = 0.07 W,

∴ Load Trans. Fwd = 0.146 W

Amount of load carried by 48.5% → 65% = 0.17 W,

∴ Load Trans. Fwd = 0.138 W

From the above, 0.146 W must be transmitted across the trailing edge attachment. Also from the above, 0.133 W must be transmitted across the relieved-out area.

Trailing Edge Joint Analysis for Typical Section

M at line of attach = 43.8 × 141

= 61.6 in-lb

Screw shear = 61.6 ÷ 0.44

= 140 lb

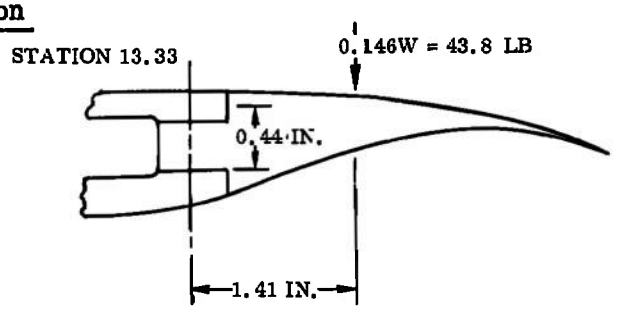

Additional $\frac{VQ}{I}$ shear:

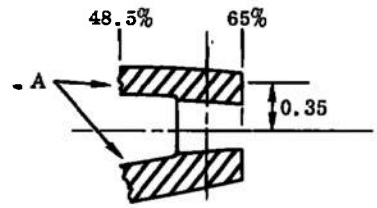

48.5% C → 65% C Inertia = 0.040 in.^{4}
(Ref. page 122)

$$V_{section} = 0.17\ (V_{total}) = 0.17 \times 3800$$

$$= 645 \text{ lb}$$

$$A = 0.82 \text{ in.} \times \overline{0.19} = 0.156 \text{ in.}^2$$

$$\text{Shear at screw shear face} = \frac{VQ}{I} = \frac{645\ (0.156 \times 0.35)}{0.040} = 880 \text{ lb/in.}$$

$$\text{Resultant screw shear} = 140 \nearrow 880 = 892 \text{ lb/in.}$$

$$\text{No. 10 screws at 1.0-in. spacing, } S_{allow} = \frac{95}{160}\ (2,892) = 1,718 \text{ lb}$$

$$\text{S.F.} = \frac{1,718}{892} = \underline{\underline{1.93}}$$

Secondary plate bending effects due to shear transferred forward in a chordwise direction across the relieved-out area.

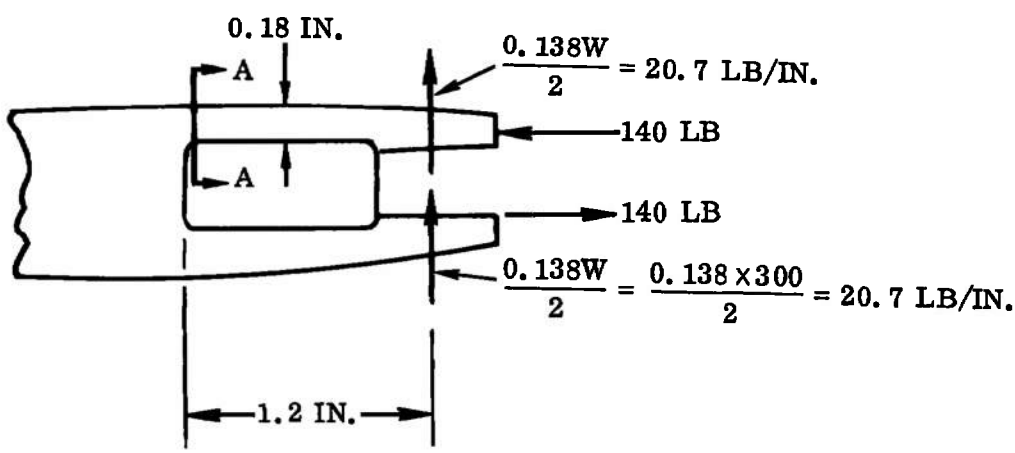

Section A-A, plate bending, 1 inch width (full fixity for shear transfer)

$$f_b = \frac{(20.7 \times 1.2)6}{1 \times 0.18^2} = \pm 4,600 \text{ psi}$$

$$f_{AX} = \frac{140}{0.18} = -775 \text{ psi}$$

$$\Sigma f_c = -5,375 \text{ psi } \underline{\underline{\text{(not critical).}}}$$

Wing Attachment to Fuselage (Ref. Figure 7)

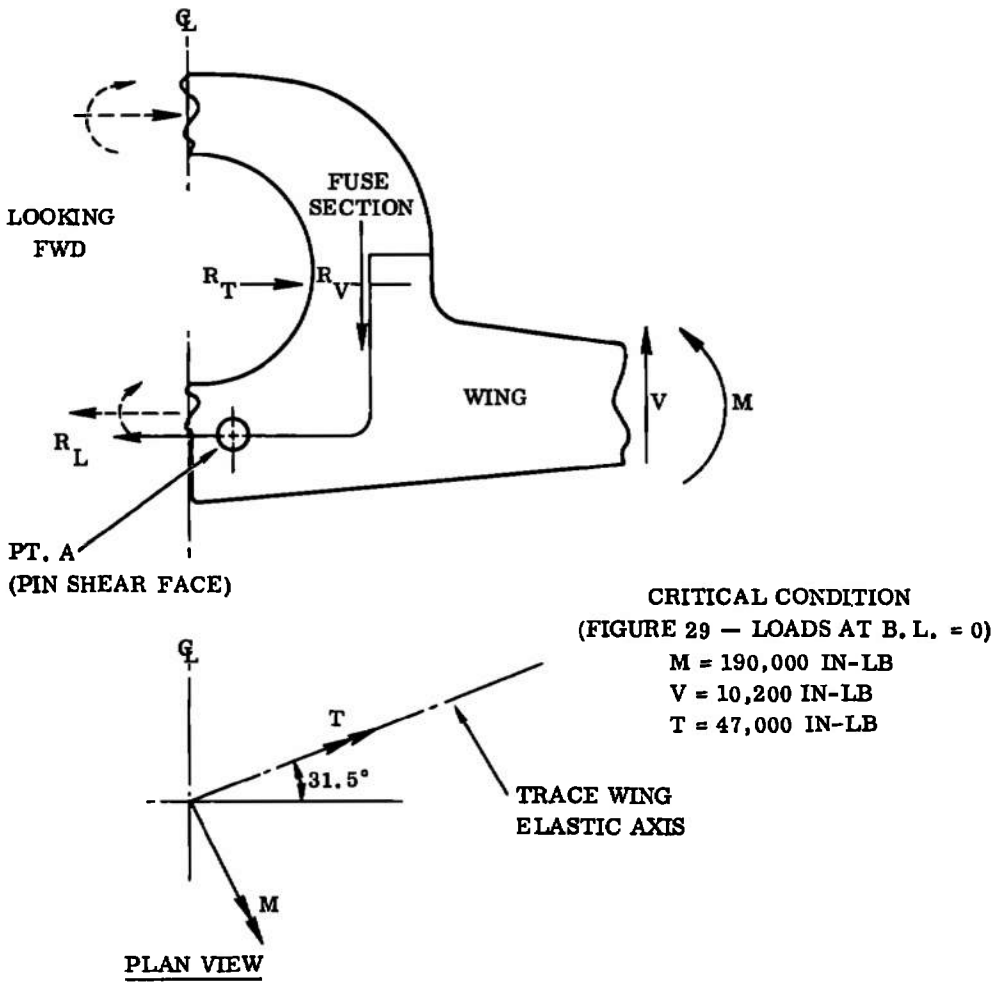

Loads Parallel and Perpendicular to Fuselage ℄ (at Fuselage ℄)

$$M' = 190,000 \cos 31.5° - 37,740 \sin 31.5° = 142,300 \text{ in-lb}$$

$$T' = 190,000 \sin 31.5° + 37,740 \cos 31.5° = -131,500 \text{ in-lb}$$

$$M \text{ at } A = 142,300 - 10,200 \times 2.25 \text{ in.} = 132,100 \text{ in-lb}$$

Row along A has 6-1/2 in. dia. dowels effective for the 65% solid wing version (which is the most critical since the trailing edge is not attached for this version).

$$\text{Couple load due to } M = \frac{132,100}{2.5} = 52,900 \text{ lb}$$

$$\text{Couple load due to } T = \frac{131,500}{2.5} = 52,500 \text{ lb}$$

$$\text{Shear/dowel} = \frac{52,900}{6} + \frac{52,500}{6} = 12,450 \text{ lb}$$

$$\text{Dowel S. F. (lower row)} = \frac{28,700^*}{12,450} = \underline{\underline{2.30}}$$

Upper Row of Dowels

V = 10,200 lb, assuming dowels take vertical shear.

$$\text{Shear/dowel (4 dowels effective)} = \frac{10,200}{4} + \frac{52,500}{4} = 13,350 \text{ lb}$$

$$\text{Dowel S. F. (upper row)} = \frac{28,700^*}{13,350} = \underline{\underline{2.15}}$$

Horizontal Tail (13-8 Mo H1000 Steel)

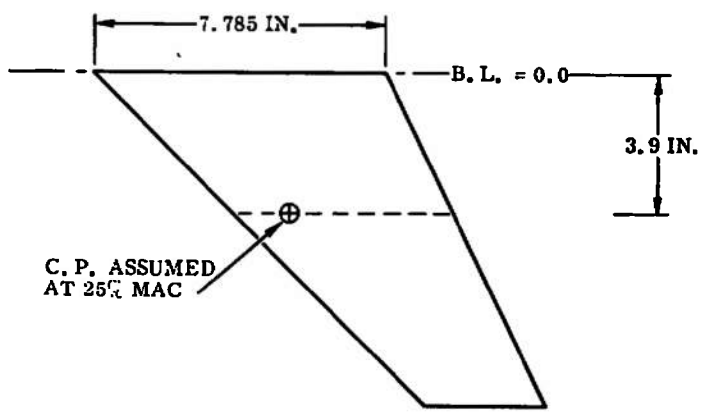

Critical condition is No. 7; total load = 1901.5 lb (Table 3).

Bending Section Check at Root

$$I_X = I_{min} = 0.1427 \text{ in.}^4$$

$$y_{max} = 0.383 \text{ in.}$$

(From a numerical integration of root cross section)

$$M = \frac{1,901.5}{2} \times 3.9 = 3,710 \text{ in-lb}$$

$$f_b = \frac{3,710 \times 0.387}{0.1427} = 10,320 \text{ psi } \underline{\underline{\text{(not critical)}}}$$

Attachment to Vertical

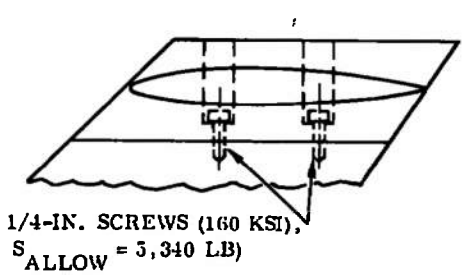

Assume the entire vertical load is taken by the forward screw.

$$\text{S. F.} = \frac{5,340}{1,901.5} = \underline{\underline{2.80}}$$

*Allowable shear load for 1/2-in. dia. dowel.

Vertical Tail (13-8 Mo H1000 Steel)

Critical vertical tail load is 3,070 lb (Table 3)

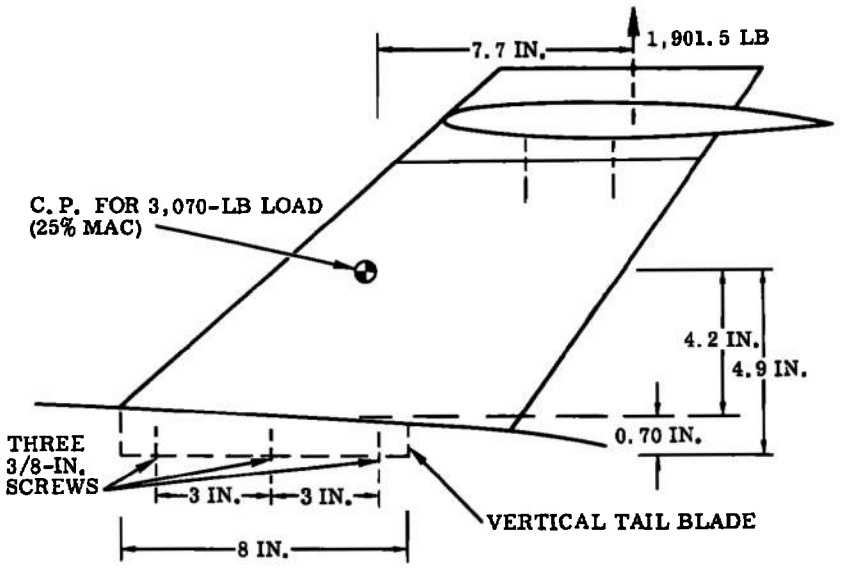

Bending Check of Blade Section at Juncture with Fuselage

Blade width = 1.0 in.

$$\text{Blade bending, } f_b = \frac{(4.2 \times 3{,}070)\,6}{8 \times 1.0^2} = 9{,}650 \text{ psi}$$

$$\text{Blade torsion, } f_s = \frac{3T}{at^2} = \frac{3\,(3 \times 3{,}070)}{8 \times 1.0^2} = 3{,}450 \text{ psi}$$

Blade and tail stresses not critical

Bearing stress distribution between blade and fuselage in reacting side shear, moment, and torque:

$$\text{Bearing stress, } f_{br} = \frac{6\,(4.55 \times 3{,}070)}{8 \times 0.70^2} + \frac{6\,(3 \times 3{,}070)}{0.70 \times 8^2} + \frac{3{,}070}{8 \times 0.70}$$

$$= 28{,}070 \text{ psi (not critical)}$$

Vertical Tail Attachment

Tension due to horizontal tail load:

$$M = 1{,}901.5 \times 10.7 = 20{,}350 \text{ in-lb}$$

Couple arm = 3 in. + (2/3)4 = 5.67 in.

$$P_T = \frac{20,350}{5.67} + \frac{1,901.5}{3} = 4,224 \text{ lb}$$

3/8-in. screw allowable = 13,180 lb tension

$$S.F. = \frac{13,180}{4,224} = \underline{\underline{3.12}}$$

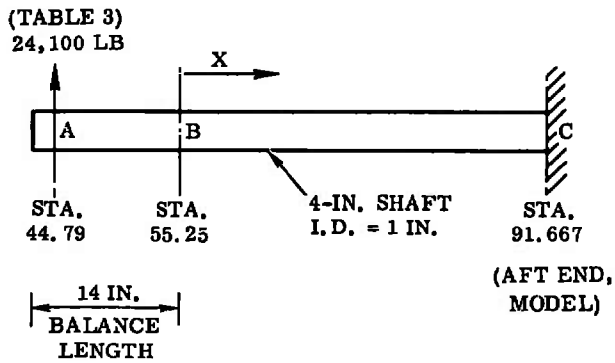

Relative Deflection of Sting Support with Respect to Aft End of Model

α = rotation of B with respect to C $= \int \frac{Mds}{EI}$

$$\alpha = \int_0^{36.417} \frac{24,100(10.46 + x)\,dx}{EI}$$

$$= 252,086\,x + \frac{24,100\,x^2}{2}\Big]_0^{36.417}$$

$$\alpha = \frac{25,160,900}{EI}$$

Where

$$I = \frac{\pi}{4}(R^4 - r^4) = \frac{\pi}{4}(2^4 - 0.5^4)$$

$$= 15.9375 \text{ in.}^4$$

$E = 27.0 \times 10^6$ psi; maraging steel 300 (MIL-S-46850A, Type 3, grade 300)

$$\therefore \alpha = \frac{25,160,900}{(15.9375 \times 27 \times 10^6)} = 0.05847 \text{ radians}$$

Relative deflection, δ_R, due to rotation at B = 36.417α

$$\delta_R = 36.417 \times 0.05847 = 2.129 \text{ in.}$$

Translation of point B, δ_V, with respect to C:

$$\delta_V = \int_0^{36.417} \frac{Mmds}{EI}$$

$$= \int_0^{36.417} \frac{24,100\,(10.46+x)\,x\,dx}{EI}$$

$$= \left.\frac{252,086\,x^2}{2} + \frac{24,100\,x^3}{3}\right]_0^{36.417} \frac{1}{EI}$$

$$= \frac{555,137,020}{27 \times 10^6 \times 15.9375} = 1.290 \text{ in.}$$

Balance rotation, δ_R: assume = 0.75°, (0.013089 radian)

$$\delta_R' = (0.013089)\ 36.417 = 0.473 \text{ in.}$$

Relative deflection at C between sting and fuselage:

$$\delta_{NET} = 2.129 + 0.473 - 1.290 = \underline{\underline{1.312 \text{ in.}}}$$

Bending Check at Point C (Station 91.667)

$$f_b = \frac{24,100\ (46.877)\,2}{15.9375} = 141,770 \text{ psi}$$

$$F_{tu} = 300,000 \text{ psi}$$

$$S.F. = \frac{300,000}{141,000} = \underline{\underline{2.116}}$$

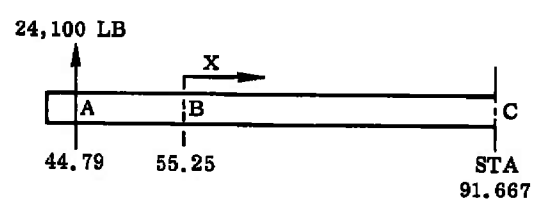

Maneuver Sting Configuration

The sting material is maraging steel 300, MIL-S-46850A, Type 3, grade 300.

The relative deflection at point C between sting and fuselage is a function of the balance rotation, α_A; the rotation and vertical displacement of point B with respect to C.

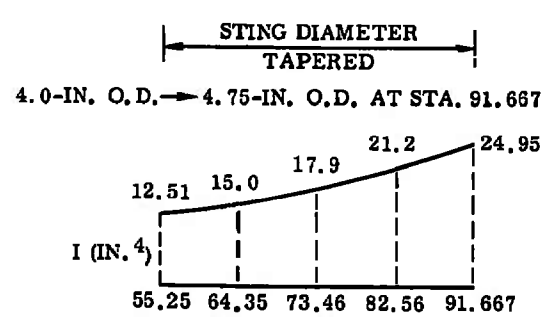

α_A, balance rotation, assume = 0.75° = (0.01309 radian)

$$\alpha_B, \text{ rotation of point B} = \int \frac{Mds}{EI} = \int_0^{36.417} \frac{24,100\,(10.46+x)\,dx}{E\,(I)}$$

α_B, from numerical integration = 0.04947 radian

$$\delta_B, \text{ displacement of B} = \int \frac{Mxds}{EI} = \int_0^{36.417} \frac{24,100\,(10.46+x)\,xdx}{E(I)}$$

δ_B, from numerical integration = 1.0048 in.

The relative deflection at C between sting and fuselage is:

$$\delta_{net} = \alpha_A\,(36.417) + \alpha_B\,(36.417) - \delta_B$$

$$= 0.01309\,(36.417) + 0.04947\,(36.417) - 1.0048$$

$$= 0.4734 + 1.7989 - 1.0048 = \underline{\underline{1.2675 \text{ in.}}}$$

Bending Check at Point C (Station 91.667)

$$f_b = \frac{24,100\,(46.877)\,2.375}{24.95^*} = 107,540 \text{ psi}$$

F_{tu} = 300,000 psi

F_b = 409,500 psi (Ref. page 122)

$$S.F. = \frac{409,500}{107,540} = \underline{\underline{3.808}}$$

Cruise Sting Configuration (13-8 Mo H1000)

The critical condition is condition 10 (300°K) - Table 2.

The relative deflection at point C between sting and fuselage is a function of the balance rotation, α_A; the rotation and vertical displacement of point B with respect to C.

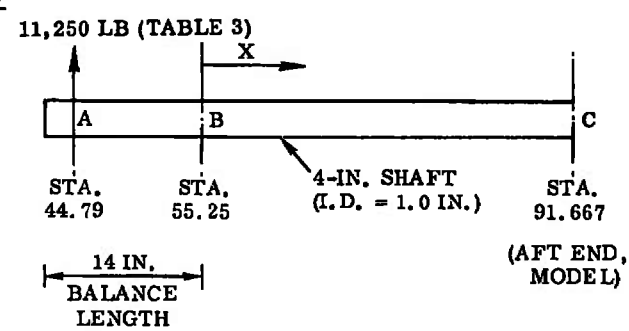

$^*I = \frac{\pi}{4}(R^4 - r^4) = \frac{\pi}{4}(2.375^4 - 0.5^4) = 24.95 \text{ in.}^4$

α_A, balance rotation, assume = 0.75 deg = 0.01309 radian

$$\alpha_B, \text{ rotation of point B} = \int_0^{36.417} \frac{M\,ds}{EI} = \int_0^{36.417} \frac{11{,}250\,(10.46+x)\,dx}{EI}$$

$$\alpha_B = \frac{11{,}744{,}777}{EI}$$

Where:

$$I = \frac{\pi}{4}\,(R^4 - r^4)$$

$$= \frac{\pi}{4}(2.0^4 - 0.5^4)$$

$$= 12.517 \text{ in.}^4$$

$$E = 28.3 \times 10^6 \text{ psi}$$

$$\therefore \alpha_B = 0.03315 \text{ radian}$$

The translation of point B, δ_B, with respect to C is:

$$\delta_B = \int_0^{36.417} \frac{M m\,ds}{EI} = \int_0^{36.417} \frac{11{,}250\,(10.46+x)\,x\,dx}{EI}$$

$$= \frac{259{,}137{,}960}{28.3 \times 10^6 \times 12.517} = 0.7315 \text{ in.}$$

The relative deflection at C between sting and fuselage is

$$\delta_{net} = \alpha_A\,(36.417) + \alpha_B\,(36.417) - \delta_B$$

$$= 0.01309\,(36.417) + 0.03315\,(36.417) - 0.7315$$

$$= \underline{\underline{0.9524 \text{ in.}}}$$

<u>Bending Check at Point C (Station 91.667)</u>

$$f_b = \frac{11{,}250\,(46.877)\,2.00}{12.517} = 84{,}264 \text{ psi}$$

$$F_{tu} = 201{,}000 \text{ psi}$$

$$F_b \simeq 1.365^* \,(201{,}000) = 274{,}365 \text{ psi}$$

---

* Form factor ≃ 1.365, Ref. page 123.

$$S.F. = \frac{274,365}{84,264} = \underline{\underline{3.256}}$$

Nacelle

The critical part of the nacelle is the weldment between the nacelle and its support.

WELD SECTION

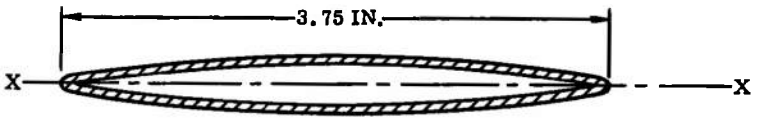

Section Properties

$A = 0.445 \text{ in.}^2$

$y = 0.18 \text{ in.}$

$I_x = 0.0046 \text{ in.}^4$

$A_{enclosed} = 0.69 \text{ in.}^2$

Load

Assume:

Lift = 100 lb

Drag = 30 lb

$M_x = 100 \times 0.9 = 90$ in-lb

$M_y = 30 \times 0.9 = 27$ in-lb

$T = 100 \times 2.1 = 210$ in-lb

Analysis

$$f_b = \frac{M_x y}{I} = \frac{90 \times 0.18}{0.0046} = 3,522 \text{ psi}$$

$$f_{s(direct)} \approx \frac{1.5 \times \text{drag}}{A} = \frac{1.5 \times 30}{0.445} = 101 \text{ psi}$$

$$q_T = \frac{T}{2A} = \frac{210}{(2 \times 0.69)} = 152.174 \text{ lb/in}$$

$$f_{s(torsion)} = \frac{q_T}{t} = \frac{152.174}{0.06} = 2,536 \text{ psi}$$

$$f_{s(total)} = 2,536 + 101 = 2,637 \text{ psi}$$

$$f_{s_{max}} = \sqrt{(f_s)^2 + (f_b/2)^2} = \sqrt{(2,637)^2 + (1,761)^2} = 3,171 \text{ psi}$$

$$f_{n_{max}} = f_{s_{max}} + \frac{f_b}{2} = 3,171 + 1,761 = 4,932 \text{ psi}$$

S. F. = large

Attachment Screws

A check shows the screws to be noncritical.

9.1.3 Detailed Stress Analysis — 1/16-Scale Model

Solid Wing

Bending stresses have been calculated (see page 112) for conditions 37, 38, 41, and 42 (Table 2) the resulting range of stresses experienced are plotted versus 1/24-scale stresses in Figure 60.

The following analysis uses section properties shown below.

TYPICAL CROSS SECTION

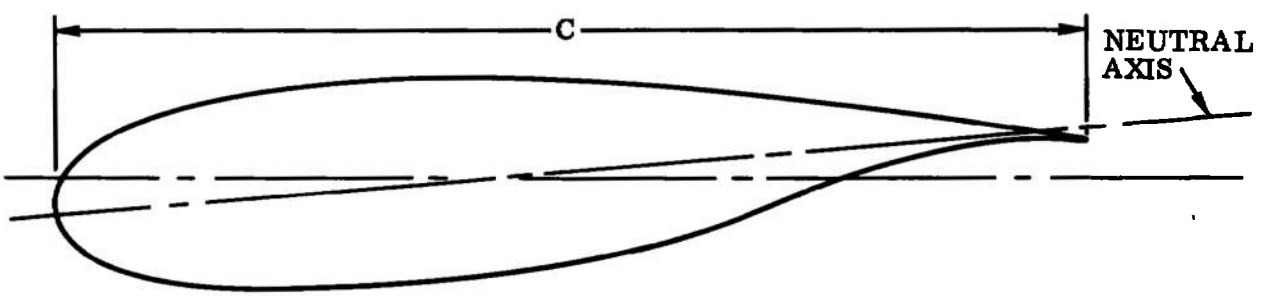

SECTION PROPERTIES (1/16 Scale ATT Wing)

Section (Ref. Fig. 57)	Wing station (in.)	C (in.)	y_T (in.)	y_L (in.)	I_{min} (in.^{4})
1	40.920	7.170	0.480	0.555	0.3225
2	26.775	9.630	0.660	0.720	1.0500
3	24.495	10.035	0.690	0.750	1.2383
4	22.305	12.300	0.720	0.780	1.4580
5	19.995	14.670	0.765	0.825	2.2629

BENDING ANALYSIS (1/16 Scale ATT Wing)

Condition	Section (Ref. Fig. 57)	Wing station (in.)	$M_{E.A.}$ (in-lb)	f_b (psi)	F_b (psi)	S. F.
37	1	40.920	4,000	6,884	201,000	29.198
	2	26.775	26,500	18,171	201,000	11.062
	3	24.495	34,500	20,895	201,000	9.620
	4	22.305	42,000	22,469	201,000	8.946
	5	19.995	51,500	18,775	201,000	10.706
38	1	40.920	8,200	14,112	201,000	14.243
	2	26.775	68,000	46,628	201,000	4.311
	3	24.495	85,200	51,602	201,000	3.895
	4	22.305	103,000	55,102	201,000	3 648
	5	19.995	123,800	45,134	201,000	4.453
41	1	40.920	4,500	7,744	201,000	25.956
	2	26.775	33,000	22,628	201,000	8.883
	3	24.495	42,500	25,741	201,000	7.809
	4	22.305	52,000	27,818	201,000	7.226
	5	19.995	64,100	23,369	201,000	8.601
42	1	40.920	12,000	20,651	201,000	9.733
	2	26.775	84,000	57,600	201,000	3.490
	3	24.495	106,200	64,321	201,000	3.125
	4	22.305	129,000	69,011	201,000	2.913
	5	19.995	155,300	56,618	201,000	3.550

9.1.4 Detailed Stress Analysis — 1/12-Scale Model

Solid Wing

The results of the stress analysis and section properties for the 1/12 scale model are shown on page 113.

TYPICAL CROSS SECTION

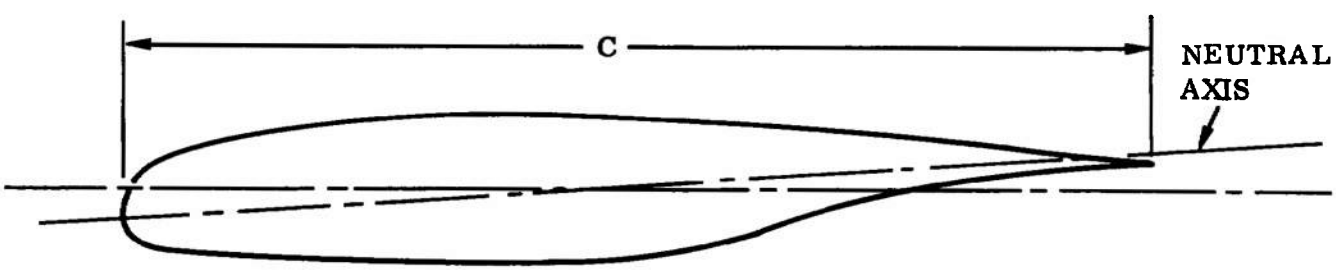

SECTION PROPERTIES (1/12 Scale ATT Wing)

Section (Ref. Fig. 57)	Wing station (in.)	C (in.)	y_T (in.)	y_L (in.)	I_{min} (in.^{4})
1	54.56	9.56	0.64	0.74	1.0192
2	35.70	12.84	0.38	0.96	3.3184
3	32.66	13.38	0.92	1.00	3.9136
4	29.74	16.40	0.96	1.04	4.6080
5	26.66	19.56	1.02	1.10	7.1520

BENDING ANALYSIS (1/12 Scale ATT Wing)

Condition	Section	Wing station (in.)	$M_{E.A.}$ (in-lb)	f_b (psi)	F_b (psi)	S. F.
39	1	54.56	7,000	5,082	201,000	39.551
	2	35.70	50,100	14,494	201,000	13.868
	3	32.66	65,200	16,660	201,000	12.065
	4	29.74	80,000	18,056	201,000	11.132
	5	26.66	96,700	14,873	201,000	13.514
40	1	54.56	18,000	13,069	201,000	15.380
	2	35.70	128,000	37,030	201,000	5.428
	3	32.66	159,900	40,857	201,000	4.920
	4	29.74	193,000	43,560	201,000	4.614
	5	26.66	231,000	35,528	201,000	5.658
43	1	54.56	8,000	5,808	201,000	34.607
	2	35.70	65,000	18,804	201,000	10.689
	3	32.66	81,900	20,927	201,000	9.605
	4	29.74	101,000	22,795	201,000	8.818
	5	26.66	122,300	18,810	201,000	10.686
44	1	54.56	23,000	16,699	201,000	12.037
	2	35.70	161,000	46,577	201,000	4.315
	3	32.66	202,400	51,717	201,000	3.887
	4	29.74	245,000	55,295	201,000	3.635
	5	26.66	293,900	45,203	201,000	4.447

9.2 F-111 AIRCRAFT

9.2.1 1/12-Scale Model

The 50-deg sweep version of the F-111 is the most highly stressed configuration. Critical wing section stresses vary from 29,300 psi (26 deg sweep) to 70,266 psi (50 deg sweep).

Wing stress vs wing sweep for the solid wings are shown in Figure 62. The structural effects of the different types of wings are illustrated in Figure 63.

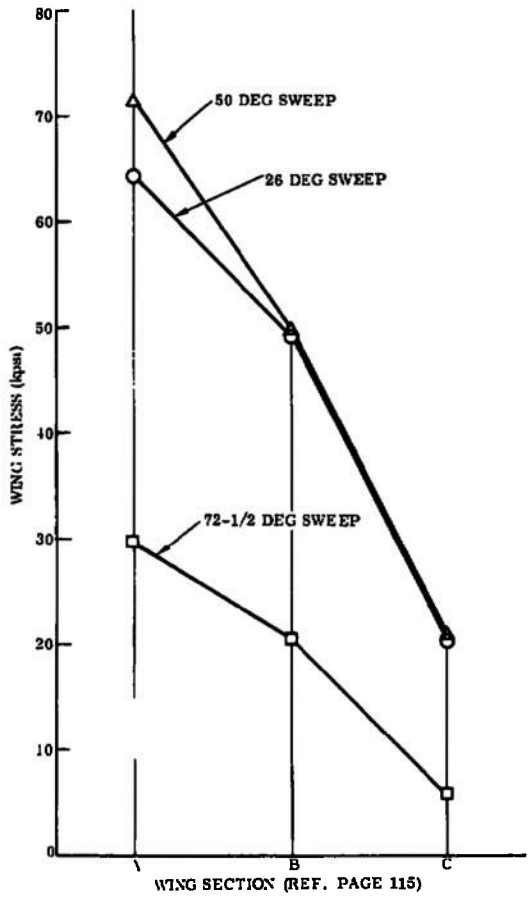

Figure 62. F-111 – Wing Stresses vs Wing Sweeps (Solid Wing)

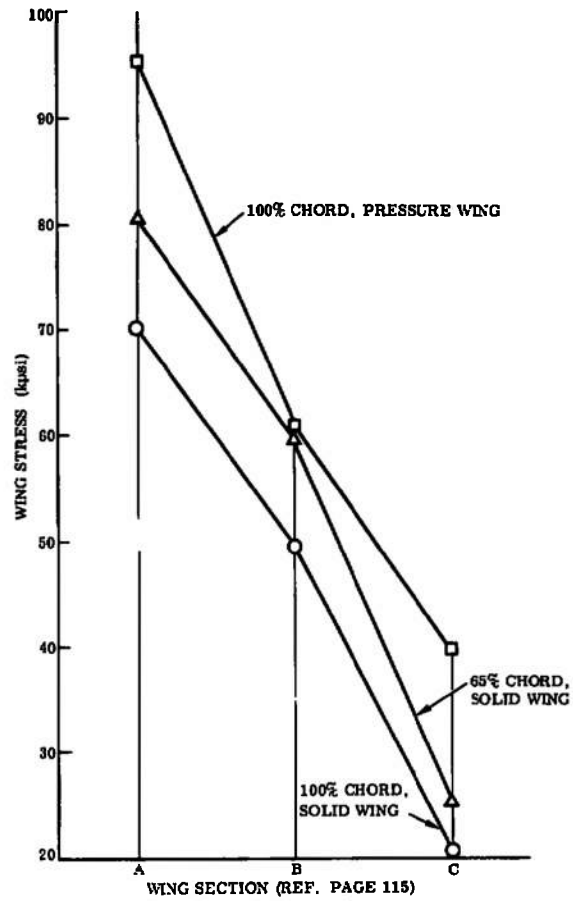

Figure 63. F-111 – Wing Types vs Stress at 50-Degree Sweep

Wing to fuselage attachment is dependent only on the bolt pattern and size. The method shown results in a SF = 4.07.

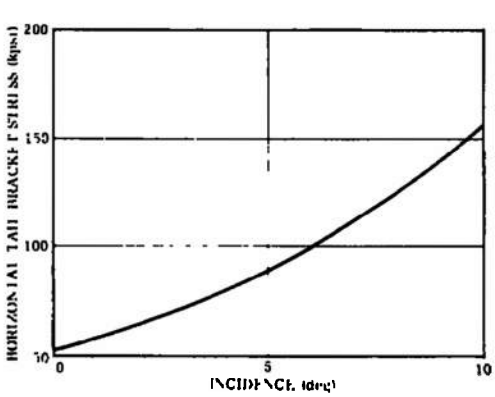

Figure 64. F-111 – Horizontal Tail Bracket Stress vs Incidence

Vertical tail stresses and attachment are no problem. The horizontal tail becomes critical when variable tail incidences are required. Due to the geometry of the tail-to-fuselage area, the horizontal tail begins to unport quickly and leaves little common material between the tail and fuselage at incidence angles of ten degrees or higher. Tail incidence requirements should be weighed carefully. The rise in stress levels vs incidence is shown in Figure 64.

High loads plus a relatively long fuselage contribute to sting stress, model clearance, and aft fuselage modification problems. The sting diameters shown in Figure 8 result in a working stress of 168,400 psi.

The use of 18 Ni-350 grade maraging steel will yield a safety factor of 2+ without the use of any form factor. Larger diameter stings would result in a very poor aft model modification.

9.2.2 Detailed Stress Analysis

Wing

This analysis is based upon the wing being machined from PH 13-8 Mo stainless steel, condition H1000. The accompanying plan view shows the locations of the sections checked.

PLAN VIEW

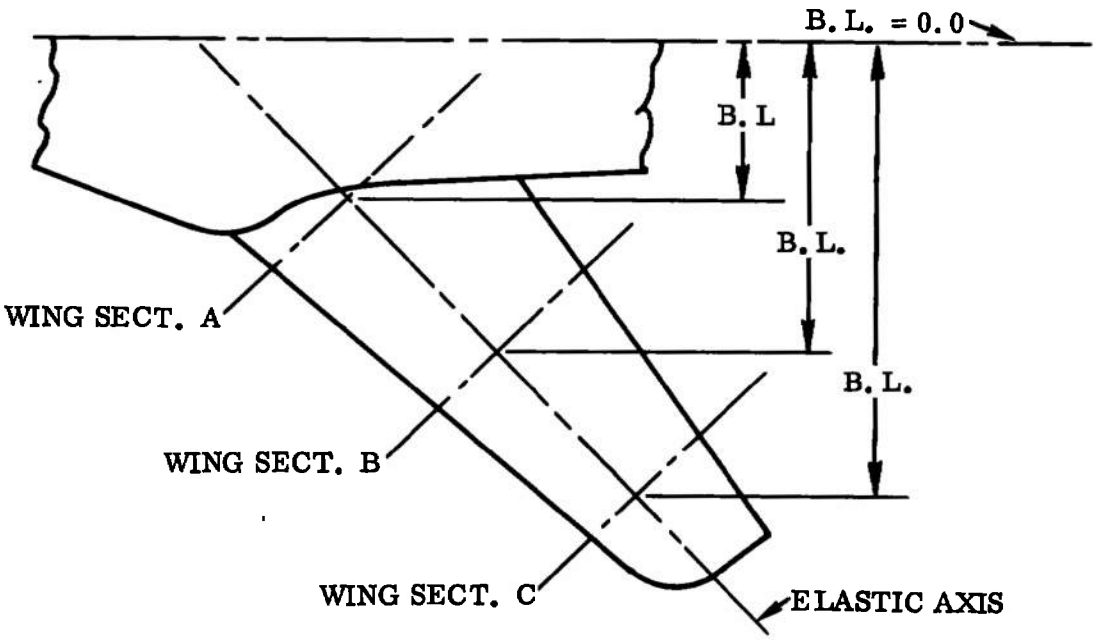

50-DEG WING SWEEP POSITION SHOWN

100% Chord Solid Wing (Ref. Figure 8)

Maximum normal stresses have been calculated for the 26, 50, and 72-1/2 degree wing sweeps. Loads for the critical conditions are shown in Figures 36, 37, 38, and 39.

TYPICAL CROSS SECTION

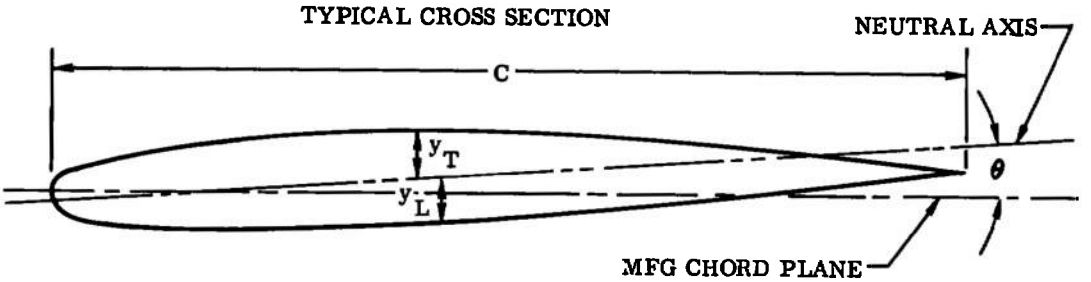

SECTION PROPERTIES (100% Chord Wing)

Wing section	Area (in.^{2})	C (in.)	y_T (in.)	y_L (in.)	θ (deg)	I_{min} (in.^{4})	I_{max} (in.^{4})
A	8.117	10.30	0.584	0.576	0.261	0.652	45.495
B	4.690	7.95	0.445	0.435	1.031	0.212	15.519
C	2.484	5.85	0.318	0.332	2.145	0.056	4.774

BENDING AND TORSION ANALYSIS

Wing section	B. L. (in.)	Moment (in-lb)	Torsion (in-lb)	$f_{n_{max}}$ (psi)	F_n (psi)	S. F.
			26-DEG SWEEP			
A	7.61	71,500	8,600	64,321	201,000	3.125
B	16.08	22,600	3,550	47,695	201,000	4.214
C	23.62	3,500	940	21,020	201,000	9.562
			50-DEG SWEEP			
A	6.46	76,000	25,300	70,266	201,000	2.861
B	12.96	23,500	4,400	49,741	201,000	4.041
C	18.76	3,500	1,300	21,347	201,000	9,416
			72-1/2-DEG SWEEP			
A	5.28	32,500	5,800	29,385	201,000	6.840
B	8.88	9,550	3,070	20,599	201,000	9.758
C	12.08	500	900	4,526	201,000	44.410

65% Chord Solid Wing (Ref. Figure 8)

The aft 35% of the wing is removable and is considered ineffective in bending and torsion. The same loads are applied as for the 100% chord wing.

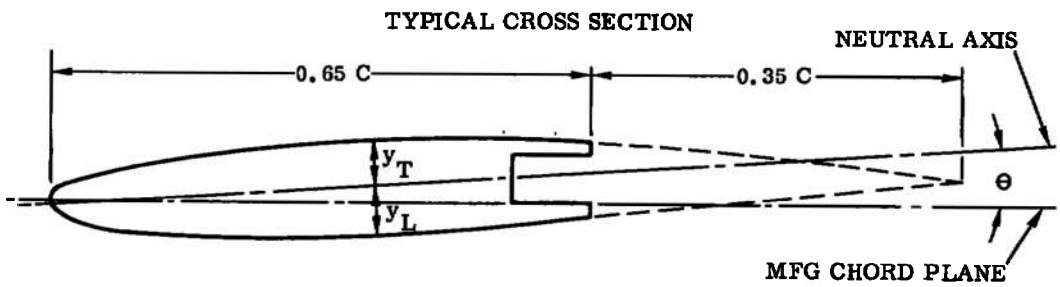

SECTION PROPERTIES (65% Chord Wing)

Wing section	Area (in.^{2})	C (in.)	y_T (in.)	y_L (in.)	θ (deg)	I_{min} (in.^{4})	I_{max} (in.^{4})
A	6.005	10.30	0.583	0.577	1.119	0.564	15.458
B	3.487	7.95	0.457	0.423	1.715	0.184	5.432
C	1.847	5.85	0.341	0.309	2.629	0.049	1.631

BENDING AND TORSION ANALYSIS – 50-DEG SWEEP

Wing section	B. L. (in.)	Moment (in-lb)	Torsion (in-lb)	$f_{n_{max}}$ (psi)	F_n (psi)	S. F.
A	6.46	76,000	25,300	81,002	201,000	2.481
B	12.96	23,500	4,400	58,919	201,000	3.411
C	18.76	3,500	1,300	25,034	201,000	8.029

100% Chord Pressure Wing (Ref. Figure 13)

This wing is subjected to the same loads as the 100% chord solid wing.

TYPICAL CROSS SECTION

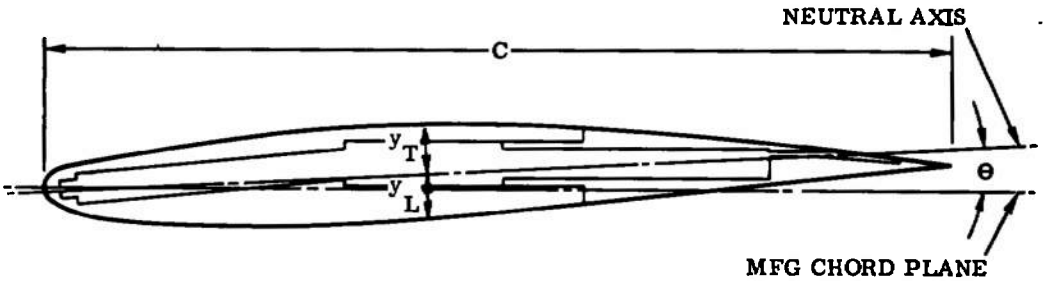

SECTION PROPERTIES

Wing section	Area (in.^{2})	C (in.)	y_T (in.)	y_L (in.)	θ (deg)	I_{min} (in.^{4})	I_{max} (in.^{4})
A	5.566	10.30	0.574	0.586	0.239	0.629	28.066
B	2.892	7.95	0.442	0.438	0.926	0.200	8.818
C	1.325	5.85	0.342	0.308	2.303	0.048	2.432

BENDING AND TORSION ANALYSIS – 50-DEG SWEEP

Wing section	B. L. (in.)	Moment (in-lb)	Torsion (in-lb)	$f_{n_{max}}$ (psi)	F_n (psi)	S. F.
A	6.46	76,000	25,300	95,203	201,000	2.111
B	12.96	23,500	4,400	60,880	201,000	3.302
C	18.76	3,500	1,300	39,221	201,000	5.125

65% Chord Pressure Wing (Ref. Figure 13)

The aft 35% of the wing is removable and discontinuous at the fuselage. As such it is considered ineffective in bending and torsion. The same loads are used as for the 100% chord wing.

TYPICAL CROSS SECTION

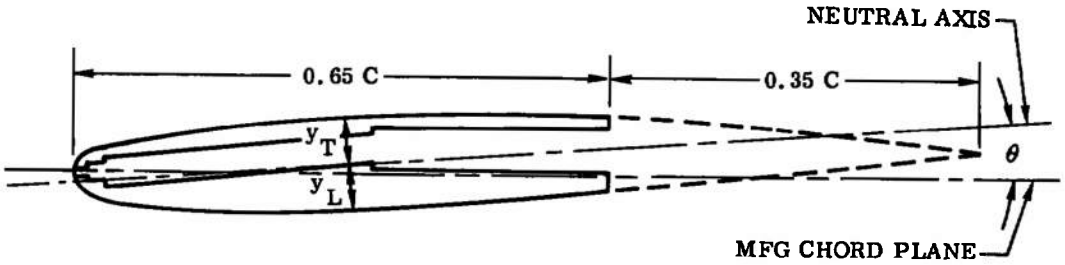

SECTION PROPERTIES

Wing section	Area (in.^{2})	C (in.)	y_T (in.)	y_L (in.)	θ (deg)	I_{min} (in.^{4})	I_{max} (in.^{4})
A	4.276	10.30	0.574	0.586	0.994	0.548	9.990
B	2.212	7.95	0.451	0.429	1.645	0.174	2.995
C	0.991	5.85	0.371	0.279	2.103	0.042	0.767

BENDING AND TORSION ANALYSIS – 50-DEG SWEEP

Wing section	B. L. (in.)	Moment (in-lb)	Torsion (in-lb)	$f_{n_{max}}$ (psi)	F_n (psi)	S. F.
A	6.46	76,000	25,300	104,969	201,000	1.915
B	12.96	23,500	4,400	69,566	201,000	2.889
C	18.76	3,500	1,300	46,213	201,000	4.349

Check of Wing Splice at 65% Chord

The load on the aft 35% of the chord is assumed to be 10% of the total chord load.

Wing shear at 40% semispan = 6,100 lb (Ref. Figure 36)
Wing shear at 60% semispan - 3,700 lb (Ref. Figure 36)
Δshear = 6,100 - 3,700 = 2,400 lb
Semispan = 23.5 in.
20% semispan = 4.7 in.
Average span loading between 40% and 60% semispan = 2400/4.7 = 511 lb/in.

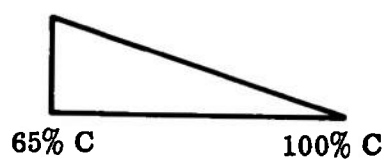

The loading on the aft 35% of the chord = 0.1 × 511 = 51 lb/in. of the span. The loading is triangular from 65% chord to the trailing edge.

Chord at wing section B = 7.95 in.
35% of chord = 2.7825 in.
Moment arm at 65% chord = 2.7825/3 = 0.9275 in.
Unit moment at 65% chord = 0.9275 x 51 = 47.4 in-lb/in. of span.

Couple arm at splice ≈ 0.5 in.

Couple per in. of span = 47.4/0.5 = 94.8 lb

3/16-in. steel screws at 2-in. spacing would be adequate.

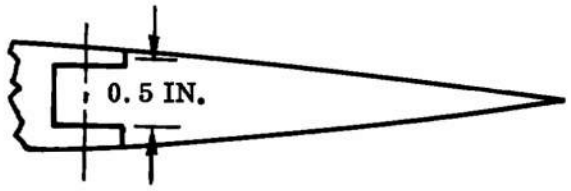

Bolts – Wing-to-Fuselage Attachment

The bolts are 1/2-20 internal wrenching heat treated to 180 ksi. The pattern is shown in Figure 8. Wing loads with respect to the wing elastic axis at model station 29.264 and B. L. 0 are as follows.

$$\left.\begin{aligned} M &= 187{,}322 \text{ in-lb} \\ T &= 28{,}092 \text{ in-lb} \\ S &= 8{,}932 \text{ lb} \end{aligned}\right\} \text{ Ref. Figure 36}$$

Resolving these loads parallel and normal to the fore and aft axis of the model gives the following data.

$$M_{parallel} = M \cos 62.11009° + T \sin 62.11009° = M_{\parallel}$$

$$= 187.322 \times 0.46777 + 28{,}092 \times 0.88385 = 112{,}453 \text{ in-lb}$$

$$M_{normal} = M \sin 62.11009° - T \cos 62.11009° = M_{\perp}$$

$$= 187{,}322 \times 0.88385 - 28{,}092 \times 0.46777 = 152{,}423 \text{ in-lb}$$

The forward bolts are at station 37.657 and the inboard bolts are at B. L. 0.5. Assume bearing along these lines.

$M_{\parallel}$ at B. L. 0 = 112,453 - 0.5 x 8932 = 107,987 in-lb

$M_{\perp}$ at station 37.657 = 152,423 - 8.393 x 8,932 = 77,457 in-lb

$\Sigma x^2 = 2(3.315^2 + 6.632^2 + 9.945^2 + 13.26^2) + 16.6^2 = 934.966 \text{ in.}^2$

$\Sigma y^2 = 6 \times 4.0^2 = 96 \text{ in.}^2$

The aft outboard bolt is critical.

$$\text{Bolt load due to M} = \frac{M_{\perp} x}{\Sigma x^2} = \frac{77,457 \times 16.6}{934.966} = 1,375.2 \text{ lb}$$

$$\text{Bolt load due to } M_{\parallel} = \frac{M_{\parallel} y}{\Sigma y^2} = \frac{107,987 \times 4.0}{96} = 4,499.5 \text{ lb}$$

$$\text{Bolt load due to S} = \frac{S}{\parallel} = \frac{8,932}{\parallel} = 812.0 \text{ lb}$$

Total critical bolt load = 1,375.2 + 4,499.5 + 812.0 = 6,686.7 lb

Allowable bolt load = 27,210 lb (Reference 16)

$$\text{S. F.} = \frac{27,210}{6,686.7} = 4.069$$

Vertical Tail (Ref. Figure 8)

This analysis is based on the vertical tail being machined from PH 13-8 Mo stainless steel, Condition H1000.

The accompanying views show the location of the sections checked.

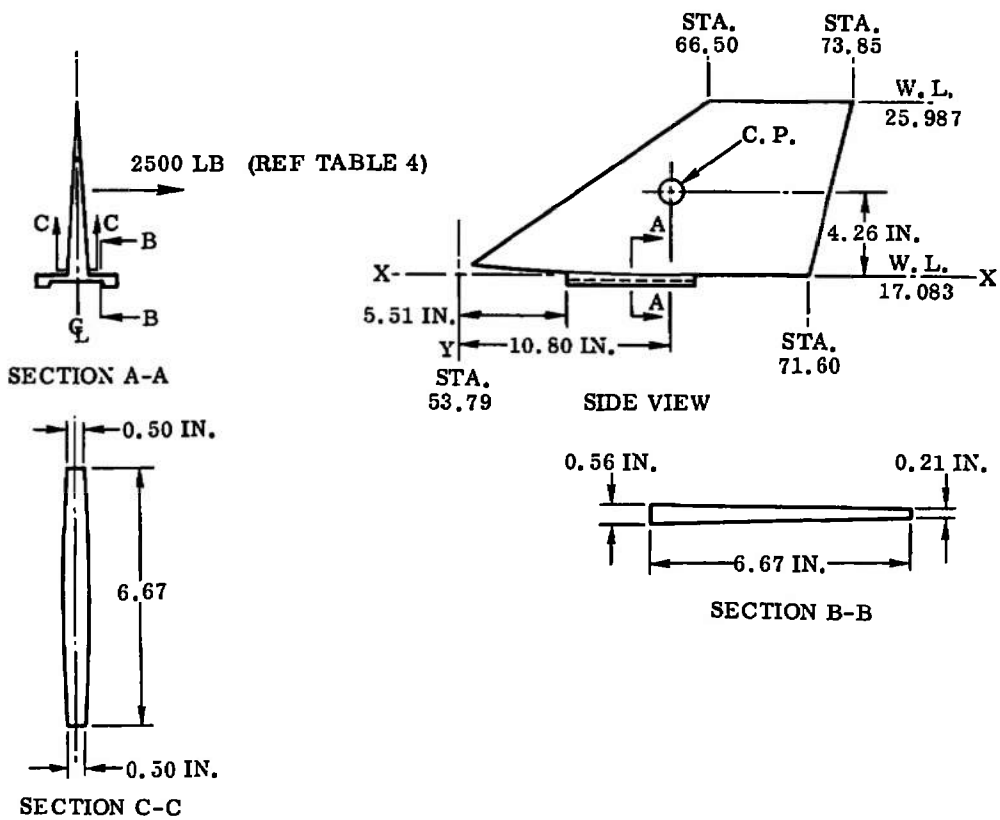

SECTION PROPERTIES

Tail section	Area (in.^{2})	y (in.)	x (in.)	I_{min} (in.^{4})	I_{max} (in.^{4})
B-B	2.537	0.28	2.83	0.0372	8.7041
C-C	3.333	0.25	3.33	0.0695	12.3642

BENDING AND/OR TORSION ANALYSIS

Tail section	$Moment_x$ (in-lb)	$Moment_y$ (in-lb)	$f_{n_{max}}$ (psi)	F_n (psi)	S. F.
B-B	5,488	3,075	41,815	213,000	5.094
C-C	10,650	4,900	40,417	213,000	5.270

Horizontal Tail (Ref. Figure 8)

The critical portion of the horizontal tail is the bracket that attaches the tail to the fuselage and the critical section is at the side of the fuselage. This analysis is based on the bracket being machined from PH 13-8 Mo stainless steel, Condition H1000.

The following sketches show the sections checked for incidence angles of 0, 5, and 10 degrees.

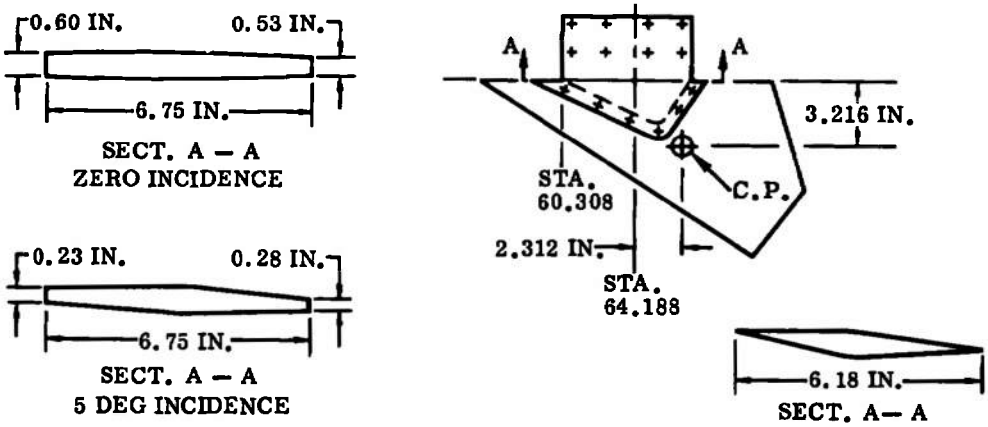

LOAD PER SIDE = 4,500 LB (REF. TABLE 3)

SECTION PROPERTIES – SECTION A-A

Incidence angle (deg)	Area (in.^{2})	y_T (in.)	y_L (in.)	I_{min} (in.^{4})	I_{max} (in.^{4})
0	3.712	0.300	0.300	0.0936	14.0959
5	2.908	0.283	0.327	0.0526	9.0426
10	1.960	0.297	0.313	0.0312	3.4635

BENDING AND TORSION ANALYSIS

Incidence angle (deg)	Moment (in-lb)	Torsion (in-lb)	$f_{n_{max}}$ (psi)	F_n (psi)	S. F.
0	14,472	12,677	50,173	201,000	4.006
5	14,472	12,002	88,038	201,000	2.283
10	14,472	10,512	155,298	201,000	1.294

Support System (Ref. Figure 8)

Two different stings were analyzed for relative deflection between the sting support and the aft end of the model: one with a constant cross section; the other with a tapered cross section.

Constant Section Sting Analysis

MAXIMUM VERTICAL FORCE = 30,370 LB (REF. TABLE 3)

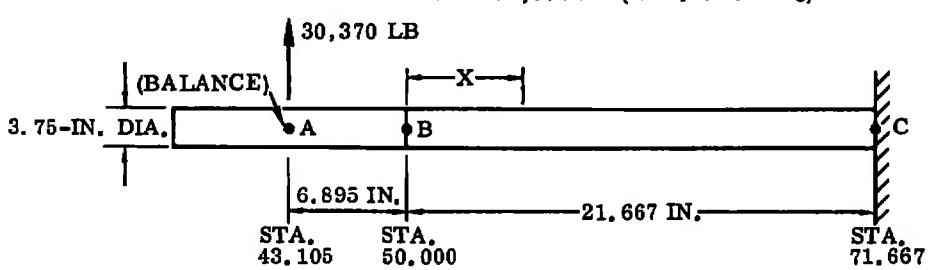

The aft end of the model is at Station 71.667. The model contacts support at point B and forward.

$$M_x = 30,370\,(6.895 + x)$$

Let

$$\alpha = \text{Rotation of Point B} = \int_B^C \frac{M\,ds}{EI}$$

$$= \int_0^{21.667} 30,370\,\frac{(6.895 + x)}{EI}\,dx = \frac{30,370}{EI}\left[6.895\,x + \frac{x^2}{2} + C\right]_0^{21.667}$$

$$= \frac{11,665,828}{EI}$$

$$I = \frac{\pi}{4}\,(R^4 - r^4) = \frac{\pi}{4}\,(1.875^4 - 0.5^4) = 9.658 \text{ in.}^4$$

$$E = 27.0 \times 10^6 \text{ for 18 NI - 300}$$

$$EI = 27.0 \times 10^6 \times 9.658 = 260.8 \times 10^6$$

$$\therefore \alpha = \frac{11,665,828}{260.8 \times 10^6} = 0.04474 \text{ radian}$$

The relative deflection due to rotation at B = $R\alpha$ = 21.667 × 0.04474 = 0.9693 in.

Let

δ = Translation Deflection of Point B

$$= \int_B^C \frac{Mm\,ds}{EI} = \int_0^{21.667} \frac{30,370(6.895 - x)x\,dx}{EI}$$

$$= \frac{30,370}{EI}\left[\frac{6.895x^2}{2} + \frac{x^3}{3} + C\right]_0^{21.667}$$

$$= \frac{152.125 \times 10^6}{EI} = \frac{152.125 \times 10^6}{260.8 \times 10^6} = 0.5833 \text{ in.}$$

Relative deflection = $R\alpha - \delta$ = 0.9693 - 0.5833 = 0.3860 in.

Assume balance rotation of 0.75° or 0.013089 radian

$R\theta$ = 21.667 × 0.013089 = 0.2836 in.

Total relative deflection = 0.3860 + 0.2836 = <u>0.6696 in.</u>

Check of Sting Bending Stress at Point C

M = 30,370 (6.895 + 21.667) = 867,428 in-lb

$$F_b = \frac{M_y}{I} = \frac{867,428 \times 1.875}{9.658} = 168,402 \text{ psi}$$

Using k = 1.5 and the modulus of rupture curve in the Convair structures manual for extra hard AISI 301 stainless, F_B/F_{TU} = 273/200 = 1.365 (Form Factor).

F_b = 1.365 × 300 ksi = 409.5 ksi

$$\text{S. F.} = \frac{409.5}{168.402} = \underline{\underline{2.432}}$$

Tapered Section Sting Analysis

The aft end of the model is at Station 71.667. The model contacts the support at point B. The forward sting is 4.25-in. O.D. at B and tapers to 3.75-in. O.D. at C. The I.D. is 1.00 in.

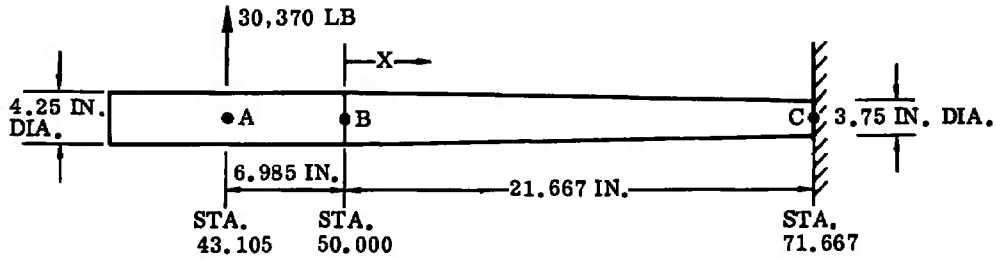

$M_x = 30,370\ (6.895 + x)$

Let α = Rotation of point B = $\displaystyle\int_B^C \frac{M\,ds}{EI}$

$$= \int_B^C \frac{30,370\ (6.895 + x)\,dx}{EI} = \frac{30,370}{EI}\left[6.895\,x + \frac{x^2}{2} + C\right]_B^C$$

Since I is not constant, the integration is made in five steps. The resulting rotation angle, α, is 0.03656 radian.

Relative deflection due to rotation at B = $R\alpha$ = 21.667 × 0.03656 = 0.7921 in.

Let δ = Translation deflection of Point B = $\displaystyle\int_B^C \frac{Mmds}{EI}$

$$\delta = \int_B^C \frac{30,370\,(6.895 + x)\,x\,dx}{EI} = \frac{30,370}{EI}\left[\frac{6.895\,x^2}{2} + \frac{x^3}{3} + C\right]_B^C$$

Integrating in five steps, to account for the variable I, results in a translation of 0.5054 in.

Relative deflection = $R\alpha - \delta$ = 0.7921 - 0.5054 = 0.2867 in.

$R\theta$ = 21.667 × 0.013089 = 0.2836 in. (due to 0.75° balance rotation)

Total relative deflection = 0.2867 + 0.2836 = <u>0.570 in.</u>

<u>Sting Bending Stress at Point C (Dia. = 3.75 in.)</u>

The stress and safety factor are the same as for the constant section.

9.3 DELTA CANARD FIGHTER

9.3.1 1/9.6-Scale Model

The low aspect ratio delta wing is inherently strong and stiff, therefore the Delta Canard model can be tested throughout its complete operating range under ambient (300°K) tunnel temperature conditions. The maximum wing stress is only 21,800 psi for the pressure-instrumented wing.

Wing-to-fuselage and vertical tail-to-fuselage attachments are more highly loaded than any other components. These attachments can be optimized by proper sizing and spacing of attachments.

A movable canard assembly is included with no large structural problems.

The model support system can be fabricated from PH 13-8 Mo steel with a safety factor of 2.88.

9.3.2 Detailed Stress Analysis

Solid Wing (Ref. Figure 9)

The wing is machined from PH 13-8 Mo H1000 stainless steel. The accompanying plan view shows the locations of the sections used for the wing bending analysis.

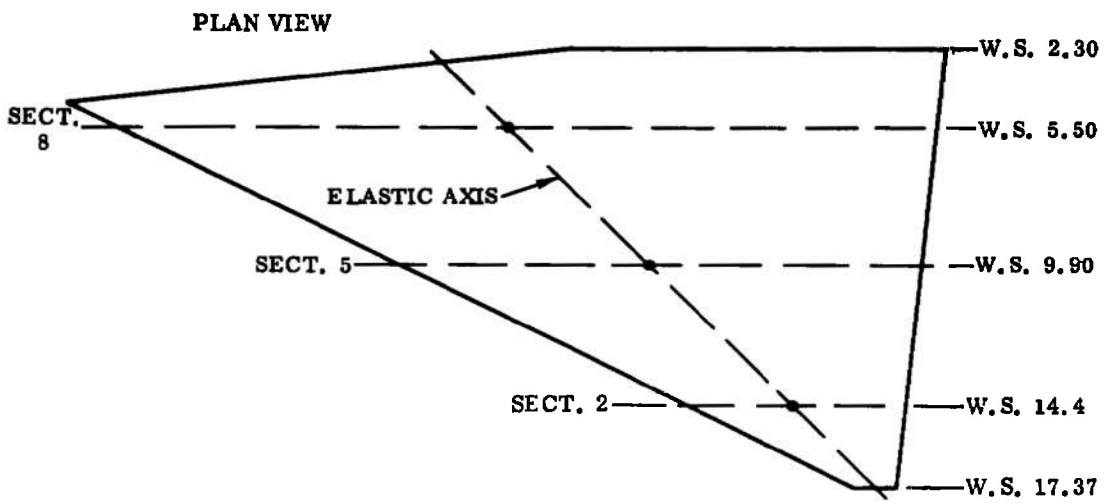

The analysis is performed on three different wing configurations for the critical loads due to the ambient (300°K) temperature condition.

a. 100% chord solid wing.

b. 70% chord solid wing.

c. 70% chord pressure wing.

Wing Bending Sections

Primary bending and torsional stresses have been calculated for the critical condition, condition 23 (300°K) (Table 2). The following table shows the resulting stresses for the three wing configurations.

BENDING ANALYSIS

Section	I^* (in.^{4})	J^* (in.^{4})	$c_U{}^*$ (in.)	$M^\dagger$ (in-lb)	$T^\dagger$ (in-lb)	$f_{st}{}^\ddagger$ (psi)	$f_b{}^\ddagger$ (psi)
			100% SOLID WING				
2	0.0050	0.010	0.14	682	190	2,660	19,100
5	0.112	0.402	0.282	5,141	1,827	1,280	12,900
8	0.650	2.55	0.448	14,627	5,160	906	10,100
			70% SOLID WING (T.E. INEFFECTIVE)				
2	0.00437	≃0.0087	0.14	682	190	3,060	21,800
5	0.098	≃0.350	0.282	5,141	1,827	1,470	14,720
8	0.636	≃2.22	0.448	14,627	5,160	1,040	10,300
			70% PRESSURE WING				
2	-		(Not Applicable)				-
5	0.082	≃0.350	0.282	5,141	1,827	1,470	17,200
8	0.620	≃2.22	0.448	14,627	5,160	1,040	10,580

* Ref. Figure 65.

† M and T, aerodynamic loads without inertia relief (conservative)

‡ $f_b = \frac{Mc_U}{I}$, $f_{st} = \frac{Tc_U}{J}$

From the table above, the most critical section is section 2 for the 70% solid wing version.

$$f_s = \frac{f_b}{2} + f_{st} = \frac{21,800}{2} + 3,060 = 11,320 \text{ psi}$$

$$f_n = \frac{f_b}{2} + f_s = 10,900 + 11,320 = 22,220 \text{ psi}$$

Material: PH 13-8 Mo H1000

$$F_{tu} = 201,000 \text{ psi}$$

$$\text{S. F.} = \frac{201,000}{22,220} = \underline{\underline{9.05}}$$

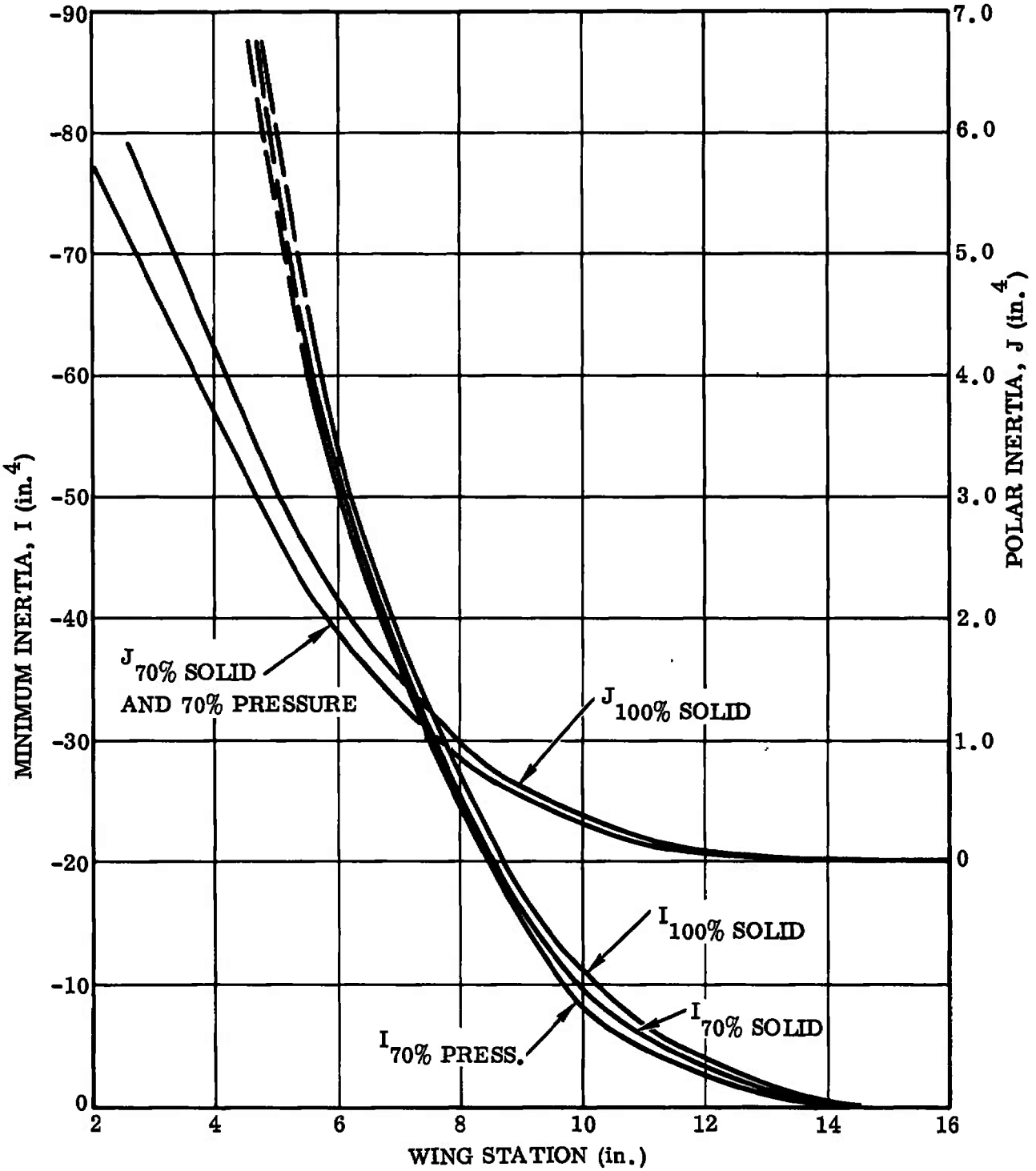

Figure 65. Delta Canard – Wing Section Properties

Wing-to-Fuselage Attachments

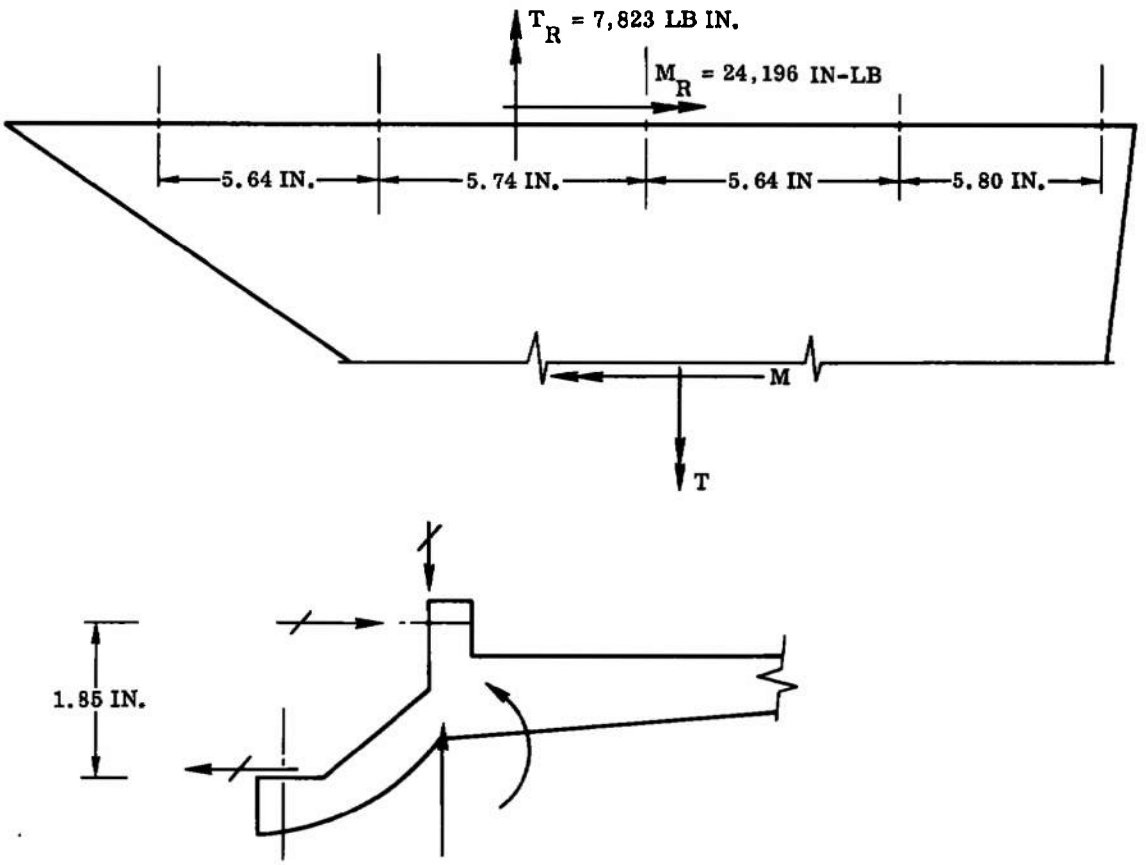

Lower Row of 3/8-in. Screws

Disregarding the aft set of attachments, the maximum shear on the lower set of screws is

$$\text{Couple due to M} = \frac{24,196}{1.85} = 13,100 \text{ lb}$$

$$\text{Couple due to T} = \frac{7,823}{1.85} = 4,220 \text{ lb}$$

$$\frac{\text{Shear}}{\text{3/8-in. screw}} = \frac{13,100}{4} + \frac{4,220}{4} = 3,450 \text{ lb}$$

$$\text{Allow } P_S = \frac{95}{160} \times 13,180 \text{ lb} = 7,800 \text{ lb}$$

$$\text{S. F.} = \frac{7,800}{3,450} = \underline{\underline{2.26}}$$

The upper row of four screws is not critical.

Vertical Tail (PH 13-8 Mo H1000 Steel)

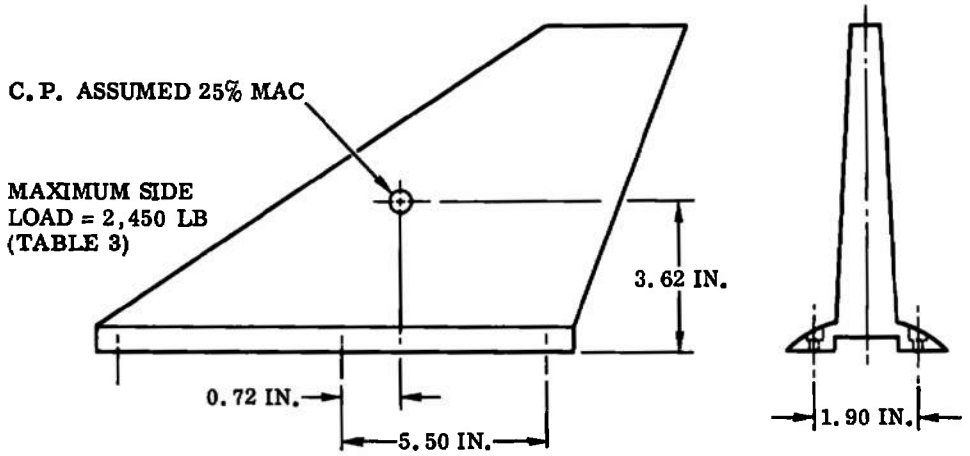

Moment at base = 3.62 × 2450 = 8,850 in-lb

Consider the aft two pairs of screws reacting side moment:

$$\text{Max screw tension} = \frac{4.78}{5.50}(8,850) \div 1.90 \text{ in.} = 4,050 \text{ lb}$$

5/16-in, 160,000 psi screws, P_{allow} = 8,590 lb

$$\text{S. F.} = \frac{8,590}{4,050} = \underline{\underline{2.12}}$$

Critical Bending at Base, Section A-A

Section A-A, 1.40-in. effective width assumed.

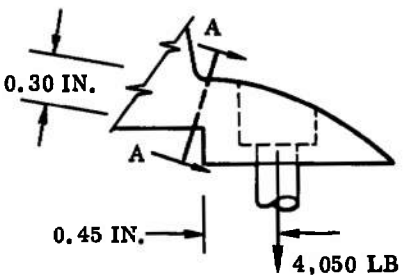

$$f_b = \frac{6M}{bt^2} = \frac{6(4,050 \times 0.45)}{1.4(0.30)^2}$$

$$= 86,600 \text{ psi}$$

PH 13-8 Mo H1000, F_{tu} = 201,000 psi

$$\text{Conservative S. F. (without form factor)} = \frac{201,000}{86,600} = \underline{\underline{2.32}}$$

Canard

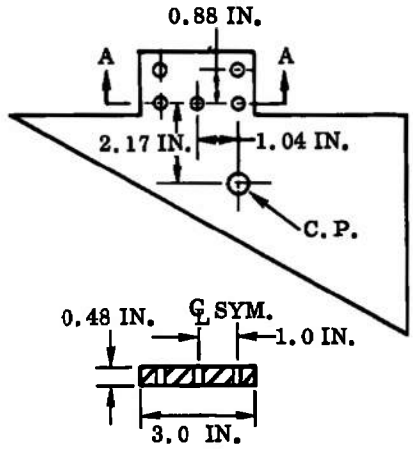

SECTION A—A

The following is a check of section A-A loads.

Assume:

Lift = 1,000 lb at C. P.

$M = 2.17 \times 1{,}000 = 2170$ in-lb

$T = 1.04 \times 1{,}000 = 1{,}040$ in-lb

Section Properties

To allow for counter sink assume holes are 0.3-in. diameter all the way through.

$$A = 2.1 \times 0.48 = 1.008 \text{ in.}^2$$

$$I = \frac{2.1 \times \overline{0.48}^3}{12} = 0.01935 \text{ in.}^4$$

Analysis

$$f_b = \frac{M_y}{I} = \frac{2{,}170 \times 0.24}{0.01935} = 26{,}915 \text{ psi}$$

$$f_s = \frac{T(3a + 1.8b)}{8a^2 b^2} = \frac{1{,}040(3 \times 1.05 + 1.8 \times 0.24)}{8 \times 1.05^2 \times 0.24^2} = 7{,}333 \text{ psi}$$

$$f_{s_{max}} = \sqrt{f_s^2 + (f_b/2)^2} = \sqrt{(7{,}333)^2 + (13{,}458)^2} = 15{,}326 \text{ psi}$$

$$f_{n_{max}} = f_{s_{max}} + \frac{f_b}{2} = 15{,}326 + 13{,}458 = 28{,}784 \text{ psi}$$

The material is PH 13-8 Mo H1000.

$$F_{tu} = 201{,}000 \text{ psi}$$

$$\text{S. F.} = \frac{201{,}000}{28{,}784} = \underline{\underline{6.983}}$$

Check of Screws

Taking moments about the inboard row:

$$R_s \times 0.88 - 1,000\ (2.17 + 0.88) = 0$$

$$R_s = \frac{1,000\ (2.17 + 0.88)}{0.88} = 3,466 \text{ lb}$$

The load per screw due to moment = 3,466/3 = 1,155 lb

Taking moments about the forward row and neglecting the screw on ℄,

$$R_s \times 2 - 1,000 \times 2.04 = 0$$

$$R_s = \frac{1,000 \times 2.04}{2} = 1,020 \text{ lb}$$

The load per screw due to torque = 1,020/2 = 510 lb

The maximum screw load = 1,155 + 510 = 1,665 lb

Use 1/4-28 internal wrenching screws heat treated to 180 ksi

P_T = 6,010 lb (Ref. MIL-HDBK-5A page 8.1.2(b))

$$\text{S. F.} = \frac{6,010}{1,665} = \underline{\underline{3.610}}$$

Relative deflection of sting support with respect to aft end of model

Relative deflection at C between sting and fuselage:

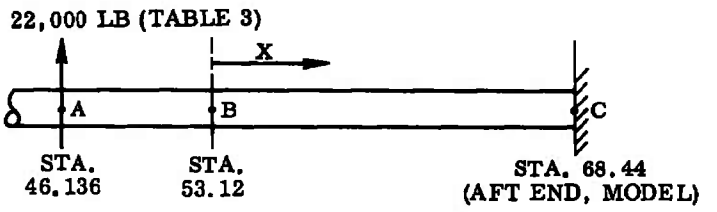

$$\delta_{net} = \alpha_A\ (68.44 - 46.136) + \alpha_B\ (68.44 - 53.12) - \delta_B$$

where

α_A = rotation of balance at A (radians) relative to B

α_B = rotation of B with respect to C (radians)

δ_B = vertical displacement of B with respect to C

$$\alpha_B = \int \frac{M\,ds}{EI} = \int_0^{15.32} \frac{22,000\,(6.984 + x)\,dx}{EI}$$

where

$$I = \frac{\pi}{4}\,(R^4 - r^4) = \frac{\pi}{4}\,(1.875^4 - 0.5^4)$$

$$I = 9.658 \text{ in.}^4$$

PH 13-8 Mo H1000 steel, $E = 28.3 \times 10^6$ psi

$$\therefore \alpha_B = 153,648x + \frac{22,000x^2}{2}\Bigg]_0^{15.32} \frac{1}{EI} = 0.01805 \text{ radian}$$

Relative deflection of sting support with respect to aft end of model:

α_A, balance rotation: assume = 0.75° = 0.013089 radian

δ_B, translation of B with respect to C $= \int \frac{Mm\,dx}{EI}$

$$\delta_B = \int_0^{15.32} \frac{22,000\,(6.984 + x)\,x\,dx}{EI}$$

$$\delta_B = \frac{153,648x^2}{2} + \frac{22,000x^3}{3}\Bigg]_0^{15.32} \frac{1}{EI} = 0.1625 \text{ in.}$$

$$\therefore \delta_{net} = \alpha_A\,(22.30) + \alpha_B\,(15.32) - \delta_B$$

$$= 22.30\,(0.013089) + 15.32\,(0.01805) - 0.1625$$

$$= \underline{\underline{0.406 \text{ in.}}}$$

<u>Bending Check at Point C (Station 68.44)</u>

$$f_b = \frac{22,000\,(22.30) \times 1.875}{9.658} = 95,245 \text{ psi}$$

F_{tu} = 201,000 psi, using the same factor as for maraging steel - Ref. page 123

$$F_b = \frac{409,500}{300,000}\ 201,000 = 274,365 \text{ psi}$$

$$\text{S. F.} = \frac{274,365}{95,245} = \underline{\underline{2.88}}$$

9.4 SPACE SHUTTLE BOOSTER

9.4.1 1/46.5-Scale Model

The space shuttle booster model is the least critical structurally of all model configurations. The complete model test plan can be covered using ambient temperature tunnel conditions (300°K).

Maximum wing stress at the wing-to-fuselage intersection results in 6,228 psi for a solid wing and 8,000 psi for a pressure wing.

Vertical tail stresses are also low (35,700 psi), and the vertical tail can be assembled to the fuselage with screws with no particular problem.

The model balance is positioned farther aft in the model than the airplane configurations, which results in a shorter sting requiring less clearance at the model aft end. Sting stresses run about 41,000 psi.

9.4.2 Detailed Stress Analysis

Solid Wing (Ref. Figure 10)

Check of section at B. L. 4.15 (side of fuselage):

The section will be conservatively checked for the air loads without inertia relief.

$$\left.\begin{aligned} M &= 59{,}296 \text{ in-lb} \\ T &= -20{,}057 \text{ in-lb} \\ S &= 8{,}763 \text{ lb} \end{aligned}\right\} \text{Ref. Figure 42}$$

Section Properties

$I_{min} = 10.762 \text{ in.}^4$

$y = 1.1 \text{ in.}$

$A = 37.071 \text{ in.}^2$

Chord = 22.251 in.

$$\text{Average depth of section} = \frac{37.071}{22.253} = 1.666 \text{ in.}$$

Analysis

$$f_b = \frac{M_y}{I} = \frac{59,296 \times 1.1}{10.762} = 6,061 \text{ psi}$$

$$f_s = \frac{T(3a + 1.8b)}{8a^2b^2} = \frac{20,057(3 \times 11.125 + 1.8 \times 0.833)}{8 \times 11.125^2 \times 0.833^2} = 1,018 \text{ psi}$$

$$f_{s_{max}} = [f_s^2 + (f_b/2)^2]^{1/2} = [(1,018)^2 + (3,031)^2]^{1/2} = 3,197 \text{ psi}$$

$$f_{n_{max}} = f_{s_{max}} + f_b/2 = 3,197 + 3,031 = 6,228 \text{ psi}$$

Using PH 13-8 Mo Condition H1000 stainless steel, $F_{tu} = 201$ ksi

$$\text{S. F.} = \frac{201,000}{6,228} = \underline{\underline{32.274}}$$

Wing-to-Fuselage Attachment

Not critical by inspection.

Pressure Wing (Ref. Figure 15)

The wing will be checked for the same loads and at the same B. L. as the solid wing.

Loads

$M = 59,296$ in-lb

$T = 20,057$ in-lb

$S = 8,763$ lb

Section Properties

$I_{min} = 9.733$ in.^{4}

$y = 1.1$ in.

$A = 20.702$ in.^{2}

Chord = 22.251 in.

$$\text{Average depth} = \frac{20.702}{22.251} = 0.930 \text{ in.}$$

Analysis

$$f_b = \frac{M_y}{I} = \frac{59,296 \times 1.1}{9.733} = 6,701 \text{ psi}$$

$$f_s = \frac{T(3a + 1.8b)}{8a^2b^2} = \frac{20,057\ (3 \times 11.125 + 1.8 \times 0.465)}{8 \times (11.125)^2 \times (0.465)^2} = 3,205 \text{ psi}$$

$$f_{s_{max}} = [f_s^2 + f_b/2)^2]^{1/2} = [(3,205)^2 + (3,351)^2]^{1/2} = 4,637 \text{ psi}$$

$$f_{n_{max}} = f_{s_{max}} + f_b/2 = 4,637 + 3,351 = 7,988 \text{ psi}$$

Using PH 13-8 Mo Condition H1000 stainless steel, $F_{tu} = 201$ ksi

$$\text{S. F.} = \frac{201,000}{7,988} = \underline{\underline{25.163}}$$

Tail (Ref. Figure 10)

The tail is critical at Section A-A.

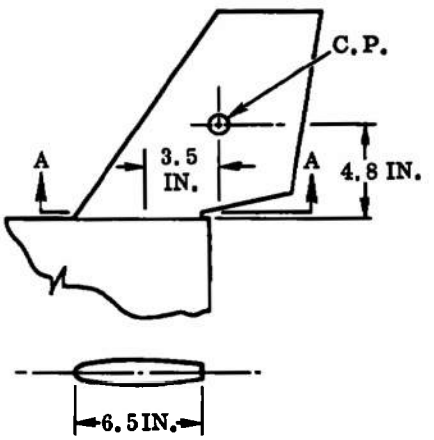

SECT. A—A

Section Properties

$A = 7.16$ in.^{2}

$y_{max} = 0.64$ in.

$I_{min} = 0.80945$ in.^{4}

$$\text{Average depth} = \frac{7.16}{6.5} = 1.102 \text{ in.}$$

Loads

Side load at C. P. = 8,320 lb (Table 3)

$M = 4.8 \times 8,320 = 39,936$ in-lb

$T = 3.5 \times 8,320 = 29,120$ in-lb

Analysis

$$f_b = \frac{M_y}{I} = 39,936 \times \frac{0.64}{0.80945} = 31,576 \text{ psi}$$

$$f_s = \frac{T(3a + 1.8b)}{8a^2b^2} = \frac{29,120\ (3 \times 3.25 + 1.8 \times 0.551)}{8 \times (3.25)^2 \times (0.551)^2} = 12,193 \text{ psi}$$

$$f_{s_{max}} = [f_s^2 + (f_b/2)^2]^{1/2} = [(12,193)^2 + (15,788)^2]^{1/2} = 19,948 \text{ psi}$$

$$f_{n_{max}} = f_{s_{max}} + \frac{f_b}{2} = 19,948 + 15,788 = 35,736 \text{ psi}$$

Using PH 13-8 Mo Condition H1000 stainless steel with F_{TU} = 201 ksi gives

$$\text{S. F.} = \frac{201,000}{35.736} = \underline{\underline{5.625}}$$

Tail-to-Fuselage Attachments (Ref. Figure 10)

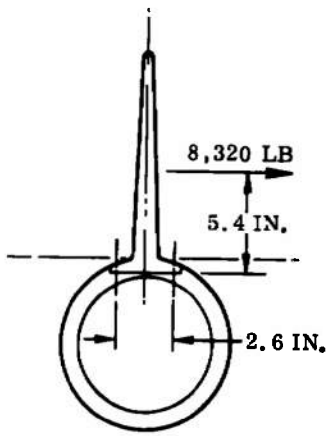

The tail is fastened to the fuselage each side of the ℄ with seven 5/16-24 steel bolts heat treated to 180 ksi.

$$\text{Couple load on bolts} = \frac{8,320 \times 5.4}{2.6} = 17,280 \text{ lb}$$

$$\text{Tension load per bolt} = \frac{17,280}{7} = 2,469 \text{ lb}$$

Allowable tension load = 9,660 lb per bolt

$$\text{S. F.} = \frac{9,660}{2,469} = \underline{\underline{3.913}}$$

Model Sting Support (Ref. Figure 10)

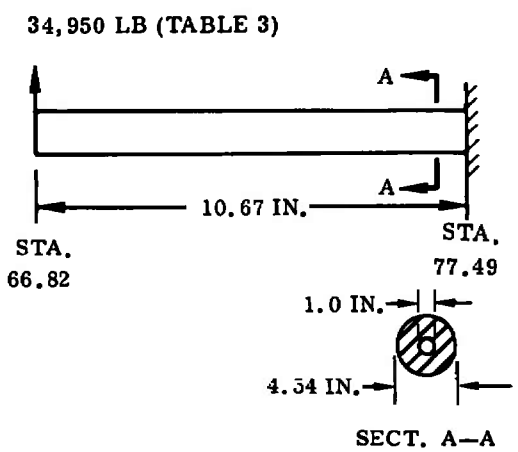

$$M = 10.67 \times 34,950 = 372,917 \text{ in-lb}$$

$$I = \frac{\pi}{4}(R^4 - r^4) = \frac{\pi}{4}(2.27^4 - 0.5^4)$$

$$= 20.805 \text{ in.}^4$$

$$f_b = \frac{M_y}{I} = \frac{372,917 \times 2.27}{20.805} = 40,688 \text{ psi}$$

Using PH 13-8 Mo Condition H1000 with F_{tu} = 201 ksi gives

$$\text{S. F.} = \frac{201,000}{40,688} = \underline{\underline{4.940}}$$

SECTION X

MATERIALS ANALYSIS

10.1 CURRENT MODEL MATERIALS

The materials commonly used for fabrication of wind tunnel test models are the high-strength steels, such as 17-4PH or AISI 4340, since strength and stiffness have been the overriding factors in the selection of model materials. The 17-4PH stainless steel is most frequently selected because it is readily available in many wrought forms and possesses an excellent combination of strength, ductility, fracture toughness, corrosion resistance, machinability, and weldability.

Another important factor is that 17-4PH can be machined in the solution-annealed condition and then hardened by a low-temperature aging treatment without distortion. In addition, 17-4PH can be heat treated to develop a wide range of properties to meet specific model requirements. The heat-treat condition most commonly used is H900, which provides a minimum ultimate tensile strength of 190 ksi.

AISI 4340 is a conventional quenched and tempered steel, which is generally used at ultimate tensile strength levels up to 200 ksi. This steel also can be used at strength levels of 260 ksi or higher, but the intermediate range between 200 and 260 ksi is not used due to embrittling encountered during tempering in the range 500 to 700°F. Since it is difficult to avoid distortion during heat treatment of quenched and tempered steels, at least the final machining operations must be performed in the fully hardened condition. AISI 4340 is not a corrosion resistant alloy and must be given a protective coating.

10.2 HIRT MODEL REQUIREMENTS

Studies of requirements for HIRT test models indicate the need for a material with a suitable combination of properties that include high strength, high modulus, good ductility, and good fracture toughness at temperatures from ambient to -30°F. In addition, the material must be machinable, weldable, dimensionally stable, available in large billet size and low cost. Most design concepts will require bar, plate or forging billets for model construction. Stress analyses of proposed HIRT models indicate that materials with ultimate tensile strength in the order of 200 ksi are needed based on a minimum safety factor of 2. The high stress level and short test duration impose requirements for good fracture toughness and impact strength for service temperatures from ambient to -30°F. A notch toughness (Charpy V-notch) of 15 ft-lb

at -30°F has been considered as a lower limit in preliminary studies of HIRT model materials (Reference 14).

The most frequently used material for contemporary wind tunnel models, 17-4PH H900, does not meet these requirements. The 17-4PH steel in the H900 condition has poor fracture toughness at -30°F and is not considered suitable for structural use at this temperature. The AISI 4340 steel has adequate fracture toughness at -30°F when tempered to strength levels up to 200 ksi but not at higher strength levels. However, several undesirable characteristics of AISI 4340 are motivating the search for a better material for HIRT models. The principal disadvantages of AISI 4340 for this application are:

a. Distortion caused by quenching and tempering.

b. Machining must be performed in fully hardened condition.

c. Marginal dimensional stability.

d. Need for a protective finish to prevent corrosion.

10.3 MATERIALS SEARCH

A search was conducted of properties and characteristics of various materials to investigate their suitability for HIRT model construction. Candidate materials were identified and grouped into material classes for comparison.

Twelve classes of materials were considered for the HIRT model application as listed in Table 10.

10.4 GENERAL DISCUSSION OF MATERIAL CLASSES

To provide the most realistic basis for evaluation, one representative alloy or material from each class was selected for the properties comparison. Where available, properties data for product form and heat treatment believed most applicable to HIRT models were used.

Three classes of materials that show the greatest promise for meeting the HIRT model requirements are

a. Precipitation hardenable stainless steels.

b. 18% Ni maraging steels.

c. Quenched and tempered steels.

Table 10. Comparative Properties of General Classes of Materials (Ambient Temperature)

Material class	Representative alloy & condition	K_{tu} (ksi)	Elong. (%)	E (10^6 psi)	K_{su} (ksi)	G (10^6 psi)	ω (lb/in.^{3})	Fracture toughness and impact strength: Charpy V-notch (ft-lb)	Fracture toughness and impact strength: K_{ic} (ksi $\sqrt{in.}$)	Q & T machinability	Weldability	Availability (bar, plate or billets)	Cost ($/lb)
Quenched & tempered steels	D6AC Q & T[a] 1,050F	230	10	29	132	11	0.283	18	90	Normalized-good Q & T[a] -poor	Good	Good	0.60
Maraging steels	18 Ni-250 grade	250	10	26.5	143	10.3	0.289	40	90	Good	Good	Good	2.00
Precipitation hardenable stainless steels	PH 13-8Mo H1000	215	13	28.3	124	11.0	0.279	30	95	Good	Good	Good	2.00
Martensitic hardenable stainless steels	AISI 410 Q & T[a] 600F	190	25	29	---	12.5	0.28	35	---	Annealed-good Q & T[a] - fair	Fair	Fair	0.70
Nickel-base superalloys	Inconel 718 STA[c]	208	21	29.6	---	11.4	0.297	21	130	Fair	Good	Good	3.00
Titanium alloys	Ti-6Al-4V STA[c]	170	8	16	98	6.2	0.160	---	60	Fair	Good	Good	4.00
Molybdenum alloys	TZM SR[b]	125	15	46	---	---	0.370	---	---	Good	Not recommended	Fair	17.00
Beryllium-nickel alloys	Be-Ni 440 STA[c]	215	12	28	15	---	0.302	---	---	Annealed-good aged - fair	Good	Not available	8.00
Aluminum alloys	7075-T6	83	11	10.4	43	3.8	0.101	---	30	Good	Not recommended	Good	0.60
Boron/aluminum composites	B/6061 unidirectional	210	< 1	30	16	6	0.096	---	---	Not applicable	Not weldable	Special fabrication	500.00
Boron/epoxy composites	B/SP-272 unidirectional	220	< 1	31	13	1.8	0.071	---	---	Not applicable	Not weldable	Special fabrication	250.00
Graphite/epoxy composites	HT-S/X-904 unidirectional	180	< 1	20	13	0.7	0.055	---	---	Not applicable	Not weldable	Special fabrication	125.00

(a) Q & T = Quenched and tempered
(b) SR = Stress relieved
(c) STA - Solution treated and aged

The rationale for eliminating the other material classes from further consideration is discussed below.

The advanced composite materials, boron/aluminum, boron/epoxy and graphite/epoxy possess excellent strength and stiffness in unidirectional layups. However, insufficient design and fabrication experience exists to effectively use these properties for general model construction. In addition, the cost of the advanced composites is extremely high compared to the more conventional materials used for wind-tunnel models. Extensive experience is presently being developed with the advanced composite materials for aircraft, spacecraft and missile systems where the superior strength/density properties offer promise of major weight savings. As the experience progresses in working with advanced composites, these materials may become attractive candidates in the future for wind tunnel models.

The aluminum alloys do not possess sufficient strength or stiffness to merit their use in highly loaded HIRT models. Molybdenum alloys exhibit the highest modulus of the material classes evaluated, but low strength, poor fracture toughness at -30° F, and high cost would make their use unattractive for this application. Titanium alloys possess sufficient strength to merit consideration, but lower modulus, more difficult machining, and higher cost make their use less attractive than steels. Superalloys exhibit much similarity in properties to the precipitation hardenable stainless steels including strength, modulus, fracture toughness, and dimensional stability. However, lower cost and better machinability favor the selection of precipitation hardenable stainless steels. From the limited data available, beryllium-nickel 440 appears to have an attractive combination of mechanical properties, but high cost and nonavailability of large billet stock precludes the selection of this alloy. Some of the martensitic stainless steels can be quenched and tempered to develop strength levels up to 280 ksi. However, the alloys of this class that can be hardened to strength levels of 200 ksi or higher have low ductility and toughness at -30° F, which make them unsuitable for HIRT models.

10.5 PROMISING MATERIAL CANDIDATES

This discussion concerns the three classes of steels that show the greatest potential for the HIRT model application. Representative high-strength steels of each of the three classes are

a. Precipitation Hardenable Stainless Steels: PH13-8Mo, 17-4PH, 15-5PH.

b. Maraging Steels: 18Ni-200 grade, 18Ni-250 grade, 18Ni-300 grade, 18Ni-350 grade.

c. Quenched and Tempered Steels: D6AC, 300M, 9Ni-4Co, 4330-V Mod, 4340, H-11.

10.5.1 Precipitation Hardenable Stainless Steels

The precipitation hardenable stainless steels provide an excellent combination of high strength, notch toughness, corrosion resistance, and dimensional stability. These steels require only a simple one-step heat treatment that avoids distortion or heat scaling. In addition, these alloys have good machinability and weldability and are available in large sections. The excellent corrosion resistance would eliminate any need for protective coating of test models. One disadvantage compared to maraging or quenched and tempered steels is that heat treating to strength levels above 220 ksi results in poor notch toughness.

The PH13-8Mo alloy has the best combination of properties for HIRT test models of the various precipitation hardenable stainless steels available. This alloy was developed primarily for large sections where notch toughness, high strength, and stress-corrosion resistance are important (Reference 15). PH13-8Mo can be used at ultimate tensile strength levels up to 220 ksi with good fracture toughness at both ambient temperature and -30° F. As previously discussed, 17-4PH is not suitable for this application because of poor fracture toughness at -30° F when heat treated to stress levels above 160 ksi. 15-5PH is a modification of 17-4PH and has similar limitations.

10.5.2 Maraging Steels

The maraging steels have an excellent combination of strength, notch toughness and resistance to fatigue and stress corrosion cracking. Other favorable factors include good machinability and weldability, availability from multiple sources, and low cost (References 16 through 19). In general, the maraging steels are applicable over the same strength ranges as the quench and tempered steels. The major advantage of maraging steels for HIRT model construction is freedom from distortion during heat treatment. The components can be completely machined and then hardened with a single, low-temperature heat treatment. A slight uniform shrinkage takes place during the aging treatment. Nominal values for dimensional changes in the maraging steels resulting from the precipitation hardening treatment are as follows:

18 Ni - 200 grade	-0.04%
18 Ni - 250 grade	-0.06%
18 Ni - 300 grade	-0.08%

This dimensional change can be compensated during machining in the case of large parts or very close tolerances. Weldments of maraging steels require only the aging treatment to achieve properties and stress relief. The maraging steels have only slightly better corrosion resistance than quenched and tempered steels and must be protected from corrosion by an appropriate coating system.

10.5.3 Quenched and Tempered Steels

The quenched and tempered steels are the most widely used high-strength steels for structural applications. These steels have an excellent combination of strength, notch toughness, and resistance to fatigue and stress corrosion cracking, both in parent metal and welds. Other factors favoring these steels are good machinability, availability from multiple sources, and low cost. These steels are weldable, but welds have lower toughness, particularly when heat treated to high stress levels. Although used extensively for highly stressed aircraft components, 4340 has lower ductility and fracture toughness than some of the more recently developed steels. D6AC, 4330V-modified, and 300M steels are essentially modifications of AISI 4340, providing improved fracture toughness and higher strength. The strength and fracture toughness relationships of these steels at room temperature and -65°F are shown in Figures 66 and 67. The 9Ni-4Co alloys also have good strength and fracture toughness. However, higher alloy content make them more costly than other steels in this class, and alloy segregation can be a problem. The H-11 steels have much lower fracture toughness compared to the modified 4340 steels (Figures 66 and 67). Warpage of complex-shaped parts during heat treatment is a major problem with the quenched and tempered steels. Machining to close dimensional tolerances must be performed in the fully hardened condition. In addition, these steels must be protected from corrosion by an appropriate coating system.

10.6 ALLOY SELECTION

The alloys recommended for construction of HIRT test models are listed below for three ranges of ultimate tensile strength. The alloys for the 200-250 ksi and 250-300 ksi ranges are listed in order of preference, with the first alloy having the best combination of properties. The alternate alloys should be used where special considerations such as availabiltiy and cost outweigh the difference in properties.

20-250 ksi

PH13-8Mo H1000*
18Ni-250 grade*
D6AC

250-300 ksi

18Ni-300 grade*
300M
D6AC

>300 ksi

18Ni-350 grade

*NOTE: If tunnel operating temperatures are reduced to -120°F, PH 13-8 Mo steel must be heat treated to condition H1100 or H1050 to maintain an acceptable Charpy V-notch of 15 or greater. 18Ni-250 grade and 18Ni-300 grade are usable at -120°F.

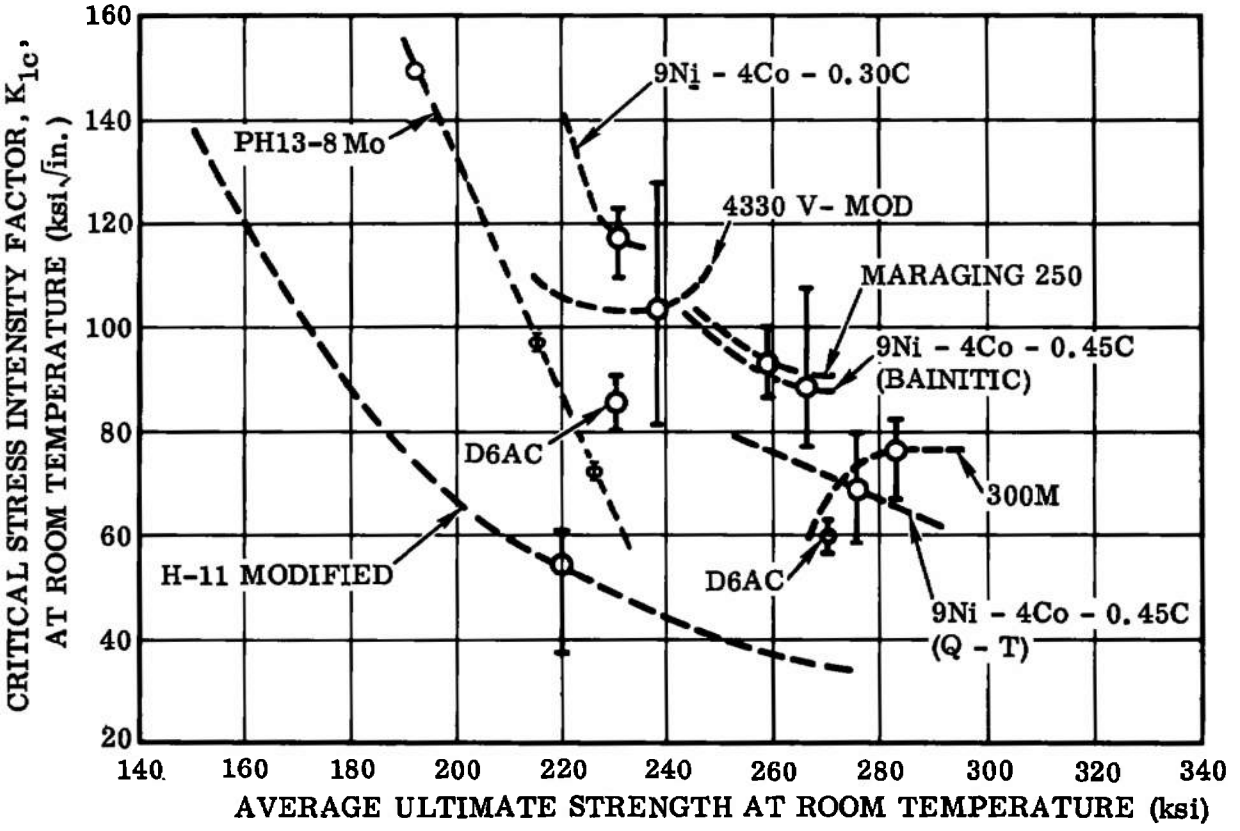

Figure 66. Strength and Room Temperature Fracture Toughness Relationships

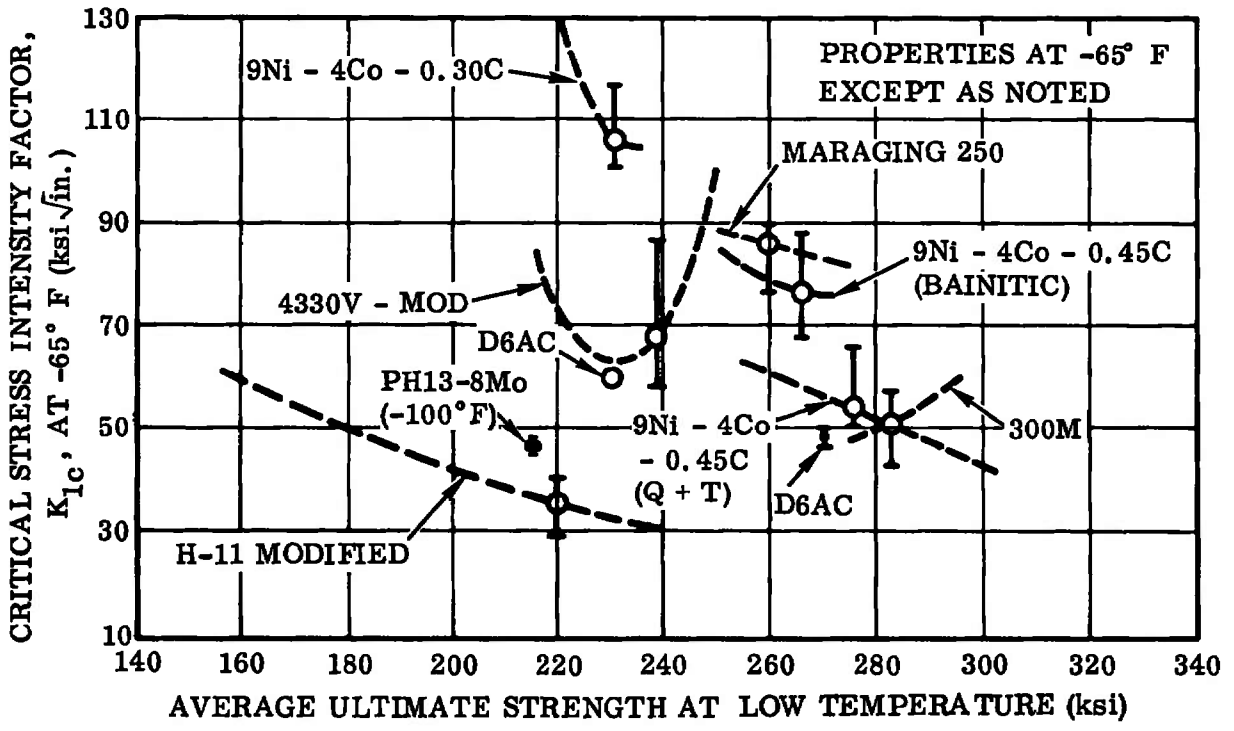

Figure 67. Strength and Low Temperature Fracture Toughness Relationships

Comparison and selection of alloys was based on use of bar, plate or forging billets for model construction. Although many of the selected alloys are available as castings, this product form is not recommended for HIRT models because of lower design allowables introduced by the casting factor and the need for optimum material quality to meet the material finish requirements as discussed in a later section.

10.7 PROCUREMENT SPECIFICATIONS

The procurement specifications, product forms, and condition for the recommended alloys are given in Table 11. Only vacuum-melted alloys are specified. Although some alloys are available in air-melted grades, these are not recommended because of the high stress level, low safety factor, and critical surface finish requirements.

Table 11. Material Specifications for Recommended Alloys

Alloy	Procurement specification	Material form	Condition
PH 13-8 Mo	AMS 5629A	Bar, forgings	Solution annealed
18Ni-250 grade	MIL-S-46850A Type III grade 250	Bar, plate, forgings	Solution annealed (A)
18Ni-300 grade	MIL-S-46850A Type III grade 300	Bar, plate, forgings	Solution annealed (A)
18Ni-350 grade	*	Bar, plate, forgings	Solution annealed (A)
D6AC	MIL-S-8949	Bar, plate, forgings	Normalized or normalized and tempered
300M	MIL-S-8844C	Bar, forgings	Normalized or normalized and tempered

*No procurement specification currently available. Material can be procured by producer specification VASCOMAX 350.

10.8 DESIGN ALLOWABLES

The design mechanical and physical properties for the recommended alloys are listed in Table 12. All mechanical properties are for product forms suitable for HIRT models; i.e., bar, plate, and forgings. The design allowables for D6AC and 300M were obtained from MIL-HDBK-5B, 1 September 1971 (Reference 20). The mechanical properties allowables are based on specified minimum values of the appropriate specification ("S"-basis).

Design allowables for PH 13-8Mo are contained in MIL-HDBK-5B but are incomplete. The tentative allowables for PH13-8Mo listed in Table 12 are proposed design mechanical

Table 12. Design Mechanical and Physical Properties of Materials Recommended for HIRT Test Models

Specification	AMS 5629A	MIL-S-46850A Type III Grade 250	MIL-S-46850A Type III Grade 300	None	MIL-S-8949		MIL-S-8844C Class 3 - 300 M
Alloy	PH13-8Mo	18Ni-250 grade	18Ni-300 grade	18Ni-350 grade	D6AC		300M
Form	Bar, Forgings	Bar, Forgings	Bar, Forgings	Bar, Forgings	Bar, Billets		Bar, Forgings
Condition	H1000	STA(a)	STA(a)	STA(a)	Q & T (b)		Q & T (b)
Basis	Tentative A	Tentative S	Tentative S	Tentative S	S		S
Mechanical properties							
F_{tu} (ksi)	201	250	300	350	220	260	280
F_{ty} (ksi)	190	240	280	330	190	215	230
F_{cy} (ksi)	200	245	280	---	213	240	247
F_{su} (ksi)	119	150	170	---	130	156	168
F_{bru} (ksi):							
(e/D = 1.5)	302	---	---	---	297	347	---
(e/D = 2.0)	402	---	---	---	385	440	---
F_{bry} (ksi):							
(e/D = 1.5)	263	---	---	---	274	309	---
(e/D = 2.0)	338	---	---	---	302	343	---
e (percent)	10	6	5	2	10L 7T	10L 3T	5
E (10^6 psi)	28.3	25.7	27.0	27.0	29.0		
E_c (10^6psi)	29.4	---	---	---	29.0		
G (10^6 psi)	11.0	---	---	---	11.0		
Poisson's ratio	0.278	0.30	---	---	0.32		
Physical properties							
ω (lb/in.^{3})	0.279	0.289	0.29	0.292	0.283		
C (Btu/ (lb) (F)	0.11 (32-212F)	0.107 (at 300F)	0.11 (at 300F)	---	0.114 (at 32F)		
K (Btu/(hr) (ft^2) (F)/ft	8.0 (at 200F)	14.6 (at 75F)	12 (at 75F)	---	22.0 (at 32F)		
α (10^{-6}in. /in. /F)	5.7 (at 200F)	5.6 (75-800F)	5.6 (75-900F)	6.3 (70-900F)	6.3 (0 to 200F)		

(a) STA = Solution treated and aged
(b) Q & T = Quenched and tempered

and physical properties from the 44th meeting of the MIL-HDBK-5 committee (References 16 and 17). The mechanical properties for PH13-8Mo were established on an "A" basis.

No design allowables for the 18Ni maraging steels have been incorporated in MIL-HDBK-5B. The values presented in Table 8 are tentative values compiled from the appropriate specifications, vendor data sheets, (References 16, 17, and 18) and the Aerospace Structural Metals Handbook (Reference 23). The design mechanical properties are established as the specification minimums where available for 18Ni-250 grade and

18Ni-300 grade. No present specification exists for 18Ni-350 grade, and properties data are very limited. The tentative design properties for 18Ni-350 grade listed in Table 8 are based on vendor data for VASCOMAX 350 (Reference 16).

10.9 SURFACE FINISH

Contemporary test models are frequently polished in critical flow areas to a finish of 32 to 16 microinch, but better surface finishes are generally not required. (The surface finish nomenclature microinch is the arithmetical average of deviation from mean centerline, as established by American Standards Association (B46.1-1962) (Reference 24). HIRT models will require a surface finish of 16 microinch or better. Surface finishes of 8 microinch or 4 microinch may be necessary in critical flow areas. However, obtaining these surface finishes on large test models will be costly. It is possible that cost considerations may result in establishing finish requirements that are less stringent than the optimum from an aerodynamic standpoint.

The requirement for superfine finishes makes it important to use the highest quality materials available, such as wrought forms of vacuum-melted alloys. Although castings are sometimes used for current test models, they are not recommended for the HIRT application. It is difficult to produce castings that are completely free from defects such as micro-porosity, inclusions, and coarse grain structure, which have an adverse effect on surface finish.

Procedures must be developed to achieve surface finishes on test models in the range of 4 to 16 microinch. Many types and sequences of polishing and buffing operations have been used to produce mirror-like finishes on metals. From this experience it would appear that the desired results could be achieved with the following sequence of operations: grinding, polishing, hard buffing, and color buffing.

Electropolishing has been found to be very effective as the final polishing operation for steels (a surface finish of 8 microinch can be obtained by removing approximately 1 mil of metal from an existing 16 microinch finish). Substitution of electropolishing for buffing and at least part of the mechanical polishing would reduce the cost of the final finishing operations by more than one-half. An electropolishing process that has achieved excellent results with the candidate steels is the proprietary Molectrics Summa process (Molectrics, Inc., Inglewood, California). (Reference 25.)

Most model fabrication shops use stoning and fine-grit papers for polishing models and have little or no experience with electropolishing. Experience with aircraft parts has shown that multi-piece components must be disassembled and cleaned after electropolishing to avoid potential stress corrosion from entrapped chemicals. Welded, brazed, and soldered parts of either similar or dissimilar metals can be satisfactorily electropolished. In addition to improving the surface finish, electropolishing provides a clean and passivated surface, which improves the corrosion resistance and toughness of the material.

10.10 PROTECTIVE COATINGS

Models constructed of maraging steels and quenched and tempered steels will require some form of corrosion protection. Although tunnel testing does not involve a corrosive environment, protection during handling and storage is necessary. In current practice, test models are frequently protected by electroplating or a chemical treatment to produce a black oxide coating. Application of either protective finish could degrade the superfine finish required for HIRT models. The black oxide finishes such as MIL-C-13924B, Class 1, provide only limited corrosion protection, and an oil film is required during storage.

The protective system recommended for HIRT models is a flash plating of chromium or nickel (0.0002-inch maximum thickness), which will provide both corrosion resistance and protection of the surface finish. The proprietary Electrolizing process (Electrolizing, Inc., Los Angeles, Calif.) produces a thin, hard, dense chromium coating of uniform thickness that would be suitable for this application. If nickel plating is used it should be applied by the electroless nickel process to ensure a thin uniform coating on complex shapes. The use of flash plating on test models will generally require final buffing after the plating operation to restore the required surface finish.

Welded, brazed, and soldered parts of either similar or dissimilar metals present no problems with these plating processes. Mechanically fastened components should be dissassembled prior to plating to avoid potential stress corrosion from entrapped chemicals. Masking can be used in any area where the plating would be undesirable.

CAUTION

Steels heat treated to high strength levels are subject to embrittlement from hydrogen absorbed during pickling and plating operations. As a precaution, all high strength steel parts should be baked for 24 hours at 375° F after plating.

SECTION XI

MODEL COSTS

The estimated cost of fabricating models for the HIRT facility will be different from present high-speed force or pressures wind tunnel models. Most models for HIRT testing will have less than a 6-foot wing span and will be fabricated mostly from high-strength steel alloys. Models with a large number of variables are not considered in this report.

Cost estimates for fabricating a variety of models are presented in Table 13.

Table 13. Model Fabrication Cost Comparisons

Type of model	Material	Surface finish			Model scales	
		A	B	C	32 to 16 μ-in. finish	
	PH 13-8 Mo	32 to 16 μ-in.	8 μ-in. to 16 μ-in.	4 μ-in. to 16 μ-in.	1.5 HIRT	2 HIRT
1. Solid wing	1.0	1.0	1.1	1.25	1.5	2.0
2. Reduced chord for deflected surfaces	1.25	1.25	1.35	1.40	1.85	2.5
3. Pressure model (400 orifices)	1.4	1.4	1.5	1.65	1.90	2.40

Three basic types of models are considered:

a. Basic solid wing model with few variables.

b. Basic model with a reduced wing chord to allow for deflected surfaces.

c. Pressure models containing approximately 400 pressure orifices.

Fabrication costs for each of these models are divided into five categories:

a. Complete model finished to a surface finish of 32 to 16 microinches.

b. Minimum of 30% of the airfoils and fuselage finished to 8 microinches with the remainder of the model finished to 16 microinches.

c. Minimum of 30% of the airfoils and fuselage finished to 4 microinches with the remainder of model finished to 16 microinches.

d. Scale equal to 1.5 × HIRT scale.

e. Scale equal to 2.0 × HIRT scale.

It should be noted that although category headings have been limited to five, items such as extra care in handling, adherence to material and fabrication specifications, inspection procedures, etc., have been considered in estimating model costs.

A baseline model is defined as a HIRT scale (approximately 5-foot span), solid-wing model fabricated from PH 13-8 Mo steel, with an overall surface finish of 16 to 32 microinches. The baseline cost factor (1.0) is assumed to be a 6,000 manhour fabrication task. (A comparable model for the Ames 11-foot Wind Tunnel is estimated to cost approximately 5,000 manhours---assuming the use of an aluminum fuselage.)

For example: Reference Table 13.

The estimated cost of a HIRT model with a reduced wing chord requiring a surface finish of 4 to 16 microinches is:

Surface finish factor of 1.40 — 6,000 × 1.40 = 8,400 manhours.

A similar model for a scale of 2 × HIRT (Surface finish of 16 to 32 microinches):

Scale cost factor of 2.50 — 6,000 × 2.50 = 15,000 manhours.

It should be noted that while the engineering task related to the HIRT models is not a part of this study, it is apparent that engineering costs will increase. Typical areas requiring additional effort are:

a. Model loads definition.

b. More detailed stress analysis.

c. Test plans.

d. Material procurement.

e. Model inspection and quality control.

f. Model distortion analysis.

It is estimated that the ratio of engineering manhour effort to the fabrication effort for a basic HIRT model will be approximately 38%.

SECTION XII

CONCLUSIONS

The results of this study clearly indicate that wind-tunnel models of the four aircraft considered can be designed and fabricated for testing throughout the entire flight envelope in the proposed HIRT facility. Conventional state-of-the-art materials and fabrication techniques can be used for these models.

Although the models can be designed to be structurally adequate for full-scale Reynolds number testing throughout their operating envelopes, some problems are associated with these models. The high loads and the requirement for better model surface finishes for high Reynolds number testing tend to dictate that HIRT models will have considerably fewer variables than present-day multipiece designs. Careful consideration must be given to minimizing streamwise joints, coverplates, fasteners, etc.

The models covered in this study were not stress limited in most cases. The high model loads produce model deformations that are larger than normal for most existing wind tunnels. Comparisons between the model deformation and the full-scale vehicle deformation (reference Figure 44) for the ATT configuration indicates that the increased flexibility of the wing may allow a closer simulation of the model to full-scale distortion over a broader range of conditions than presently attainable in existing wind tunnels.

It is estimated that a ratio of engineering effort to fabrication effort for a HIRT model will be higher than for a present-day model. Whereas it has been shown that the fabrication costs for the basic HIRT model will be 20% higher, the combined task of engineering and fabrication is estimated as 33% higher than present-day models.

The selection and quality control of materials used for HIRT models must be accomplished with special care. Since operating the HIRT tunnel at -30°F results in a large reduction in the dynamic pressure required to produce a given Reynolds number per foot, the selection of materials for that operating condition is important. The precipitation hardenable stainless steels are recommended as the first choice for general model fabrication. These steels provide an excellent combination of high strength, notch toughness, corrosion resistance and dimensional stability. These steels are simple to heat treat and require no special protective coatings for models. PH 13-8 Mo Alloy is recommended as the best choice of materials for models requiring an ultimate tensile strength of 220 ksi or less. For ultimate tensile strengths of 250 to 300 ksi, 18 Ni-300 grade maraging steel is recommended. 18 Ni-350 grade maraging steel is recommended for requirements of ultimate tensile strengths greater than 300 ksi.

Admissible roughness estimates computed for the models in this study indicate that acceptable surface finishes in critical areas run from 11 to 70 microinches (Reference Table 1). Finishes of that quality are within the present-day state of the art in the fabrication of wind tunnel models.

SECTION XIII

RECOMMENDATIONS

13.1 RECOMMENDATIONS FOR FURTHER ANALYSES

Due to the scope of the subject of wind tunnel models for the HIRT facility, it was necessary to limit the depth of study in many areas. It is recommended that additional work be performed in various areas where a more specific detailed analysis of a particular problem could yield useful information regarding the design and fabrication of models for testing in the HIRT facility.

13.2 ADDITIONAL STUDY AREAS

The following recommendations concern areas that were not covered in the original study program.

a. Conduct a study to determine the possibility of designing a model wing for testing in the HIRT facility with a predetermined jig twist, which would enable the model wing to distort under a given load to match the full-scale airplane distortion. Techniques of varying test conditions should be analyzed to determine a range of test conditions that would allow the model wing to match the full-scale wing twist and/or vertical deflection within a specified tolerance.

b. Determine the model limitations of a present-day multipiece model design and upgrade the design, where necessary, to achieve a test range capable of encompassing the airplane operating envelope. The model should include:

   1. Inlets with provisions for air flow through the fuselage.

   2. Sting support.

   3. Deflected control surfaces.

c. Model loads in the HIRT facility will be very large for the size of model when compared to the normal transonic models of today. A new family of six-component strain gage balances must be designed, built, and calibrated. A study should be conducted to verify the predicted load capability versus diameter of these balances. External balance dimensions should be accumulated for a variety of load capacities that will be in the HIRT range. Balance deflections should also be studied since balance deflection contributes a large increment to the clearance requirement at the model/sting exit.

d. This study was limited to the use of conventional sting-mounted models. Various model support systems and their effect on the design and structural limitations of models for the HIRT facility is of great importance. A study should be conducted to investigate alternate model support systems and their effects on HIRT models.

e. A reflection plane model would offer several advantages in HIRT testing. Model scale could be increased considerably, which would decrease model stress levels and distortions. Model variable surfaces would be fabricated and rigged for less cost (due to the singlehanded parts). Wall or floor mounting would eliminate the need for aft fuselage distortion for sting clearances. A study should be conducted to determine the model limitations of a reflection plane model for the HIRT facility.

f. The high loads imposed on the models in the HIRT tunnel can produce considerable aeroelastic deformation to the primary aerodynamic surfaces. Wing twist and deflection will be produced, and since the models cannot be fabricated to be structurally similar to the flight vehicle, the aeroelastic behavior as a function of dynamic pressure will be different. An undesired wing twist would cause a disturbed span loading, which alters the configuration-induced drag characteristics. Lift and moment characteristics are also affected and lead to errors in trim characteristics caused by a lower lift curve slope and a more unstable configuration. Changes to the wing twist also imply a disturbed chordwise pressure distribution, and at supercritical Mach numbers the upper surface shock wave location and strength can be affected. The latter could bear directly on the drag divergence-buffet characteristics. Experience with supercritical wings has shown considerable angle-of-attack sensitivity. Currently the ability to predetermine the magnitude of these effects outside the tunnel is limited to empirical analysis for supercritical conditions. For subcritical conditions, linear theories may prove to be adequate for data corrections in the linear lift range but will be inadequate for assessing the effects on flow separation characteristics. A study should be directed toward analyzing the aerodynamic corrections dictated by the elastic differences between the model and the full-scale vehicle.

SECTION XIV

REFERENCES

1. J. D. Whitfield, C. J. Schueler, and R. F. Starr, ARO, Inc., "High Reynolds Number Transonic Wind Tunnels – Blowdown or Ludwieg Tube," AGARD – CP-83-71, Page 29, April 26, 1971.

2. R. G. Roepke, "The High Reynolds Number Transonic Wind Tunnel HIRT Proposal as Part of the National Aeronautical Facilities Program," AIAA Paper No. 72-1035, September 13-15, 1972.

3. "Report of the AGARD Ad Hoc Committee on Engine – Airplane Interface & Wall Corrections in Transonic Wind Tunnel Tests," AGARD-AR-36-71.

4. "Hypersonic Research Facilities Study," McDonnell Aircraft Company, NASA CR 114323, Volume II, Part I, Pages 6-52, October 2, 1970.

*5 R. F. Starr, ARO, Inc., " Aerodynamic and Systems Considerations for Short-Duration Transonic Testing."

6. H. Schlichting, Boundary Layer Theory, p. 559, McGraw-Hill.

7. "Application of Lifting Line Theory to Aircraft Aeroelastic Loads Analysis," General Dynamics Convair Report No. GDC-ERR-AN-1128, February 1968.

8. W. L. Gray and K. M. Schenk, Boeing Aircraft Co., "A Method for Calculating the Subsonic Steady-State Loading on an Airplane with a Wing of Arbitrary Plan Form and Stiffness," NACA 3030, December 1953.

9. L. H. Schindel, "An Evaluation of Procedures for Calculating Aerodynamic Loads," AFFDL-TR-65-18, May 1965.

10. C. J. Borland, "Methods of Calculating Aerodynamic Loads on Aircraft Structures," AFFDL-TR-66-37, August 1966.

11. J. A. Blackwell, Jr., "A Finite Stop Method for Calculation of Theoretical Load Distribution for Arbitrary Lifting-Surface Arrangements at Subsonic Speeds," NASA TN D-5335, 1969.

12. USAF Stability and Control DATCOM, AFFDL Wright-Patterson Air Force Base, Ohio.

*13. Curves of Flow Properties for HIRT Operation, USAF, June 28, 1972.

*14. R. Underwood, "Possible Materials Suitable for HIRT Models," preliminary draft dated June 15, 1972, USAF-AEDC.

* References supplied by the Government for this contract.

15. Product Data S-33c, "Armco PH 13-8 Mo Precipitation-Hardening Stainless Steel, Bar, Wire, Plate and Forging Billets," Armco Steel Corporation, Advanced Materials Division, Baltimore, Maryland.

16. 18% Nickel Ultra High Strength Maraging Steels, VASCOMAX 200-250-300-350, Vanadium-Pacific Steel Co., Montibello, Calif.

17. Data Sheets, "Specialty Alloys" Latrobe Steel Company, Latrobe, Pennsylvania.

18. Data Bulletin, "18% Nickel Maraging Steels," International Nickel Company, June 1969.

19. A. M. Hall and C. J. Slunder, "The Metallurgy, Behavior, and Application of the 18-Percent Nickel Maraging Steels," NASA SP-5051, 1968.

20. MIL-HDBK-5B, Military Standardization Handbook, "Metallic Materials and Elements for Aerospace Vehicle Structures," Vols. 1 and 2, 1 September 1972.

21. Agenda 44th Meeting MIL-HDBK-5 Committee, Item 70-16, "Additional Data for PH13-8Mo."

22. Private Communication H. Garvin, Armco to R. Tryon, General Dynamics Convair Aerospace Division, November 3, 1972, on Proposed Properties of PH13-8Mo for MIL-HDBK-5.

23. Aerospace Structural Metals Handbook, AFML-TR-68-115, 1972 publication.

24. American Standard ASA B46. 1-1962, "Surface Texture – Surface Roughness, Waviness and Lay," American Society of Mechanical Engineers.

25. "Molectrics Summa Processing," Manufacturing Process Specification GJ-6-289-A, Molectrics, Inc., Inglewood, California.

APPENDIX I

TYPICAL COMPUTER RUN PROGRAM 4278

Model loads and deformations for this report were computed using a method and digital program identified as Program 4278. A description of Program 4278 can be found in Section 8. All computer data generated for this report is on file in Department 666-0 at the Convair Aerospace Division of General Dynamics Corporation, San Diego operation, San Diego, California. A typical run (in this case Condition 7, Table 2) is included as an illustration of the type of information available for each test condition shown in Table 2.

1. EXPLANATION OF SYMBOLS AND ABBREVIATIONS (See Page 158)

2. SAMPLE COMPUTER PRINTOUT (See Page 169)

1. EXPLANATION OF SYMBOLS AND ABBREVIATIONS

```
P427R      FORTRAN LOADS AEROELASTIC PROGRAM  (IN FORTRAN IV)

           R L HOLT  EXT.2194LF


NOTE- (1) ALL ANGULAR INPUT AND OUTPUT DATA ARE IN DEGREES.
          ANGULAR QUANTITIES INVOLVED IN INTERNAL PROGRAM
          COMPUTATIONS ARE IN RADIANS WITH THE EXCEPTION OF
          ALPHAR WHICH IS IN DEGREES

      (2) ONLY ONE LENGTH UNIT MUST BE USED IN THE PROGRAM

SET  INGM=0  IF WING GEOMETRY IS TO BE COMPUTED FROM PLANFORM
             DATA

SET  INWNO=1  IF WIND TUNNEL DATA IS TO BE USED

SET  INBAL= NUMBER OF SETS OF BALANCE DATA

SET  IFLGS = 0 IF SYMMETRIC LOADS ARE WANTED

SET  IFLGA = 0 IF ASYMMETRIC LOADS ARE WANTED

SET  LTAIL= NSECT+1 FOR CONVENTIONAL TAIL LOAD CONFIGURATIONS

SET  RIGID=1. FOR RIGID CASE

SET  NFUS= NUMBER OF WING STRIPS OF THE HALF WING THAT LIE
           INBOARD OF THE WING-FUSELAGE JUNCTION

SET  NEXTW  = NUMBER OF WEIGHTS THAT LIE ON A WING SEMISPAN.


     LIST OF PROGRAM PARAMETERS ,THEIR UNITS AND DEFINITIONS
*****-*****-*****-*****-*****-*****-*****-*****-*****-*****-


 OTHER FORCE AND LENGTH UNITS  DIFFERENT FROM THOSE SPECIFIED
 IN THE FOLLOWING LIST CAN BE USED

PARAMETER
 NAME        UNITS                  DEFINITIONS
 *****-*****-*****-*****-*****-*****-*****-*****-*****-*****-

 ACLC         IN.       ASYMMETRIC PORTION OF LEFT-WING LOCAL LIFT
                        COEFFICIENT MULTIPLIED BY LOCAL CHORD

 ADG          DEG       INCREMENTAL ANGLE OF ATTACK OF WING SECTION DUE TO
                        AEROELASTIC EFFECTS FROM LOADINGS WHICH ARE NOT
                        EXPLICIT FUNCTIONS OF ANGLE OF ATTACK.

 ADFL         -         FLAP    EFFECTIVENESS

 ADSL         -         SLAT    EFFECTIVENESS

 ADSP         -         SPOILER EFFECTIVENESS
```

*	AFAD	DEG	LOCAL WING ELASTIC AXIS SWEEPBACK ANGLE
	AFXT	PER LB	EXTERNAL STORES MATRIX ALPHAF DEPENDANT COMPONENT
	AINCB	DEG	INCIDENCE OF BODY WITH RESPECT TO SECTION CHORD LINE
	AINCF	DEG	INCIDENCE OF FUSELAGE WITH RESPECT TO ROOT CHORD LINE (MINUS. WING INCIDENCE ANGLE)
	AINCT	DEG	HORIZONTAL TAIL INCIDENCE ANGLE WITH RESPECT TO FUSELAGE REFERENCE LINE
	ALAM	--	WING TAPER RATIO
*	ALFND	DEG	TOTAL ANGLE OF ATTACK OF WING SECTION INCLUDING ALL AEROELASTIC EFFECTS
	ALGIB	DEG	INTERFERENCE TWIST DUE TO AERODYNAMIC INTERFERENCE EFFECTS OF NEIGHBORING BODIES (FUSELAGES.NACELLES.EXTERNAL STORES.ETC.) UPON THE WING. DATA IS REDUCED FROM WIND TUNNEL TEST RESULTS
	ALPH1	DEG	KNOWN LOCAL Z.L.L. ANGLE OF ATTACK FOR FIRST MODEL ANGLE OF ATTACK
	ALPH2	DEG	KNOWN LOCAL Z.L.L. ANGLE OF ATTACK FOR SECOND MODEL ANGLE OF ATTACK
*	ALED	DEG	LOCAL WING LEADING EDGE SWEEPBACK ANGLE
	ALFWT	DEG	ANGLE OF ATTACK AT WING CENTERLINE OF MODEL IN WIND TUNNEL
	ALPHAF	DEG	WING SECTION ZERO-LIFT-LINE ANGLE OF ATTACK (SAME AS ALFNO)
*	ALREFD	DEG	WING ROOT-CHORD ZERO-LIFT-LINE ANGLE OF ATTACK
	AOLSE	DEG	CLEAN WING SECTION ZERO LIFT LINE ANGLE RELATIVE TO ITS CHORDLINE
	AOLRT	DEG	ROOT WING SECTION ZERO LIFT LINE ANGLE RELATIVE TO ITS CHORDLINE.(-) FOR LIFT LINE ABOVE CHORDLINE
	AR	-	WING GEOMETRIC ASPECT RATIO
	ASELD	DEG	INCREMENTAL ANGLE OF ATTACK OF WING SECTION DUE TO AEROELASTIC EFFECTS FROM STORE LOADS WHICH ARE EXPLICIT FUNCTIONS OF ANGLE OF ATTACK
	ATAU	DEG	WING JIG TWIST RELATIVE TO ROOT CHORD
*	ATED	DEG	LOCAL WING TRAILING EDGE SWEEPBACK ANGLE

NOTE: * DENOTES ITEMS OF PARTICULAR INTEREST

*	ATELD	DEG	TWIST DUE TO THE ELASTICITY OF THE WING
	ATPAR	-	RATE OF CHANGE OF HORIZONTAL TAIL ANGLE OF ATTACK (AT) WITH ANGLE OF ATTACK OF WING ROOT-SECTION ZERO-LIFT-LINE (ALREFO). (ONE MINUS DERIVATIVE OF DOWNWASH ANGLE WITH RESPECT TO ALREFO) (1-D EPSILON/D ALPHA)
	ATPDDE	-	RATE OF CHANGE OF HORIZONTAL TAIL ANGLE OF ATTACK WITH ELEVATOR DEFLECTION (DDF)
	AWELD	DEG	INCREMENTAL ANGLE OF ATTACK OF WING SECTION DUE TO AERDELASTIC EFFECTS FROM CLEAN WING LOADS WHICH ARE EXPLICIT FUNCTIONS OF ANGLE OF ATTACK.
*	BARL	-	FOR SYMMETRIC LOADINGS----- SOLUTION TO THE SET OF SIMULTANEOUS EQUATIONS COMPRISED OF WING SYMMETRIC DOWNWASH EQUATIONS. VERTICAL FORCE EQUATION. AND PITCHING MOMENT EQUATION. IT IS COMPOSED OF THE WING SYMMETRIC LIFT DISTRIBUTION (CLC). WING ROOT ZERO-LIFT LINE ANGLE OF ATTACK (ALREFO). AND THE BALANCING TAIL LOAD (PT). ***OR*** FOR ASYMMETRIC LOADINGS----- SOLUTION TO THE SET OF SIMULTANEOUS EQUATIONS COMPRISED OF WING ASYMMETRIC DOWNWASH EQUATIONS. SIDEFORCE EQUATION. ROLLING MOMENT EQUATION. AND YAWING MOMENT EQUATION. IT IS COMPOSED OF THE LEFT-WING ASYMMETRIC LIFT DISTRIBUTION (ACLC). AIRPLANE SIDESLIP ANGLE (BETA). RUDDER DEFLECTION(DELTR). AND EITHER AIRPLANE ROLLING VELOCITY (PHID) OR AIRPLANE ROLL ACCELERATION (PHIDD) DEPENDING ON WHICH VARIABLE HAS BEEN SELECTED (SEE ROLL).
	BEXT	PER LB	EXTERNAL STORES MATRIX ALPHAF=0. COMPONENT
	BLAMD	DEG	WING QUARTER CHORD LINE SWEEPBACK ANGLE. DEFINED POSITIVE AFT OF LATERAL AXIS
*	BMWNG	IN.LB.	AERODYNAMIC WING BENDING MOMENT (ABOUT AXIS PARALLEL TO X-AXIS)
	BP	-	WIND TUNNEL MODEL SCALE
	C	IN.	LOCAL CHORD PARALLEL TO PLANE OF SYMMETRY
*	CBAR	IN.	WING MEAN AERODYNAMIC CHORD
	CDEA	PER DEG	EXT. STORE DRAG COEFF. VAR. WITH ALPHAF
	CDEZ	-	EXT. STORE DRAG COEFF. AT ALPHAF=0.
	CLC	IN.	SYMMETRIC PORTION OF WING LOCAL LIFT COEFFICIENT MULTIPLIED BY LOCAL CHORD
	CFS	NON DIMEN.	LOCATION OF FRONT SPAR FROM L.E.(PER CENT CHORD/100)

CLFA	PER DEG	SLOPE OF FUSELAGE LIFT CURVE COEFF
CLFO	-	LIFT COEFF OF FUSELAGE AT ALREFO=AOLRT
CLEA	PER DEG	EXT. STORE LIFT COEFF. VAR. WITH ALPHAF
CLEZ	-	EXT. STORE LIFT COEFF. AT ALPHAF=0.
CLWS	-	WING LIFT COEFFICIENT FOR TOTAL WING PLUS STORE AERODYNAMIC LOAD
CMEA	PER DEG	EXT. STORE PITCH MOMENT COEFF. VAR. WITH ALPHAF
CMEZ	-	EXT. STORE PITCH MOMENT COEFF. AT ALPHAF=0.
CMFA	PER DEG	SLOPE OF FUSELAGE MOMENT COEFF AT QUARTER CHORD OF MAC
CMFO	-	MOMENT COEFF OF FUSELAGE AT ALREFO=AOLRT AND QUARTER CHORD OF MAC
CMOTO	-	TOTAL SECTION MOMENT COEFF. AT SECTION QUARTER CHORD

ABOVE AERO COEFFS. RELATED TO FUSELAGE AND EXTERNAL STORE EFFECTS ARE BASED ON WINGA AND CBAR.

CNAFR	PER RADIAN	SLOPE OF CURVE OF CNA VS ALPHA FOR AIRPLANE WITH FLEXIBLE WING. THIS IS AN EXCEPTION TO THE USUAL PER DEG. INPUT.
CONONO	-	CONDITION NUMBER (10-ALPHANUMERIC CHAR.)
CONSJ	NON DIMEN.	CONSTANT WHICH IS USED IN THE CALCULATION OF TORSIONAL MOMENT OF INERTIA. USUAL RANGE IS .172 TO .186
* CR	IN	WING CHORD AT AIRCRAFT CENTERLINE
CPS	NON DIMEN.	LOCATION OF REAR SPAR FROM L.E.(PER CENT CHORD/100)
* CT	IN	WING CHORD AT TIP
DCDF	-	INCREMENT DRAG COEFFICIENT OF FUSELAGE
DCOT	-	INCREMENT DRAG COEFFICIENT OF TAIL
* DOE	DEG	ELEVATOR DEFLECTION
DELFL	DEG	FLAP DEFLECTION
DELSL	DEG	SLAT DEFLECTION
DELSP	DEG	SPOILER DEFLECTION
DEWT	DEG	ELEVATOR DEFLECTION IN WIND TUNNEL

	DNZ	-	POSITIVE INCREMENT OF NORMAL LOAD FACTOR TO BE USED IN THE ITERATIVE PROCESS OF OBTAINING THE DESIRED VALUE OF ALREFO WHEN USPLR.NE.0
*	EA	-	LOCAL WING ELASTIC AXIS POSITION. IN FRACTION OF LOCAL CHORD
	EAL	-	ELASTIC AXIS POSITION FROM LOCAL WING LEADING EDGE .IN FRACTION OF LOCAL CHORD.
	ECLTA	PER DEG.	EFFECTIVE LIFT CURVE SLOPE OF THE HORIZONTAL TAIL BASED ON WING AREA (WINGA) AND FREE-STREAM DYNAMIC PRESSURE (QDYN). TAIL EFFICIENCY FACTOR INCLUDED.
*	EI	LBS.IN.SQD.	EFFECTIVE VALUE OF PRODUCT OF MODULUS OF ELASTICTICITY AND WING SECTION BEAM BENDING MOMENT OF INERTIA
	ELFT1	LBS. PER IN.	WIND TUNNEL MODEL TEST LOCAL SPANWISE LOADING FOR FIRST MODEL ANGLE OF ATTACK
	ELFT2	LBS. PER IN.	WIND TUNNEL MODEL TEST LOCAL SPANWISE LOADING FOR SECOND MODEL ANGLE OF ATTACK
	[illegible]	-	SET.NE.ZERO TO ENTER AEROX FROM SYBAL (INSERT SET OF AEROX INPUT CARDS AFTER INPUT CARDS FOR SYBAL)
	ENST	-	[illegible] .NE.ZERO TO ENTER STORE FROM SYBAL (INSER[illegible]T OF STORE INPUT CARDS AFTER ANY AEROX INPUT [illegible]S FOLLOWING INPUT CARDS [illegible] FOR SYBAL)
*	ETA	-	POSITION OF WING STRIP ALONG Y-A[illegible] IN FRACTION OF HALFSPAN
	ETABAR	-	POSITION OF TOTAL WING PLUS STORE AERODYNAMIC LOAD ALONG Y-AXIS IN FRACTION OF SEMISPAN
*	GJ	LBS.IN.SQD.	EFFECTIVE VALUE OF SHEAR MODULUS OF ELASTICITY AND WING SECTION POLAR MOMENT OF INERTIA
	GUSTF	I	SET.NE.ZERO IF GUST CONDITION IS DESIRED
	H	IN.	LOCAL WING STRIP HALFWIDTH
	IAEROX	-	BODY IMAGE/OVERVELOCITY EFFECT FLAG.... SET.EQ.ZERO FOR BOTH IMAGE/OVERVELOCITY EFFECTS SET.EQ.1 FOR ONLY IMAGE EFFECTS SET.EQ.2 FOR ONLY OVERVELOCITY EFFECTS SET.EQ.3 FOR NO BODY EFFECTS
	IFUS	-	FUSELAGE IMAGE/ OVERVELOCITY EFFECT FLAG... SET.EQ.ZERO FOR BOTH IMAGE/OVERVELOCITY EFFECTS SET.EQ.1 FOR ONLY IMAGE EFFECTS SET.EQ.2 FOR ONLY OVERVELOCITY EFFECTS SET.EQ.3 FOR NO BODY EFFECTS

	ITIME	-	SET = 1 EACH TIME OVERLAYD.0 IS ENTERED (USED IN SYBALA TO SAVE DISK2 FOR THE NTH CASE)
	LTAIL	-	TAIL BOOM ENTRY STATION NUMBER (SET EQUAL TO NSTRP+1 FOR CONVENTIONAL TAIL CONFIG.)
*	MACHN	NON DIMEN.	MACH NUMBER. (READ INTO BOTH WINDT AND GUST)
*	MEAPIL	IN.LB.	WING BENDING MOMENT (AIR PLUS INERTIA) ABOUT ELASTIC AXIS
	MD	PER DEG	TWO-DIMENSIONAL LIFT-CURVE SLOPE PER DEG. INCLUDING COMPRESSIBILTY EFFECTS .FOR SECTIONS PARALLEL TO THE PLANE OF SYMMETRY
	NB	-	NUMBER OF BODIES PER SEMISPAN FOR WHICH IMAGE/OVERVELOCITY EFFECTS DESIRED (IN ADDITION FOT THE FUSELAGE)
	NBSEC	-	SECTION NUMBER WHERE BODY CENTERED
	NEXTR	-	NUMBER OF EXTERNAL STORES ATTACHED TO WING
	NFUS	-	NUMBER OF WING STRIPS/SECTIONS WITHIN FUSELAGE
	NG	NON DIMEN.	STATION NUMBER WHERE WEIGHT IS LOCATED
	NJ	-	EXT. STORE LOCATION STATION NUMBER
	NSTRP	-	NUMBER OF STRIPS ON WING HALFSPAN. STRIPS ARE ASSIGNED STATION NUMBERS.ONE TO NSTRP.FROM LEFT WING TIP TO WING ROOT
	PHID	DEG	WING QUARTER CHORD LINE DIHEDRAL ANGLE DEFINED POSTIVE ABOVE LATERAL AXIS NOTE. ALSO USED IN ASBAL.
	PT	LBS	BALANCING HORIZONTAL TAIL LOAD = PTAT + PTDDE
	PTAT	LBS.	PORTION OF HORIZONTAL TAIL LOAD DUE TO ANGLE OF ATTACK
	PTDDE	LBS.	PORTION OF HORIZONTAL TAIL LOAD DUE TO ELEVATOR DEFLECTION
	PTWT	LB	SUM OF ALPHA AND DELTA LOADS ON HORIZONTAL TAIL IN THE WIND TUNNEL
	PTZER	PER LB	TAIL LOAD STRUCTURAL MATRIX INFLUENCE ON WING
*	QDYN	LBS./SQ.IN.	FREE STREAM DYNAMIC PRESSURE
	QM	LBS./SQ.IN.	WIND TUNNEL MODEL TEST DYNAMIC PRESSURE
	RAERO	-	SET.NE.ZERO TO REUSE SYMMETRIC SECTION DATA
	RB	IN.	RADIUS OF BODY FOR WHICH EFFECTS DESIRED
	RF	IN.	EFFECTIVE RADIUS OF FUSELAGE(INFL. CALC.)

*	RHOAL	INLBSEC2/FT4	DENSITY OF AIR AT ALTITUDE.
	RWTS	-	SET.NE.ZERO TO REUSE WTS DATA
	S1A	PER IN	WING ASYMMETRIC DOWNWASH MATRIX
	S1S	PER IN	WING SYMMETRIC DOWNWASH MATRIX
	S2P	PER IN	WING ELASTICITY MATRIX
	SAIA	PER IN	ASYMMETRIC IMAGE-VORTEX EFFECT MATRIX. (CORRECTION TO SIA EXPOSED WING COMPONENTS)
	SAIS	PER IN	SYMMETRIC IMAGE-VORTEX EFFECT MATRIX. (CORRECTION TO SIS EXPOSED WING COMPONENTS)
*	SCLCQ	LB/IN	AERODYNAMIC WING LOADING (CONSTANT ACROSS EACH STRIP)
*	SHAPIL	LB	WING SHEAR DUE TO AIR PLUS INERTIA
*	SHWNG	LB	AERODYNAMIC WING SHEAR
*	SPAN	IN.	WING SPAN
	SZERO	-	OVERVELOCITY EFFECT MATRIX. (EFFECT OF K-TH BODY STORED IN THE NBSEC(K)-TH COLUMN. EFFECT OF FUSELAGE STORED IN THE NSTRP-TH COLUMN)
*	TEAPIL	IN.LB.	WING PITCHING MOMENT (AIR PLUS INERTIA) ABOUT ELASTIC AXIS
	THTDD	DEG/SEC.SOD.	PITCH ACCELERATION OF VEHICLE
	TSECT	NON DIMEN	MAXIMUM THICKNESS/CHORD RATIO OF A WING SECTION.
*	TQBR4	IN.LB.	TORQUE ABOUT CBAR DUE TO WING AERODYNAMIC FORCES
*	TQCHK	IN.LB.	TORQUE ABOUT CBAR DUE TO AIR PLUS INERTIA LOADS
*	TQFUA	IN.LB.	TORQUE ABOUT CBAR DUE TO FUSELAGE AT ANGLE OF ATTACK
*	TQFUO	IN.LB.	TORQUE ABOUT CBAR DUE TO FUSELAGE AT ZERO ANGLE OF ATTACK
*	TQINR	IN.LB.	TORQUE ABOUT CBAR DUE TO INERTIA OF TOTAL AIRCRAFT
*	TOTAL	IN.LB.	TORQUE ABOUT CBAR DUE TO HORIZONTAL TAIL LOAD
*	TOWNG	IN.LB.	AERODYNAMIC WING PITCHING MOMENT (ABOUT AXIS PERPENDICULAR TO X-AXIS)
	UDEGF	FT/SEC.	GUST VELOCITY (EAS)

	USPLR	DEG	SYMMETRIC PORTION OF UNSYMMETRIC SPOILER DEFLECTION. USE ONE-HALF ACTUAL DEFLECTION--OTHER HALF OBTAINED WITH DLASP.
	VEL	FT/SEC.	THE SPEED AT WHICH THE AIRPLANE MOVES THROUGH THE AIR SURROUNDING IT. THIS IS TAS DO NOT CONFUSE WITH CAS, EAS, OR IAS.
*	VFCHK	LB	VERTICAL FORCE AT CBAR DUE TO AIR PLUS INERTIA LOADS
	VFFUA	LB	VERTICAL FORCE ON FUSELAGE DUE TO ANGLE OF ATTACK
	VFFUO	LB	VERTICAL FORCE ON FUSELAGE AT ZERO ANGLE OF ATTACK
	VFINR	LB	VERTICAL FORCE DUE TO INERTIA OF TOTAL AIRCRAFT
*	VFTAL	LB	VERTICAL FORCE ON HORIZONTAL TAIL
*	VNZ	-	VERTICAL LOAD FACTOR ALONG Z-AXIS
*	W	LBS.	GROSS WEIGHT OF VEHICLE ALSO WEIGHT DISTRIBUTION ON WING SEMI-SPAN I USED IN SYBAL AND WTS)
*	WINGA	SQ.IN.	WING AREA
*	WTSH	LB	WING SHEAR DUE TO INERTIA
*	WTMEA	IN.LB.	WING BENDING MOMENT DUE TO INERTIA ABOUT ELASTIC AXIS
*	WTTEA	IN.LB.	WING PITCHING MOMENT DUE TO INERTIA ABOUT ELASTIC AXIS
*	XBAR4	IN.	FUS. STA. OF CBAR/4 ALONG X-AXIS
*	XC4	IN.	LOCAL QUARTER CHORD POSITION ALONG X-AXIS
*	XCG	IN.	FUS. STA. OF VEHICLE C.G. ALONG X-AXIS
	XDDE	IN.	DIFFERENCE BETWEEN ANGLE OF ATTACK TYPE AND ELEVATOR TYPE HORIZONTAL TAIL LOAD CENTER POSITIONS ALONG THE X-AXIS.--NEGATIVE IF ELEVATOR TYPE LOAD CENTER AFT OF ANGLE OF ATTACK TYPE LOAD CENTER.
	XE	IN.	EXT. STORE POS'N. ALONG X-AXIS
	XEA	IN.	FUS. STA. OF ELASTIC AXIS ALONG X-AXIS
	XEAIE	IN.	LOCATION ALONG X-AXIS OF INBOARD EDGE OF WING SECTION.
*	XFUS	IN.	FUS. STA. OF C.P. OF FUSELAGE LIFT

*	XLE	IN.	POSITION OF WING ROOT LEADING EDGE ALONG THE X AXIS.
	XTAIL	IN.	POSITION OF ANGLE OF ATTACK TYPE HORIZONTAL TAIL LOAD CENTER ALONG X-AXIS
	XW	IN.	FUSELAGE STATION OF DISTRIBUTED WEIGHT.
	YC4	IN.	LOCAL QUARTER CHORD POSITION ALONG Y-AXIS
	YE	IN.	EXT. STORE POS'N. ALONG Y-AXIS
	YIY	IN.LBS.SEC.SQD.	MOMENT OF INERTIA OF VEHICLE ABOUT PITCH AXIS THROUGH C.G.
	YTAIL	IN.	POSITION OF HALF TAIL LOAD ENTRY ALONG Y-AXIS
	YW	IN.	DISTANCE FROM FUSELAGE CENTERLINE TO DISTRIBUTED WEIGHT ALONG THE Y AXIS.
	ZBAR4	IN.	WATERLINE OF CBAR/4 ALONG Z-AXIS
	ZC4	IN.	LOCAL QUARTER CHORD POSITION ALONG Z-AXIS
	ZCDF	IN.	WATERLINE POSITION OF FUSELAGE DRAG
	ZCDT	IN.	WATERLINE POSITION OF TOTAL TAIL DRAG
	ZCG	IN.	WATERLINE OF VEHICLE C.G. ALONG Z-AXIS
	ZE	IN.	EXT. STORE POS'N. ALONG Z-AXIS
	ZEA	IN.	WATERLINE OF ELASTIC AXIS ALONG Z-AXIS
	ZFUS	IN.	FUSELAGE CENTER LINE POSITION ALONG Z-AXIS
	ZLE	IN.	POSITION OF WING ROOT LEADING EDGE ALONG Z-AXIS
*	ZOEDGE	IN.	DISPLACEMENT ALONG Z-AXIS OF ELASTIC AXIS AT OUTBOARD EDGE OF WING SECTION.
	ZW	IN.	WATER LINE OF DISTRIBUTED WEIGHT.

*****-*****-*****-*****-*****-*****-*****-*****-*****-*****-

THE FOLLOWING VARIABLES OCCUR IN THE ASYMMETRIC SECTION

*****-*****-*****-*****-*****-*****-*****-*****-*****-*****-

ABAL	-	FLAG WHICH IS SET EQUAL TO 1.0 FOR THE LAST ASYMMETRIC CASE PRIOR TO RESETTING INBAL. AND IS SET GREATER THAN ONE FOR ALL PRE-CEEDING ASYMMETRIC CASES

AIX	IN LB SECSQDMDMENT DF INERTIA VEHICLE ABOUT THE LONGITUDINAL ROLL AXIS.	
APDA	NDN DIMEN.	WING SECTION ANGLE OF ATTACK PEP DLAIL
APDSP	NDN DIMEN.	WING SECTION ANGLE DF ATTACK PER DLASP
AWD	DEG.	ASYMMETRIC WING TWIST. + WHEN RIGHT WING HAS INCREASED ANGLE DF ATTACK AND VICE VERSA FDR LEFT WING.
BETA	DEG.	SIDESLIP ANGLE OF AIRPLANE. + WHEN RELATIVE WIND VECTOR STRIKES DN THE RIGHT SIDE OF THE AIRPLANE CENTERLINE.
CNBT	PER DEG.	TDTAL AIRPLANE YAWING MDMENT CDEFF.CAUSEO BY BETA. (+FDR +BETA) NDTE.WING COMPONENT IS ABDUT 3X VERTICAL TAIL CDMPDNENT
CNPD	SEC.SQD./DEG	TDTAL AIRPLANE YAWING MDMENT CDEFF. CAUSED BY ROLLING VELDCITY PHID. THE WING CDMPONENT IS DPPDSITE IN SIGN TD THE TAIL CDMPDNENT AND ABDUT 4X AS LARGE. (-FDR+PHID)
CNRU	PER DEG.	TDTAL AIRPLANE YAWING MDMENT CDEFF. CAUSED BY RUDDER DEFLECTIDN. (-FDR+DELTR)
CRLBT	PER DEG.	TDTAL AIRPLANE RDLLING MDMENT CDEFFICIENT CAUSED BY BETA. (-FDR +BETA)
CRLPD	SEC.SOD./DEG	VERTICAL AND HDRIZDNTAL TAIL RDLLING MOMENT CDEFF. CAUSEO BY RDLLING VELDCITY, PHID. (WING CDNTRIBUTION IS CALCULATED INTERNALLY) (-FOR+PHID)
CRLRU	PER DEG.	TDTAL AIRPLANE RDLLING MDMENT COEFFICIENT CAUSED BY RUDDER DEFLECTIDN. (+FOR+DELTR)
CYBT	PER DEG.	TDTAL AIRPLANE SLOPE DF SIDE FDRCE CDEFF. VS BETA. (-FOR+BETA)
CYPD	SEC.SQD./OEG	VERTICAL AND HDRIZONTAL TAIL SLOPE DF SIDE FORCE COEFF. VS ROLLING VELDCITY.(-FOR+PHID)
CYRU	PER DEG.	TDTAL AIRPLANE SLOPE DF SIDE FDRCE CDEFF. VS RUDDER DEFLECTIDN. (+FDR+DELTR)
DELTR	DEG.	RUDDER DEFLECTION. A + DELTR YAWS THE NDSE TD THE LEFT.
DLAIL	DEG.	AILERDN DEFLECTIDN. + DLAIL ROLLS AIRPLANE WITH LEFT WING DESCENDING FIRST.
DLASP	OEG	ASYMMETRIC PART OF UNSYMMETRIC SPOILER DE-FLECTIDN. +DLASP RDLLS AIRPLANE WITH RIGHT WING DESCENDING FIRST. USE ONE-HALF ACTUAL DEFLECTION--OTHER HALF OBTAINED WITH USPLR.
PHID	DEG./SEC.	AIRPLANE RDLLING VELDCITY. + WHEN RIGHT WING IS DESCENDING.

PHIDD	DEG./SEC.SQD	AIRPLANE ROLLING ACCELERATION. +PHIDD WHEN RIGHT WING INITIALLY MOVES DOWN.
PSIDD	DEG./SEC.SQD	AIRPLANE YAWING ACCELERATION. + WHEN RIGHT WING MOVES BACK.
RASYA	-	SET.NE.ZERO TO REUSE ASYMMETRIC SECTION DATA
POLL	NON-DIMEN	SET = 1. IF PHIDD IS KNOWN AND PHID IS THE VARIABLE. OTHERWISE PHID IS KNOWN AND PHIDD IS THE VARIABLE.
VIZ	IN LB SEC SQD	MOMENT OF INERTIA OF VEHICLE ABOUT THE VERTICAL YAW AXIS.
VNY	NON.DIMEN.	LATERAL LOAD FACTOR ALONG Y AXIS. A + YNY TRANSLATES VEHICLE TOWARD RIGHT WING TIP.

2. SAMPLE COMPUTER PRINTOUT

```
P$MAIN2
C            P _ HOLT      HIPT ADVANCED TECHNOLOGY TRANSPORT UNBALANCED
 INGM=0,INWND=0,INBAL=10,IFLGS=0,          IFPRT=0,NOPLT=0,IGEOM=0,
 INBAL = 1,
 SYM4020 = 3HYES,                                                          PROGRAM FLAGS
 SYM4020 = 2HNO,
 ABAL = 0.,
 ASY4020 = 2HNO,          ITIMF=1,
 $END OF DATA

P$INPT14                  GEOMETRIC DESCRIPTION
 CR=28.313,
 PHID(1)=11*0.0,
 SPANBP(1)=.9135, .8279, .7406, .6541, .5577, .4812, .3945, .2961,
 SPANPP(9)=.2073, .1116, 0.,
 NSTPP=11,
 LTAIL=12,
 NFUS =1,
 SPAN =67.550,
 XLE  =25.14,
 ZLE  =8.05,
 XTAIL=96.00,
 YTAIL=0.0,
 EAL  =.405,
 ALED(1)=7*43.5, 45.0, 33.5, 59.0, 47.5,
 ATED(1)=7*36.0, 4*5.0,
C          SOLID WING WITH AFT 75 PERCENT OF CHORD REMOVED      10/13/72
 EI(1)=1.1E+06, 1.4E+06, 2.3E+06, 2.9E+06, 4.6E+06, 5.7E+06,  7.7E+06,
 EI(8)=18.8E+05, 68.4E+06, 242.3E+06, 427.5E+06,


 GJ(1)= 1.6E+05, 2.5E+05, 3.5E+05, 4.9E+05, 7.4E+06, 10.4E+06, 14.3E+06,
 GJ(8)= 33.4E+06, 91.8E+06, 408.4E+06, 638.4E+06,                          WING 6
C          ATT SOLID WING   10/13/72                                       STRUCTURAL BENDING AND
 EI(1)=1.43E+05, 1.98E+05, 2.34E+06, 3.59E+06, 5.30E+06, 7.41E+06, 10.3E+06,  TORSIONAL PROPERTIES
 EI(8)=20.2E+05, 71.8E+06, 251.4E+06, 427.5E+06,
 GJ(1)= 1.79E+05, 2.78E+06, 3.86E+06, 5.54E+06, 7.95E+06, 11.3E+06, 15.4E+06,
 GJ(8)= 37.7E+06, 99.7E+06, 526.4E+06, 639.4E+06,
 $END
                          FUSELAGE DESCRIPTION
P$INPT12
  RF= 3.77,  ZFUS=10.0,
  $END OF DATA
CBAR CALCULATED= 15.955025 AT( 46.823935, 11.594778,  9.050100)
```

CALCULATED GEOMETRY (SEE FIGURE 23 FOR USE OF THIS INFORMATION)

ETA	C	2H	XC4	YC4	ZC4	EA	ALED	AFAD	ATED	EI	GJ
ND	IN	IN	IN	IN	IN	ND	DEG	DEG	DEG	LBIN2	LBIN2
.95	5.03	2.92	64.63	32.31	8.05	.40	43.50	40.66	36.00	1.43E+06	1.79E+06
.87	5.68	2.92	62.02	29.39	8.05	.40	43.50	40.66	36.00	1.88E+06	2.78E+06
.79	6.33	2.92	59.42	26.47	8.05	.40	43.50	40.66	36.00	2.34E+06	3.86E+06
.70	6.98	2.92	56.81	23.55	8.05	.40	43.50	40.66	36.00	3.59E+06	5.54E+06
.61	7.63	2.92	54.20	20.63	8.05	.40	43.50	40.66	36.00	5.70E+06	7.95E+06
.52	8.28	2.92	51.59	17.71	8.05	.40	43.50	40.66	36.00	7.41E+06	1.13E+07
.44	8.93	2.92	48.98	14.79	8.05	.40	43.50	40.66	36.00	1.05E+07	1.56E+07
.35	10.78	3.33	46.39	11.67	8.05	.40	45.00	32.23	5.00	2.02E+07	3.77E+07
.25	14.61	3.00	43.24	8.56	8.05	.40	58.50	45.18	5.00	7.18E+07	9.97E+07
.16	21.00	3.23	38.18	5.39	8.05	.40	60.00	57.76	5.00	2.51E+08	3.25E+08
.05	28.59	3.77	37.60	1.88	8.05	.40	43.50	33.97	5.00	4.27E+08	5.38E+08

CR= 28.31 CT= 4.71 SPAN= 67.55 WING A= 791.84 AR= 5.84

CALCULATED CRAR= 15.855 AT(X= 40.82 Y= 11.39 Z= 8.05)

```
P$MATPS1
  RIGTD =0.0,
 $END OF DATA

P$AEROX1
 IFUS=0,NB=0,NBSEC(1)=0,IAEPOX(1)=0,RR(1)=0,ZD(1)=0,AINCB(1)=0,
 $END OF DATA

P$STOPE1
 NEXTR=0,CBAR=15.AF, XE(1)=0,YE(1)=0,ZE(1)=0,CLEZ(1)=0,CLFA(1)=0,CMEZ(1)=0,
 CMFA(1)=0,CDEZ(1)=0,CDEA(1)=0,NJ(1)=0,
 $END OF DATA

P$SYBAL1
C        ALT= 30000, SF= 24.0,    TEMP= 240 DEG K      MANEUVER
 XFUS=23.17, AINCF=-3.0, DCDF=.0072, ZCDF=10.0, DCDT=.0022, ZCDT=20.0,
 CLFA=.0030, CLFO=0.,   CMFA=.0141, CMFO=0.,   DELFL=0.,  DELSP=0.,
 DELSL=0.,  DDYN=52.78, THTDD=0.,  WG=11250.,  XCG=44.79,  XBAR4=44.79,
C        IF AINCF AND AO.PT BOTH = 0, DIVISION BY 0 WILL OCCUR AT 580 IN SYBALC
 YIY=200.0, ZBAR4=7.25, ZCG=7.25, AOLPT=-.008,CONSJ=.174, UDEOF=0.,
 CNAFR=.111, RADAL=.02145,  VEL=334.84,GUSTF=0., MACHN=1.0, USPLP=0.00,
 ECLTA=.0073, ATPAP=.794, AINCT=0.,   ATPODE=1.00, XDDE=-1.0, PWTS=0.,
 RAERO=0., ENAX=0., ENST=0., IFPPT=0., CONDNO=9H 7 ATT   ,
 DNZ= 0.00001,
 VNZ=2.5,
 ALFWT=7.95 ,DEWT=0., HPT4020 = 3HYES,
 HPT4020 = 2HNO,
 $END OF DATA
```

SINGULAR INPUT VARIABLES

CONDITION NUMBER 7 ATT

```
P&SYBAL7
 AOLSC(1)=10*-2.7, 0.,
 ADFL(1)=11*0.,
 ADSP( 1)=11*0.,
 ADSL(1)=11*0.,
      ATAU(1)= -5.0, -4.4, -3.8, -3.2, -2.6, -2.0, -1.4, -.8, -.4, -.2, 0.,      JIG TWIST
 CMOTO(1)=10*-.13, 0.,          SECTION PITCHING MOMENT
 TSECT(1)=11*.11,
 CRS(1)= 11*.61,
 CFS(1)= 11*.15,
 MO(1)= 9*.157, .106, .001,     SECTION LIFT CURVE SLOPE
 $END OF DATA

P&WTS1
 NEXTW=10,
 NG(1)= 1, 2, 3, 4, 5, 6, 7, 8, 9, 10,
 W(1)= .89, .92, .99, 1.00, 1.02, 1.05, 1.11, 1.32, 1.27, 1.55,
 XW(1)= 65.3, 62.7, 60.2, 57.7, 55.2, 52.7, 50.2, 47.9, 45.3, 41.2,
 YW(1)= 32.3, 29.4, 26.5, 23.6, 20.6, 17.7, 14.8, 11.7, 8.5, 5.4,
 ZW(1)= 10*8.35,
 $END OF DATA
```

WING INERTIA

INTEGRATED WING INERTIA

	SHNZ	EMONZ	ETONZ	SHTH	EMOTH	ETOTH	SHPH	EMOPH	ETOPH
NSECT= 1	8.90000E-01	1.63779E+00	6.90397E-02	-1.44453E-04	-2.85798E-04	1.32140E-05	-2.17284E-04	-3.99[illegible]E-[illegible]	-1.68553E-05
NSECT= 2	1.81000E+00	6.71898E+00	2.16655E-01	-2.93776E-04	-1.13319E-03	1.44977E-05	-4.41892E-04	-1.64136E-[illegible]	-5.28939E-05
NSECT= 3	2.80000E+00	1.54788E+01	3.82450E-01	-4.34460E-04	-2.57870E-03	1.47515E-05	-6.83589E-04	-3.77[illegible]E-03	-9.33709E-05
NSECT= 4	3.80000E+00	2.80998E+01	5.56936E-01	-6.16767E-04	-4.65035E-03	1.38675E-05	-9.27728E-04	-6.66[illegible]E-[illegible]	-1.35970E-04
NSECT= 5	4.82000E+00	4.45328E+01	6.75615E-01	-7.82321E-04	-7.34158E-03	2.25930E-05	-1.17675E-03	-1.[illegible]722E-02	-1.64944E-04
NSECT= 6	5.87000E+00	6.49877E+01	8.05153E-01	-9.52743E-04	-1.06863E-02	3.03778E-05	-1.43310E-03	-1.58[illegible]E-02	-1.96569E-04
NSECT= 7	6.98000E+00	8.95883E+01	9.49882E-01	-1.13290E-03	-1.47053E-02	3.73431E-05	-1.73439E-03	-2.18720E-02	-2.31903E-04
NSECT= 8	8.30000E+00	1.18789E+02	-1.13902E+01	-1.34715E-03	-1.94404E-02	2.20004E-03	-2.02635E-03	-2.90[illegible]E-02	2.92727E-03
NSECT= 9	9.57000E+00	1.56290E+02	1.51223E+01	-1.55329E-03	-2.56125E-02	-2.21037E-03	-2.33641E-03	-3.81564E-02	-3.69208E-03
NSECT=10	1.11200E+01	2.11634E+02	4.93014E+01	-1.80496E-03	-3.45809E-02	-7.77871E-03	-2.71483E-03	-5.16681E-02	-1.19631E-02
NSECT=11	1.11200E+01	2.59884E+02	-5.16547E+01	-1.80486E-03	-4.27879E-02	8.72891E-03	-2.71483E-03	-6.34477E-02	1.26109E-02
CMOTO=	-.1300	-.1300	-.1300	-.1300	-.1300	-.1300	-.1300	-.1300	0.0000

MATRIX BARL

```
NSECT=  1          1.92246E+00
NSECT=  2          2.74001E+00
NSECT=  3          3.41456E+00
NSECT=  4          4.17053E+00
NSECT=  5          5.02998E+00
NSECT=  6          5.99255E+00
NSECT=  7          7.09651E+00
NSECT=  8          8.59329E+00
NSECT=  9          9.70193E+00
NSECT= 10          9.60128E+00
NSECT= 11          6.05400E+00
```

SOLUTION OF SIMULTANEOUS EQUATIONS ($C_\ell c\ q$)

```
NOGO=  1

PTAT= 1.90151E+03          PTDOS= 0.                    DDF= 0.

   DELSP          USPLR          VNZ            DNZ            ALPEFD
  0.             0.             2.50000E+00    1.30000E-05    7.95000E+00

   VFFUA          VFTAL          VFINP          VFFUO          VFCHK
  1.01968E+03    1.90151E+03   -2.81250E+04    0.            -4.02884E+03

   TDBR4          TOFUA          TOTAL          TOINP          TOFUO          TOCHK
 -4.63972E+04    1.08781E+05   -2.59675E+04    -0.            -3.91841E+04   -1.09165E+05
```

FORCES AND MOMENTS ON TOTAL VEHICLE AND COMPONENTS

```
   CLWS           STABAR
  5.13177E-01    5.95934E-01
```

```
VERTICAL AERODYNAMIC FORCE ON THE WIND TUNNEL MODEL AT THE QUARTER MAC =   24026.16 LBS
AND THE AERODYNAMIC MOMENT ON THE WIND TUNNEL MODEL AT THE QUARTER MAC =   -109163.40 IN LB
```

STING REACTION

SHWNG THROUGH TOTEA ARE AERODYNAMIC LOADS AND MOMENTS. WTSH, WTMEA, AND WTTEA ARE INERTIA LOADS AND MOMENTS.

SHAPI, MEAPI, AND TEAPI ARE AIR + INERTIA LOADS AND MOMENTS.

ALL SHEAR/MOMENT VALUES ABOUT ELASTIC AXIS AT INBOARD EDGE OF SECTION

+SIGN CONVENTION = NOSE UP, RIGHT WING DOWN AND BACK

	XFATE	SHWNG	BMWNG	TOWNG	SHSTC	BMSTC	TCSTO
NSECT= 1	5.41533E+01	2.96441E+02	4.33122E+02	-5.48471E+02	0.	0.	0.
NSECT= 2	5.16535E+01	7.19947E+02	1.91824E+03	-2.19763E+03	0.	0.	0.
NSECT= 3	5.91443E+01	1.24466E+03	4.78163E+03	-4.96532E+03	0.	0.	0.
NSECT= 4	5.60356E+01	1.88737E+03	9.35796E+03	-9.17035E+03	0.	0.	0.
NSECT= 5	5.41287E+01	2.66226E+03	1.49377E+04	-1.51095E+04	0.	0.	0.
NSECT= 6	5.16134E+01	3.58674E+03	2.51267E+04	-2.33186E+04	0.	0.	0.
NSECT= 7	4.91131E+01	4.67975E+03	3.71582E+04	-3.35818E+04	0.	0.	0.
NSECT= 8	4.70115E+01	6.25961E+03	5.53563E+04	-4.51252E+04	0.	0.	0.
NSECT= 9	4.39331E+01	7.74511E+03	7.62642E+04	-6.71004E+04	0.	0.	0.
NSECT= 10	3.88686E+01	9.38738E+03	1.33946E+05	-1.17435E+05	0.	0.	0.
NSECT= 11	3.66358E+01	1.05875E+04	1.41583E+05	-1.33037E+05	0.	0.	0.

AIR LOADS AND MOMENTS PERPENDICULAR TO FREE STREAM

	CWMEA	CWTEA	STMEA	STTEA	SHTEA	BMTEA	TCTEA
NSECT= 1	7.51312E+02	-2.59732E+02	0.	0.	2.96441E+02	7.51312E+02	-2.59732E+02
NSECT= 2	2.36597E+03	-4.16586E+02	0.	0.	7.18447E+02	2.36597E+03	-4.18586E+02
NSECT= 3	5.94950E+03	-5.36072E+02	0.	0.	1.24466E+03	6.59950E+03	-5.36072E+02
NSECT= 4	1.30653E+04	-8.49394E+02	0.	0.	1.88797E+03	1.30653E+04	-8.49394E+02
NSECT= 5	2.19835E+04	-1.03779E+03	0.	0.	2.56286E+03	2.19835E+04	-1.03779E+03
NSECT= 6	3.41372E+04	-1.18130E+03	0.	0.	3.58674E+03	3.41372E+04	-1.18130E+03
NSECT= 7	5.00914E+04	-1.24540E+03	0.	0.	4.67975E+03	5.00914E+04	-1.24540E+03
NSECT= 8	7.38771E+04	-9.56145E+03	0.	0.	5.20931E+03	7.38771E+04	-9.56144E+03
NSECT= 9	1.01353E+05	8.80189E+03	0.	0.	7.74511E+03	1.01353E+05	8.80189E+03
NSECT= 10	1.53383E+05	2.63356E+04	0.	0.	9.38738E+03	1.53383E+05	2.63356E+04
NSECT= 11	1.89825E+05	-4.12256E+04	0.	0.	1.05875E+04	1.89825E+05	-4.12256E+04

AIR LOADS AND MOMENTS PERPENDICULAR TO ELASTIC AXIS

+SIGN CONVENTION = NOSE UP, RIGHT WING DOWN AND BACK

	INERTIA SHEARS AND MOMENTS			AIR + INERTIA SHEARS AND MOMENTS			WING LOADING (AIR ONLY)
	WTS4	WTMEA	WTTEA	SHEAFIL	MEAFIL	TORFIL	SCLCO
NSECT= 1	-2.22503E+01	-4.29447E+03	-1.72593E-01	2.94216E+02	7.46917E+02	-2.34954E+02	1.51467E+02
NSECT= 2	-4.32503E+01	-1.67974E+01	-5.41638E-01	7.14422E+02	2.96377E+03	-4.13127E+02	1.44618E+02

NSECT= 3	-7.00000E+00	-3.86959E+01	-9.26125E-01	1.27786E+03	6.91280E+03	-6.3[illegible]E+02	1.[illegible]E+02
NSECT= 4	-9.50000E+00	-7.02435E+01	-1.39234E+00	1.87847E+03	1.29350E+04	-9.5[illegible]E+02	2.2[illegible]E+02
NSECT= 5	-1.20500E+01	-1.11372E+02	-1.68904E+00	2.60063E+03	2.18592E+04	-1.0[illegible]E+03	2.2[illegible]E+02
NSECT= 6	-1.46750E+01	-1.62469E+02	-2.31293E+00	3.57207E+03	3.59748E+04	-1.1[illegible]E+03	4.1[illegible]E+02
NSECT= 7	-1.74500E+01	-2.23971E+02	-2.37471E+00	4.66238E+03	4.38674E+04	-1.2[illegible]E+03	3.7[illegible]E+02
NSECT= 8	-2.07500E+01	-2.96972E+02	2.39754E+01	6.1[illegible]56E+03	7.3581[illegible]E+04	-8.6[illegible]E+03	4.5[illegible]E+02
NSECT= 9	-2.39250E+01	-3.93724E+02	-3.73072E+01	7.7211[illegible]E+03	1.0[illegible]362E+05	6.7[illegible]E+03	5.12[illegible]E+02
NSECT= 10	-2.78000E+01	-5.29045E+02	-1.22503E+02	9.3552[illegible]E+03	1.5256[illegible]E+05	2.5217[illegible]E+04	5.06[illegible]E+02
NSECT= 11	-2.78000E+01	-5.49709E+02	1.29137E+02	1.0[illegible]597[illegible]E+04	1.3920[illegible]E+05	-4.1[illegible]E+04	3.14[illegible]E+02

	CALC EI	CALC GJ	ZOEDGE VERTICAL DEFLECTION
NSECT= 1	1.75179E+05	2.24239E+05	1.721
NSECT= 2	4.09235E+05	4.39147E+05	1.401
NSECT= 3	8.48439E+05	9.27353E+05	1.092
NSECT= 4	1.57937E+06	1.46054E+06	.819
NSECT= 5	2.70623E+06	2.42406E+06	.562
NSECT= 6	4.35919E+06	3.82576E+06	.359
NSECT= 7	6.68814E+06	5.78570E+06	.206
NSECT= 8	1.14523E+07	9.93158E+06	.103
NSECT= 9	2.30202E+07	2.02659E+07	.042
NSECT= 10	5.27432E+07	4.75871E+07	.016
NSECT= 11	8.79794E+07	9.13951E+07	.004

	ALFND ELASTIC EQUILIBRIUM ANGLE OF ATTACK	ATELD ELASTIC WING TWIST	AWELD ELASTIC TWIST DUE TO C_{ℓ}^{c}	ASELD	QSBEXTD	ACMOED	ACMOGD
				ELASTIC TWIST DUE TO STORES		ELASTIC TWIST DUE TO C_{M_0}	
NSECT= 1	2.30457E+00	-3.40387E+00	-2.62226E+00	0.	0.	-4.0[illegible]E-01	-3.76044E-01
NSECT= 2	3.01752E+00	-3.33462E+00	-2.57916E+00	0.	0.	-3.77[illegible]E-01	-3.48[illegible]E-01
NSECT= 3	3.87306E+00	-3.06755E+00	-2.43664E+00	0.	0.	-3.27374E-01	-3.03541E-01
NSECT= 4	4.86914E+00	-2.69690E+00	-2.18301E+00	0.	0.	-2.5[illegible]E-01	-2.49906E-01
NSECT= 5	5.96534E+00	-2.23729E+00	-1.83653E+00	0.	0.	-2.0[illegible]E-01	-1.93998E-01
NSECT= 6	7.15154E+00	-1.70625E+00	-1.41866E+00	0.	0.	-1.4[illegible]E-01	-1.39959E-01

NSECT= 7	8.42553E+00	-1.12120E+00	-9.41528E-01	0.	0.	-9.29990E-02	-9.65733E-02
NSECT= 8	9.70169E+00	-6.14976E-01	-5.18363E-01	0.	0.	-5.35953E-02	-4.50021E-02
NSECT= 9	1.07624E+01	-3.10930E-01	-2.61436E-01	0.	0.	-7.1[illegible]E-03	-1.77133E-02
NSECT= 10	1.19476E+01	-1.39145E-01	-1.17793E-01	0.	0.	-1.24122E-02	-4.73915E-03
NSECT= 11	7.99773E+00	-3.42651E-02	-2.90113E-02	0.	0.	-1.78[illegible]E-03	-3.48424E-03

```
P$PLOTDAT
 PLTTITL(1)=10HATT M=1.0 , 10HH=30000 T=, 10H24CK A=7.9, 10H5 SOLTD X-,
 PLTTTTL(5)=10HC UNBAL   ,  10H          ,
 SYU(1) = 14000., 300000., 1000.,  60.,      5., 0.1,
 SYL(1) =    1.0, -100000.,   1.0,.04, 0.,  -7.,
 PLOT=3HYES,
 PLOT=2HNO,
 $END OF DATA
```

SC4020
PLOTTING
INFORMATION

APPENDIX II

SAFETY FACTOR BASED ON FRACTURE MECHANICS

Design procedures using fracture mechanics have not been rigidly established, because the entire field is still under development. However. it is important in selection of high-strength materials and design of structures operating at high stress levels that consideration be given to fracture resistance to ensure reasonable safety from catastrophic failure. This is particularly true for high-strength steels, where toughness generally decreases with increasing yield strength and decreasing temperature.

The most commonly used measure of crack propagation resistance of high-strength alloys for use in heavy sections* is plane strain fracture toughness, K_{1c}. Variations in K_{1c} can be expected for any given alloy and strength level due to metallurgical aspects and nonstandardization of testing procedures. For example. variations in K_{1c} have been observed for melting practice, processing history, size and shape of product form, and grain orientation. This variability makes the selection of a "design allowable" for K_{1c} extremely difficult.

Flaws are inherent in all materials, and these defects can propagate under an applied stress, depending on a number of factors including size, shape, location and orientation. Therefore, the minimum flaw size that can be detected by available nondestructive testing (NDT) inspection processes is important in application of fracture mechanics. The detection capability of most NDT techniques varies with different types of materials. Fabrication of highly stressed models from high-strength steels will generally require ultrasonic inspection of the raw stock and magnetic particle inspection of the finish machined components. Both inspection requirements must be specified on the drawings, since present material specifications do not define these inspection requirements.

The minimum flaw size that can be detected in high-strength steels by these NDT inspection techniques has not been established. In application of fracture mechanics to design, some investigators have assumed minimum initial crack dimensions of 0.15 inch deep by 0.75 inch long as "standard minimum-detectable values" (Reference 2). These are considered conservative values, but are useful for safety factor calculations.

---

*ASTM E399-72 (Reference 1) defines that for plane strain conditions, material thickness must exceed $2.5\ (K_{1c}/\sigma_{ys})^2$.

The tensile strength and fracture toughness properties at room and subzero temperatures for three high strength steels are shown below (References 3, 4, and 5).

Alloy & Condition	Temperature (°F)	F_{tu} (ksi)	F_{ty} (ksi)	Fracture Toughness, K_{1c} (ksi $\sqrt{in.}$)
PH13-8 Mo	RT	201(1)	190(1)	90
H1000	-110	230	220	18
18 Ni Maraging	RT	250(1)	240(1)	90
250 Grade	-65	260	245	85
	-110	270	260	71
18 Ni Maraging 300 Grade	RT	300(1)	285(1)	52

All values are typical except as noted.

(1) MIL-HDBK-5 or material specification minimums.

Using the above data, calculations were made of the critical flaw size for an operating stress of one-half the yield strength, critical stress for "minimum detectable flaw size", and safety factor for PH13-8Mo H1000 and 18Ni maraging 250 grade steel at room temperature. The calculations assumed a "standard minimum detectable flaw size" of 0.15 inch deep by 0.75 inch long. The safety factor is defined as the ratio of the operating stress to the critical stress for the "standard minimum detectable flaw size."

	PH13-8 Mo H1000	18 Ni Maraging 250 Grade
Operating Stress $\sigma = 0.5\,\sigma_{ys}$ (ksi)	95	120
Critical Flaw Size for $0.5\,\sigma_{ys}$ (in.) (a = flaw depth)	0.29	0.18
Minimum Detectable Flaw Size (in.) (a = flaw depth)	0.15	0.15
Critical σ for Minimum Detectable Flaw Size (ksi)	130	130
Safety Factor ($\sigma_{\text{Minimum Detectable Flaw Size}}/0.5\,\sigma_{ys}$)	1.36	1.08

The resulting safety factors of 1.36 and 1.08 appear reasonable in view of the conservative value used for the minimum detectable flaw size.

The calculations were made using the following equations (Reference 6):

$$\left(\frac{a}{Q}\right)_c = \frac{1}{1.21\pi}\left(\frac{K_{1c}}{\sigma}\right)^2 \tag{1}$$

where

$\left(\frac{a}{Q}\right)_c$ = critical normalized flaw size

K_{1c} = plane strain fracture toughness

σ = applied stress

a = flaw depth

Q = flaw shape parameter

The equations for determining Q are:

$$Q = \phi^2 - 0.212\left(\frac{\sigma}{\sigma_{ys}}\right)^2$$

where

$$\phi^2 = \int_0^{\pi/2} \sqrt{1 - \frac{c^2 - a^2}{c^2}\sin^2\theta}\, d\theta$$

For the "standard minimum detectable flaw size" (a = 0.15 and c = 0.75 inch), the eliptical integer ϕ = 1.3 (from table of eliptical integers), and Q = 1.2 (by calculation). The fracture toughness data are shown in Figure I-1.

The observations from these preliminary studies are that PH13-8Mo H1000 and maraging 250 grade steels have good fracture toughness at room temperature. However, the limited data available for PH13-8Mo H1000 show a drastic decrease in fracture toughness at subzero temperatures, which should be more fully explored for low-temperature service. Changes in heat treatment or alloy may be necessary; for example, the use of maraging 200 grade, which has a K_{1c} value of 160 ksi$\sqrt{\text{in.}}$ at -100°F compared to PH13-8Mo H1000, which has a K_{1c} of 18 ksi$\sqrt{\text{in.}}$ at -110°F (Reference 7).

The lower fracture toughness of maraging 300 grade steel at room temperature and lack of data at subzero temperatures indicate a vital need for further investigation of this alloy.

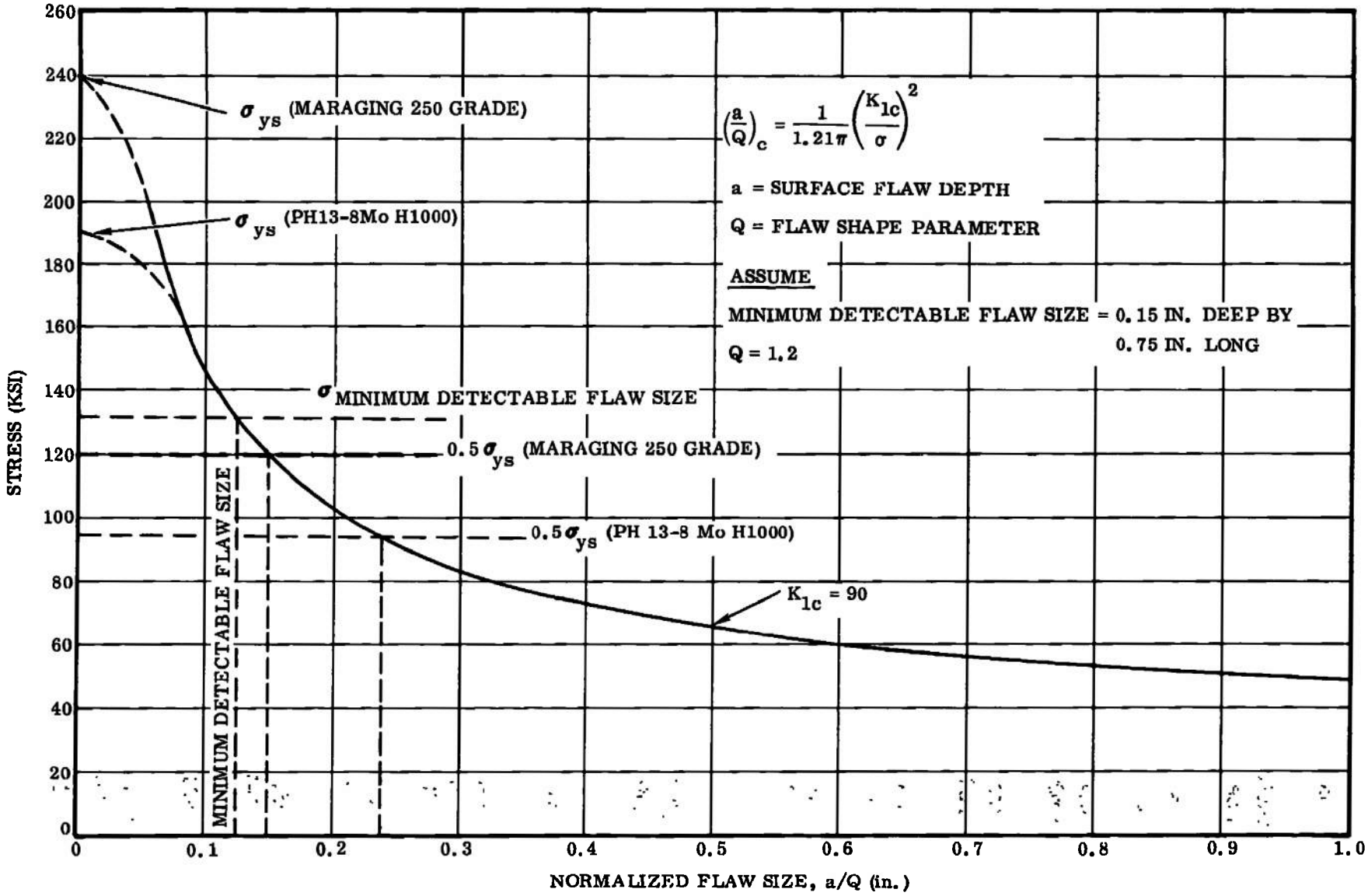

Figure I-1. Relationship Between Critical Flaw Size $(a/Q)_c$, Applied Stress (σ), and Plane Strain Fracture Toughness (K_{1c})

The following studies are recommended:

a. Comprehensive compilation of available fracture toughness data on selected high-strength steels for the full range of potential service temperatures.

b. Determine safety factors and critical flaw sizes using the above fracture toughness data for the full range of potential service temperatures.

c. Establish statistically significant "minimum detectable flaw sizes" for selected high-strength steels, based on currently available NDT techniques.

d. Establish fracture toughness "design allowables" for the recommended high-strength steels, based on the wind tunnel operating temperature and environment.

e. Analyze the effect of cyclic loading and sustained-stress loading on subcritical flaw growth.

f. Evaluate the feasibility of proof testing highly stressed wind tunnel models to ensure an adequate safety factor from catastrophic failure.

REFERENCES

1. ASTM E399-72 "Standard Method of Test for Plane Strain Fracture Toughness of Metallic Materials."

2. C. C. Osgood, "What is Fracture Mechanics," Machine Design, July 22, 1971, August 5, 1971, August 19, 1971, September 2, 1971, September 16, 1971.

3. R. T. Bubsey, and W. F. Brown, Jr., "Crack Toughness Characteristics of Several Alloys for Use in Heavy Sections of High Speed Aircraft," NASA TN D-4998, January 1969.

4. W. F. Brown, Jr. and J. E. Srawley, "Plane Strain Crack Toughness Testing of High Strength Metallic Materials," ASTM STP 410, 1966.

5. H. A. Wood, "Fracture Control Procedures for Aircraft Structural Integrity," AFFDL-TR-71-89, July 1971.

6. NASA SP-8040 , "Fracture Control of Metallic Pressure Vessels," May 1970.

7. C. Vishnevsky and E. A. Steigerwald, "Plane Strain Fracture Toughness of Some Cryogenic Materials at Room and Subzero Temperatures," ASTM STP 496, Fracture Toughness Testing at Cryogenic Temperatures, August 1971.

UNCLASSIFIED
Security Classification

DOCUMENT CONTROL DATA - R & D

(Security classification of title, body of abstract and indexing annotation must be entered when the overall report is classified)

1. ORIGINATING ACTIVITY *(Corporate author)* General Dynamics Corporation Convair Aerospace Division San Diego, California	2a. REPORT SECURITY CLASSIFICATION UNCLASSIFIED 2b. GROUP N/A

3. REPORT TITLE
WIND TUNNEL MODEL PARAMETRIC STUDY FOR USE IN THE PROPOSED 8 FT X 10 FT HIGH REYNOLDS NUMBER TRANSONIC WIND TUNNEL (HIRT) AT ARNOLD ENGINEERING DEVELOPMENT CENTER

4. DESCRIPTIVE NOTES *(Type of report and inclusive dates)*
Final Report - June through December 1972

5. AUTHOR(S) *(First name, middle initial, last name)*
Walter K. Alexander, Stanley A. Griffin, Robert L. Holt, et al.

6. REPORT DATE March 1973	7a. TOTAL NO. OF PAGES 175	7b. NO. OF REFS 25

8a. CONTRACT OR GRANT NO F40600-72-C-0015 b. PROJECT NO. c. d.	9a. ORIGINATOR'S REPORT NUMBER(S) AEDC-TR-73-47 9b. OTHER REPORT NO(S) *(Any other numbers that may be assigned this report)* GDCA-DHJ72-001

10. DISTRIBUTION STATEMENT
Approved for public release; distribution unlimited.

11. SUPPLEMENTARY NOTES Available in DDC	12. SPONSORING MILITARY ACTIVITY Arnold Engineering Development Center, Air Force Systems Command, Arnold AF Station, Tenn. 37389

13. ABSTRACT The need for a High Reynolds Number Transonic Wind Tunnel (HIRT) has been recognized throughout the industry for some years. The proposed HIRT facility at Arnold Engineering Development Center will provide a much needed tool for the study of phenomena sensitive to Reynolds number. The usefulness of the HIRT facility will be largely influenced by the ability of industry to design and build wind-tunnel models for an acceptable cost capable of operating within the severe environment of the tunnel. The object of this study is to determine the feasibility of designing and building models capable of withstanding the loads and environmental conditions of the facility. The aircraft configurations chosen for study cover a wide spectrum of flight conditions. A test plan is developed for each configuration which encompasses its complete flight envelope. Model loads and deformations, stress analyses of each configuration, a summary of materials suitable for use in the HIRT facility, and cost comparisons are presented. The study concluded that models capable of running in the HIRT facility can be built at a reasonable cost with present-day techniques and materials.

DD FORM 1 NOV 65 1473

UNCLASSIFIED
Security Classification

14. KEY WORDS	LINK A ROLE	LINK A WT	LINK B ROLE	LINK B WT	LINK C ROLE	LINK C WT
wind tunnel models						
configurations						
design						
fabrication						
high Reynolds number testing						
materials						
model distortion						
aerodynamic loads						

AFSC
Arnold AFS Tenn